Mitteilungsblatt

der

Bundesanstalt für Wasserbau

Nr. 88

Karlsruhe • August • 2005

ISSN 0572-5801

Bulletin

No. 88

of the
Federal Waterways Engineering
and Research Institute
(Bundesanstalt für Wasserbau)

Principles for the Design of Bank and Bottom Protection for Inland Waterways

Karlsruhe • August• 2005

ISSN 0572-5801

Published by:

Bundesanstalt für Wasserbau
Kußmaulstrasse 17, 76187 Karlsruhe, Germany
Postfach 21 02 53, 76152 Karlsruhe, Germany
Phone: +49 721 9726-0
Fax: +49 721 9726-4540
e-mail: info.karlsruhe@baw.de
Internet: http://www.baw.de

Cover photograph:
Field tests on the Wesel-Datteln Canal below Flaesheim Lock (at km 46.500), in October 2002 with the tug Mignon sailing close to the slope at almost critical speed. The motor vessel MS Main can be seen in the background.

Foreword

The Federal Waterways and Shipping Administration designs and constructs bank and bottom protection for inland waterways in compliance with the Code of Practice Use of Standard Construction Methods for Bank and Bottom Protection on Waterways (*Merkblatt Anwendung von regelbauweisen für Böschungs- und Sohlensicherungen*) (MAR) which describes tried and tested standard methods of construction. However, the standard methods are only applicable in certain circumstances, depending on the impact of waves and currents caused by shipping and the loads acting on the subsoil. A new concept for the design of bank and bottom protection, which took ten years to develop, is proposed in this publication; it describes a more general approach to design and extends beyond the scope of the MAR. Apart from the specially developed geotechnical calculation methods and the well-known principles for calculation used in waterway design, it is now also possible to take account of

- the effects of propeller wash and bow thrusters on the banks and botttoms of waterways
- secondary waves caused by small ships sailing at high speeds
- the influence of the ratio of the length of a ship to the width of the waterway
- running waves, slope supply flow and
- wind waves.

Compliance with the speeds and modes of operation stipulated in the shipping regulations was assumed when specifying the parameters of ships in motion for design purposes. The loads to which bank protections are exposed increase disproportionately whenever ship speeds approach or reach a critical level and taking account of such cases would result in very uneconomic designs. It is therefore assumed that ships do not exceed a maximum of 97 % of the critical ship speed, as has hitherto been the case for designs based on the MAR and which is also in keeping with an economic mode of operation.

Large, very powerful recreational craft or pusher craft sailing alone can give rise to wave loads on bank protections that exceed those caused by the vessels and modes of operation on which this publication is based. The inclusion of such load cases, which occur very rarely these days, as design load cases would lead to a considerable increase in the cost of constructing bank and bottom protection. Owing to the unlikelihood of such loads occurring, it is recommended that any damage resulting from overloading caused in this way be repaired during maintenance work. However, it will also be necessary to consider whether the current shipping regulations need to be revised, taking account of economic considerations.

In addition to this, attention must be paid to the new types of propulsion and vessels that are being developed so that prompt action can be taken if they seriously affect the durability of bank protection. To this end, it will be necessary to document and analyse the cost of maintaining bank protection more systematically in future.

This publication describes the theoretical and experimental principles for the design of bank and bottom protection for inland waterways. Thus it is not intended as a practical aid to design. The Code of Practice Use of Standard Construction Methods for Bank and Bottom Protection on Waterways (MAR) is one such practical aid for design engineers. It is currently being revised on the basis of this publication.

The publication has been drawn up by the working group “Revetments for Waterways” in which members of staff of the Waterways and Shipping Administration, the Federal Ministry for Transport, Building and Housing and the Federal Waterways Engineering and Research Institute participated, assisted by external experts on certain matters. I should like to thank the members of the working group for their intensive and successful work, their perseverance in discussions on what were often controversial subjects and for conducting and evaluating the required field tests. I should also like to thank Professor Schulz (University of the German Federal Armed Forces in Munich), the former head of the working group, our colleagues in the “AK 17” group of experts on revetment construction, as well as Professor Römisch and Professor Wagner (both formerly of the Technical University of Dresden) and Dr. Daemrich (University of Hanover) who assisted us in recent years by taking a critical look at the text and putting forward proposals for its improvement.

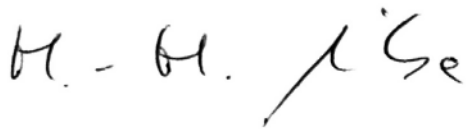

Dr. H.-H. Witte
Director and Professor
of the Federal Waterways Engineering
and Research Institute

Principles for the Design of Bank and Bottom Protection for Inland Waterways

Working Group "Revetments for Waterways"

Founded in October 1992

Members:

ABROMEIT, Uwe	BOR, Bundesanstalt für Wasserbau Karlsruhe
ALBERTS, Dirk †	Dipl.-Ing., Bundesanstalt für Wasserbau, Dienststelle Hamburg
BARTNIK, Wolfgang	BDir, Wasserstraßen-Neubauamt Datteln
FISCHER, Uwe	BOR, Bundesministerium für Verkehr, Bau- und Wohnungswesen Bonn
FLEISCHER, Petra	BOR, Bundesanstalt für Wasserbau Karlsruhe
FUEHRER, Manfred (until February 2000)	Dr. rer. nat., ehem. Bundesanstalt für Wasserbau Karlsruhe
HEIBAUM, Michael	BDir, Dr.-Ing., Bundesanstalt für Wasserbau Karlsruhe
KAYSER, Jan	BDir, Dr.-Ing., Bundesanstalt für Wasserbau Karlsruhe
KNAPPE, Gerd	Dipl.-Ing., Wasserstraßen-Neubauamt Datteln
KÖHLER, Hans-Jürgen	Dipl.-Ing., Bundesanstalt für Wasserbau Karlsruhe
LIEBRECHT, Arno	Dipl.-Ing., Wasser- und Schifffahrtsdirektion Mitte Hannover
REINER, Wilfried	LBDir, Wasser- und Schifffahrtsdirektion Mitte Hannover
SCHMIDT-VÖCKS, Dieter	LBDir a. D., Wasser- und Schifffahrtsdirektion Mitte Hannover
SCHULZ, Hartmut (Obmann bis 1996)	Prof. Dr.-Ing., Universität der Bundeswehr München
SCHUPPENER, Bernd (Obmann seit 1996)	LBDir, Dr.-Ing., Bundesanstalt für Wasserbau Karlsruhe
SÖHNGEN, Bernhard	BDir, Prof. Dr.-Ing., Bundesanstalt für Wasserbau Karlsruhe
SOYEAUX, Renald	Dr.-Ing., Bundesanstalt für Wasserbau Karlsruhe

Content

1 Preliminary remarks 15

2 Terms and definitions 17

3 Summary of the hydraulic actions on the banks and bottoms of rivers and canals 23

3.1 General 23
3.2 Currents 23
3.3 Waves 23
3.3.1 General 23
3.3.2 Effect of unbroken run-up wave 24
3.3.3 Effect of breaking run-up wave 24
3.3.4 Effect of breaking waves travelling parallel to a bank 24
3.4 Effect of water level drawdown 25
3.4.1 General 25
3.4.2 Slowly falling water levels 25
3.4.3 Rapidly falling water levels 25
3.4.3.1 General 25
3.4.3.2 Effect of excess pore water pressure 25
3.4.3.3 Magnitude and development of excess pore water pressure 25
3.5 Groundwater inflow 26

4 Safety and design concept 27

4.1 General 27
4.2 Hydraulic analyses 28
4.2.1 Aspects of the specification of the design values 28
4.2.2 Recommendations for hydraulic design 29
4.2.2.1 Primary wave field 29
4.2.2.2 Secondary wave field 30
4.2.2.3 Propeller wash 31
4.2.2.4 Wind waves 31
4.2.2.5 Recommendations for hydraulic design in standard cases 31
4.3 Geotechnical verifications 32

5 Determination of the hydraulic actions 33

5.1 General 33
5.2 Data on waterways 33
5.2.1 Geometry of waterways 33
5.2.2 Geometry of fairways 33
5.3 Data on vessels 34

5.4 Hydraulic actions due to shipping 35
5.4.1 Components 35
5.4.2 Sailing situations 35
5.4.2.1 Sailing at normal speed 35
5.4.2.2 Manoeuvring 37
5.5 Magnitude of ship-induced waves (design situation: "sailing at normal speed") 37
5.5.1 Hydraulic effective cross-section of canals and ships 38
5.5.1.1 Influence of shallow water 38
5.5.1.2 Influence of boundary layers 43
5.5.2 Critical ship speed for canal conditions 44
5.5.3 Mean drawdown and return flow velocity for vessels sailing in the centre of a canal 45
5.5.4 Hydraulic design parameters and geotechnically relevant drawdown parameters for any sailing position 49
5.5.4.1 Definition of wave height 49
5.5.4.2 Maximum drawdown at bow and associated return flow velocity without the influence of eccentricity 49
5.5.4.3 Maximum drawdown at stern and associated return current velocity without the influence of eccentricity 49
5.5.4.4 Maximum heights of bow and stern waves due to eccentric sailing 50
5.5.4.5 Slope supply flow 51
5.5.4.6 Increase in wave heights for vessels sailing with drift 53
5.5.4.7 Drawdown velocity of ship-induced waves 53
5.5.5 Secondary waves 55
5.5.5.1 General 55
5.5.5.2 Calculation of the heights of secondary waves 57
5.5.5.3 Additional secondary waves in analogy to an imperfect hydraulic jump 58
5.5.5.4 Secondary waves caused by small boats at sliding speed and when sailing close to a bank 58
5.5.6 Passing and overtaking 59
5.6 Hydraulic actions on waterways due to flow caused by propulsion (propeller wash) 59
5.6.1 Induced initial velocity of the propeller jet for stationary vessels (ship speed $v_S = 0$) 59
5.6.2 Velocity of the propeller jet at ship speed $v_S \neq 0$ 61
5.6.3 Jet dispersion characteristics 62
5.6.3.1 Standard jet dispersion situations 62
5.6.3.2 Characteristics of the decrease in the main velocity 63
5.6.3.3 Calculation of the distribution of the jet velocity orthogonal to the jet axis 65
5.6.3.4 Multi-screw drives 67
5.6.4 Simplified calculation of the maximum near bed velocity 67
5.6.5 Loads due to bow thrusters 68
5.7 Wind set-up and wind waves 69
5.7.1 General 69
5.7.2 Wind data 70
5.7.3 Fetch and period of wind action 70

5.7.4 Wind set-up 71
5.7.5 Wind waves 72
5.8 Wave deformation 74
5.8.1 General 74
5.8.2 Wave shoaling and breaking of waves 74
5.8.3 Diffraction 76
5.8.4 Refraction 77
5.8.5 Reflection 78
5.8.6 Wave run-up 78
5.8.6.1 Incoming waves 79
5.8.6.2 Parallel waves 80
5.8.7 Change in wave height at the transition from a vertical bank to a slope revetment 80
5.9 Other waves 80
5.9.1 General 80
5.9.2 Positive surge/drawdown waves 80
5.9.3 Flood waves 81
5.10 Excess pore water pressure as a function of rapid drawdown z_a 82
5.10.1 General 82
5.10.2 Maximum drawdown z_a and drawdown velocity v_{za} 82
5.10.3 Magnitude of excess pore water pressure Δu 82

6 Hydraulic design of unbound armourstone cover layers 85
6.1 General 85
6.2 Stone size required to resist loading due to transversal stern waves 86
6.3 Stone size required to resist flow due to propulsion 87
6.3.1 Stone size required to resist jet attack 87
6.3.2 Stone size required to limit the depth of scour due to propeller wash 88
6.4 Stone size required to resist loading due to secondary diverging waves 89
6.5 Stone size required to resist wind waves 89
6.6 Stone size required to resist combined loads due to ship-induced waves and wind waves 90
6.7 Stone size required to resist attack by currents 90
6.7.1 Stone size required to resist attack by currents flowing largely parallel to the slope 90
6.7.2 Stone size required to resist loads on the slope due to slope supply flow 91
6.8 Stone size as specified in the Technical Supply Conditions for Armourstones (TLW) 91
6.9 Thickness of the cover layer 92
6.10 Determination of hydraulically equivalent revetments 93
6.11 Minimum thicknesses 93

6.12 Length of revetments in the line of the slope required to resist wave loads 94
6.12.1 General 94
6.12.2 Above the still-water level 94
6.12.3 Below the still-water level 94
6.13 Design for the transition from a vertical bank to a slope revetment 94

7 Geotechnical design of unbound cover layers 97
7.1 General 97
7.1.1 Guidance on design 97
7.1.2 Input parameters 97
7.2 Local stability of permeable revetments 98
7.2.1 General 98
7.2.2 Depth of the critical failure surface d_{krit} 98
7.2.3 Weight per unit area of cover layers required to protect slope revetments against sliding failure 98
7.2.3.1 General 98
7.2.3.2 Method of calculation 99
7.2.3.3 Procedure for stratified ground 100
7.2.4 Weight per unit area of cover layers to inhibit hydrodynamic soil displacement 100
7.2.4.1 General 100
7.2.4.2 Method of calculation 100
7.2.5 Weight per unit area of cover layers taking a toe support into account 100
7.2.5.1 General 100
7.2.5.2 Failure mechanism 1 at the toe of a slope 101
7.2.5.3 Failure mechanism 2 for toe blankets 102
7.2.5.4 Failure mechanism 2 for embedded toes 104
7.2.5.5 Failure mechanism 2 for a sheet pile wall at the toe 106
7.2.6 Weight per unit area of cover layers taking a suspension of the revetment into account 107
7.2.6.1 General 107
7.2.6.2 Verification of the external load-bearing capacity 108
7.2.6.3 Verification of the internal load-bearing capacity 108
7.2.7 Slope revetment above the lowered water level 108
7.3 Local stability of impermeable revetments 109
7.3.1 General 109
7.3.2 Weight per unit area of impermeable cover layers required to resist sliding 109
7.3.3 Weight per unit area of impermeable cover layers required to resist uplift 109
7.4 Verification of the global safety of the water-side slope 110

8 Hydraulic design of partially grouted armourstone cover layers 111

9 Geotechnical design of partially grouted armour-stone cover layers 111

9.1 General 111

9.2 Local stability of permeable revetments with partially grouted cover layers 111

9.3 Local stability of impermeable revetments with partially grouted cover layers 111

9.4 Verification of the global stability of the water-side slope 111

10 Literature 113

11 Nomenclature 125

11.1 Abbreviations 125

11.2 Symbols 125

Annex A

1 Preliminary remarks

This publication describes in detail the principles of the design of bank and bottom protection for inland waterways, taking into account the results of recent research. The principles include the verification by calculation of the stability and resistance to erosion of canal embankments and, with certain limitations, the banks of rivers exposed to natural hydraulic influences and to those caused by shipping.

The publication is devided into three main sections:

- The first section includes definitions of the relevant terminology, explanations of the hydraulic and geotechnical principles and an introduction to the safety philosophy and the design concept (see chapters 2 to 4).
- The second section deals with the determination of the hydraulic actions (see chapter 5), that constitute the input parameters for the design.
- The third section deals with hydraulic and geotechnical design procedures (see chapters 6 to 9).

The **scope** of the hydraulic design approaches primarily covers waterways with predominantly parallel banks, with confined fairways, whose depths are virtually constant (i.e. no berms) except in the vicinity of the banks, that have a maximum ratio of the water surface width to ship's length (b_{ws}/L) of around 2:1 and with shipping traffic comprising mostly displacement craft (including recreational craft), the displacement being relevant to the design. Within certain limitations, the methods described can also be applied to widened stretches of canals and to canalized rivers, if vessels sail close to the banks and those banks are regular, i.e. without any projections or funnels where ship-induced waves can accumulate. Within these limitations, the influence of the shape of the bank, the turbulence and the current on wave propagation can be disregarded. The influence of shallow water (i.e. if b_{ws}/L is greater than 2/1) on possible ship speeds and drawdown in the vicinity of ships can be taken into account by considering an equivalent canal cross-section by way of an approximation. Approximation equations have been included to enable the decrease in wave height as the waves move away from a vessel to be calculated. Approximation methods are also used to estimate the hydraulic actions caused by recreational craft and craft with short stocky hulls (such as pusher craft and tugs).

Methods of calculating the hydraulic design parameters (wave height, flow velocity) described in chapter 5 do not cover the following situations:

- Very irregular waterway cross-sections and waterways with irregular banks.
- Unconventional propulsion such as Schottel propellers or jet propulsion.
- Craft that do not displace water such as hovercraft and planing recreational craft.
- Ocean-going vessels and other vessels whose design differs from the usual design of inland navigation vessels, e.g. ships with bulbous bows (which give rise to different types of secondary waves).
- Depth-based Froude numbers greater than 0.8
  $v_S / \sqrt{g\, h_m} > 0.8$
  (where the secondary wave system is altered significantly).
- Sailing lines whose axis deviates considerably from that of the canal (causing pronounced changes in the primary and secondary wave systems).

Design procedures based on readings, e.g. for ship-induced wave heights, if available, can be applied directly when determining the size of armourstones (see chapter 6).

The following points are not covered by the procedure for determining the size of armourstones given in chapter 6. (This does not affect the geotechnical design process.)

- Banks with gradients of less than approx. 1:5 (at which significant deformation of the incoming waves occurs) and greater than approx. 1:2.
- Wave deformation at the slope (although this is taken into account indirectly in the design procedures covering wave heights at the toe of the slope).
- Slope revetments comprising shaped stones, gabions or asphalt.

The design of bank and bottom protection comprises a hydraulic and a geotechnical component (see Figure 1.1). The two design components must be carried out separately.

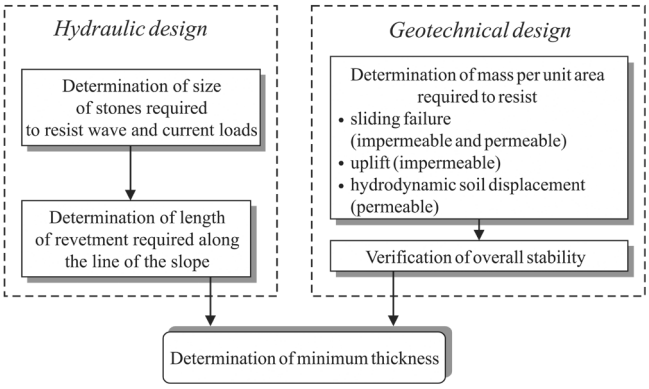

Figure 1.1 Procedure for the design of bank and bottom protection

Hydraulic design deals with the determination of the required stone size and the length of the revetment along the line of the slope, depending on the wave and current loads. The purpose of **geotechnical design** is to establish the required mass per unit area of the revetment to ensure adequate resistance to sliding failure, uplift and hydrodynamic soil displacement. In addition to this, a geotechnical verification of the overall stability is required.

Finally, the results of hydraulic and geotechnical design serve as the basis for determining the required minimum thickness of armour or cover layers. It must also be checked whether sufficient protection is ensured in the event of a ship colliding with the revetment as well as against anchor cast and ultraviolet radiation and that the filtration length is sufficient to safeguard against the transport of particles.

The methods described in this publication apply in conjunction with the latest versions of the following **specifications and codes of practice** for bank and bottom protection on waterways:

- Code of Practice Use of Standard Construction Methods for Bank and Bottom Protection on Waterways (*Merkblatt Anwendung von Regelbauweisen für Böschungen und Sohlsicherungen an Wasserstraßen*) /*MAR*/
- Code of Practice Use of Granular Filters on Waterways (*Merkblatt Anwendung von Kornfiltern an Wasserstraßen*) /*MAK*/
- Code of Practice Use of Geotextile Filters on Waterways (*Merkblatt Anwendung von geotextilen Filtern an Wasserstraßen)* /*MAG*/
- Use of Cement Bonded and Bituminous Materials for Grouting of Armorstones on Waterways *(Merkblatt Anwendung von hydraulisch und bitumengebundenen Stoffen zum Verguss von Wasserbausteinen an Wasserstraßen)* /*MAV*/
- Technical Supply Conditions for Armourstone (*Technische Lieferbedingungen für Wasserbausteine)* /*TLW*/
- Guidelines for Standard Cross Sections of Shipping Canals *(Richtlinien für Regelquerschnitte von Schifffahrtskanälen)* /*BMV 1994*/

2 Terms and definitions

Advance ratio of a propeller: Ratio J of the velocity of the approach flow towards the propeller v_A to the product of the propeller speed n and propeller diameter D ($J = v_A/nD$)

Armour layer: The upper layer of a ⇒ revetment; it must be resistant to erosion and have adequate resistance to anchor cast and impacts by shipping.

Backwater at the bow: Accumulation of water in front of the bow over the influence width, caused by vessels on accelerating or when sailing steadily along channels with rough surfaces (water surface elevation); unlike ⇒ bow waves, backwater at the bow occurs over large widths (canal width).

Bow thruster: A ship's propeller (standard model) that accelerates water in a tube in the bow section orthogonal to the axis of the vessel. It exerts a transversal thrust that acts in the same way as a rudder. It is most effective at low speeds over ground.

Bow wave: Accumulation of approaching water directly in front of the bow of a vessel (stagnation point) that gives rise to the formation of ⇒ secondary waves on either side of the vessel.

Breaking of waves: A wave will break if the ⇒ wave steepness reaches a critical value as a result of ⇒ shoaling. The process is accompanied by the formation of a water-air mix and a loss of wave energy (⇒ plunging breakers).

Breaking waves ⇒ breaking of waves

Canal conditions: Confined waterway (with restricted depth and width). Canals are the most common type of inland waterway.

The effect of the width limit ("canal case") becomes noticeable when the ratio of the water surface width b_{ws} to the length of the vessel L is equal to or less than 2 to 3 ($b_{WS}/L \leq 2 - 3$) /*Schuster 1952*/.

Canal conditions exist at low blockage ratios. As a rough estimate, $n = A/A_M \leq 25 - 35$ for motor vessels and large inland cargo vessels, the higher value applying to long, narrow vessels with a shallow draught and the lower value to short, wide vessels with a deep draught.

Channel: Wetted perimeter of a canal or river comprising the bed and banks.

Cross-section ratio: The ratio n of the cross-sectional area A of a waterway at a particular water level (which affects the return flow) to the cross-sectional area A_M of the submerged part of a vessel ($n = A/A_M$). The reciprocal value of the blockage ratio, $k = 1/n$, (known as the blockage coefficient) is mostly used in the literature in Britain and North America.

Deep water: Waves can propagate or diminish entirely unhindered due to the absence of any depth or width restriction; this situation obtains in large, deep lakes and in seas.

Depth, critical: The depth at which a failure surface parallel to and close to the surface of a slope occurs in the underlying soil after the shear resistance of the soil has been reduced to a minimum as a result of the ⇒ excess pore water pressure caused by ⇒ rapid drawdown (⇒ local stability).

Diffraction: Occurs when a wave front hits an obstacle. Waves are generated at the end of the obstacle that is exposed to waves and propagate on its leeside as each point of a wave crest is the starting point for new circular wavelets. The wave celerity is not altered but the wave height and direction change at the open flanks.

Diverging waves: Part of the ⇒ secondary wave system in which the wave crests diverge at an acute angle to the vessel's direction of travel.

Drawdown: Lowering of the water level adjacent to a vessel caused by the displacement flow.

Vessels in motion cause the water to flow around them in a particular way which is accompanied by deformation of the water surface. The relevant terminology is given in Figure 2.3 (longitudinal section) and in Figure 2.1 and Figure 2.2 (top views).

Drawdown, rapid: Drawdown in which the rate at which the water level drops is higher than the permeability of the bed and banks of the river or canal.

Drawdown velocity: Average rate at which the water level falls at any point on a bank.

Ducted propeller: Propeller enclosed in a cylindrical duct to increase its efficiency.

Excess pore water pressure: The water pressure in the pores of a soil in excess of the hydrostatic pore water pressure. It arises when the volume of the pore water is prevented from increasing (if the pore water pressure changes) or when the volume of the granular structure is prevented from decreasing (if there are changes in the total or effective tension of the granular structure). It is caused by ⇒ rapid drawdown. As a result, the pressure in the subsoil is higher than at the water/soil interface.

Fetch: Area of the surface of a body of water in which ⇒ wind waves are generated. The **effective fetch** takes into account any restrictions in length or width owing to topographical features (such as banks or islands) and/or meteorological conditions (e.g. wind direction).

Fetch length: Linear extent of a ⇒ fetch.

Fetch width: Width of a ⇒ fetch.

Influence width (~, effective): The effective influence width b_E is the imaginary width in which the entire return flow field is concentrated around a vessel. It enables the maximum drawdown and return flow

velocities of vessels sailing in shallow water to be calculated for an equivalent waterway cross-section of the same width.

Manoeuvring situation: Navigation at low speed for the purposes of manoeuvring $v_S \sim 0$, i.e. at an ⇒ advance ratio of the propeller of $J \sim 0$ and maximum propeller thrust loading (for starting, stopping and turning).

Midship section, submerged: Maximum cross-sectional area submerged in the water of a vessel at rest (beam multiplied by the draught).

Plunging breaker: The velocity of approaching waves decreases close to the ground as the water becomes shallower; at the same time, the steepness of the wave front increases without any significant absorption of air. Intensive absorption of air occurs when the wave front is more or less vertical and the wave front plunges. When a plunging wave hits a bank, it breaks with substantial force, releasing a great deal of its energy, owing the compressibility of the absorbed air. This type of breaker can be observed at steep banks.

Positive surge/drawdown waves: Variations in the water level are caused by sudden changes in the flow of water owing to the operation of the waterway. They are similar to single waves in shallow water.

Primary wave (primary wave system): Consequence of the interaction between a vessel and the waterway as a result of the flow around the hull due to displacement. The lowering of the water level on either side of the vessel and the backwater at the bow and stern are part of the displacement flow. The primary wave advances with the vessel, diminishing with its distance from the sides (see Figure 2.1 and Figure 2.2).

Reflection: When waves strike a boundary surface (wall, groyne, training wall, steep bank, etc.) they are partially reflected, resulting in a loss of wave energy. The height of the reflected wave is usually lower than that of the incoming wave. Incoming waves and reflected waves are superimposed on each other.

Refraction: Change in the direction and magnitude of a wave front owing to friction on the river or canal bed caused by a change in the depth of the water in the vicinity of a bank. Applies to waves that initially travel parallel to the bank but are bent towards it, and to diverging ship-induced secondary waves. One side of the ⇒ wave crest is in shallower water than the other. As the velocity of shallow water waves diminishes with the depth of the water, the wave flank closest to the bank moves more slowly than the flank furthest away from the bank, resulting in curvature of the wave crest. Refraction causes the ⇒ wave height to diminish and is accompanied by ⇒ wave shoaling.

Return flow: Water flowing in the opposite direction to the vessel; it is caused by the displacement action of the vessel and drawdown.

Revetment: Permeable or impermeable lining of a waterway intended to prevent changes in its bed and banks.

Permeable revetments allow an unhindered exchange of water between the subsoil and the waterway. They generally comprise an armour layer placed on a filter.

Impermeable revetments prevent the exchange of water between the waterway and the subsoil. They comprise an impermeable armour layer – generally placed on a geotextile separation layer - or a permeable armour layer placed on a flexible lining – generally with a geotextile or mineral separation layer as an intermediate layer.

Running wave: When ⇒ transversal stern waves travelling along a bank break they are referred to as running waves. Running waves are particularly high when a vessel is moving at a speed approaching critical speed.

Sailing at normal speed: Navigation at a speed permitted on open stretches of canals in the Regulations for Navigation on Inland Waterways or at a technically feasible ship speed.

Sailing line: Position of the actual axis of the path of a vessel in relation to the axis of the waterway.

Secondary waves (secondary wave system): The secondary wave system is caused by two centres of pressure at the bow and the stern that ideally move in unison and generate wavelets. Unlike the ⇒ primary wave system it is a disturbance of the equilibrium that propagates away from the vessel and comprises ⇒ diverging- and ⇒ transversal waves (see Figure 2.1 and Figure 2.2).

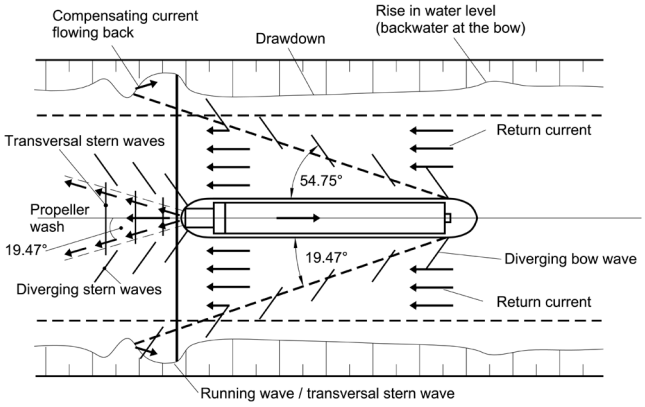

Figure 2.1 Deformation of the water surface (top view). Least favourable superimposition of primary and secondary wave systems.

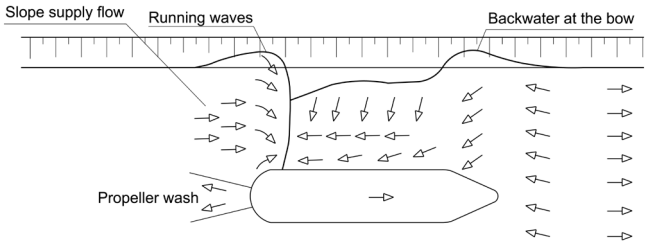

Figure 2.2 Deformation of the water surface (top view). Primary wave system and running wave at critical speed caused by a short vessel sailing close to the bank.

Shallow water: Fairway of limited depth but unconfined laterally. Unlike ⇒ deep water, shallow water affects wave movements (⇒ wave deformation). Lateral wave movements can diminish unhindered (for example, in wide, free-flowing rivers).

Shallow water starts to affect the shape of waves when the ratio of the wave length L to the mean water depth h_m is greater than 2 ($L/h_m > 2$).

Shallow water starts to affect the resistance of vessels when the ratio of the water depth h to the draught of a vessel T is equal to or less than 4 ($h/T \leq 4$). The effect is very pronounced at $h/T \leq 2$ /*Binek, Müller 1991*/.

Ship-induced waves: The moving vessel generates waves on the surface of the water owing to hydrodynamic effects.

Ship speed, critical: Speed of a ship v_{krit} in shallow water or in a canal at which the water displaced by the vessel is prevented from flowing fully in the opposite direction to the ship and past its stern at subcritical flow. The transition from subcritical to supercritical flow begins (the Froude number in the narrowest cross-section adjacent to the vessel is equal to 1). In general, displacement craft cannot exceed v_{krit}. Any attempts by displacement craft to sail faster than v_{krit}, e.g. by increasing the driving power, generally result in even higher return flow velocities and in a greater drawdown than at v_{krit}, causing the speed of the vessel over ground to diminish further and/or the vessel to be drawn towards the bed of the river or canal.

Sliding failure: Specific case of ⇒ slope failure on a sliding surface close to the surface and parallel to the slope.

Sliding speed: Speed at which a vessel (recreational craft) begins to slide and ride up on its bow wave.

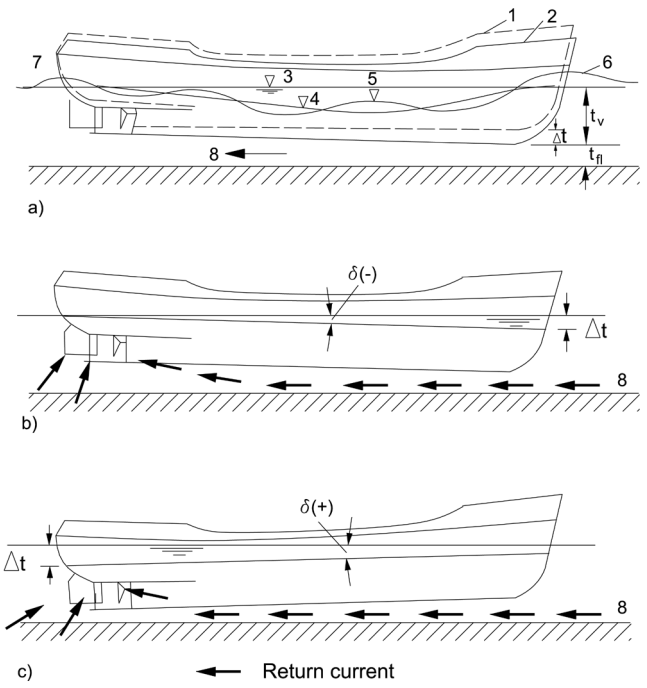

Figure 2.3 Deformation of water surface in the direction of travel, squat and direction of return flow (vector arrows) for a conventional inland navigation vessel with a full bow as described by /Kuhn 1985/

(a) Lowered water level and ship-induced waves

1 vessel at rest, 2 vessel in motion, 3 still-water level, 4 lowered water level (primary wave), 5 superimposed secondary wave,
6 backwater at the blow, 7 stern wave,
8 return flow,
Δt squat,
t_{fl} dynamic underkeel clearance,
t_v draught of vessel while sailing,

(b) δ(-) trim angle, bow-heavy

(c) δ(+) trim angle, stern-heavy

(b) and (c) without deformation of the water surface

Slope failure: Slippage of part of an embankment, generally on a deep sliding surface due to the shear resistance of the soil being exceeded.

Slope supply flow: The depression caused by drawdown at a sloping bank is refilled from astern by a ⇒ running wave.

Soil displacement, hydrodynamic: The flow of groundwater from the slope into open water due to ⇒ excess pore water pressure in the soil causes deformation of the slope (loosening of soil, heave) if the surcharge is insufficient. It can result in a deleterious displacement of particles, sometimes down the slope, once the plastic limit state has been reached (Mohr-Coulomb failure conditions) if the excess pore water pressure in the soil below the armour layer is sufficiently high.

Spilling breaker: Air is absorbed at the crest of a wave once a ⇒ critical wave steepness has been reached. A water-air mixture (spume) then develops at the front of the wave. The steepness of the front remains approximately the same as the wave crosses the surf zone. This type of breaker occurs particularly at slopes with gentle gradients.

Squat: Hydrodynamic effect produced by a vessel when sailing. Inland navigation vessels sail in the zone of the lowered water level (⇒ drawdown) and therefore drop below the still-water level (see Figure 2.3). In addition to this, local peaks in the velocity of the water flowing past the vessel caused by the curvature of the contour of the ship and its propulsion system give rise to negative pressures that pull the hull towards the bed at varying degrees at bow and stern. As a result, squat can increase or decrease and cause the vessel to float at an unwanted angle of trim (⇒ trim).

Stability, global: The resistance of the water-side slope to failure conditions in the ground in which the curved sliding surface of the sliding wedge penetrates relatively far down into the ground, i.e. to below the depth that is critical for local stability (failure surface) ⇒ critical depth.

Stability, local: The resistance of the water-side slope to failure conditions in the ground in which the sliding surface of the sliding wedge is relatively close to the surface, i.e. at the ⇒ critical depth.

Stand-by propeller test: The propeller operates at an advance ratio J equal to 0.

Superposition of waves: Waves of different origins, directions or celerities are superposed upon each other when they meet, their heights being added together if the waves are low in relation to the depth of the water.

Surging breaker: Air is absorbed once a ⇒ critical wave steepness has been reached. The wave does not plunge although the steepness of the wave front diminishes. The very extensive water-air-mix at the wave front surges up the embankment as a wall of surf. Surging breakers occur on steep slopes.

Toe protection: Lower part of a slope revetment.

(Transversal) stern waves: Type of wave at the stern of a vessel caused by the primary and the secondary wave systems, the ⇒ wave crest being perpendicular to the vessel's direction of travel. Transversal stern waves caused by primary and secondary wave systems may be superimposed on each other. ⇒ Running waves are a particular type of transversal stern wave.

Transversal waves: These form part of the ⇒ secondary wave system in which the wave crests are perpendicular to the direction of travel of the vessel.

Trim, dynamic: Additional inclination of the longitudinal axis of a vessel in relation to the horizontal caused by dynamic processes occurring while the vessel is in motion (⇒ squat).

Trim, static: A greater draught at the bow than at the stern can be chosen to ensure, for safety reasons, that the bow of the vessel (not the stern) touches the bed first at shallows in bodies of water with moving beds, e.g. rivers.

Water depth, mean: Depth of a waterway obtained by dividing the flow cross-section by the water surface width.

Some important terms relating to the hydraulic features of rivers and canals as well as to the dimensions of waterways and fairways as used in this publication are given in Figure 2.4.

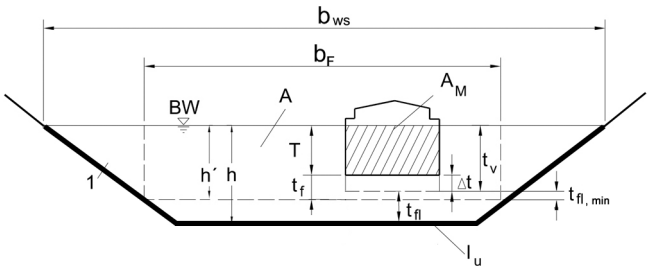

Figure 2.4 Dimension of canal and fairway according to /Kuhn 1985/
1 canal cross-section or river channel relevant to the design, b_F width of fairway, b_{WS} water surface width, h' depth of fairway, h water depth, T draught, Δt squat, t_v draught while sailing = T + Δt, t_f underkeel clearance = h' - T, t_{fl} dynamic underkeel clearance, $t_{fl,min}$ minimum dynamic underkeel clearance, A canal cross-section, A_M submerged midship section of vessel, l_u wetted perimeter of canal (without vessel), BW *operating water level*

Water depth-to-draught ratio: Ratio of the water depth h to the draught of a vessel T (h/T).

Wave crest: Peak line of a wave orthogonal to its direction of propagation.

Wave deformation: Changes occur in the wave crest and in the wave heights in particular if waves are unable to propagate unhindered (e.g. due to a change in the water depth in ⇒ shallow water, beds of rivers or canals, structures, approach angles etc.). The principal types of deformation are ⇒ wave shoaling, ⇒ breaking, ⇒ diffraction, ⇒ refraction and ⇒ reflection.

Wave height: The wave height of regular waves or specified design waves is defined as the vertical difference between a wave trough and the preceding crest, for example. The length of time between the two points is half a wave length or wave period. Statistical methods can be used to determine the design wave height of natural, irregular waves.

Wave length: Defined as the horizontal distance between two wave crests or troughs, for example, for regular waves or specified design waves. Statistical methods can be used for natural, irregular waves.

Wave run-up: Occurs when a wave, either broken or unbroken, runs up the bank for a certain distance.

Wave shoaling: Waves in ⇒ shallow water are always in contact with the bed. A reduction in the depth of the water causes a decrease in the wave celerity and the wave length as well as an increase in the wave height although the wave period remains constant. The front and back of the wave become steeper. ⇒ Refraction also occurs when waves run up a bank at an angle.

Wave steepness: Ratio of ⇒ wave height to ⇒ wave length. It is a variable geometrical wave characteristic.

Wave steepness, critical: ⇒ Wave steepness at which an incoming wave breaks (⇒ breaking of waves).

Wind set-up: Rise in the water level at the lee of a ⇒ fetch due to the shear stress between the air flow and the surface of the water during constant wind action over a relatively long period of time.

Wind waves: Waves caused by the action of the wind on the surface of the water.

3 Summary of the hydraulic actions on the banks and bottoms of rivers and canals

3.1 General

The bottoms and banks of rivers and canals are exposed to the following hydraulic actions that can occur alone or at the same time:

- currents
- waves
- drawdown
- inflow of groundwater

Currents and waves can cause erosion of the bottoms and banks of a canal or river while rapid drawdown or a considerable inflow of groundwater may result in sliding or loosening of the soil (heave).

The resistance of the bottoms and banks of rivers and canals to such hydraulic actions must be verified if any changes to the cross-section of the waterway are unacceptable. Protection methods of banks and/or bottoms must be provided if resistance (stability) is inadequate.

3.2 Currents

Only **turbulent** currents are of significance for waterways as they can cause erosion, depending on the particle size of the material present in the banks and beds. Highly turbulent currents occur, in particular, in

- the tail water of weirs
- the propeller wash
- the return flows due to shipping
- in the slope supply flow.

3.3 Waves

3.3.1 General

Waves on waterways are generated by shipping and strong winds. However, they can also be caused by the operation of weirs, locks and power stations (surge/drawdown). Ship-induced waves are divided into primary wave system and secondary waves. The primary wave system includes drawdown which occurs in the vicinity of a vessel and moves at the same speed. Secondary waves can travel a long way from the vessel and then behave in the same way as free waves. Free waves are dealt with in 3.3.2 and 3.3.3. Primary wave system is described in 3.3.4 and 3.4.

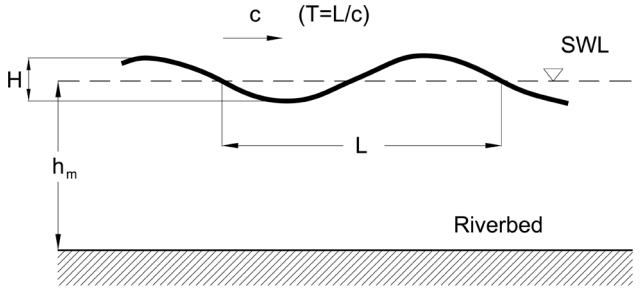

Figure 3.1 Characteristic quantities of a sinusoidal wave movement with a low wave height

The behaviour of free waves and their effect on the beds and banks of rivers and canals is not affected by the way in which the waves are generated. Free waves are identified by the following characteristic parameters (see also Figure 3.1):

- wave height (H)
- wave length (L)
- wave celerity (c)
- wave period (T)
- wave depth, mean (h_m)

As wave behaviour is influenced by a variety of factors as of a particular water depth (see 5.8 on wave deformation), it is common practice to make a distinction between deep and shallow water, depending on the ratio of the mean water depth h_m to the wave length L (see Figure 3.2).

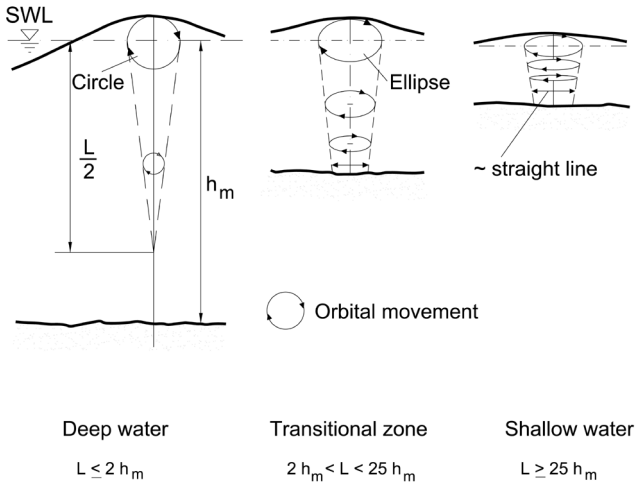

Figure 3.2 Waves zones as a function of the mean water depth ($h_m = A/b_{WS}$) and the wave length L

The celerity c in **deep water** of free waves, i.e. waves not bound to a vessel as primary and secondary wave systems are, depends on the wave length only:

$$c = \sqrt{\frac{Lg}{2\pi}} \qquad (3\text{-}1)$$

where

L is the wave length [m]

g is the acceleration due to gravity [m/s^2]

The celerity of free waves in **shallow water**, c or c_0, is determined by the mean water depth only:

$$c = c_0 = \sqrt{g\, h_m} = \sqrt{\frac{g\, A}{b_{ws}}} \qquad (3\text{-}2)$$

where

A is the flow cross section [m^2]

b_{ws} is the water surface width [m]

h_m is the mean water depth [m]

The celerity of free waves in **transitional zones** depends on the water depth and the wave length:

$$c = \left(\frac{g\, L}{2\,\pi} \tanh \frac{2\,\pi\, h_m}{L} \right)^{1/2} \qquad (3\text{-}3)$$

The celerity of ship-induced secondary waves is linked to the speed of the vessel (see 5.5.5).

In general, the following distinctions are sufficient for practical calculations according to /*Press, Schröder 1966*/*:*

Deep water: $h_m / L \geq 0.5$

Shallow water: $h_m / L < 0.5$

Accordingly, ship-induced secondary waves are generally regarded as deep water waves and the primary wave due to drawdown as shallow water wave.

3.3.2 Effect of unbroken run-up wave

Rapid hydrostatic pressure changes occur at slopes below water level when an unbroken wave passes. As the pore water pressure in the subsoil cannot keep up with such changes in pressure (see 3.4), the pore water pressure in the soil may be greater or less than the external hydrostatic pressure (i.e. caused by wave troughs and wave crests respectively), depending on the water level at any given moment. As a result, water either flows out of or into the subsoil.

The flow of pore water out of the subsoil reduces the weight of individual soil particles, which has already been diminished by buoyancy, and may cause loosening of the soil. It may promote erosion if actions due to flow occur at the same time.

In **transitional zones** and in **shallow water**, the orbital movement of a wave can give rise to a reciprocating motion in individual soil particles, causing them to shift slightly. In some cases, it may even result in armourstones being moved. A significant degree of erosion does not occur until the flow forces at the bottom of a river or canal reach a level at which the particles that have been set in motion are transported along the bed.

3.3.3 Effect of breaking run-up wave

Breaking waves are divided into three types of breaker, depending on their shape /*Pilarczyk 1990*/. These are spilling breakers, plunging breakers and surging breakers (see 5.8.2).

For waves running up slopes, the shape of the breakers depends essentially on the inclination of the slope on which the wave breaks (see Figure 5.42 and Table 5.2).

The way in which free waves and ship-induced secondary waves affect the stability of slopes is determined primarily by plunging breakers.

The plunging water and the resulting run-up and run-down caused by plunging breakers have a highly erosive effect (displacement of stones) on the slope zone concerned (zone of fluctuating water levels) owing to the flow force and high level of turbulence.

The impact of plunging breakers also generates excess pore water pressure, which may be several times the hydrostatic head of the waves, in the saturated subsoil in the zone in which water levels fluctuate. Its effect is relatively small if the waves break in a water cushion or an armour layer with a large number of cavities (e.g. rip-rap). It is also associated with a very turbulent run-up and run-down flow.

The impact of the breaker reduces the stability of the bank as the resulting excess pore water pressure in the subsoil is unable to diminish quickly enough. If several plunging breakers follow each other the excess pore water pressures are superimposed on each other, reducing the shear strength of the soil.

3.3.4 Effect of breaking waves travelling parallel to a bank

The shape of breakers caused by waves travelling parallel to a bank, such as those that occur at the stern of a vessel, depends primarily on the wave steepness and the Froude number or on the ratio of the ship speed to the critical speed. If the waves are steep and the Froude numbers are high, it is primarily the transversal stern wave (running waves or slope supply flow) that breaks. Combined with the slope supply flow, the local flow velocities occurring at the wave front may be so high that armourstones are dislodged from the revetment.

3.4 Effect of water level drawdown

3.4.1 General

Natural and man-made influences can cause the water level of a river or canal to change slowly or rapidly. To ensure the geotechnical stability of the channel it is important to establish whether the pore water in the underlying soil is able to follow the changes in the water level of the river or canal without significant excess pressures being generated.

A comparison of the drawdown rate of the water level (v_{za}) and the permeabiliy of the soil (k) can initially provide a conservative estimate of whether excess pore water pressure is being generated:

(a) slowly falling water level: $v_{za} < k$

(b) rapidly falling water level: $v_{za} \geq k$

3.4.2 Slowly falling water levels

There is always a delay in the decrease in the hydrostatic pore water pressure in the soil of the bed and banks of a river or canal when drawdown occurs as pore water can only flow out of a slope when a pressure differential exists.

If the drawdown rate is lower than the permeability of the soil of the bed and banks ($v_{za} < k$) the possible gradient is also small and the pore water pressure is only slightly above the effective free water level at any given moment. The associated flow force can be disregarded with respect to the stability of the banks and the bed of the waterway.

3.4.3 Rapidly falling water levels

3.4.3.1 General

Rapidly falling water levels cause excess pore water pressures in the soil (see 3.4.1) and can occur in conjunction with the following:

a) over large areas

- drawdown due to shipping (depending on the draught and cross-section of the waterway)
- tides
- receding flood waves (immediately after the flood peak has passed)
- impoundment (initial phase)
- positive surge/drawdown waves due to the operation of weirs, locks and power stations
- failure of embankments

b) over small areas

- bow and stern waves of sailing vessels, particularly of unladen vessels, passenger crafts and recreational crafts sailing at high speed
- wind waves

The dimensions of the rapidly falling water surface do not affect the level of excess pore water pressure.

3.4.3.2 Effect of excess pore water pressure

Excess pore water pressure in the soil occurs when the drawdown rate exceeds the rate at which the hydrostatic pore water pressure in the soil is able to adapt ($v_{za} \geq k$) (cf. Figure 3.4). Excess pore water pressure is caused by the delay in pressure equalization owing to gas bubbles that increase in size as the pressure decreases /*Köhler 1993; Köhler 1996*/.

The excess pore water pressure gives rise to seepage flow towards the ground surface (see Figure 3.3) which reduces the stability of the bank and/or bed and may result in slides or loosening of the soil.

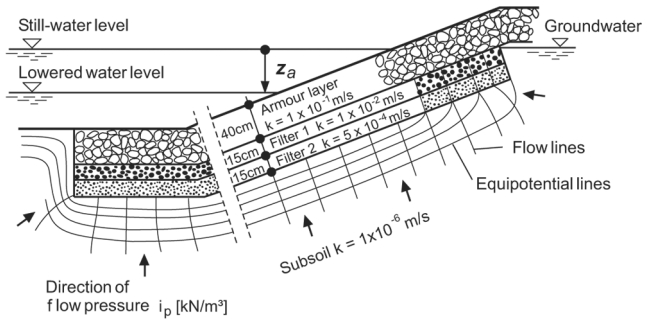

Figure 3.3 Flow lines and equipotential lines in the ground below a permeable slope revetment during rapid drawdown of the water level

3.4.3.3 Magnitude and development of excess pore water pressure

The magnitude and development of excess pore water pressure due to rapid drawdown are governed primarily by the drawdown z_a, the drawdown time t_a, the permeability of the soil k and the compressibility of the water-soil-mix (including the gas that it contains) in the zone of the banks and bed of the river or canal that is close to the surface. The last three parameters are reflected in the pore water pressure parameter b (see 5.10.3).

The excess pore water pressure Δu, which increases exponentially with the depth z, is at its highest when the maximum drawdown is reached, after which it decreases over time (see Figure 3.4).

The excess pore water pressure can reduce the effective stresses in the soil, and thus the frictional forces to such an extent that sliding failure occurs in banks (with or without a revetment) along a failure interface parallel to the slope at depth d_{krit} (Annex A).

If sliding is prevented (e.g. by means of supported or suspended revetments, on very gentle slope inclinations or at the bed of a waterway), loosening of the soil

may occur near the surface, resulting in hydrodynamic displacement of the soil.

The provision of a sufficiently heavy revetment can prevent such limit states occurring in the ground.

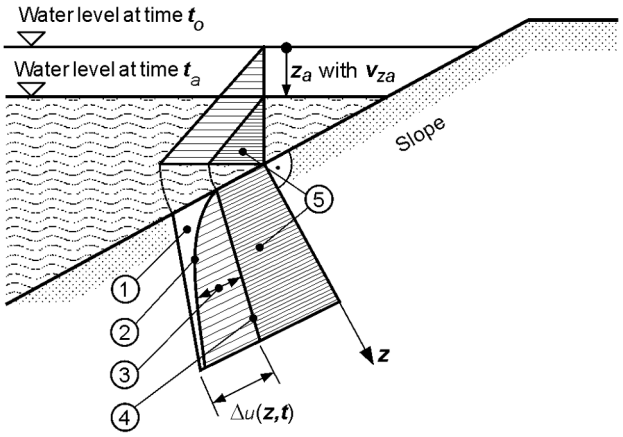

Key:
① Pore water pressure at time t_o
② Pore water pressure at time t_a
③ Excess pore water pressure Δu when $t = t_a$
④ Pore water pressure when $t = t_\infty$
⑤ Hydrostatic pressure component when $t = t_a$
z_a Drawdown
v_{za} Drawdown rate $\left(v_{za} = \frac{z_a}{t_a}\right)$
Δu Excess pore water pressure
z Depth in soil perpendicular to slope

Figure 3.4 Hydrostatic pore water pressure and excess pore water pressure during rapid drawdown

3.5 Groundwater inflow

Groundwater will flow into a river or canal if the groundwater table in the slope is higher than the still-water level, e.g. where a river flows through a cutting or after a flood. The inflow means that a higher hydrostatic water pressure acts in the subsoil of the slope, giving rise to flow forces in the direction of the river or canal. All geotechnical design calculations must take such actions into account.

If groundwater flows out of an unprotected slope, the limit state for local slope stability will be reached at a slope inclination of

$$\beta \leq \varphi'/2 \tag{3-4}$$

where

β is the slope angle [°]

φ' is the effective angle of shearing resistance of the soil [°]

Any outflow of groundwater from the surface over a fairly long period of time should therefore be avoided. A continuous grass cover will provide an adequate level of protection for slope angles β of less than $\varphi'/2$ if groundwater emerges rarely or only for short periods of time.

4 Safety and design concept

4.1 General

No distinction according to the load cases specified in /*DIN 1054*/ is made for the design of bank and bottom protection.

An appropriate extreme load constellation with a very low probability of occurrence is determined for geotechnical analyses. Unless explicitly stated otherwise, the analysis must demonstrate that the limiting equilibrium state is maintained under the relevant combination of actions. A higher safety level involving the use of partial safety factors as laid down in /*DIN 1054*/ will only be specified if verification of global stability is required (see 7.4).

The requirements regarding the probability of occurrence of the actions to be used in the design are less stringent for hydraulic analyses, the purpose of which is to determine the stone size required to provide resistance to movement on exposure to currents and wave loads, than for geotechnical analyses. This is because the displacement of individual stones – despite accumulating over time – does not jeopardize the stability of revetments or canal embankments. Hydraulic design should therefore really be based on a cost-benefit analysis in which the additional cost of providing a heavier or partially grouted revetment is compared with the cost of repairing and maintaining a lighter revetment over its lifetime instead of on the method applied here in which limit values of the loads are used. In addition to the structure of the revetment, the most important parameters as regards maintenance costs are the volume of shipping and fleet composition. The number of stones that are displaced from a revetment and move to its toe increases with the volume of traffic as passing ships subject revetments to high levels of loading.

However, such cost-benefit analyses require comprehensive and detailed data on the cost of maintaining the various types of revetment, which depends on the volume of shipping and fleet composition. Such data are not yet available.

Nevertheless, sailing tests conducted recently with various types of vessel /BAW 2002/ have been used in addition to published calculation methods and test results in order to establish an initial design approach. The sailing tests caused considerable, but quantifiable, displacement of stones in new revetments as a result of loads due to waves and currents. More systematic documentation of the level of maintenance required for revetments should be conducted in future so that, in conjunction with the test results for the actions, a broader and more reliable experience-based understanding of the problem can be developed as a basis for the design of revetments.

The design concept presented in this chapter includes the following hydraulic analyses:

- Determination of the size of stones required to withstand loads due to transversal stern waves (for ships sailing at normal speed) in accordance with 6.2
- Determination of the size of stones required to withstand loads due to propulsion-induced flow (while a ship is manoeuvring) in accordance with 6.3
- Determination of the size of stones required to withstand loads due to secondary waves in accordance with 6.4
- Determination of the size of stones required to withstand loads due to wind waves in accordance with 6.5
- Determination of the size of stones required to withstand loads due to a combination of ship-induced waves and wind waves in accordance with 6.6
- Determination of the size of stones required to withstand actions due to currents in accordance with 6.7
- Determination of the minimum thickness of the armour layer, which depends on the size of the stones as required by the hydraulic design, in accordance with 6.9, if necessary, modified as specified in 6.10
- Compliance with the minimum thicknesses of the armour layer specified in 6.11
- Determination of the length of the armour layer above and below the still-water level as specified in 6.12

The design values required for the hydrodynamic analyses, such as the height of transversal stern waves or the flow velocities caused by propeller wash near the bed of a river or canal, can either be measurement data or obtained by means of the formulae given in 5 if the appropriate measurement values are not available, e.g. in the case of forecasts.

The following geotechnical analyses are required:

- Determination of the mass per unit area of permeable armour layers in accordance with 7.2
- Determination of the mass per unit area of impermeable revetments to ensure resistance to sliding failure (7.3.2) and uplift (7.3.3)
- Global stability of the water-side slope including the revetment as specified in 7.4

The values relevant to the design are either the largest stone size required and the greatest thickness of the armour layer as determined in the various analyses or the greatest mass per unit area of the armour layer.

4.2 Hydraulic analyses

The design method discussed below applies primarily to revetments comprising non-grouted rip-rap. Some aspects of the use of partial grouting are dealt with in chapters 8 and 9.

4.2.1 Aspects of the specification of the design values

The appropriate limits for the design values must be selected when designing bank protection. The values are determined primarily by the ship chosen for design purposes, the ship speed, position in the cross-section of the river and the sailing situation (a ship sailing alone, one ship passing or overtaking another). When selecting these parameters, their probability of occurrence and any possible damage should be taken into account. Consideration must be given to the following aspects:

- **Risk of failure:** The stability of a bank can be endangered by the drawdown caused by a single vessel passing at high speed. The highest realistic ship speed (critical ship speed v_{krit} or the maximum permitted speed v_{zul}) must therefore be used in analyses of the global stability of banks. A representative maximum ship speed may be used if failure of the structure cannot be caused by single cases of damage, such as displacement of stones, but would result from the sum of such cases (permanent damage). Generally speaking, it is recommended that 97 % of the critical ship speed be used in the analysis, as specified in /*MAR*/.
- **Volume of shipping and fleet composition:** If modern vessels whose engine power enables them to reach the critical speed v_{krit} predominate in the stretch of the canal being considered and/or it can be argued that the vessels in that stretch sail at particularly high speeds the design speeds will have to be higher than if older vessels and units with less powerful engines are more common. The percentages of recreational craft, tugs and pusher craft sailing alone, including their respective engine powers and sizes, must also be taken into account when the composition of the fleet is considered. For these types of vessel, it is the sliding speed that limits the possible ship speed, and thus the wave height, rather than the critical ship speed. It will be necessary to check whether the vessel's engine power will enable it to reach this speed.
- **Traffic volume:** The rate at which permanent damage accumulates is proportional to the volume of traffic. The greater the volume of traffic, the higher the probability that the high ship speeds relevant to the design will be reached, whether intentionally or not, especially when vessels sail close to the bank, for example during evasion manoeuvres. The design ship speeds can therefore be lower for low volumes of traffic than for high volumes.
- **Size of canal cross-sections:** In narrow canal cross-sections, e.g. in those designed for one-way traffic, boatmasters have only limited scope for varying the speed of their vessels (between the nautical minimum speed and v_{krit}), with the exception of manoeuvring courses, in order to sail with ease and safety. The probability that v_{krit} will be reached is higher in such cross-sections than in wide canals as even vessels with not particularly powerful engines may also reach the critical ship speed in narrow canal cross-sections. Supercritical sailing conditions have also been observed in narrow canal cross-sections when vessels sailing at v_{krit} in the centre of the canal change course and sail towards the bank. The reason for this is that the critical ship speed is lower for vessels sailing steadily close to a bank than for those sailing in the middle of a canal. The probability of this load case occurring is lower in wide canals as vessels lose speed on approaching the (initially distant) bank.
- **Sailing situation (ships sailing alone, passing or overtaking):** Observations have shown that the greatest loads are usually caused by vessels sailing close to the bank. This applies to wide canals in particular in which ships can pass or overtake each other without having to reduce their speed considerably. Such situations must therefore also be taken into account when designing wide canals.
- **Permitted ship speeds:** The ship speeds permitted on German canals vary. They mostly depend on whether vessels are loaded or empty although usually only a draught-related limit is stated. Observations of shipping traffic have shown that vessels sometimes sail at far higher speeds than permitted if their engine power and the blockage ratio enable to do so. Conversely, modern loaded vessels are not always able to reach the permitted speeds owing to the low blockage ratio, i.e. the critical ship speed limits the possible speed. This must be taken into account when the design speed is specified.

4.2.2 Recommendations for hydraulic design

The relevant hydraulic actions on the bed and banks of rivers and canals are obtained from the parameters described below.

4.2.2.1 Primary wave field

The primary wave field comprises the following components:

- **Drawdown:** The maximum drawdown is caused by large inland cargo vessels and units sailing at their maximum draught and governs the following quantities:
  - The required minimum depth of the revetment below still-water level (see 6.12.3),
  - The dynamic underkeel clearance owing to the squat associated with drawdown of a sailing ship. As a result of that there is an increase in the impact of the propeller wash on the bed of the waterway. The impact determines the size of the stones required to protect the bed of the waterway (see 6.3),
  - The period of time during which the water level drops, thus reducing the stability of the slope. It will need to be examined on a case-to-case basis whether a shorter drawdown time, such as in the case of vessels sailing at high speed where the drawdown at the bow is less than at the stern, results in less favourable design values than a longer drawdown time. The latter occurs between the bow and the stern and is associated with a greater drawdown at the stern (see 5.5.4.7).
- **Transversal stern wave:** When vessels approach critical speed the transversal stern wave (see 5.5.4.4) may break and form a running wave (like a moving hydraulic jump), especially if the vessel is sailing close to the bank in which case the wave length will decrease and the wave steepness, and thus the wave height, will increase. It is the running waves that are usually responsible for the displacement of stones in bank revetments. Very high transversal stern waves occur in the following situations in particular:
  - eccentric paths, in particular those close to the banks;
  - empty vessels, which usually exhibit a stern-heavy dynamic trim and vessels that are statically trimmed by the stern (i.e. sailing with ballast);
  - pusher craft, tugs and recreational craft sailing alone that generate large diverging waves at the bow (which may be blunt) that may be superimposed on the transversal stern wave (see 5.5.5.1 Distance case B and 5.5.5.2);
  - vessels travelling close to the critical ship speed which will usually have a stern-heavy dynamic trim, increasing the drawdown and thus the height of the stern wave (see 5.5.4.4). Additional transversal stern waves similar to the rippling flow of an imperfect hydraulic jump may also occur (see 5.5.5.3);
  - recreational craft designed for planing but which displace water when accelerating to sliding speed, in which case the transversal waves of the bow and stern wave systems are superimposed (see 5.5.5.1 Distance case C and 5.5.5.4).

  The required stone size (see 6.2) is determined by the pressure gradients and flow velocities caused by the orbital movement and the plunging water of the broken wave that also occur at banks. The height of the bank revetment (see 5.8.6.2) is determined by the height of the waves above the still-water level – which is much greater than the wave trough owing to the asymmetrical shape of such waves – even if the waves stay mainly parallel to the bank, i.e. where there is little wave run-up due to refraction.

  In the case of vessels with a considerable static trim, the greatest degree of drawdown may occur at the bow as opposed to the stern. The transversal stern wave may also break under such sailing conditions. The exposure of banks to this type of loading is not dealt with here.
- **Slope supply flow:** Running waves close to a bank are usually accompanied by a current flowing parallel to the bank that refills the depression caused by drawdown from astern. In limiting cases, the slope supply flow velocity u_{max} may even reach the same speed as the vessel (see 5.5.4.5). This occurs when the momentum of high transversal stern waves causes the wave celerity to increase to such an extent that the wave threatens to overtake the vessel. However, the fact that the wave system is bound to the vessel prevents this from happening and the wave breaks. This effect is most pronounced in narrow canal cross-sections and when vessels sail close to a bank at a speed approaching the critical ship speed. The higher speeds at which empty vessels or tugs may sail means that this case may be relevant to the design despite the fact that the ratio of u_{max} to v_s is lower than for vessels sailing at their maximum draught (see 6.7.2).
- **Return flow:** The mean return flow velocity increases with the ship speed, the displacement by the vessel and the reciprocal value of the effective cross-sectional area. The local return flow in the vicinity of the bed and bank will exceed the mean value, especially at the bilge at the bow or, more generally, at all pronounced curvatures of the contour of traditional inland navigation vessels as the vessel approaches the bottom or the banks.

Significant local lowering of the water level may occur at these points, resulting in a further increase in the return flow velocity owing to the narrowing of the flow cross-section. This effect is most noticeable between the ship's side and a sloping bank when a vessel sails close to the bank (see 5.5.4.4). It must be established which of the following load cases give rise to the highest return flow velocities:

- Vessels at their maximum draught sailing along the centre of a fairway where higher ship speeds are possible, resulting, in conjunction with the greater displacement, in high return flow velocities,
- Vessels at their maximum draught sailing close to the bank where, although the ship speed tends to be lower, the narrowing effect results in an increase in the return flow velocity at the bank,
- Empty vessels sailing at high speed close to the bank where the higher ship speed, together with the greater draught of such vessels at the stern, may be more significant than the displacement effect of an empty vessel which is less pronounced than for a vessel at its maximum draught.

The influence of an eccentric sailing line on the distribution of the return flow velocities and thus their local maximum values is small compared with that of the wave height.

Generally speaking, the return flow in narrow canals, e.g. those designed for one-way traffic, influences the size of the stones required for a slope revetment to a greater extent than waves. In the case of wide canals, it is usually the height of the transversal stern wave that is relevant to the design.

The hydraulic parameters described above are determined by means of the one-dimensional canal theory (see 5.5.3) which is based on the following important simplifications:

- a constant return flow velocity over the canal cross-section,
- a constant drawdown over the length of the vessel,
- the drawdown corresponds to the squat (the draught at the bow and at the stern is the same),
- frictionless flow.

The one-dimensional canal theory provides the correlation between the mean drawdown, the mean return flow velocity and the ship speed. It also provides a reference value for the critical ship speed.

Owing to the simplifications listed above, corrections are required to take the following influences into account:

- Shallow water conditions in wide canals or vessels that are short in relation to the canal: an equivalent canal cross-section and approximation equations are used to modify the height of the wave between the vessel and the bank (see 5.5.1),
- The inclination of the water surface between bow and stern and the shape of the vessel: the mean drawdown and mean return flow velocity are increased to enable the maximum values at the bank closer to the vessel to be estimated (see 5.5.4.2 to 5.5.4.4),
- Eccentric sailing line: a smaller equivalent canal cross-section is used to take account of the possible ship speed and the mean drawdown and mean return flow,
- Vessel shape and dynamic trim: the mean values of the hydraulic parameters are increased (see 5.5.4.3 and 5.5.4.4),
- Flow supply flow rate: stated as a function of the ship speed and wave height (see 5.5.4.5).

4.2.2.2 Secondary wave field

The waves generated by the discontinuities and pronounced curvature of the ship's contours are divided into diverging waves and transversal waves. They originate primarily at the bow and stern and give rise to interferences that diverge at stern along a line at an angle. It is at these interferences where the highest waves occur. The diverging wave system is focused on a narrow strip along the line. For energy-related reasons it diminishes exponentially at –1/3 with its distance from the vessel. Transversal waves diminish more rapidly, i.e. at a power of –1/2, in the direction of the bank. Therefore, the highest waves at the bank are generally caused by the diverging wave systems when vessels sail far from the bank and by the transversal wave systems when vessels sail close to the bank (see 5.5.5).

Generally speaking, it is the distance of a ship from the bank at which the interferences generated result in the highest waves locally at the bank that is relevant to the design. Thus, the sailing line closest to the bank needs not necessarily to result in the highest waves in spite of the fact that the wave height diminishes least at the bank. This must be checked on a case-to-case basis (see 5.5.5.1).

The secondary wave system determines

- the wave run-up and thus the maximum height of the slope revetment (see 6.12.2), the largest waves being caused by vessels with a blunt bow form sailing at high speeds and by pusher craft, tugs or recreational craft with powerful engines sailing alone; and
- the size of the stones required to prevent erosion due to the impact of waves (see 6.4).

Furthermore, secondary waves generated at the bows of short vessels and transversal stern waves may be superimposed (see case B in 5.5.5.1). Large stern waves are caused by recreational craft designed for high speeds, and thus for planing, when the craft reach sliding speed. Long deep-going recreational craft produce the largest stern waves (see 5.5.5.2 and 5.5.5.4). It will have to be checked on a case-to-case basis whether such waves need to be taken into consideration in the design and whether speed limits need to be set and effective speed controls enforced. The equations for the wave heights provided in this publication can also be used to estimate which ship speeds should be permitted in order to minimise the damage caused by waves.

4.2.2.3 Propeller wash

The weight of the stones forming a bed revetment and, in certain cases, an embankment is determined by the propulsion-induced flow velocities (see 6.3). The flow velocities near the bed are greatest for

- ship's propellers with large diameters and high design pitch ratios,
- ship's propellers designed for high rotational speeds or high performance,
- unducted propellers with middle rudders located behind them owing to the division of the jet caused by the angular momentum,
- if propagation of the propeller wash is limited, e.g. in the vicinity of a quay wall, and for
- small dynamic underkeel clearances (see 5.6.3).

Generally speaking, the load case of relevance to the design will be a vessel remaining in a certain position or starting off, which makes full use of its installed engine power when manoeuvring to leave a mooring, for instance. Moving vessels generate lower impacts.

The main propulsion of a vessel causes significant loads on the bank when the main rudder directs the propeller jet towards the bank, for instance when the vessel is leaving a mooring. It can also subject banks to high levels of loading when a vessel is manoeuvring in order to turn.

If directed towards a bank, the jet produced by an active bow rudder when a vessel is leaving a mooring can cause local scour and hence a great deal of damage to unanchored revetments (see 5.6.5 and 6.3.2). Any revetment design that includes the loads produced by bow thrusters may result in over-dimensioning when compared to a design that only covers the other loads. It will need to be considered whether such damage should be repaired during maintenance work or if it is advisable to anchor the revetments in the affected areas.

4.2.2.4 Wind waves

In comparison with ship-induced waves, wind-induced waves may be relevant to revetment design if a canal is wide and the fairway is far from the bank (see 5.7, 5.8 and 6.5). The relevant equations are therefore dealt with in this bulletin. In many cases it will also be important to consider the comparative sizes of wind-induced and ship-induced waves.

4.2.2.5 Recommendations for hydraulic design in standard cases

Based on present-day (as at 2003) fleet on German inland waterways and experience with constructed revetments, designs that take account of the following loads due to shipping will provide embankments with sufficient resistance to erosion and adequate stability, although a certain minimum amount of maintenance is assumed:

Vessels sailing alone and close to the bank (vessels sailing over the toe of the slope or edge of the fairway less the safety margin), i.e.

- large loaded inland cargo vessels (return flow, running waves and slope supply flow determine the size of the stones; drawdown and drawdown time define the thickness of the revetment and the required depth of anchoring below still-water level) and
- large inland cargo vessels that are empty or are stern-heavy owing to ballast (running waves and slope supply flow at the slope determine the size of the stones and the height of secondary waves the required height of the bank revetment above still-water level) and
- large inland cargo vessels that are capable of reaching the critical ship speed owing to their engine power.

The erosion resistance of bank and bottom protection exposed to the propeller wash of ships is determined by a vessel with a powerful engine, a large propeller diameter and a small dynamic underkeel clearance after casting off (i.e. remaining in a given position in the relevant design situation for a short time only). Loads exerted on banks by bow thrusters will need to be taken into account at moorings. The damage can be minimised by anchoring the stones.

The loads on revetments and wave run-up heights caused by pushers and recreational craft sailing alone will need to be taken into account if they occur frequently or if it is not possible to limit them by supporting measures, such as speed restrictions.

All other types of damage must be dealt with during maintenance work.

4.3 Geotechnical verifications

The purpose of the geotechnical verifications is to determine the mass per unit area of the revetment or the armour layer.

- The most unfavourable combination of bank geometry and water level must be established for each analysis as it will determine the design water level. The upper operating water level BW_o (resulting in the greatest slope length under water L_u) will apply to analyses in accordance with 7.2 for banks with unchanging geometry of canals while the greatest potential difference between the groundwater level and canal water level will apply in all other cases.
- Unscheduled emptying of a canal due to damage needs not be taken into account in the design of the bank revetment. However, any damage to adjacent property caused by failure of the slope revetment must be ruled out.
- If a canal section is emptied as scheduled, the slope revetment can be designed for the combination of actions occurring at that time. Structural measures (such as ponding) may be taken into account.
- Geotechnical design does not take into account actions due to currents.
- The drawdown due to wind set-up is taken into account by the water level BW_u in canals.
- The maximum difference between the lowered water level and the groundwater level occurring at the slope must be included in the design to take account of the drawdown due to tidal fluctuations, the operation of locks or other relatively slow changes in the water level.
- The maximum possible drawdown over the toe of the slope caused by a vessel passing at the selected design ship speed must to be taken into account if conditions are such that the design ship speed may be reached.
- The design drawdown due to pure wind waves is to be taken as a quarter of the wave height and considered as a steady state for design purposes.
- Secondary waves due to drawdown of the ship need not be taken into account.
- The design rapid drawdown due to long waves, e.g. drawdown waves (wave length $L > 20$ m) is half the wave height H and is to be considered as a steady state for design purposes.
- The following equations are to be used to calculate the drawdown rate and drawdown time of wind waves or ship-induced secondary waves:

$$v_{za} = \pi \, H/T \tag{4-1}$$

$$t_a = T/2 \tag{4-2}$$

where

H is the wave height [m]

t_a is the drawdown time [s]

T is the wave period [s]

- The design groundwater level is the maximum possible groundwater level (e.g. as established by measurements taken over many years). A safety margin may be added in certain cases if insufficient experience is available.
- Imposed loads shall be taken into account as area loads of 10 kN/m^2 as from the slope edge. The most unfavourable load position shall be used if it is not possible to position the load directly on the slope edge owing to structural measures.
- The various stages of construction need only be taken into account if they give rise to even more unfavourable combinations of actions.

The design soil resistance shall be the characteristic soil resistance without a safety factor as the probability of a limit state occurring is considered to be sufficiently low. However, partial safety factors as specified in /*DIN 1054*/ must be applied in analyses of the global stability in accordance with /*DIN 4084*/. The characteristic value selected should be on the "conservative side" of the mean value, as stated in /*DIN 4020*/. The difference between the characteristic value and the mean value may be small if the data pool is large enough; however, it must be large if insufficient data are available.

The angle of shearing resistance required to ensure the appropriate shear strength of armour or cover layers may, without further verification, be taken as $\varphi_D' = 55°$ (cohesion $c' = 0$) for loose armourstones of classes II to IV in accordance with the 1997 edition of /*TLW*/ or classes $CP_{90/250}$, $LMB_{5/40}$, $LMB_{10/60}$ to $LMB_{40/200}$ in accordance with the 2003 edition of /*TLW*/ and as $\varphi_D' = 70$ ($c' = 0$) for partially grouted cover layers.

5 Determination of the hydraulic actions

The procedures described in chapter 5 are not required if the hydraulic characteristics needed to determine the size of the stones and the thickness of the revetment have been obtained from measurement data for each of the relevant design situations. Measurement data are preferable to calculated values as the latter are subject to the following limitations:

(1) Generally speaking, they are obtained by calculation methods that are based on assumptions regarding the relevant physical processes, that work with simplified fundamental equations and use simplified geometrical data for the boundary conditions (for instance, the flow field around a moving vessel is approximated as one-dimensional in an equivalent canal cross-section).

(2) Any necessary empirical corrections to the design approaches based on the simplifications, such as those taking account of wave shoaling when vessels sail close to a bank, only apply to the cases for which measurement data are available.

(3) Experience is not available on the applicability of all of the methods described here to the individual design situation (e.g. for the wave heights caused by recreational craft).

It is for this reason that partially more than one equation, e.g. for the wave height, will be offered to the user, that may deliver equally plausible results. They also can be used to illustrate different aspects of design, e.g. the influence of the slope inclination or wave steepness on the stability of individual revetments. It is the responsibility of the project engineer to select the appropriate design parameters by comparing the results of calculations based on equally feasible methods.

As regards the accuracy of the calculation methods it should be noted that the loads resulting from the primary wave field can be determined more accurately than those arising from the secondary wave field, the slope supply flow and wind waves. Particularly it is very difficult to determine the loads due to the propulsion units of ships as the latter depend largely on the ship design and it is not possible to deal with each special case.

5.1 General

The following design parameters are required for the design of revetments as described in chapters 6 und 7 below to resist possible hydraulic actions on the bottom and banks of rivers and canals:

a) for hydraulic design (chapter 6)

- maximum wave height
- maximum flow velocity

b) for geotechnical design (chapter 7)

- maximum drawdown velocity
- maximum rapid drawdown or excess pore water pressure in the soil

The values of these parameters can be determined either by measurements or by calculation.

Calculation methods are specified below along with a guide on how to determine the values of the following hydraulic actions and the reactions of the soil:

- wave height (wind, shipping)
- return flows of vessels
- propeller wash
- rapid drawdown due to shipping
- rapid drawdown due to the operation of weirs, locks or power stations
- rapid drawdown in conjunction with a receding flood wave
- value of the excess pore water pressure in the soil when rapid drawdown occurs

Furthermore, certain input parameters for the waterway and shipping as well as meteorological data are required for the design. Guidance on how to determine such parameters is also given below.

5.2 Data on waterways

5.2.1 Geometry of waterways

The geometry of the river or canal affects both the natural and the ship-induced hydraulic actions. Therefore, the dimensions, shape and course of the waterway in the reach or section considered must be known in order to perform a stability analysis.

Actual profiles must be used for rivers. The “Guidelines for Standard Cross-sections of Shipping Canals” /*BMV 1994*/ apply to the cross-sections of canals.

5.2.2 Geometry of fairways

Minimum **fairway widths** are specified in the “Guidelines for Standard Cross-sections of Shipping Canals” /*BMV 1994*/.

The **fairway depth** depends on the waterway class stated in the CEMT Classification of European Inland Waterways /*BMV 1996*/.

The fairway must be known and the positions of the design ship must be selected in a meaningful way to enable the ship-induced hydraulic actions on the banks and bottom of rivers and canals to be determined.

5.3 Data on vessels

The length, width, draught, installed engine power and propeller diameter of the design ship are important input data for the determination of the hydraulic actions on the bed and banks of rivers and canals. The upper limits that apply to common classes of waterways are laid down in /*BMV 1996*/. Data for powered coastal vessels, pushed lighters and push tow units are included in /*EAU 1996*/. The values for large inland cargo vessels are specified in Figure 5.1.

The different types of pushed barge trains sailing on the section of waterway under consideration need to be taken into account when specifying the dimensions of the design ship. Large inland cargo vessels may also operate as composite units.

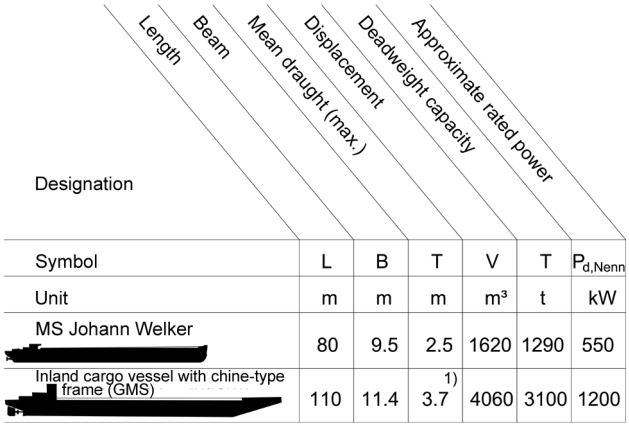

Figure 5.1 Examples of common types of inland cargo vessel according to /Kuhn 1985/; [1] a value of 2.8 m only is permitted on canals in Western Germany

Propeller wash is not generally a relevant action for bank and bottom protection when a ship sails at normal speed. However, revetments may be damaged by the wash caused by the main propulsion unit or by bow thrusters when a vessel is manoeuvring (e.g. while mooring, casting off, turning, etc.). The diameter and rotation rate of the propellers, the number of propellers and the thrust coefficient of the propeller and/or bow thruster or, alternatively, the propeller diameter and the propulsion power of the types of vessel under consideration need to be known for designs taking account of such actions. Guide values are given in Table 5.1.

Table 5.1 Technical data for inland navigation vessels in use today (Guide values; it will be necessary to obtain data for inland navigation vessels to be used in future)

Type of vessel	Length/ beam/ max. draught *L/B/T* [m/m/m]	Propeller diameter *D* [m]	Approx. rated power $P_{d,Nenn}$ [kW]	Rated propeller rotation rate n_{Nenn} [1/min]
Inland cargo vessels				
Large powered Rhine vessel GMS	95-110/ 11.4/ 2.5-2.8	1.70	1200	310 - 400
Europe ship ES (Johann Welker)	80-85/ 9.5/ 2.5	1.70	550	250 - 310
Gustav Koenigs	67-80/ 8.2/ 2.5	1.50	375	270 - 340
Kempenaar	50-55/ 6.6/ 2.5	1.30	≈ 200	290 - 370
Peniche	38.5/ 5.05/ 1.8-2.2	1.10	150	330 - 420
Pusher craft and tugs				
Small pusher craft 1 or 2 propellers	Details to be obtained from the ship-builder or shipping company.	1.50	375 or 750	270 - 340
Long-distance pusher craft, small, 2 propellers		1.70	750-1500	280 - 350
Long-distance pusher craft, large, 2 propellers, 3 propellers		1.85	2 x 750 = 1500 3 x 875 = 2625	240 - 300 250 - 320
Large pusher craft (Lower Rhine) 2 propellers 3 propellers		2.10	2 x 1313 = 2625 3 x 1500 = 4500	240 - 300 250 - 310
Tugs	31/5/2.20	1.50	290	-
Lighters				
Europe II	76.5/ 11.4/ 2.5			
Europe I	70/ 9.5/ 2.5			

Type of vessel	Installed power P_{Bug} [kW]	Propeller diameter D [m]
Bow thrusters		
Large inland cargo vessel, Lighter (GMS)	150-200	1.10
Europe ship (ES)	≈150	0.80

If no exact data are available for the design ship, propeller rotation rates n between 300 [1/min] (large propeller diameter) and 500 [1/min] (small propeller diameter] can be used for inland navigation vessels. The relevant rotation rates will have to be obtained for pusher craft. The rated rotation rates given in Table 5.1 are approximate values and may be exceeded by up to 20% in certain cases. The lower limits apply to ducted propellers.

Bow thrusters are generally installed such that they are flush with the bottom of the ship hull. Special forms such as pump jets must also be considered. The jet is discharged at a speed of up to 14 m/s and strikes the bed at an angle of between 8° and 17°.

5.4 Hydraulic actions due to shipping

5.4.1 Components

The hydraulic actions on the bed and banks of a river or canal due to shipping are caused by

- drawdown,
- ship-induced waves (primary and secondary wave systems),
- return flow (flow due to displacement) and
- propeller wash (flow due to propulsion).

These factors, which usually act simultaneously, affect the bed and banks in different ways depending on the way in which the fairway is restricted (laterally unrestricted shallow water or canal) and the range of ship speeds (subcritical, critical or supercritical) (see 4.2.2).

5.4.2 Sailing situations

A distinction must be drawn between the two situations described below for design purposes.

5.4.2.1 Sailing at normal speed

The vessel sails at the permitted speed. For example, the following speeds, which depend on the ship's draught, apply on canals (DEK, RHK, WDK, etc.) (see Section § 15.04 of the German Code for Inland Navigation Waterways (Binnenschifffahrtsstraßenordnung BinSchiStrO)).

$T < 1.3$ m $\quad v_{zul} = 12$ km/h

$T > 1.3$ m $\quad v_{zul} = 10$ km/h

v_{zul} is lower for small canal cross-sections.

The ship may sail along the centre of the canal or its sailing line may be eccentric. In theory, the highest critical ship speeds are associated with sailing lines along the centre of a river or canal and with shallow draughts. The critical ship speed tends to decrease with an increase in the draught and/or if the sailing line becomes more eccentric (e.g. closer to one of the banks). The following must be considered with regard to the effect of eccentricity:

(1) The effect of eccentricity, which would result in a reduction of the possible ship speed during a steady course, is disregarded below in order to take account of the unsteady sailing situation in a canal in which a vessel approaching a bank maintains the higher ship speed possible in the centre of the canal.

(2) By contrast, the much greater influence of the eccentricity of the sailing line or of the proximity to the bank on the critical ship speed is taken in account in shallow water conditions.

(3) The influence of eccentricity on the drawdown and wave height at the slope must always be taken into account, not only for vessels sailing on canals but also where shallow water effects occur.

The draught and bank distance must therefore be regarded as parameters of fundamental importance when specifying design situations.

Vessels sailing alone usually travel either along the centre of the waterway or eccentrically at the edge of a single lane along the canal axis (see Figure 5.2 a/b). As a general rule, a value of 0.97 v_{krit} is recommended for the design ship speed of vessels sailing in the centre of a waterway. When a vessel is preparing to pass or overtake, it can also sail along the outer edge of the double lane specified in the Guidelines for Standard Canal Cross-sections /*BMV 1994*/ (see Figure 5.2 c). The ship's bilge in the midship section will then lie over the toe of the slope. Given a draught of 2.8 m, a squat of 0.5 m and a minimum dynamic underkeel clearance of 0.2 m, a lateral clearance of 1.5 m between the vessel and the bank will be required in accordance with the aforementioned guidelines. This value can also be used for other canal cross-sections in order to specify the position of the vessel when it is sailing close to a bank. The ship speed stated above should also be assumed for eccentric sailing positions when a vessel is sailing alone.

The special cases involving vessels passing or overtaking each other are dealt with in 5.5.6.

The shallowest draught that can be considered in the methods described in this chapter is approx. one third of the water depth.

a) Europe ship (ES) sailing in the centre of the lane, without a drift angle

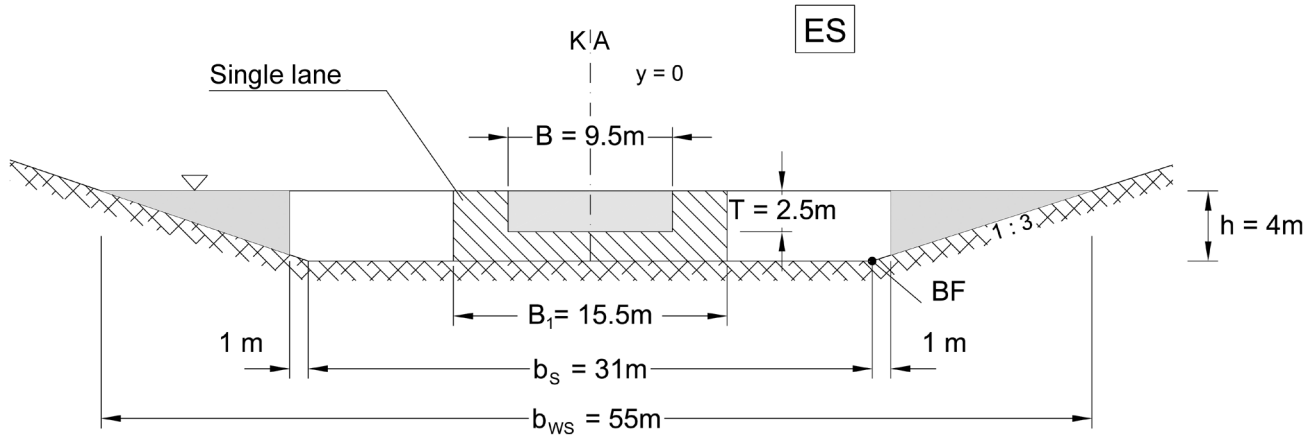

b) Europe ship (ES) sailing on an eccentric course over the edge of the single lane (B_1 = 15.5 m), without a drift angle

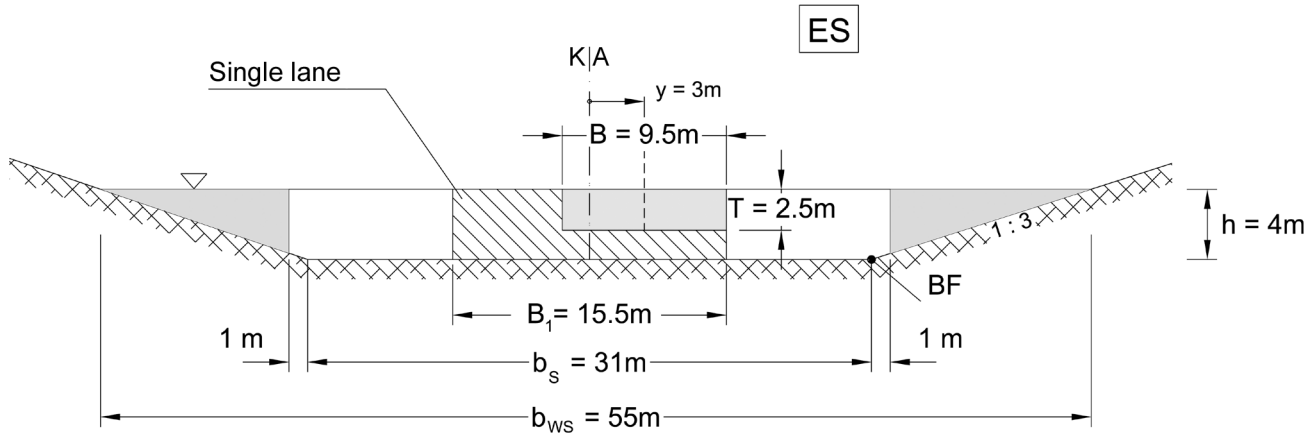

c) Large inland cargo vessel (GMS) sailing on an eccentric course, at the outer edge of the double lane, without a drift angle

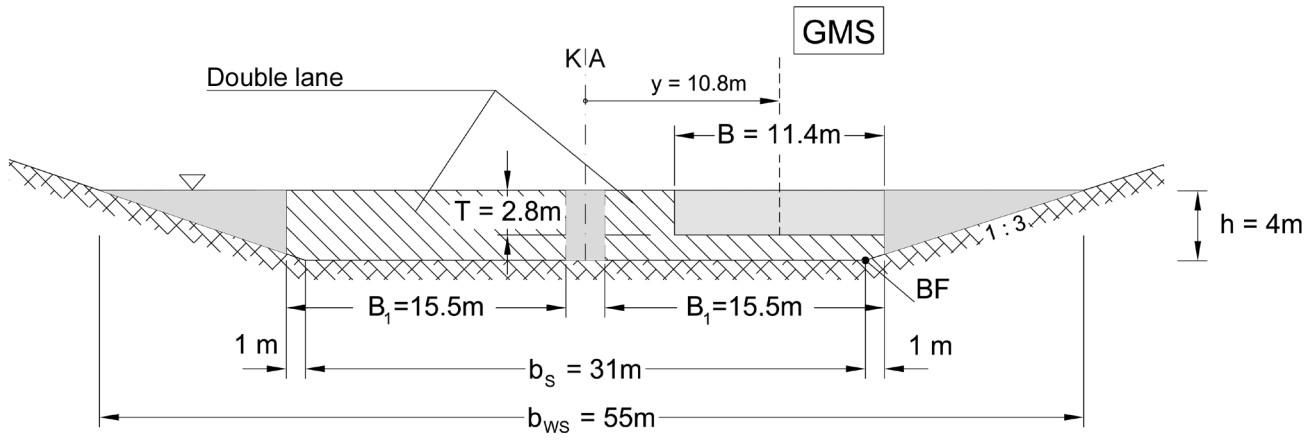

Figure 5.2 Examples of positions of a Europe ship (ES) and of a large inland cargo vessel (GMS) in a standard trapezoidal profile

Abbreviations: KA – *canal axis* BF – *toe of slope*
Symbols: B – *beam of a vessel* b_{WS} – *width at water level*
B_1 – *width of single lane* h – *depth of water*
b_S – *width of bed of waterway* T – *draught of vessel*

The relevant hydraulic actions on the bed and banks of a waterway or on the slope and bank revetment that result from the above sailing conditions are as follows:

- drawdown due to the ship-induced primary wave system and
- wave run-up and run-off at the banks due to the ship-induced secondary wave system.

Other hydraulic actions are

- return flow and
- propeller wash (which decreases as the advance ratio of the propeller increases, i.e. it diminishes as the ship speed increases).

5.4.2.2 Manoeuvring

Ships manoeuvre at low speed, $v_s \cong 0$ (propeller advance ratio $J = 0$) and with maximum propeller thrust in the following situations:

- mooring and casting off,
- acceleration phase when a vessel sails out of a lock (situation similar to stand-by propeller test).

The relevant hydraulic action on the bed and banks of a canal or river or on the slope and bank revetment results from

- the propeller wash that is caused by the main and bow thrusters and strikes the slope and bed.

5.5 Magnitude of ship-induced waves (design situation: "sailing at normal speed")

The primary wave field around a moving vessel is unevenly distributed. When the vessel is sailing in shallow water, the greatest return flow velocity occurs directly at the vessel and rapidly diminishes with the distance from it. This effect does not occur at the bank nearest the vessel when the latter is sailing close to a bank and the water is shallow. In this case, the drawdown and return flow velocity at the bank may even exceed those in the vicinity of the vessel. The return flow and drawdown caused by ships sailing on canals are distributed more or less uniformly.

The lack of uniformity of the return flow field is taken into consideration in the calculations by assuming that the entire return flow is concentrated in the influence width b_E, i.e. occurs in an equivalent canal cross-section, with the same values of the return current speed as in the vicinity of the vessel. This enables the one-dimensional canal theory to be applied. The theory provides the drawdown and return flow velocity in the vicinity of the vessel and thus the critical ship speed.

Approximation equations are included in 5.5.1.1 to enable the cross-sectional area of the equivalent canal cross-section to be determined as a function of the relevant influence parameters, which are the length of the vessel, the width of the canal and the distance of the vessel from the bank. The approximation equations are based on the 2D potential theory for vessels /BAW 2002/.

Approximation equations for the ratio of the drawdown at the bank to that at the vessel are also included in 5.5.1.1 on the basis of the same theory. The ratio is taken into account when specifying the hydraulically equivalent slope inclination of the equivalent canal cross-section, which is approximated to a trapezoidal profile. This enables the mean water depth of the equivalent canal cross-section to be calculated. The effective cross-section of the vessel required for the application of the 1D canal theory is determined in 5.5.1.2, taking account of the draughts at the bow and stern and the displacement effect of the boundary layer.

These data are used in 5.5.2 to calculate the critical ship speed upon which the choice of design ship speed is based. The latter is generally specified as a percentage of the critical ship speed. The mean drawdown and mean return flow velocity at the design ship speed in the equivalent canal cross-section are determined in 5.5.3. They are subsequently used to calculate the values at the bank, using the approximation equations given in 5.5.1.1. The drawdown and return flow velocity are corrected in 5.5.4.3 to take account of the effects of the difference in the water levels between the bow and stern and the dynamic trim. This is necessary as the 1D canal theory does not take into account the potential flow due to the difference in the water levels at the bow and stern.

The continuity equation is used to calculate the maximum return flow velocity at the bank from the maximum local drawdown obtained above. Finally, the design wave heights at the bow and stern are determined (see 5.5.4.4). In doing so, the influence of the wave steepness and shoaling effects have to be taken into account. This can be done by applying an empirical equation for the effect of the eccentricity of the sailing line /*PIANC 1987a*/.

The diagram in Figure 5.3 illustrates the entire procedure described here.

Further aspects of the primary wave field are examined below in sections 5.5.4.5 to 5.5.4.7. These are the slope supply flow, influence of the drift angle and drawdown velocity. Finally, section 5.5.5 deals with secondary waves which generally occur independently of the primary wave field and can therefore be considered separately.

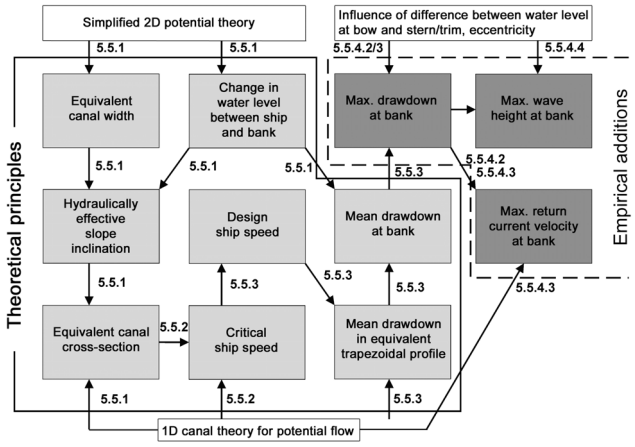

Figure 5.3 Procedure for determining the hydraulic design parameters such as the maximum return flow velocity and maximum wave heights due to the primary wave field of ships sailing in shallow water when subject to shallow water and boundary layer effects, including the relevant sections of this publication

Particular hydraulic actions on canal linings such as propeller wash, wind waves and other types of wave (positive surge/drawdown waves, flood waves) are considered in sections 5.6 to 5.9. Finally, the excess pore water pressures required for the geotechnical analyses are determined in section 5.10.

5.5.1 Hydraulic effective cross-section of canals and ships

5.5.1.1 Influence of shallow water

The partial waterway cross-section that governs the drawdown and return flows and determines the equivalent canal cross-section depends on the calculated width of the waterway

$$b_r = A/h \qquad (5\text{-}1)$$

(where

A flow cross-section [m²] not modified

h water depth [m] (see Figure 5.4))

in accordance with Figure 5.4, the effective influence width of the return flow field (b_E) and the position of the vessel (eccentricity) within the cross-section of the waterway. As a result, there are three width cases, which are illustrated in Figure 5.4. The differences between the width cases and the associated design principles apply to ratios of water depth h to draught T where $1.25 \leq h/T \leq 5$ /*Kreibel 2003*/ and ratios of ship's length L to beam B where $L/B \geq 5$.

A sketch showing the dimensions of the cross-section, influence width and position of the vessel is recommended in practice to enable the correct case to be established.

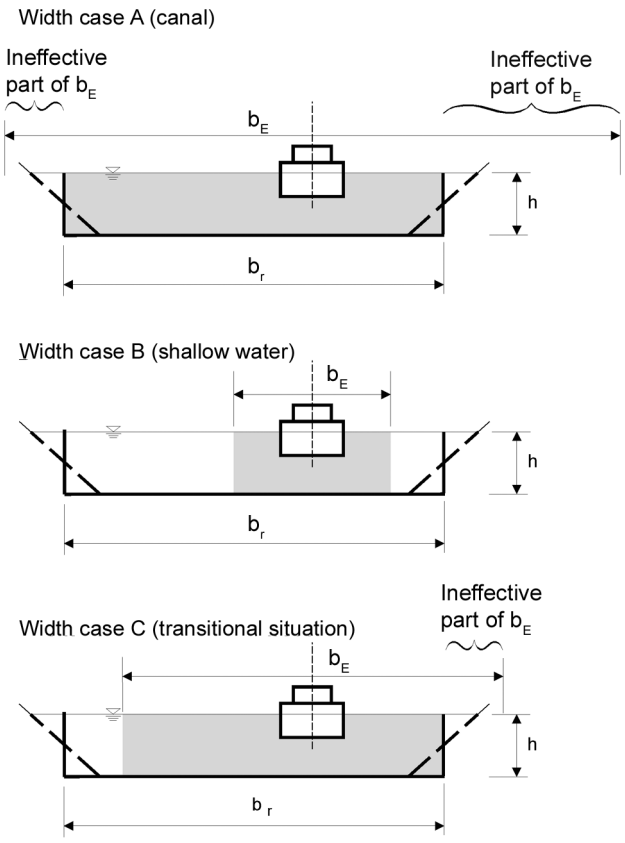

Figure 5.4 Basic cases for the ratio of the influence width b_E of the return flow field to the average width b_r of the waterway (approximative rectangular profile of the same cross-section and the same water depth):
A: canal: $b_E > b_r$
B: shallow water: $b_E < b_r$
C: transitional situation: b_E includes one bank

Width case A: "Canal"
Long vessels, narrow canals

The return flow acts over the entire width of the canal when a ships' hull is long in relation to the canal width. A canal cross-section with the dimensions

b_{WS} width of the canal at water level [m]

h depth of water [m]

m slope inclination [-], corresponding to the cotangent of the slope angle β ($\tan \beta = 1/m$)

can be used without modification for the following calculations based on the 1D canal theory:

$$A_{K,äqui} = A_K \qquad (5\text{-}2)$$

$$A_{S,äqui} = A_{S,eff} \qquad (5\text{-}3)$$

$$m_{K,äqui} = m \qquad (5\text{-}4)$$

where

A_K is the canal cross-section [m²],
$A_K = h\,(b_{WS} - m\,h) > u b_r$

$A_{K,äqui}$ is the equivalent canal cross-section [m²]

$A_{S,äqui}$ is the equivalent cross-sectional area of the ship [m²]

$A_{S,eff}$ is the effective cross-sectional area of the ship [m²], taking into account boundary layer effects and the drift angle, where appropriate

$m_{K,äqui}$ is the equivalent slope inclination [-]

This situation, which applies only to canals, occurs when the maximum of the left or right distance between the ship's axis and the imaginary banks of the approximative rectangular profile, $u_{r,max}$ (see Figure 5.5), given a constant water depth, satisfies the following equation:

$$u_{r,max} \le b_E / 2 \tag{5-5}$$

where

$u_{r,max}$ is the maximum bank distance in the approximative rectangular profile [m] (see Figure 5.5)

b_E is the influence width of the return flow field [m]

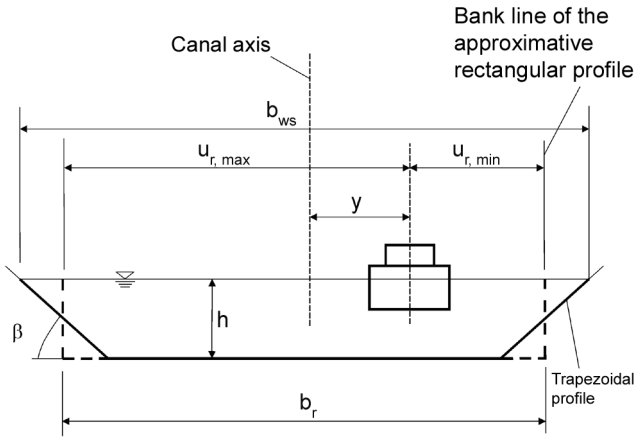

Figure 5.5 Definition of the bank distances $u_{r,min}$ and $u_{r,max}$

Equation (5-6) applies to trapezoidal profiles featuring slopes with the same inclination:

$$\left\{ \begin{array}{l} b_r = b_{WS} - m\,h \\ u_{r,min} = ½\, b_r - y \\ A = b_r\, h \end{array} \right\} \tag{5-6}$$

The following approach applies to b_E; it is dependent on the type of ship.

Influence width b_E of the return flow field [m]

$$b_E = \frac{\pi}{2}\,(L + f_B\,B) \tag{5-7}$$

where

B is the ship's beam [m]

f_B is the factor of the influence width [-], which is dependent on the type of ship

$f_B = 3$ common inland navigation vessel

$f_B \approx 1.5$ modern sea-going vessel that can also navigate inland waterways; ship with bulbous bow

$f_B = 0$ elliptical body plan (in accordance with theory)

L is the overall ship's length [m]

The diagrams in Figure 5.7 and Figure 5.8 illustrating more precise calculations are based on equation (5-7) for $f_B = 3$.
Equation (5-7) can also be applied in general cases, i.e. where $f_B \neq 3$, by substituting L_{eff}/B for the ratio L/B in Figure 5.7 and Figure 5.8 The following applies to the effective ship's length for slender ships:

Effective ship's length L_{eff} [m]

$$L_{eff} = L + B(f_B - 3) \tag{5-8}$$

Slight shallow water effects may occur in canals and can be taken into account in the equivalent cross-sectional area for a more precise calculation in accordance with Figure 5.7, which has been derived from the simplified 2D potential theory. The equivalent cross-sectional area of the canal $A_{K,äqui}$ is obtained as follows:

Equivalent cross-sectional area of the canal $A_{K,äqui}$

$$A_{K,äqui} = b_{r,äqui}\,h \tag{5-9}$$

where

$b_{r,äqui}$ is the calculated width of the equivalent canal cross-section [m]

h is the water depth [m]

The change in the return flow velocity and drawdown between the ship and the bank is slight for canals and can generally be disregarded. The following procedure can be followed for the transition from width case A

to width cases B and C to achieve a more precise calculation:

The parameters determined using the equivalent cross-sectional area of the ship, i.e.

- mean drawdown $\Delta\overline{h}$ in accordance with eq. (5-25) in 5.5.3 and
- mean return flow velocity $\overline{v}_{rück}$ in accordance with eq. (5-23) in 5.5.3

diminish or increase between the ship and the bank (index "u"), resulting in different values (see eqs. (5-26) and (5-27)):

$$\Delta\overline{h} \rightarrow \Delta\overline{h}_u$$

$$\overline{v}_{rück} \rightarrow \overline{v}_{rück,u}$$

where

$\Delta\overline{h}$ is the mean drawdown in the longitudinal and transverse directions [m]

$\Delta\overline{h}_u$ is the drawdown averaged in a longitudinal direction at the bank [m]

$\overline{v}_{rück}$ is the mean return flow velocity averaged in the longitudinal and transverse directions [m/s]

$\overline{v}_{rück,u}$ is the mean return flow velocity averaged in a longitudinal direction at the bank [m/s]

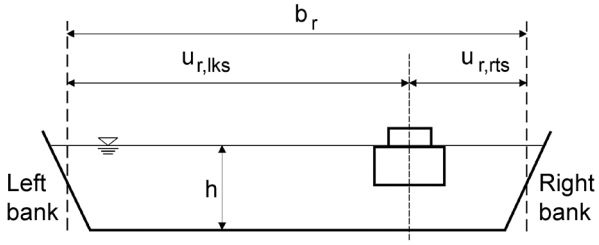

Figure 5.6 Sketch showing the equivalent bank distances and the calculated width of the approximative rectangular profile of the waterway

Depending on the ratio of the ship's length to the average canal width L/b_r, the ratios $\Delta\overline{h}_u / \Delta\overline{h}$ and $\overline{v}_{rück,u} / \overline{v}_{rück}$, which apply to the right bank, can be determined approximately from Figure 5.8 as a function of the equivalent right-hand bank distance $u_{r,rts} / b_r$ (see Figure 5.6 for definitions), with the ship acting as a dipole with a flow around it. Figure 5.8 must be reversed for the left bank (substituting $u_{r,lks}$ for $u_{r,rts}$). The figure makes a distinction between important cases of L/B. Typical length-to-width ratios (L/B) are:

Europe ship ES:	8.4
Large inland cargo vessel GMS:	9.7
Push tow unit with 2 lighters 2SV:	16.2
Push tow unit with 4 lighters 4SV:	8.1

These exact values will need to be interpolated as appropriate when Figure 5.7 and Figure 5.8 are applied.

The slope inclination $m_{K,äqui}$ to be used in this case to obtain a more exact calculation for the equivalent canal cross-section may differ slightly from that of the original canal cross-section. It is obtained as follows:

Equivalent slope inclination $m_{K,äqui}$ [-] in an equivalent canal cross-section

$$m_{K,äqui} \approx \frac{1}{2}\left(m_{lks}\frac{\Delta\overline{h}_{u,lks}}{\Delta\overline{h}} + m_{rts}\frac{\Delta\overline{h}_{u,rts}}{\Delta\overline{h}}\right) \qquad (5\text{-}10)$$

where

$m_{K,äqui}$ is the equivalent slope inclination [-], only for the hydraulic calculation of drawdown and return flow (equivalent slope inclination = cotangent of the angle of the slope of an equivalent canal cross-section)

$m_{K,äqui}$ does not apply to the calculations in chapters 6 und 7

m_{lks} is the slope inclination on the left bank [-]

m_{rts} is the slope inclination on the right bank [-]

$\frac{\Delta\overline{h}_{u,lks}}{\Delta\overline{h}}$ is the relative drawdown at the equivalent left bank [-] in accordance with Figure 5.8

$\frac{\Delta\overline{h}_{u,rts}}{\Delta\overline{h}}$ is the relative drawdown at the equivalent right bank [-] in accordance with Figure 5.8

The values $A_{K,äqui}$, $m_{K,äqui}$ and h thus apply to the calculated equivalent trapezoidal profile, i.e. the one used in subsequent calculations. The equivalent width at water level $b_{WS,äqui}$ can then be obtained from those values, i.e.

Equivalent width at water level $b_{WS,äqui}$ [m]

$$b_{WS,äqui} = m_{K,äqui}\,h + A_{K,äqui} / h \qquad (5\text{-}11)$$

where

$A_{K,äqui}$ is the equivalent canal cross-section [m^2] in accordance with eq. (5-9) in 5.5.1

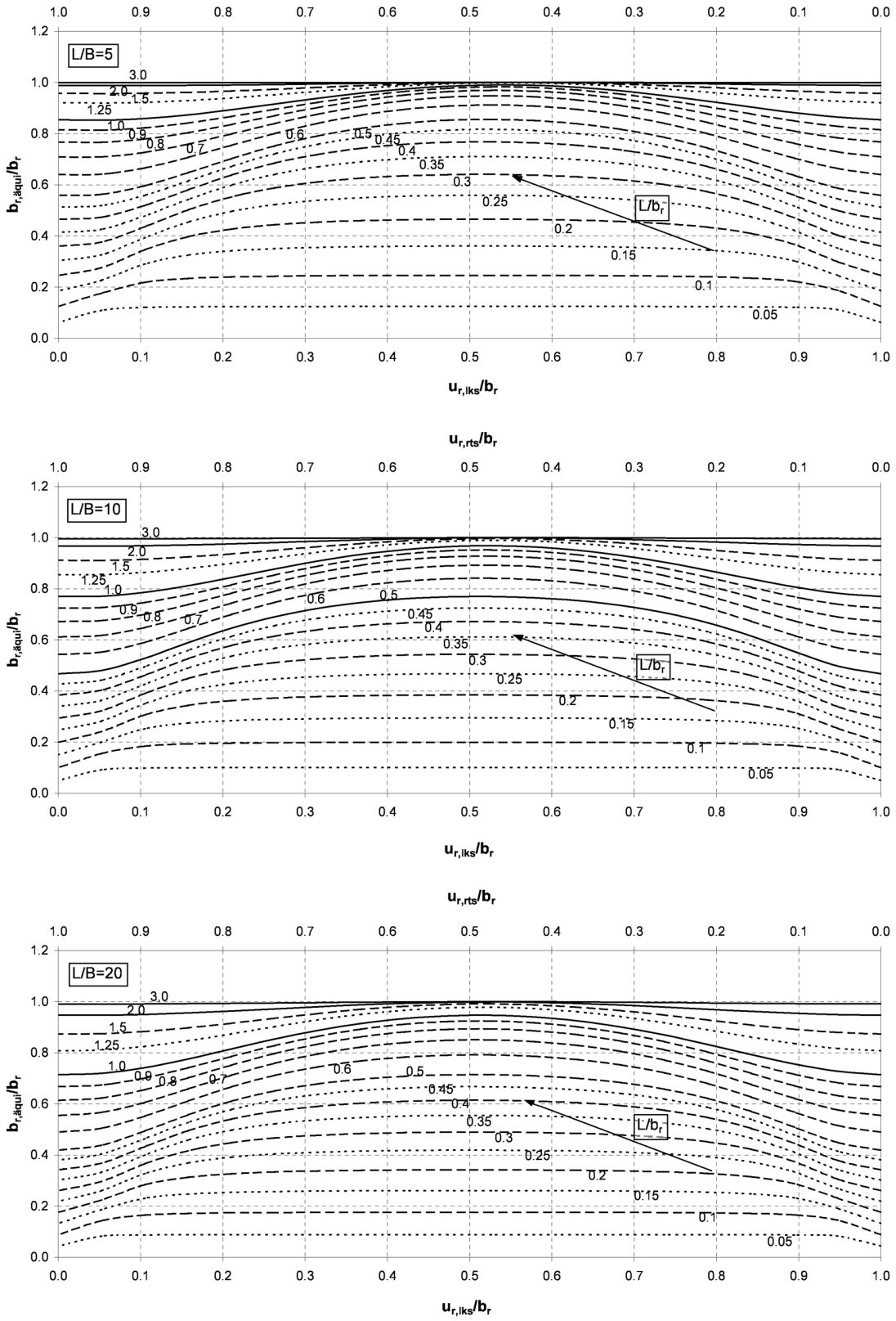

Figure 5.7 Average width of an equivalent canal cross-section $b_{r,äqui}$ as a function of the calculated canal width b_r (see Figure 5.5 and Figure 5.6 for definition); the equivalent bank distances $u_{r,rts}$ and $u_{r,lks}$ for the right and left banks respectively (see Figure 5.6 for definition); ship's length L and beam B for L/B = 5, 10 and 20. (Substitute L_{eff} in accordance with eq. (5-8) for L where where $f_B \neq 3$ in eq. (5-7))

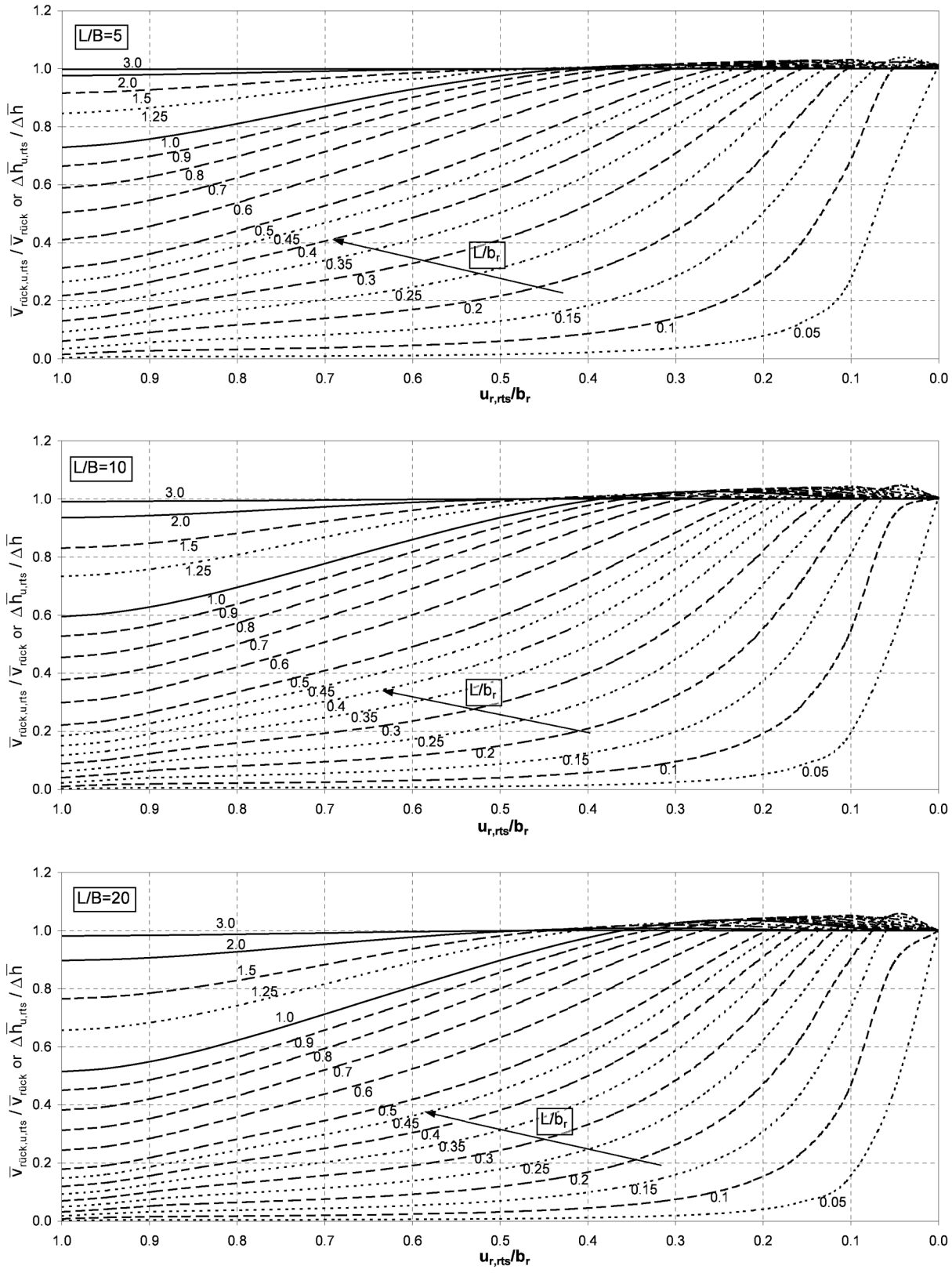

Figure 5.8 Mean return flow velocity ($\overline{v}_{\text{rück,u,rts}}$) or drawdown ($\Delta\overline{h}_{\text{u,rts}}$) at the equivalent (Index r*) right (Index* rts*) bank (Index* u*) in relation to the corresponding values at the ship ($\overline{v}_{\text{rück}}$, $\Delta\overline{h}$); the bank distances $u_{\text{r,rts}}$ and $u_{\text{r,lks}}$ for the equivalent right and left banks respectively (see Figure 5.6 for definitions) ship's length L and beam B for L / B = 5, 10 and 20.*
(Substitute $u_{\text{r,lks}}$ for $u_{\text{r,rts}}$ to calculate the values for the left bank)

Width case B: "Shallow Water"
Short vessels, large bank distances

Shallow water conditions exist when a vessel is short in relation to the width of the canal and for very large bank distances. This width case occurs when the smallest bank distance $u_{r,min}$ as shown in Figure 5.5 satisfies the following criterion:

$$u_{r,min} > \frac{b_E}{2} \tag{5-12}$$

where

b_E is the influence width in accordance with eq. (5-7) [m]

$u_{r,min}$ is the minimum bank distance in an equivalent canal cross-section [m] (see Figure 5.5 for definition)

The 1D canal theory can then be applied to the following equivalent canal cross-section $A_{K,äqui}$, its width being limited by b_E by way of approximation:

$$A_{K,äqui} = b_E \, h \tag{5-13}$$

The slope inclination of the equivalent canal cross-section $m_{K,äqui}$ for very large bank distances, i.e. where $u_{r,min} >> b_E/2$, is approximately equal to zero. In this case, the return flow velocity and the drawdown diminish towards the bank (distance u_r) approximately as follows:

$$\frac{\overline{v}_{rück,u}}{\overline{v}_{rück}} = \frac{\Delta\overline{h}_u}{\Delta\overline{h}} \approx \frac{1}{1+\left(\frac{u_r \pi}{b_E}\right)^2} \tag{5-14}$$

The much smaller decrease in the return flow field must be taken into account if a more exact calculation is required. This applies in particular to the transition from width case B to width cases A or C. In this case, the following procedure should be followed:

- $A_{K,äqui}$ in accordance with eq. (5-9)
- $b_{r,äqui}$ in accordance with Figure 5.7
- $m_{K,äqui}$ in accordance with eq. (5-10)
- $b_{WS,äqui}$ in accordance with eq. (5-11)
- Change $\Delta\overline{h}$ and $\overline{v}_{rück}$ between the ship and the bank to the new values $\Delta\overline{h}_u$ and $\overline{v}_{rück,u}$ as shown in Figure 5.8

Width case C: "Transitional situation"
Transition from canal to shallow water conditions

The influence width b_E and the bank nearest the vessel overlap in the transitional area between a canal and shallow water conditions. The transitional area thus satisfies the following criterion:

$$u_{r,min} \le \frac{b_E}{2} \le u_{r,max} \tag{5-15}$$

The approximate equivalent canal cross-section is obtained by disregarding the ineffective portion of the influence width b_E (see Figure 5.4). The associated equivalent cross-sectional area $A_{K,äqui}$ is then:

$$A_{K,äqui} = \left(\frac{b_E}{2} + u_{r,min}\right) h \tag{5-16}$$

The associated equivalent slope inclination $m_{K,äqui}$ is approximately equal to $m/2$.

It can be assumed in the first approximation for the bank nearest the ship that $\overline{v}_{rück,u} = \overline{v}_{rück}$ and $\Delta\overline{h}_u = \Delta\overline{h}$. For a more exact calculation, see equations (5-9), (5-10) and (5-11) as well as Figure 5.7 and Figure 5.8

5.5.1.2 Influence of boundary layers

The effects of boundary layers are taken into consideration separately for the bow and stern by means of an effective cross-sectional area of the ship $A_{S,eff}$ in the prismatic section of the hull (midship). They enable the energy losses disregarded in the 1D canal theory to be determined approximately.

Bow (negligible boundary layer effects):

Effective cross-sectional area of the ship at the bow $A_{S,eff,B}$ [m²]

$$A_{S,eff,B} = A_{S,B} = B_B \, T_B \, \gamma_B \tag{5-17}$$

where

$A_{S,B}$ is the cross-sectional area of the ship at the bow [m²]

B_B is the beam at the bow [m]

T_B is the draught of the ship at the bow [m]

γ_B is the block coefficient of the cross-sectional area of the ship at the bow [-]; it is generally equal to 1.0 (prismatic midship section)
N.B.: Not to be confused with the block coefficient of the ship's volume.

Stern (greatest boundary layer thickness):

Effective cross-sectional area of the ship at the stern $A_{S,eff,H}$ [m²]

$$\left\{ \begin{array}{l} A_{S,eff,H} = A_{S,H} + \delta_{1H} \left(B_m + 2\,T_m \right) \\ A_{S,H} = T_H\; B_H\; \gamma_H \\ \delta_{1H} = 0.645\, L_H \left(1.89 + 1.62\, \log_{10} \dfrac{L_H}{K_{SS}} \right)^{-2.5} \end{array} \right. \qquad (5\text{-}18)$$

where

$A_{S,H}$ is the cross-sectional area of the ship at the stern or at the point of greatest displacement [m²]

B_H is the beam at the stern [m]

B_m is the mean beam between bow and stern [m]

K_{SS} is the equivalent sand roughness of the ship's hull [m]
$K_{SS} \approx 0.3 \cdot 10^{-3} - 0.5 \cdot 10^{-3}$ m

L_H is the development length of the boundary layer between the bow and the end of the midship section [m]

T_H is the draught of the vessel at the stern [m]

T_m is the mean draught of the vessel between bow and stern [m]

γ_H is the block coefficient of the cross-sectional area of the ship at the stern [-] generally equal to 1.0 (prismatic midship section)
N.B.: Not to be confused with the block coefficient of the ship's volume.

δ_{1H} is the thickness of the boundary layer at the stern [m]; it cannot exceed the depth of the dynamic underkeel clearance

If the vessel does not have a prismatic hull, as is often the case for tugs, the cross-section with the greatest displacement may be selected by way of an approximation of $A_{S,eff}$. The thickness of the boundary layer will then need to be determined for that cross-section.

5.5.2 Critical ship speed for canal conditions

The flow around a ship and wave formation are subject to typical changes in restricted cross-sections when the ship speed increases. While the water displaced by the ship flows in the opposite direction to the ship in case of subcritical ship speed, the critical gradient required for the transition to supercritical flow in the vicinity of the ship starts to develop unsteadily when the critical ship speed has been reached.

An analysis of the results of field tests conducted with a modern large inland cargo vessel /BAW 2002/ in a canal (with approx. the standard trapezoidal profile in accordance with /*BMV 1994*/) indicates that calculations of the critical ship speed should include $A_{K,äqui}$ and $A_{S,eff}$ to account for the boundary layer around the ship's hull and the shallow water effects described in 5.5.1. The tests /BAW 2002/ showed that the influence of eccentricity on the critical ship speed only proved to be significant for width case C in 5.5.1, i.e. when ships that are short in relation to the width of the canal sail close to a bank, taking into account the unsteady course on approaching the bank. The influence of eccentricity is taken into consideration below by reducing the width of the original canal cross-section. The critical ship speed observed during the tests was slightly affected by the trim. The critical ship speed of vessels with a static trim by the stern or with a loaded stern dynamic trim tends to be lower, leading to higher waves, than for vessels without a dynamic trim. Accordingly, the following equations apply to the mean drawdown at critical ship speed $\Delta\bar{h}_{krit}$ and the critical ship speed v_{krit} (speed in relation to the water) (Figure 5.9):

Critical ship speed v_{krit} [m/s], associated mean drawdown $\Delta\bar{h}_{krit}$ [m]

$$\left\{ \begin{array}{l} \Delta\bar{h}_{krit} = x_{krit}\; h_m \\ v_{krit} = y_{krit} \sqrt{g h_m} \end{array} \right. \qquad (5\text{-}19)$$

The values of x_{krit} and y_{krit} are calculated iteratively using the following auxiliary equations:

$$\beta = 1 - \frac{1}{n}$$

$$\tilde{f} = \frac{m h_m}{b_{WS}}$$

$$f = 1 - x_{krit}\, \tilde{f}$$

(The value of x_{krit} (see below) must be provided here – return address for iteration.)

$$f^* = \frac{2}{f}(1 - 2f)$$

$$\tilde{r} = \frac{1 - f^*}{3}$$

$$\tilde{x}_{krit} = -2\tilde{r}^{1/2}\cos\left\{\frac{\pi}{3} + \frac{1}{3}\arccos\left[\frac{\beta f^*}{2\tilde{r}^{3/2}}\right]\right\}$$

N.B.: Calculations in radian measure

$$x_{krit} = \frac{\beta - \tilde{x}_{krit}}{f}$$

N.B.: At this point return to calculation of *f* until the result is sufficiently stable.

$$y_{krit} = \left[\frac{2\,x_{krit}}{\left(\beta - x_{krit} f\right)^{-2} - 1}\right]^{1/2}$$

The auxiliary functions are associated with the following parameters of the canal and the ship:

$A_{K,äqui}$ equivalent canal cross-section [m²] in accordance with eq. (5-9) in 5.5.1

$A_{S,eff}$ effective cross-section of vessel [m²], allowing for boundary layer effects at bow and stern in accordance with 5.5.1 and 5.5.4.6.

b_{WS} width at water level [m]
$b_{WS} = b_{WS,äqui}$ in accordance with eq. (5-11) in 5.5.1.1

h_m mean water depth [m], $h_m = A_{K,äqui} / b_{WS,äqui}$

m inclination of slope [-]
$m = m_{K,äqui}$ in accordance with eq. (5-10) in 5.5.1.1

n blockage ratio [-]
$n = n_{äqui} = A_{K,äqui} / A_{S,eff}$ (equivalent blockage ratio)

During iteration, the solution for a rectangular cross-section can be used as an initial estimate of x_{krit} as follows:

$$x_{krit} = \beta + 2\cos\left[\frac{\pi}{3} + \frac{1}{3}\arccos(-\beta)\right]$$

The dimensionless values y_{krit} for the critical ship speed and x_{krit} for the critical drawdown depend primarily on the blockage ratio *1/n*. The form parameter $\tilde{f}$, describing the shape of the canal cross-section has a slight effect on v_{krit} (see Figure 5.9). The influence of $\tilde{f}$ on v_{krit} can be disregarded in rough calculations. The value of v_{krit} is then obtained from Figure 5.9 for typical blockage ratios. The influence of $\tilde{f}$ on x_{krit} can be seen in Figure 5.9 and Figure which can be used to determine approximate values.

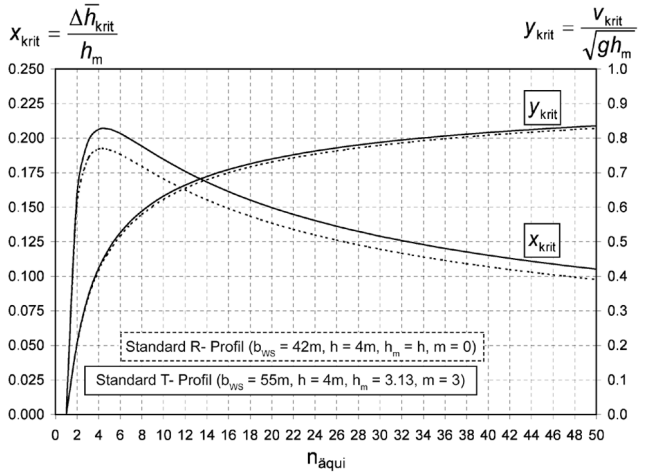

Figure 5.9 Graph illustrating how the critical ship speed v_{krit} and the associated mean drawdown $\Delta\bar{h}_{krit}$ are dependent on $n_{äqui}$ by reference to a standard trapezoidal cross-section (T-Profil) and a standard rectangular cross-section (R-Profil)

Modified approaches, which are described *inter alia* in /*Römisch 1989*/ and may serve as an alternative to the approximation equation (5-19) given here, apply to the critical speed in special cases such as waterway cross-sections with a very irregular water depth (e.g. cross-sections with berms or dredged fairways).

A larger effective ship's cross-section must be used for vessels sailing with drift (see 5.5.4.6).

5.5.3 Mean drawdown and return flow velocity for vessels sailing in the centre of a canal

The one-dimensional calculation of the return flow velocity and drawdown occurring when a vessel sails steadily along a canal is based on Bernoulli's equation (energy conservation) and the continuity equation (conservation of mass). The equations are applied to the undisturbed canal cross-section in front of the vessel and the restricted cross-section adjacent to the vessel reduced by the plunged midship section and drawdown (see Figure 5.10). The canal cross-section flows towards a hypothetical "fixed" vessel at the ship speed v_s (in relation to the water). It is assumed in this case that the flow distribution over the cross-section is uniform, the squat of the vessel corresponds to the mean drawdown in the narrowest flow cross-section (cross-section with the greatest drawdown) (simplified assumption: squat = drawdown) and any energy losses are disregarded. Furthermore, the dynamic trim of the vessel, if any, is not taken into consideration. With the exception of flow cross-sections with rough beds and high levels of turbulence due to a pronounced flow field, the 1D canal theory provides reliable results, in spite of the simplifications referred to above, if the influences that are not taken into account are subsequently corrected empirically.

Allowance for boundary layer effects at a vessel and shallow water effects can be made to enable the 1D canal theory to be applied approximately using the algorithms given in 5.5.1 with an equivalent cross-sectional area of the canal $A_{K,äqui}$ and an effective cross-sectional area of the ship $A_{S,eff}$. The influence of a natural current on the calculation of the drawdown for a specified ship speed over ground $v_{SüG}$ is taken into account by calculating the ship speed through water v_s:

Ship speed through water v_S [m/s]

$$v_S = v_{SüG} \pm v_{Str} \qquad (5\text{-}20)$$

(+: travel upstream, -: travel downstream)

where

v_{Str} is the flow velocity [m/s] of the currents

$v_{SüG}$ is the ship speed over ground [m/s]

If it is assumed for design purposes that $v_s = 0.97 v_{krit}$, it is this speed that will correspond to the ship speed through water. The flow velocity is then irrelevant to the calculation of the drawdown. Accordingly, each of the speeds given below is measured in relation to the surrounding body of water. The effect of the currents must be considered when determining the required size of stones as it will result in either an increase or a decrease in the size, see eq. (6-13) in 6.7.2

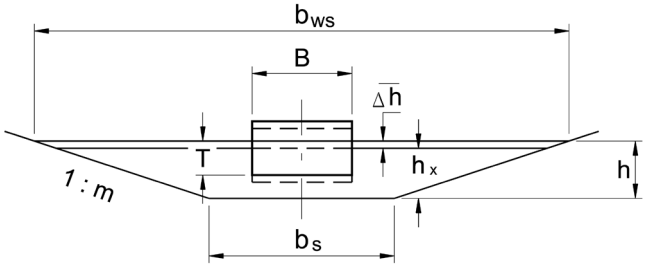

Figure 5.10 Diagram illustrating how to calculate the flow due to displacement; see text and eqs. (5-21) and (5-22) for symbols

The following two basic relationships then apply:

1. The maximum drawdown $\Delta\overline{h}$ in the narrowest flow cross-section adjacent to the ship, averaged over the width of the canal, is obtained by means of Bernouilli's equation (see Figure 5.10):

$$\Delta\overline{h} = h - h_x = \\ = \frac{1}{2g}\left[\alpha_1 \left(v_S + \overline{v}_{rück}\right)^2 - {v_S}^2\right] \qquad (5\text{-}21)$$

2. In accordance with the continuity equation

$$A v_S = \left[A - \left(A_M + b_m \Delta\overline{h}\right)\right]\left(v_S + \overline{v}_{rück}\right) \qquad (5\text{-}22)$$

the associated return flow velocity at the bow and stern, averaged over the cross-section, is:

Return flow velocity averaged over the cross-section $\overline{v}_{rück}$ [m/s]

$$\overline{v}_{rück} = \frac{A_M + b_m \Delta\overline{h}}{A - (A_M + b_m \Delta\overline{h})} v_S = \frac{\Delta A}{A - \Delta A} v_S \qquad (5\text{-}23)$$

where

A is the canal cross-section [m^2]
$A = A_{K,äqui}$ as defined in 5.5.1.1

A_M is the plunged midship section (making allowance for boundary layer effects and shallow water effects at bow and stern) [m^2]
$A_M = A_{S,eff}$ as defined in 5.5.1.2 and 5.5.4.6.

ΔA is the reduction in the cross-section of the canal due to the cross-section of the ship and drawdown [m^2]
$\Delta A = A_M + b_m \Delta\overline{h}$

b_m is the mean width at water level in the drawdown area [m]

$b_m = b_{WS} - \Delta\overline{h}\ m$

b_S is the width of the bed [m]

b_{WS} is the width at water level [m]

$b_{WS} = b_{WS,äqui}$ in accordance with eq. (5-11) in 5.5.1.1

g is the acceleration due to gravity [m/s^2]

h is the depth of the water in the canal [m]

h_x is the depth of water in the narrowest flow cross-section [m]

$\Delta\overline{h}$ is the maximum drawdown in the narrowest flow cross-section, averaged over the width of the canal [m]

m is the slope inclination [-]

$m = m_{K,äqui}$ in accordance with eq. (5-10) in 5.5.1.1

v_S is the ship speed through water [m/s] in accordance with eq. (5-20)

$\overline{v}_{rück}$ is the mean return flow velocity [m/s] (in relation to an observer moving at v_{Str})

α_1 is the correction coefficient [-] in accordance with eq. (5-24)

A correction coefficient describing, amongst other things, the influence of the irregularity of the return flow field depending on how close the actual ship speed is to the critical ship speed is stated by /*Przedwodjski et al. 1995*/:

$$\alpha_1 = 1.4 - 0.4\frac{v_S}{v_{krit}} \tag{5-24}$$

The implicit method of calculating the relationship $\Delta\overline{h} = f(v_S)$ is derived from eq. (5-21):

Correlation between ship speed v_S [m/s] and mean drawdown $\Delta\overline{h}$ [m]

$$v_S = \sqrt{\frac{2\,g\,\Delta\overline{h}}{\alpha_1\left(\frac{A}{A-\Delta A}\right)^2 - 1}} \tag{5-25}$$

The calculation is performed iteratively after specifying $\Delta\overline{h}$ (usually a value between 0.2 and 0.5 m) until the calculated speed corresponds to the design ship speed. Plotting the calculated ship speed v_s against $\Delta\overline{h}$ is recommended (see Figure 5.11). $\overline{v}_{rück}$ can then be calculated using eq. (5-23).

An exact calculation in accordance with eq. (5-25) is not necessary if only a rough estimate is required in which case calculations can be performed with v_s/v_{krit}, the blockage ratio *1/n*, form parameter $\tilde{f}$ and Figure 5.12 instead.

The return flow velocities $\overline{v}_{rück}$ and the drawdown $\Delta\overline{h}$ must be multiplied by the ratios given in 5.5.1.1 and Figure 5.8 to allow for their reduction between the ship and the bank and to obtain the corresponding values at the bank, $\overline{v}_{rück,u}$ and $\Delta\overline{h}_u$:

$$\Delta\overline{h}_u = \Delta\overline{h}\left\{\frac{\Delta\overline{h}_u}{\Delta\overline{h}}\right\}\Bigg|_{\text{Fig. 5.8}} \tag{5-26}$$

$$\overline{v}_{rück,u} = \overline{v}_{rück}\left\{\frac{\overline{v}_{rück,u}}{\overline{v}_{rück}}\right\}\Bigg|_{\text{Fig. 5.8}} \tag{5-27}$$

$\Delta\overline{h}$ and $\overline{v}_{rück}$ are design values for ships sailing in the centre of the waterway. They serve as input data for other empirical calculations to allow for the influence of the water surface gradient and eccentric sailing lines in accordance with 5.5.4.2 to 5.5.4.4.

Numerous other calculation methods have been developed for the 1D canal theory /*Bouwmeester 1977; Dand, White 1978; Führböter et al. 1983; Jansen, Schijf 1953; Söhngen 1992*/. The mean drawdown $\Delta\overline{h}$ provided by each of the methods referred to here is obtained by averaging over the primary wave only.

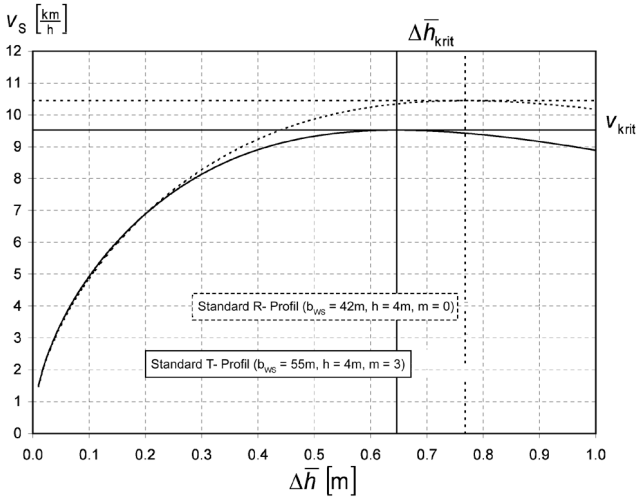

Figure 5.11 Ship speed v_S as a function of the mean drawdown $\Delta\overline{h}$ in accordance with the 1D canal theory for a large inland cargo vessel (length L = 110 m, beam B = 11.4 m, draught T = 2.8 m, thickness of boundary layer at bow section δ_{1H} = 0.19 m) in standard trapezoidal and rectangular profiles, calculated using eq. (5-25)

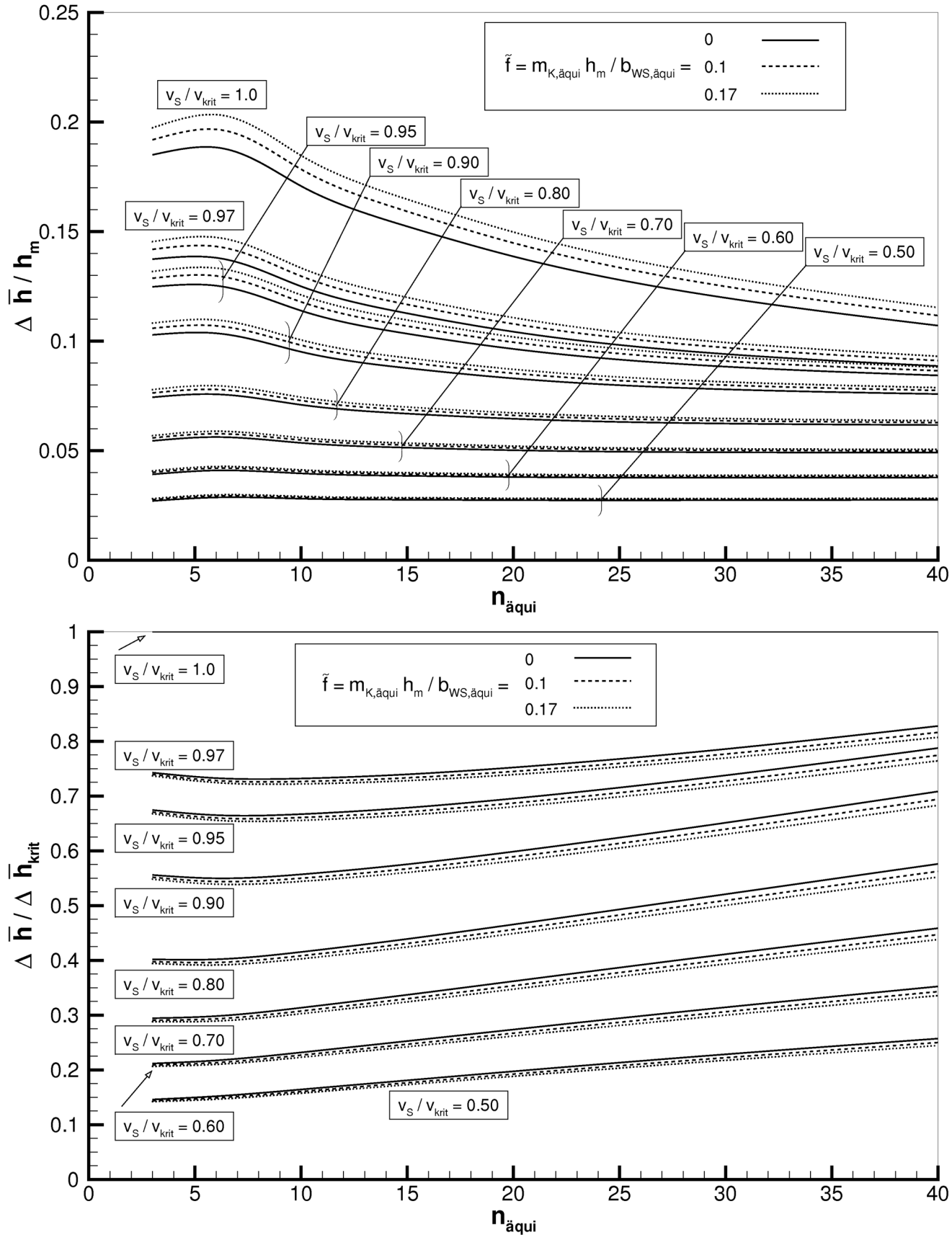

Figure 5.12 Relative values (in relation to $\Delta\bar{h}_{krit}$ and h_m) of the mean drawdown $\Delta\bar{h}$ as a function of $n_{äqui}$ and the form parameter $\tilde{f}$ for typical relative ship speeds v_S / v_{krit} calculated using the 1D canal theory

5.5.4 Hydraulic design parameters and geotechnically relevant drawdown parameters for any sailing position

5.5.4.1 Definition of wave height

The design ship-induced wave heights H at the bow (H_B) and stern (H_H) are calculated taking account of the canal width in the centre of the slope. Any changes in the waves running up the slope are not dealt with separately but are incorporated into the overall design calculations.

The basic primary and secondary wave patterns, as they would be perceived by a stationary observer on the bank, are shown in in Figure 5.13.

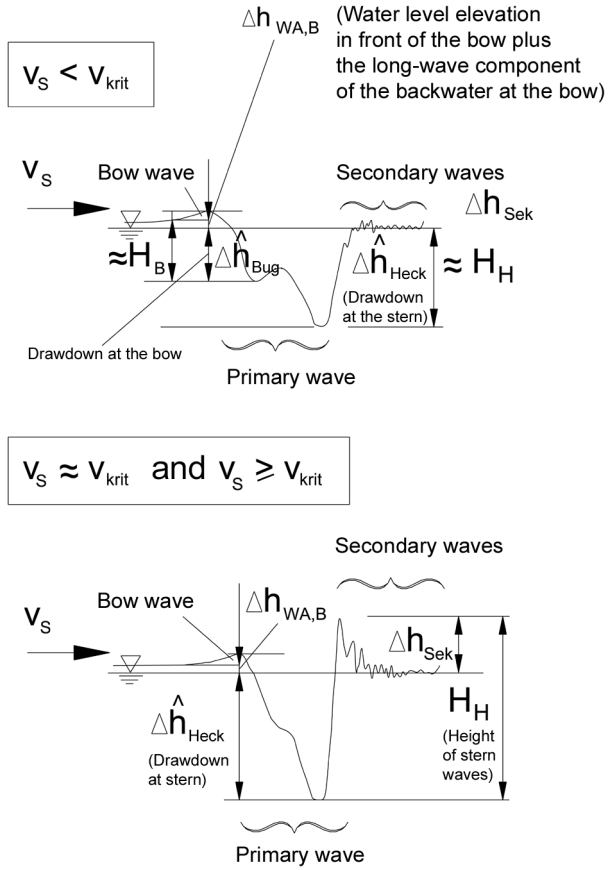

Figure 5.13 Formation of ship-induced primary waves at subcritical ($v_S < v_{krit}$) and critical ($v_S \approx v_{krit}$) speeds

5.5.4.2 Maximum drawdown at bow and associated return flow velocity without the influence of eccentricity

The cross-section of the vessel at the bow must be known in order to calculate the maximum drawdown at the bow. Boundary layer and shallow water effects as described in 5.5.1 must be taken into account, if necessary. The following equation /*Przedwojski et al. 1995*/ applies to the height of bow waves at the bank for modern large inland cargo vessels and tugs, except in cases where the influence of eccentricity needs to be considered. The equation takes account of, amongst other things, the water level elevation $\Delta h_{WA,B}$ in front of the bow:

Maximum drawdown near the bank at the **bow** $\Delta \hat{h}_{u,Bug}$ [m] without the influence of eccentricity

$$\Delta \hat{h}_{u,Bug} = 1.1\, \Delta \overline{h}_{u,Bug} \qquad (5\text{-}28)$$

where

$\Delta \hat{h}_{u,Bug}$ is the maximum drawdown near the bank at the bow [m]

$\Delta \overline{h}_{u,Bug}$ is the mean drawdown near the bank at the bow [m], calculated for the blockage ratios at the bow as described in 5.5.3

Remark: The coefficient may be greater than 1.1 for full bows.

The influence of eccentricity on the bow wave is taken into account in 5.5.4.4.

The maximum return flow at the bow $\hat{v}_{rück,u,Bug}$ can be calculated approximately by means of the continuity equation (eq. 5-23) substituting $\Delta \hat{h}_{u,Bug}$ for $\Delta \overline{h}$. It should be borne in mind that both b_m and ΔA are effected by $\Delta \hat{h}_{u,Bug}$.

5.5.4.3 Maximum drawdown at stern and associated return current velocity without the influence of eccentricity

The difference between the maximum drawdown at the stern and $\Delta \overline{h}_u$ (see eq. (5-26)) depends on the following influences:

(1) Ratio of draught to water depth. (The ratio $\Delta \hat{h}_{u,Heck} / \Delta \overline{h}_{u,Heck}$ tends to be greater for smaller T / h ratios.)

(2) Type of propulsion. ($\Delta \hat{h}_{u,Heck}$ tends to be greater for twin-screw vessels sailing close to a bank than for single-screw vessels.)

(3) Closeness to v_{krit}. (Due to the increase in the water surface gradient between the bow and the stern, the associated stern-heavy trim and the secondary waves caused by the transversal stern wave as described in 5.5.5.)

(4) Superimposition of secondary waves originating at the bow for short vessels or wide canals. (Distance case B as described in 5.5.5.1.)

Influences (1) and (3) can be taken into consideration approximately by means of the following equation according to the approach of /*Przedwojski et al. 1995*/:

Maximum drawdown near the bank at the **stern** $\Delta\hat{h}_{u,Heck}$ [m] without the influence of eccentricity

$$\Delta\hat{h}_{u,Heck} = C_H \, \Delta\overline{h}_{u,Heck} \qquad (5\text{-}29)$$

where

C_H is the factor for consideration of the influence of the type of ship, draught, trim and different in water levels between bow and stern [-]

$C_H \approx 1.3$ for modern inland navigation vessels ($T / h \approx 0.7$)

$C_H \approx 1.5$ for partially laden, in particular ballasted, modern inland navigation vessels and tugs ($T / h \approx 0.4$)

$C_H \approx 1.1$ for sea-going vessels that can also navigate inland waterways, as they usually have a bow-heavy trim.

$\Delta\overline{h}_{u,Heck}$ is the mean drawdown near the bank [m], calculated in accordance with 5.5.3 for the blockage ratios at the stern

$\Delta\hat{h}_{u,Heck}$ is the maximum drawdown near the bank at the stern [m]

Additional transversal stern waves may occur at ship speeds close to v_{krit}; they are described in 5.5.5.3. They may affect $\Delta\hat{h}_{u,Heck}$ to a greater extent than the influences (1) to (3) described above, in particular if the additional influence (4) occurs.

If this is the case, $\Delta\hat{h}_{u,Heck}$ is obtained by using the following equation instead of eq. (5-29) */BAW 2002/*.

$$\Delta\hat{h}_{u,Heck} \approx \Delta\overline{h} + \tfrac{1}{2} H_{Sek,q} \qquad (5\text{-}30)$$

where

H_{Sek} is the height of the additional secondary wave in accordance with 5.5.5.3 obtained by eq. (5-47), taking eq. (5-50) into consideration

If influence (4) occurs, the part of the height of the secondary bow wave below the still-water level (SWL), obtained by means of eq. (5-43) (see 5.5.5.2) must be added to $\Delta\hat{h}_{u,Heck}$ in accordance with eq. (5-29) or eq. (5-30).

The maximum return flow velocity at the stern $\hat{v}_{rück,u,Heck}$ can be calculated approximately by means of the continuity equation (5-23), substituting $\Delta\hat{h}_{u,Heck}$ for $\Delta\overline{h}$. It should be borne in mind that both b_m and ΔA are affected by $\Delta\hat{h}_{u,Heck}$.

5.5.4.4 Maximum heights of bow and stern waves due to eccentric sailing

There is a steep increase in the wave heights at the slope as the distance between the vessel and the banks decreases. One of the reasons for this effect is the reduction in the length of the waves between the vessel and the bank. As stated in 6.2 the wave length depends on the bank distance (eq. (6-6)) which is why the wave height increases as the bank distance decreases, given a constant wave energy level. The increase in wave height at the bank nearest the ship is calculated as follows as described by /*Przedowojski et al. 1995*/ as a function of the ratio of the cross-sectional area between the ship and the bank to the canal cross-section (or, for vessels sailing in shallow water, to the equivalent cross-sectional area of the canal in accordance with 5.5.1) (see Figure 5.14):

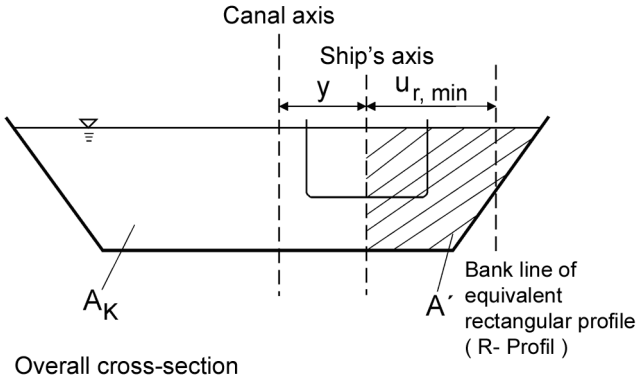

Figure 5.14 Definition of A' for eccentric sailing in width case A in accordance with 5.5.1.1

Maximum bow wave height $H_{u,Bug}$ [m] at the bank closest to the vessel for eccentric sailing

$$H_{u,Bug} = (2.0 - 2\frac{A'}{A}) \, \Delta\hat{h}_{u,Bug} \qquad (5\text{-}31)$$

Maximum stern wave height $H_{u,Heck}$ [m] at the bank closest to the vessel for eccentric sailing

$$H_{u,Heck} = (2.0 - 2\frac{A'}{A})\Delta\hat{h}_{u,Heck} \quad (5\text{-}32)$$

where

A is the relevant cross-sectional area of the canal [m^2]

A' is the cross-sectional area between the ship's axis and the bank [m^2] (see Figure 5.14)

A'/A is the blockage ratio [-] in accordance with the individual cases described in 5.5.1.1 and Figure 5.4

Width case A: $\frac{A'}{A} = \frac{u_{r,min}}{b_r} \geq 0$

Width case B: $\frac{A'}{A} = 0.5$

Width case C: $\frac{A'}{A} = \frac{u_{r,min}}{\frac{b_E}{2} + u_{r,min}} \geq 0$

$\Delta\hat{h}_{u,Bug}$ is the maximum drawdown near the bank at the bow [m] in accordance with 5.5.4.2

$\Delta\hat{h}_{u,Heck}$ is the maximum drawdown at the bank near the stern [m] in accordance with 5.5.4.3

If a vessel is sailing very close to a bank, the point of impact of the interferences caused by the diverging waves of the secondary bow wave system may coincide with the maximum drawdown at the bow that occurs at the transition to the midship section. In this case, half the height of the secondary wave must be added to the height of the bow wave by way of approximation (special situation for distance case A in 5.5.5.1).

$H_{u,Bug}$ and $H_{u,Heck}$ can be taken as $\Delta\hat{h}_{u,Bug}$ and $\Delta\hat{h}_{u,Heck}$ respectively at the bank furthest from the vessel for design purposes.

The influence of the proximity to the bank on the return flow velocity is small and is disregarded. The design values are therefore obtained directly as described in 5.5.4.2 and 5.5.4.3.

5.5.4.5 Slope supply flow

A significant slope supply flow parallel to the bank occurs when stern waves break or in case of unbroken stern waves, if a vessel sails close to the bank. It is indicated by the area of spume travelling alongside the vessel, Figure 5.15.

The flow velocity u_{max}, occurring at the height of the revetment stones can reach the same velocity as the ship if the waves are very high. In the case of lower wave heights, the flow velocity depends above all on the ratio of the ship speed to the celerity of the breaking wave (calculated with the local water depth corresponding to the wave height) (characteristic $\tilde{Fr}$). The following approximation equation for u_{max} has been derived from data obtained in measurements performed on the Wesel-Datteln Canal by the Federal Waterway Engineering and Research Institute /BAW 2002/*:*

Maximum velocity of slope supply flow u_{max} [m/s]

$$\begin{cases} u_{max} \approx 0.3\, v_s & \text{for } \tilde{Fr}^2 > 1.83 \\ u_{max} \approx 0.3\, v_s + 0.7\left(1 - \frac{\tilde{Fr}^2 - 0.71}{1.12}\right) v_s & \text{for } 0.71 \leq \tilde{Fr}^2 \leq 1.83 \\ u_{max} \approx 1.0\, v_s & \text{for } \tilde{Fr}^2 < 0.71 \end{cases} \quad (5\text{-}33)$$

where

$\tilde{Fr}$ is the Froude number at the location of the maximum height of the stern waves [m]

$$\tilde{Fr}^2 = \frac{{v_s}^2}{g\, H_{u,Heck}}$$

$H_{u,Heck}$ is the maximum height of the stern waves [m] in accordance with 5.5.4.4, eq. (5-32) (design wave height)

v_s is the ship speed [m/s]

u_{max} is the maximum velocity of the slope supply flow at the height of the revetment stones [m/s]

An approach in which the roughness of the slope revetment is taken into consideration has been described by /*Verhey, Bogaerts 1989*/.

In addition to the characteristic $\tilde{Fr}$, the local Froude number and the ratio of the wave height $H_{u,Heck}$ to the stern wave length L_H, respectively to the bank distance u_{eff} (for the correlation see eq. (6-6) in 6.2), determine whether a significant slope supply flow will occur or not. Sailing tests carried out on the Wesel-Datteln Canal /*BAW 1994*/ have enabled to define a breaker criterion, see Figure 5.16. The Froude number is obtained from the maximum return flow velocity and maximum wave height at the stern in accordance with 5.5.4.3 and 5.5.4.4.

The equations given above and the breaker criterion can only provide an initial rough estimate. However, they show that waves break when a vessel sails close to the bank in particular and that there is a pronounced slope supply flow.

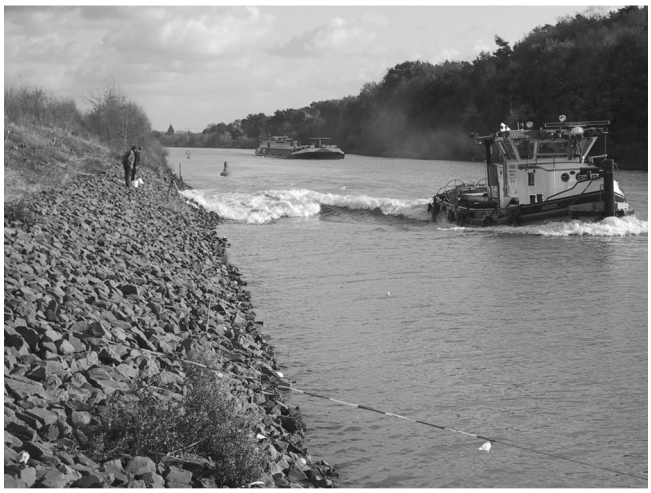

Figure 5.15 Slope supply flow for vessels sailing close to a bank. The photos show a laden inland cargo vessel (GMS) (top), an empty inland cargo vessel (GMS) (centre) and a tug boat (bottom) in a standard trapezoidal profile (T-Profil)

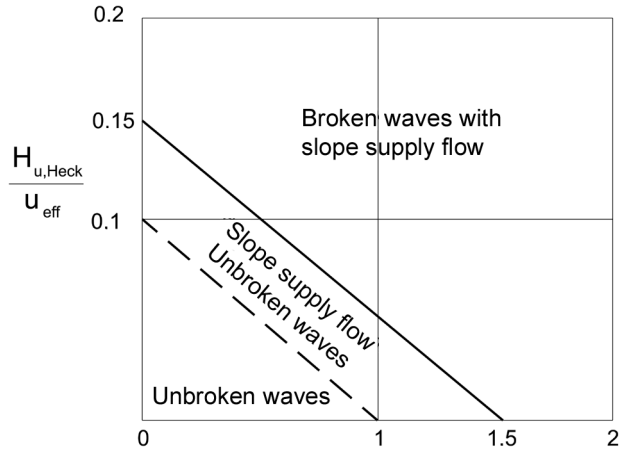

$$Fr^2 = \frac{(v_S + \hat{v}_{rück,\,u,\,Heck})^2}{g\,(h_m - H_{u,Heck})}$$

h_m	is the mean water depth [m]
$H_{u,Heck}$	is the maximum stern wave height disregarding the secondary wave height component [m]
u_{eff}	is the effective bank distance in accordance with figure 5.19
$\hat{v}_{rück,u,Heck}$	is the maximum return current velocity [m/s] at the bank near the stern
v_S	is the ship speed [m/s]
Fr	is the Froude number at stern [-]

Figure 5.16 Threshold between unbroken waves, waves without slope supply flow, waves with significant slope supply flow and fully broken waves with high slope supply flow at slopes for vessels sailing close to a bank (breaker criterion)

5.5.4.6 Increase in wave heights for vessels sailing with drift

Even when a vessel is sailing along a **straight stretch** a nautical drift angle β_D can occur between the axis of the ship and that of the canal. The drift angle can be taken to be approx. 2.1° (for large inland cargo vessels GMS) or approx. 1.25° (for push tow units with a length of 185 m) as stated in /*BMV 1994*/ (see Figure 5.17a).

The drift angle β_D is considerably larger when a vessel navigates a **bend** (see Figure 5.17b). It can be obtained from the relative position of the tactical centre of rotation c_F in accordance with Figure 5.17b. c_F is approximately equal to 0.9 for push tow units and approximately equal to 1.0 for large inland cargo vessels in shallow water as stated by /*Dettmann 1998*/. Reference should be made to /*Dettmann, Jurisch 2001*/ if the influence of currents is to be considered.

The effect of the drift angle is taken into account by defining a notionally enlarged plunged midship section $A_{S,eff,D}$ (boundary layer effects being disregarded).

Midship section $A_{S,eff,D}$ of a ship sailing with drift [m^2]

$$A_{S,eff,D} = \frac{(B + 0.25\, L \sin \beta_D)}{B} A_M \qquad (5\text{-}34)$$

where

A_M is the plunged midship section [m^2] (the boundary layer being disregarded)

B is the beam of the ship [m]

L is the length of the ship [m]

β_D is the drift angle [°]

The changes in the loads on the slope that occur when a ship sails with a drift angle are introduced into the design by means of $A_{S,eff,D}$ (instead of $A_{S,eff}$ in accordance with 5.5.1) and the eccentricity of the vessel, which is increased if appropriate (depending on the position of the stern), (as $A_{S,eff,D} > A_M$). The influence of the drift angle on the hydraulic design parameters is small for vessels sailing alone and is only relevant for long push-tow units. Both cases may need to be considered as it is not possible to decide in advance whether sailing with or without drift will be relevant to the design.

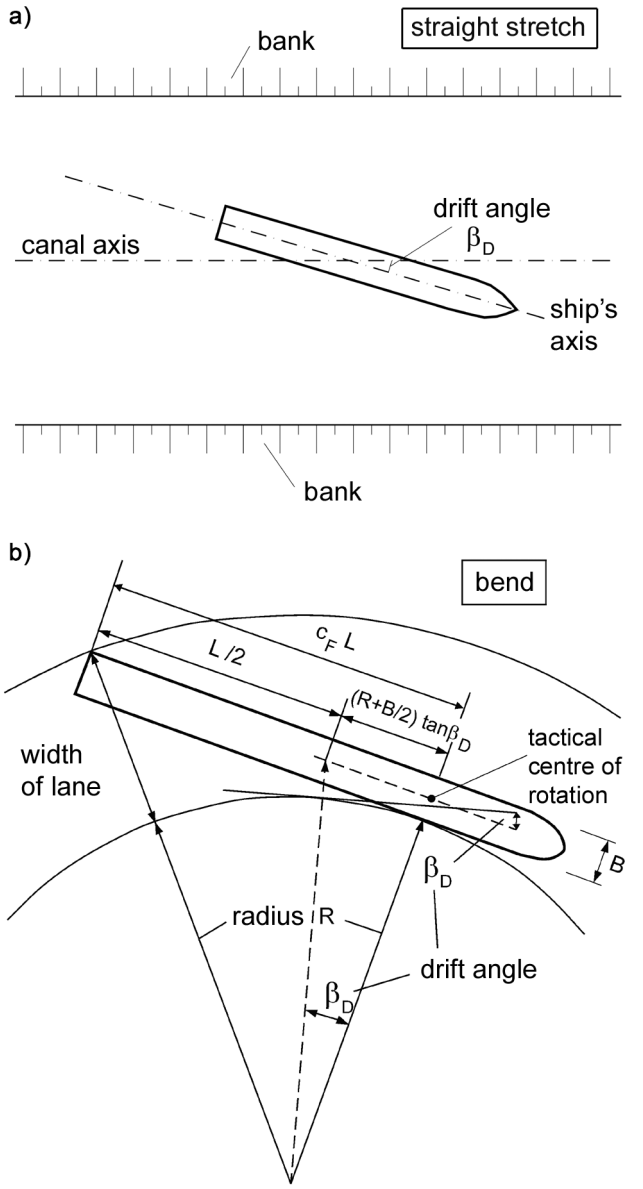

Figure 5.17 Diagram showing how to determine the drift angle on straight stretches (a) and on bends (b)

5.5.4.7 Drawdown velocity of ship-induced waves

A moving vessel will cause the water to flow around it, giving rise to backwater at the bow, drawdown and a stern wave owing to the local and temporal changes in the blockage ratios. The greatest wave heights $H_{u,Bug}$ and $H^*_{u,H}$ at the bank (depending on the water level in front of the ship at any given moment without the bow wave height and the rise in the water level caused by the ship), the associated drawdown time t_a and thus the drawdown velocity $\overline{v}_{za}$ must be known for geotechnical design considerations (see 5.10.3).

The following design values, which have been derived from measurements of the wave system at the bow

/BAW 2002/, are recommended for rough calculations (see Figure 5.18):

Average drawdown velocity at bow $\overline{v}_{za,B}$ [m/s]

$$\overline{v}_{za,B} = 0.12 \text{ m/s} \tag{5-35}$$

Associated drawdown time $t_{a,B}$ [s]

$$t_{a,B} = 5 \text{ s} \tag{5-36}$$

This values apply to vessels with a bulk full form sailing close to the bank at critical ship speed (ship's side over the toe of the slope).

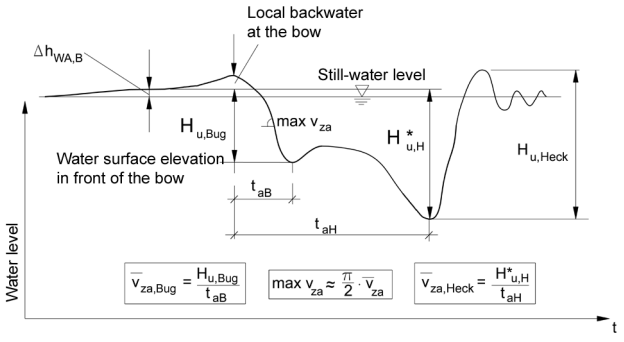

Figure 5.18 Correlation betweeen wave height $H_{u,Bug}$ or $H^{*}_{u,H}$ (corresponding to drawdown z_a in geotechnical calculations) and drawdown time t_a

The following approximation equation can be used for the minimum drawdown time at the bow $t_{a,B}$ (including the water surface elevation in front of the bow where $H_{u,Bug}$ as shown in Figure 5.18 is approximately equal to the height of the bow wave in accordance with 5.5.4.4, eq. (5-31)) for small bank distances in other situations:

$$t_{a,B} \approx C \frac{u_{eff}}{v_{SüG}} \tag{5-37}$$

where

C is a constant [-]
C = 1.7 for modern large inland cargo vessels
C = 1.5 for tugs
C = 1.3 for relatively old vessels with a full form

$t_{a,B}$ is the drawdown time at the bow [s] (see Figure 5.18)

u_{eff} is the effective bank distance [m] (distance between the ship's axis and the equivalent bank line at still-water level as shown in Figure 5.19)
N.B.: The equivalent bank line is situated in the centre of the remaining slope on the bank nearest the ship.

$v_{SüG}$ is the ship speed over ground [m/s] which is linked with the ship speed through water v_S and the flow velocity v_{Str} in accordance with eq. (5-20)

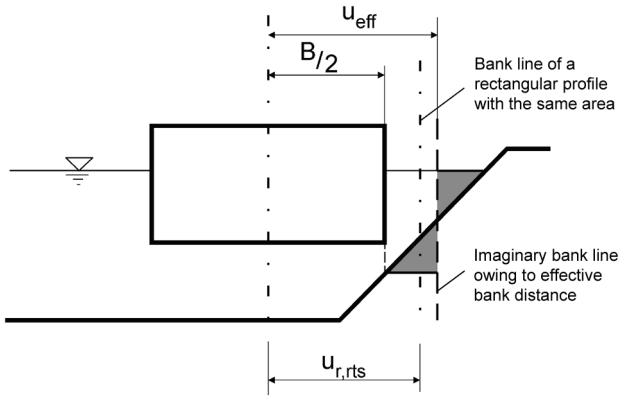

Figure 5.19 Definition of effctive bank distance u_{eff} (distance between ship's axis and equivalent bank line) in a symmetrical trapezoidal profile

The following equations apply to the effective bank distance in symmetrical trapezoidal profiles, depending on the position of the vessel (for definitionen cf. Figure 5.19):

- Smaller bank distances:

$$u_{r,rts} < \frac{B}{2} + \frac{mh}{2}:$$

$$u_{eff} = \frac{u_{r,rts}}{2} + \frac{mh}{4} + \frac{B}{4}$$

N.B.: The bilge line of the vessel must not pass over the slope.

- Larger bank distances:

$$u_{r,rts} \geq \frac{B}{2} + \frac{mh}{2}:$$

$$u_{eff} = u_{r,rts}$$

There is a limit to the reduction in the drawdown time, even when a vessel is sailing extremely close to a bank, as in this case the reduction is limited by the secondary wave system.
The following equation applies to the shortest possible drawdown time for $v_S / \sqrt{g h_m} < 0.8$:

$$t_{a,B} \geq t_{a,B,Sek} \tag{5-38}$$

where

$t_{a,B}$ is the drawdown time at the bow in general [s]

$t_{a,B,Sek}$ is the drawdown time of the secondary bow wave [s] in accordance with eq. (5-39)

The drawdown time of the secondary bow waves is calculated as follows:

$$\left\{ \begin{array}{l} t_{a,B,Sek} = \pi \dfrac{{v_S}^2}{g\, v_{SüG}} \text{ for transversal waves} \\ t_{a,B,Sek} = \dfrac{2}{3}\pi \dfrac{{v_S}^2}{g\, v_{SüG}} \text{ for diverging waves} \end{array} \right\} \quad (5\text{-}39)$$

The values determined using e.g. (5-39) also apply whenever secondary wave loads occur.

The stern wave system predominates in the case of vessels with a static trim by the stern, for instance during empty runs (runs with ballast) and small craft that can sail at relatively fast speeds, tugs or recreational craft. In this case, the drawdown between the bow and stern or the associated relevant wave height $H^*_{u,H}$ as shown in Figure 5.18, together with the associated drawdown time $t_{a,H}$, are relevant to geotechnical assessments. The following applies to $t_{a,H}$:

$$t_{a,H} \approx t_{a,B} + \frac{L_{pris}}{v_{SüG}} \quad (5\text{-}40)$$

where

L_{pris} is the length of the hull with a largely prismatic cross-section [m]

- $L_{pris} \approx 0.9\, L$ for push tow units with 2 lighters (2SV)
- $L_{pris} \approx 0.8\, L$ for large inland cargo vessels (GMS) and Europe ships (ES)
- $L_{pris} \approx 0.3\, L$ for recreational craft with a flat stern
- $L_{pris} \approx 0.0\, L$ for tugs

For $H^*_{u,H}$

$$H^*_{u,H} \approx 0{,}1\, H_{u,Bug} + H_{u,Heck} - \frac{1}{2} H_{Sek,q} \quad (5\text{-}41)$$

applies, where

$H^*_{u,H}$ is the relevant wave height near the bank at the stern [m] used to calculate the drawdown time

$H_{u,Bug}$ is the maximum bow wave height [m] at the bank for eccentric sailing in accordance with eq. (5-31)

$H_{u,Heck}$ is the maximum stern wave height [m] at the bank for eccentric sailing in accordance with eq. (5-32)

$H_{Sek,q}$ is the height of secondary transversal stern waves [m] in accordance with eq. (5-47)

The average drawdown velocity $\bar{v}_{za}$ is obtained by dividing the relevant wave height by the associated drawdown time.

5.5.5 Secondary waves

5.5.5.1 General

Vessels in motion generate diverging and transversal waves that originate at the bow and stern (Figure 5.20). It is these waves that form the secondary wave system. The waves are superimposed on each other and form pronounced interference lines at which the highest waves occur.

For Froude numbers based on depth $Fr_h = v_S / \sqrt{gh}$ up to 0.7, or up to 0.8 for rough estimates, the interference line is inclined towards the ship's axis at a Kelvin angle α_K of approx. 19°. The fronts of the diverging waves are inclined at an angle $\beta_W \approx 55°$ in relation to the ship's axis and thus in relation to the canal bank when the ship is sailing more or less parallel to the bank. The angle of impact of the diverging waves will be modified if the ship is not sailing parallel to the bank and this will have to be taken into consideration in the following equations.

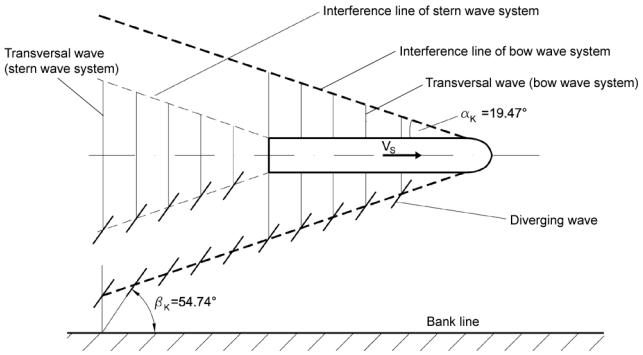

Figure 5.20 Secondary wave system for $Fr_h \leq 0.8$

The secondary waves diverge as they travel towards the bank, decreasing in height in the process. Transversal waves diminish to a greater extent than diverging waves. The three design cases described below must generally be taken into account as the transversal waves of the stern wave system are more pronounced than those of the bow wave system, particularly for short, fast ships and vessels on empty runs, although the diverging bow waves are larger than the diverging stern waves (see Figure 5.21).

The drawdown due to the return flow field may need to be taken into account in the case of high values of $\Delta\bar{h}$ when determining u or u'. In this case, u and u' are reduced by around $m\,\Delta\bar{h}_u$ ($\Delta\bar{h}_u$ in accordance with eq. (5-26) in 5.5.3).

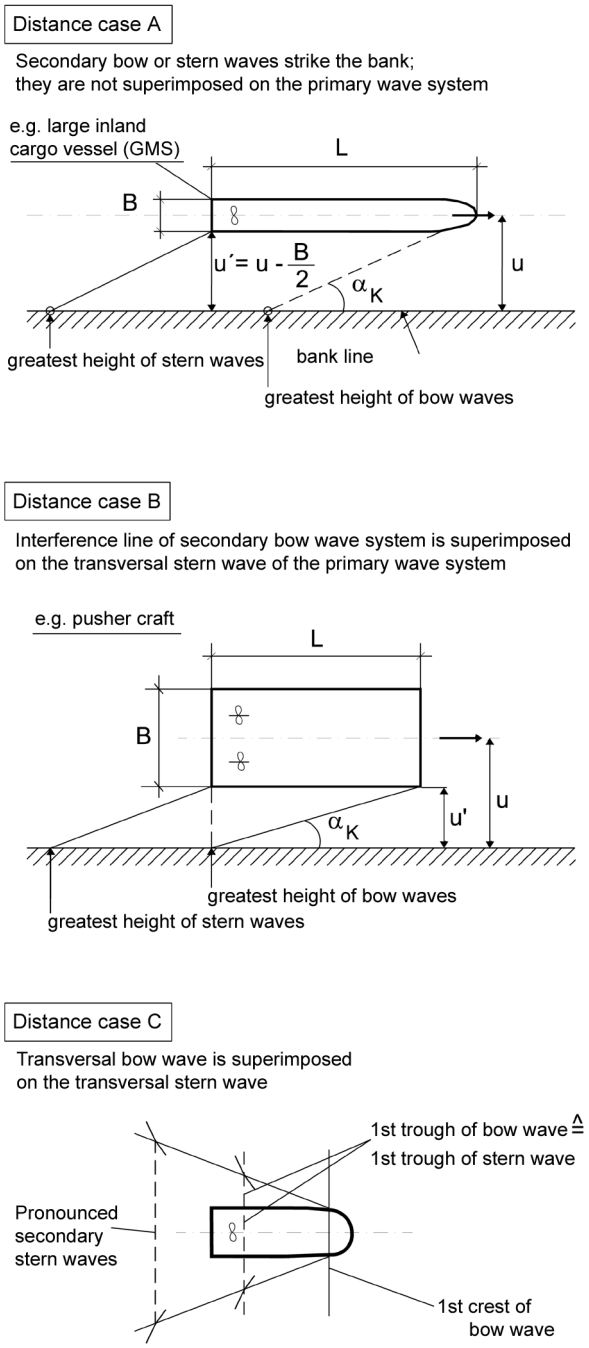

Figure 5.21 Standard distance cases for secondary waves

Distance case A

The primary and secondary wave systems are not usually superimposed on each other in a way that is relevant to the design where $u' < L \tan\alpha_K$, i.e. when they are generated by vessels that are long in relation to the width of the canal or for short bank distances (the standard situation for Europe ships (ES), large inland cargo vessels (GMS) and push tow units (SV) in canals). The heights of the secondary waves are obtained as described in 5.5.5.2. The stone size required for stabilisation of the slope can therefore be calculated separately for the primary and secondary wave fields (cf. 6.2 und 6.4).

Distance case B

The transversal stern wave of the primary wave system may be superimposed on the interferences of the secondary bow waves in wide canals or in the case of short vessels. This situation obtains where $u' = L \tan\alpha_K$. The wave height at the stern needed to determine the required size of the stones results from the superimposition of the secondary bow wave in accordance with in 5.5.5.2 and the transversal stern wave of the primary wave system in accordance with 5.5.4.4. As the length of the waves in the primary wave system differs from that of the waves in the secondary wave system, the entire height of the primary wave and half the height of the secondary wave are used in the design if the waves are superimposed.

Superimposed waves are particularly high when the bow is full or blunt, i.e. for pusher craft sailing alone, and when a vessel is moving at a speed close to the critical ship speed. The speed of pusher craft sailing alone or of large recreational craft may therefore need to be restricted in order to avoid very high wave loads on the banks, even though they only occur occasionally as a rule.

Distance case C

Short boats with powerful engines such as recreational craft may reach, and exceed, the sliding speed, even in confined fairways. The most unfavourable case as regards wave development, which coincides with the maximum power requirement, occurs when the ship reaches sliding speed. This happens when the wave-generating ship length L_W is equal to half the length of the secondary waves. In this case, the bow is at the first wave crest of the bow wave system while the stern lies in the trough of the bow wave and in the trough of the secondary stern wave system at the same time. The ship must travel “uphill”, so to speak, in its own secondary wave system. This special case is dealt with in in 5.5.5.2, eq. (5-47) and also in 5.5.5.4. The following equation applies:

$$\left\{ \begin{array}{l} \lambda_q \overset{!}{=} 2\,L_W \\ L_W \approx \beta_\lambda\, L \\ \lambda_q \approx 2\pi \dfrac{v_s^{\,2}}{g} \end{array} \right\} \qquad (5\text{-}42)$$

where

L is the ship length [m]

L_W is the wave generating ship length [m] (corresponding to the length at the waterline)

v_S is the ship speed [m/s]

β_λ is the coefficient for considering the wave-generating length of the ship [-]
$\beta_\lambda \approx 0.72$ for fast ships, in accordance with /*Horn 1928*/
$\beta_\lambda \approx 0.90$ for common types of inland navigation vessel and push-tow units

λ_q is the length of the transversal waves [m]

Eq. (5-42) can be used to calculate, for a given ship's length, the ship speed at which a ship, to which distance case C applies, starts to slide.

Transversal bow and stern waves are superimposed to a significant degree when λ_q exceeds 4/3 L_W.

5.5.5.2 Calculation of the heights of secondary waves

The following applies to the interference points of the diverging bow and stern waves in accordance with /*Blaauw et al. 1984*/ and /*Gates, Herbrich 1977*/:

Height of secondary waves H_{Sek} [m] at the interference line of diverging bow and stern waves

$$H_{Sek} = A_W \frac{v_s^{8/3}}{g^{4/3}\,(u')^{1/3}} f_{cr} \qquad (5\text{-}43)$$

where

A_W is the wave height coefficient [-], dependent on the shape and dimensions of the ship, draught and water depth

The following values can be used in rough calculations:

$A_W \approx 0.25$ for conventional inland navigation vessels and tugs

$A_W \approx 0.35$ for empty, single-line push tow units

$A_W \approx 0.80$ for fully laden, multi-line push tow units

f_{cr} is the coefficient of velocity [-] according to eq. (5-44)

g is the acceleration due to gravity [m/s^2]

H_{Sek} is the height of the secondary waves [m]

u' is the distance between the ship's side and the bank line [m]
$u' = u - B/2$ (cf. Figure 5.21)

The coefficient of velocity f_{cr} in eq. (5-43) accounts for the increase in the height of the secondary waves near the critical ship speed. The following approximation applies in analogy to the increase in the resistance of the ship, where the sheep speed approaches the wave celerity.

$$\begin{cases} f_{cr} \approx 1.0 \quad \text{for } v_s / v_{krit} < 0.8 \\ f_{cr} \approx 1.0 + 0.7\left\{\sin\left[\frac{2\pi}{0.8}\left(\frac{v_s}{v_{krit}} - 0.8\right)\right]\right\}^2 \\ \text{for } 0.8 \le v_s / v_{krit} \le 1.2 \end{cases} \qquad (5\text{-}44)$$

N.B.: sine (radian measure)

Strictly speaking, eq. (5-43) is only valid for such u' at which the secondary waves interfere at the bank. Because of irregularities of the ship path and the secondary wave system, eq. (5-43) appears generally, if u' fulfills the following condition:

$$u' \ge \frac{1}{2}\lambda_q \tan\alpha_K \qquad (5\text{-}45)$$

where

α_K is the Kelvin angle [°]

λ_q is the length of the transversal stern wave [m]
$\lambda_q \approx 2\pi\left(v_s^2/g\right)$

The length of the diverging waves is obtained as follows for $v_S/\sqrt{gh} < 0.8$:

$$\lambda_s = \frac{2}{3}\lambda_q \qquad (5\text{-}46)$$

where

λ_S is the length of the diverging wave [m]

λ_q is the length of the transversal stern wave [m]
$\lambda_q \approx 2\pi\left(v_s^2/g\right)$

The following applies to pure transversal stern waves:

Height $H_{Sek,q}$ [m] of pure secondary transversal stern waves

$$H_{Sek,q} = A_W \frac{v_s^2}{g}\left(\frac{B}{2\,u}\right)^{1/2}\left(f_{cr} + f_\lambda\right) \qquad (5\text{-}47)$$

where

A_W is the wave height coefficient [-] in accordance with eq. (5-43)

B is the beam [m]

f_{cr} is the coefficient of velocity [-] (see eq. (5-44))

f_λ is the coefficient of wave length [-] (see eq. (5-48))

u is the distance between the ship's axis and bank line [m] (cf. Figure 5.19 and Figure 5.21)

v_S is the ship speed through water [m/s]

The coefficient of wave length f_λ covers the superimposition of the transversal stern waves and the transversal bow wave. The following equation applies:

$$\left\{ \begin{array}{l} f_\lambda \approx 0 \qquad \text{for } \lambda_q \le \frac{4}{3} L_W \\ \\ f_\lambda = 0.9 \sin\left\{ \pi \left(\frac{2\,L_W}{\lambda_q} - \frac{1}{2} \right) \right\} \\ \qquad \text{for } \frac{4}{3} L_W \le \lambda_q \le 2\,L_W \end{array} \right\} \qquad (5\text{-}48)$$

N.B.: sine (radian measure)

The following restriction applies to the heights of secondary waves previously determined by means of eqs. (5-43) and (5-47) as such waves break when they exceed a certain steepness:

$$H_{Sek} \text{ or } H_{Sek,q} \le \lambda_{Sek} / 2\pi \qquad (5\text{-}49)$$

Eqs. (5-43), (5-47) and (5-49) form the basis of the calculations in chapter 6. They are used to obtain the wave heights that have not been deformed by the vicinity of the bank (wave height near a bank).

Secondary waves approaching a bank are deformed by the decrease in the depth of the water. This behaviour is extremely complex. By way of simplification, it can be said that the influence of the bank is taken into account indirectly for the slope inclinations considered here, i.e. between 1:2 and 1:5, by using the wave height near the bank in the derivation of the design equations, for example for the required size of stones.

5.5.5.3 Additional secondary waves in analogy to an imperfect hydraulic jump

Even before the critical ship speed is attained a Froude number of 1.0, calculated by considering the maximum local return flow velocity and the drawdown can be reached in the vicinity of the ship. Because the Froude number is lower than one behind the ship, there will be a flow transition in the stern region of the ship. The latter is combined with a stable hydraulic jump roller - the breaking transversal stern wave – only in case of higher ship speeds and thus at higher Froude numbers. In the range of speeds considered here, additional large transversal stern waves may occur in the case of an imperfect hydraulic jump (see Figure 5.22). Their transverse propagation corresponds to the transversal stern wave. In a first approximation, their height, which interferes with the transversal stern wave of the primary wave system as described in 5.5.4.4, can be determined from eq. (5-47) for secondary transversal waves.

The height of such waves is also limited as follows for energy-related reasons and owing to the fact that they break when they become very steep:

$$H_{Sek} \le \frac{v_S^{\,2}}{g} \qquad (5\text{-}50)$$

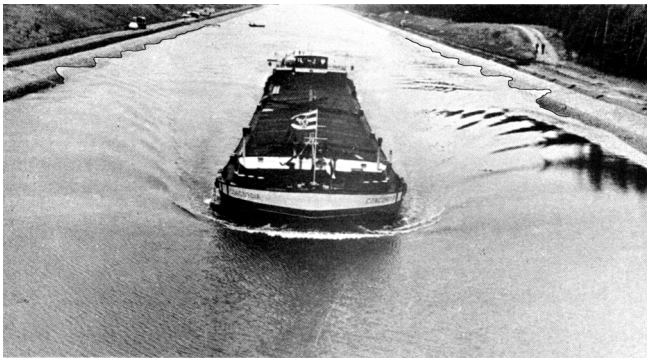

Figure 5.22 MS Concordia sailing on the Main-Danube-Canal (measurements taken at Kriegenbrunn) close to the critical ship speed (v_S = 12 km/h) /Schäle, Mollus 1971/

5.5.5.4 Secondary waves caused by small boats at sliding speed and when sailing close to a bank

According to */Przedwojski et al. 1995/,* the sliding speed $v_{S,gl}$ of small recreational craft designed to slide can be estimated as follows:

$$v_{S,gl} = 0.37 \sqrt{g\,L} \qquad (5\text{-}51)$$

where

L the length of the recreational craft [m]

$v_{S,gl}$ is the sliding speed [m/s]

The greatest wave height at the interference points of the diverging waves of the stern wave system is calculated as follows where $v_s = v_{S,gl}$:

$$H_{\mathrm{Sek,gl}} \approx 1.4\, T \left(\frac{L}{u}\right)^{1/3} \tag{5-52}$$

where

$H_{\mathrm{Sek,gl}}$ is the height of secondary waves for vessels sailing at sliding speed [m]

T is the draught of the recreational craft [m]

u is the bank distance [m]

The greatest wave height occurs at a bank distance u^* at which the first group of interference waves strikes the bank:

$$u^* \approx 0.5\, B + 0.4\, L \tag{5-53}$$

The permissible ship speed through water can be estimated as follows by specifying a tolerated wave height in order to avoid the great wave heights associated with interference waves:

$$v_{\mathrm{S,zul}} = v_{\mathrm{S,gl}} \sqrt{\frac{H_{\mathrm{tol}}}{H_{\mathrm{Sek,gl}}}} \tag{5-54}$$

where

H_{tol} is the tolerated wave height [m]

$v_{\mathrm{S,zul}}$ is the permissible ship speed through water [m/s]

5.5.6 Passing and overtaking

Situations in which two ships **pass** each other occur frequently. The ships will usually approach each other at reduced speed and then accelerate when the last thirds of the ships are opposite each other to prevent the sterns from coming into contact. The associated loads on revetments can be approximated by considering the following limiting case:

The two vessels are sailing at the same speed when they pass each other. Each vessel generates its own return flow field in the associated part of the canal or river cross-section. In a first approximation, this limiting case can be dealt with by considering the ships to be sailing in the same direction and adding the plunged midship sections together. The overall canal cross-section is the reference cross-section.

The other situation on canals, which rarely occurs, is **overtaking** in which one ship (usually at its maximum draught) is moving very slowly and the other (usually empty) is travelling very fast, see case (1). A special case occurs when both vessels sail next to each other at approximately the same speed for a short period of time, see case (2). Two limiting cases can therefore be assumed:

(1) The ship that is being overtaken is stationary; the ship that is overtaking will generally pass it at 0.8 v_{krit} (of a single ship alone in the original canal cross-section). In this case, the first ship is sailing in a canal cross-section that has been reduced by the cross-sectional area of the second ship. The recommended design value of the relative speed of the ship that is overtaking, 0.8 v_{krit}, (relative to the original canal cross-section) may even exceed 1.0 v_{krit} (relative to the reduced canal cross-section) in the smaller canal cross-section. If this is the case, a value of 1.0 v_{krit} (relative to the reduced canal cross-section) must be assumed.

(2) Both ships are moving at approximately the same speed, 0.8 v_{krit} (of a single ship in the original canal cross-section). The relevant plunged cross-sectional area is equal to the sum of the cross-sectional areas of both ships. The speed 0.8 v_{krit} of one of the ships may exceed 1.0 v_{krit} of both ships together, in which case the latter must be used in the design.

5.6 Hydraulic actions on waterways due to flow caused by propulsion (propeller wash)

The following sections refer to canals without a ground swell, the latter being considered in 6.3.

5.6.1 Induced initial velocity of the propeller jet for stationary vessels (ship speed v_s = 0)

The induced initial velocity of a propeller is calculated for a ship speed v_s equal to zero (propeller advance ratio J = 0). This applies to bollard pull propeller test conditions or manoeuvres under similar conditions and is based on the methods described below.

- **Unducted propellers** (see Figure 5.23)

Maximum induced initial velocity v_0 in accordance with the simplified momentum theory [m/s]

$$v_0 = 1.60\, f_{\mathrm{N}}\, n_{\mathrm{Nenn}}\, D \sqrt{K_{\mathrm{T}}} \tag{5-55}$$

where

D is the diameter of the propeller [m] (taken from Table 5.1)

f_{N} is the factor for the applicable propeller rotation rate [-]

Value recommended in /*EAU 1996*/:

$f_{\mathrm{N}} \approx 0.75$ for start-off manoeuvres from standing

K_{T} is the thrust coefficient of the propeller for J = 0 [-]

n_{Nenn} is the design propeller rotation rate [1/s]
see Table 5.1
N.B.: Values in Table 5.1 are given in [1/min]

v_0 is the induced initial velocity after contraction of the jet [m/s]

The induced initial velocity v_0 of unducted propellers reaches its maximum value at a distance of D/2 behind the plane of the propeller where the maximum contraction of the jet occurs. The diameter of the jet for unducted propellers at this point is:

$$d_0 \geq \frac{D}{\sqrt{2}} \tag{5-56}$$

where

d_0 is the jet diameter at the point of maximum contraction [m]

D is the propeller diameter [m] as stated in Table 5.1

The upper limit of K_T can be estimated as follows (in accordance with /*Peters 2002*/):

$$K_T = 0.55 \cdot \frac{P}{D} \quad \text{for} \left\{ \begin{matrix} 0 < \frac{P}{D} < 1.4 \\ J = 0 \end{matrix} \right\} \tag{5-57}$$

where

P is the design pitch [m]

P/D is the design pitch ratio [-]

$P/D \approx 0.7$ for inland navigation vessel
$P/D \approx 1.0$ for pusher craft

A polynomial approximation obtained from tests /*Oosterveld, Oossannen 1975*/ can be applied if, in addition to P/D, the ratio of the areas A_A / A_0 (A_A – area of approach flow in front of the propeller, A_0 – cross-sectional area at the narrowest contraction behind the propeller; see Figure 5.23) and the number of blades on the propeller z are known. Calculation programmes (e.g. /*PROFIX 2002*/) may also be used if sufficient geometric data are available.

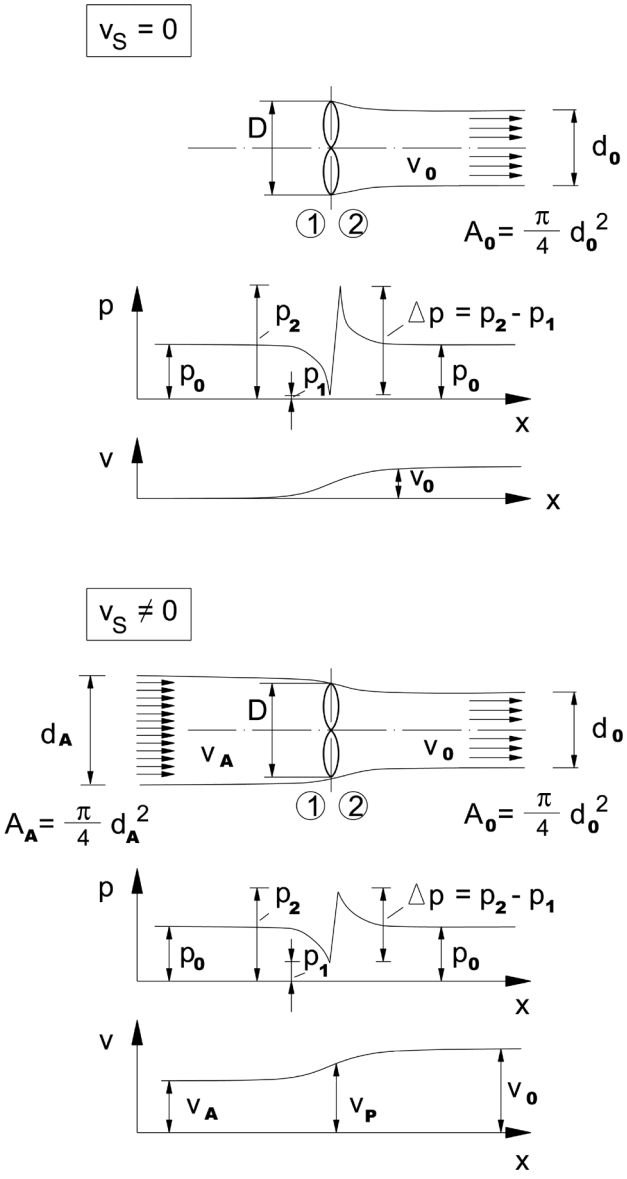

Figure 5.23 Unducted propeller as the ideal thrust accelerator (a) $v_S = 0$, (b) $v_S \neq 0$
Top: change in velocity as water flows through the propeller
Middle: associated pressures
Bottom: associated velocities

- **Ducted propellers**

Maximum induced initial velocity v_0 due to the ducted propellers [m/s]

$$v_0 = 1.60 \sqrt{0.5}\, f_N\, n_{Nenn}\, D \sqrt{K_{T,DP}} \tag{5-58}$$

where

$K_{T,DP}$ is the thrust coefficient of ducted propeller system as a whole for $J = 0$ [-]

The upper limit of K_T can be estimated as follows (in accordance with /*Peters 2002*/):

$$K_{T,DP} = 0.67 \cdot \frac{P}{D} \quad \text{for} \left\{ \begin{array}{l} 0 < \frac{P}{D} < 1.8 \\ J = 0 \end{array} \right\} \tag{5-59}$$

A polynomial approximation obtained in tests /*Yosifov et al. 1986*/ can also be used in this case to calculate K_T if, in addition to *P/D*, the ratio of the areas A_E / A_0 (A_E – area of inlet into the propeller plane, A_0 – cross-sectional area at the narrowest contraction behind the propeller) and the number of blades on the propeller *z* are known. The calculation programme /*DVPFIX 2002*/ may be used if sufficient geometric data are available.

- **Approximation calculation** based on **installed engine power**

Maximum induced initial velocity v_0 due to the installed engine power [m/s]

$$v_0 = C \left(\frac{f_P \, P_{d,Nenn}}{\rho_W \, D^2} \right)^{1/3} \tag{5-60}$$

where

C is a coefficient [-]

$C \approx 1.2$ - 1.4 for ducted propellers
$C \approx 1.5$ for unducted propellers

f_P is the factor for the applicable engine power [-]

Value recommended in /*EAU 1996*/:

$f_P \approx 0.42$ for start-off manoeuvres from standing ($f_P \approx f_N{}^3$)

$P_{d,Nenn}$ is the nominal power per propeller [W]
see Table 5.1
N.B.: The values in Table 5.1 are stated in [kW]

v_0 is the induced initial velocity [m/s] (after contraction of jet)

ρ_W is the density of water [kg/m^3]

5.6.2 Velocity of the propeller jet at ship speed $v_S \neq 0$

The propeller inflow velocity (propeller advance ratio $J \neq 0$) increases as a ship gathers speed. The velocity of the propeller jet also changes, to v_{0J}. The value of v_{0J} for unducted propellers initially diminishes slightly with increasing ship speed in relation to v_0 (in relation to the ship) for low propeller advance ratios, after which it increases. The increase depends essentially on the design pitch ratio *P/D* of the propeller, with the values of v_{0J} returning to approximately v_0 in the *P/D* range relevant to actual practice as the propeller advance ratio increases. The reduction does not occur at low propeller advance ratios in the case of ducted propellers.

$$v_{0J} \approx v_0$$

applies to unducted propellers and ducted propellers alike.

More exact estimates of the upper limit of the thrust coefficients K_{TJ} and $K_{T,DPJ}$ and thus the jet velocity v_{0J} are possible if *D*, *n* and *P/D* are known for the propeller:

- **Unducted propellers**

$$K_{TJ} = 0.55 \frac{P}{D} - 0.46 J \tag{5-61}$$

Induced initial velocity of jet v_{0J} [m/s] for an unducted propeller at any ship speed

$$v_{0J} = \frac{\sqrt{\left(J^2 + 2.55 K_{TJ} \right)}}{\sqrt{1.40 \frac{P}{D}}} v_0 \tag{5-62}$$

- **Ducted propellers**

$$K_{T,DPJ} = 0.67 \frac{P}{D} - 0.77 J \tag{5-63}$$

Induced initial velocity of jet v_{0J} [m/s] for a ducted propeller at any ship speed

$$v_{0J} = \frac{J + \sqrt{\left(J^2 + 5.10 K_{T,DPJ} \right)}}{\sqrt{3.41 \frac{P}{D}}} v_0 \tag{5-64}$$

$$J = \frac{v_A}{n \, D} = \frac{v_S (1 - w)}{n \, D} \tag{5-65}$$

where

D is the propeller diameter [m]

J is the advance ratio of the propeller [-]

$K_{T,DPJ}$ is the thrust coefficient of a ducted propeller at $J \neq 0$ [-]

K_{TJ} is the thrust coefficient of an unducted propeller at $J \neq 0$ [-]

n is the propeller rotation rate [1/s]

P is the design pitch [m]

P/*D* is the design pitch ratio [-]

v_S is the ship speed [m/s]

v_A is the velocity of the propeller in flow [m/s]

v_0 is the induced initial velocity at $J = 0$ [m/s]

v_{0J} is the induced initial velocity of the propeller jet at $J \neq 0$ [m/s] (in relation to the ship)

w is the wake factor [-]
$w \approx 0.3$

Calculation programmes (such as */DVPFIX 2002; PROFIX 2002/*) may be used for ducted and unducted propellers if sufficient geometric data are available.

5.6.3 Jet dispersion characteristics

5.6.3.1 Standard jet dispersion situations

The geometry of the jet depends primarily on the following conditions:

- rudder configuration
- limitation of the dispersion area due to quay walls beside the ship and in the direction of jet dispersion

These conditions are considered under the standard situations described below (see Figure 5.24).

- **Standard situation 1 (no splitting of the jet)**

Propeller without a middle rudder located behind it; the jet is restricted by the depth of the water but there are no lateral limits to the dispersion of the jet.

The jet is dispersed

- along the jet axis being diverted towards the bed of the river or canal at an angle α_0 of approx. 2.5° for unducted propellers
- along the jet axis being diverted towards the bed at an angle α_0 of approx. 0° for ducted propellers and vessels with a tunnel stern
- in all cases, at an angle of the outer jet boundary α_0 of approx. 13° (defined at the v_{xr}/v_{xmax} = 0.1 location in accordance with eq. (5-74))

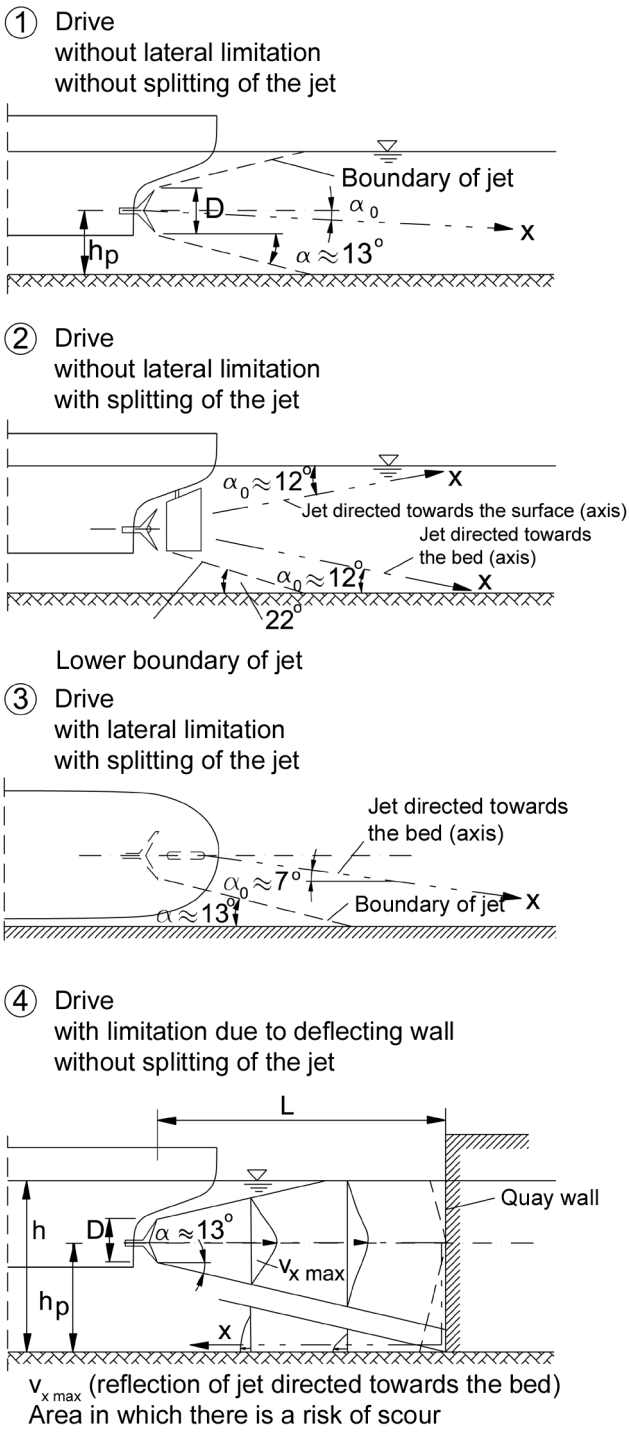

Figure 5.24 Standard jet dispersion situations

The following applies to the increase in the diameter of the jet cone:

Increase in the diameter of the jet cone d_x [m]

$$d_x = D + 2x \tan\alpha \qquad (5\text{-}66)$$

where

x is the distance from the plane of the propeller [m]

α is the angle of the outer jet boundary [°]

There is no division of the jet for ducted propellers with a middle rudder located behind them. In this case, standard situation 1 applies.

- **Standard situation 2 (jet splitting)**

Unducted propeller with a middle rudder located behind it; jet splitting is limited by the depth of the water but not laterally.

The angular momentum causes the jet to split at the rudder into a jet that is directed towards the bed of the waterway and another jet that is directed towards the water surface, the former giving rise to the relevant hydromechanical loads. The jets are dispersed

- by the axes of the jets being diverted towards the bed of the waterway and towards the water surface respectively at angles α_0 of approx. 12°
- at an angle of the outer jet boundary α_0 of approx. 10° to the axes of the two jets directed towards the bed and the surface of the waterway respectively

- **Standard situation 3 (jet splitting)**

Unducted propeller with a middle rudder located behind it; additional lateral limitation of jet dispersion (by quay wall).

When a vessel casts off from a vertical wall, the jet is divided. At the same time, the jet is diverted towards the lateral boundary. The jet directed towards the bed is dispersed

- by the axis of the jet being diverted laterally towards the quay wall at an angle α_0 of approx. 7° (horizontally)
- at angles of the outer jet boundary α_0 of approx. 13° horizontally and approx. 12° vertically

- **Standard situation 4 (no jet splitting)**

Ducted propeller (also with a middle rudder) or unducted propeller without a middle rudder located behind it; dispersion of the jet is limited vertically in the direction of propagation (e.g. by a quay wall).

The jet is deflected by the wall to the sides and towards the bed of the waterway where it is deflected again. The jet is dispersed

- without the jet axis being diverted towards the bed (α_0 being approx. 0°)
- at an angle of the outer jet boundary α_0 of approx. 13°
- at angles of the outer jet boundaries α_0 of the deflected jets and the jet reflected off the bed of approx. 13°

- **Other situations**

The standard situations described above do not include all possible load situations. Intermediate situations can be covered by selecting the appropriate parameters.

5.6.3.2 Characteristics of the decrease in the main velocity

The characteristic quantity of the propeller jet is the main velocity $v_{x,max}$ that is reached on the jet axis at a distance x from the propeller plane. It is required for the calculation of the entire three-dimensional velocity field acting on the surfaces of the fairway

- with reference to the induced initial velocity v_0 (see 5.6.1) or v_{0J} (see 5.6.2),
- from the relative decrease in the main velocity v_{xmax}/v_0 = function of (x/D) and
- in conjunction with the radial velocity distribution assumed in accordance with the normal distribution law and the relevant standard jet dispersion situation (see 5.6.3.3).

The velocity v_0 must be substituted by the reference velocity v_{0J} (cf. 5.6.2) in the following equations (5-67), (5-68), (5-70) and (5-73) whenever the ship speed v_S is greater than 0.

The reduction in the main velocity can be divided into three sections:

(1) Main velocity in the approach area ($x/D \leq 2.6$ from the propeller plane) for all standard situations

Main velocity v_{xmax} in the approach area [m/s]

$$\frac{v_{xmax}}{v_0} = 1 \qquad (5\text{-}67)$$

(2) Area in which dispersion of the jet is not obstructed by the water level, bed or any lateral boundaries ($2.6 < x/D \leq x_{gr}/D$) for all standard situations

Main velocity v_{xmax} for unobstructed jet dispersion [m/s]

$$\frac{v_{xmax}}{v_0} = 2.6 \left(\frac{x}{D}\right)^{-1} \qquad (5\text{-}68)$$

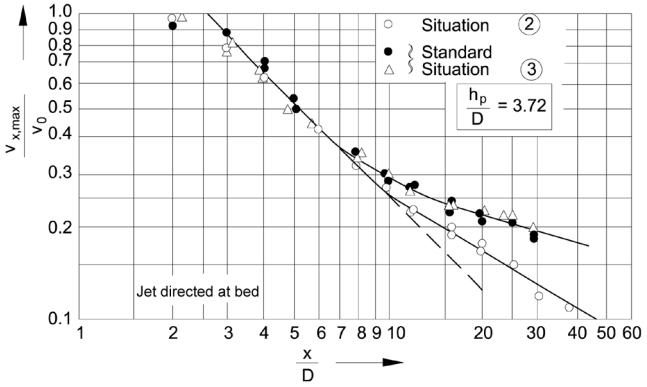

Figure 5.25 Characteristics of the decrease in the main velocity for $h_p/D = 3.72$

The point at which the dispersion of the jet is obstructed by the bed of the river or canal is located at a distance x_{gr} behind the plane of the propeller. The following applies:

$$\frac{x_{gr}}{D} = \left(\frac{A}{2.6}\right)^{1/(a-1)} \qquad (5\text{-}69)$$

where

a, A are quantities depending on the "standard situation" of the jet dispersion field, the design of the stern of the vessel and the propeller/rudder configuration [-], see (3) below

D is the propeller diameter [m]

x_{gr} is the distance beyond which the dispersion of the jet is obstructed [m]

(3) Area of jet dispersion influenced by the water level, bed of the river or canal and lateral boundaries ($x/D > x_{gr}/D$)

Central speed v_{xmax} for obstructed jet dispersion [m/s]

$$\frac{v_{x\,max}}{v_0} = A \left(\frac{x}{D}\right)^{-a} \qquad (5\text{-}70)$$

where

a, A are quantities depending on the "standard situation" of the jet dispersion field, the shape of the stern of the vessel and the propeller/rudder configuration [-]

The following applies to the exponent *a*, depending on the standard situation:

a = 0.6 where jet dispersion is limited by the bed and the water level (standard situation 1, standard situation 2 (jet directed at the bed) and standard situation 4 for $x \leq L$ (approach area up to quay wall))

a = 0.3 where jet dispersion is limited by an additional lateral wall (standard situations 3 and 4)

a = 0.25 for jet dispersion behind a twin-screw drive (only if it is treated as a single-screw drive)

a = 1.62 for the dispersion of the jet reflected from the bed in front of a quay wall (standard situation 4, for $x > L + h_p$ (deflection area at quay wall)

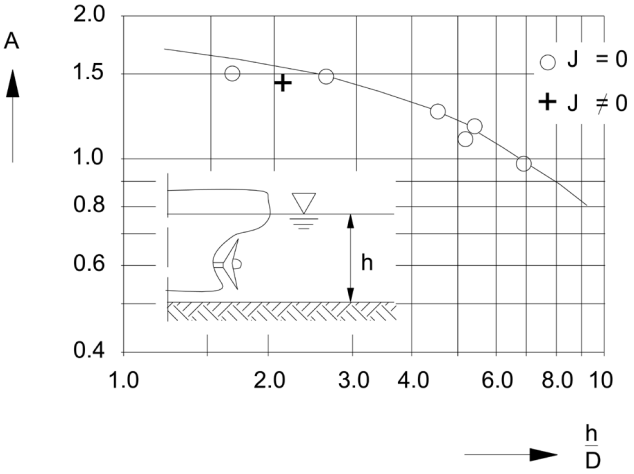

Figure 5.26 Coefficient A = function of (h/D) (standard situation 1)

The following applies to coefficient *A*:

(1) For jet dispersion limited only by the bed and water level behind a propeller without division of the jet, i.e. for propellers without a middle rudder located behind them or for ducted propellers (in this case also with a middle rudder located behind the propeller) for $1.0 \le h/D \le 9$ (standard situation 1, see Figure 5.26):

$$A = 1.88\ e^{-0.092\ (h/D)} \qquad (5\text{-}71)$$

where

h is the water depth [m]

(2) For a splitted jet by the middle rudder located behind the propeller ($0.7 \le h_p/D \le 5$) (standard situations 2 and 3, see Figure 5.27):

$$A = 1.88\ e^{-0.061\left(h_p/D\right)} \qquad (5\text{-}72)$$

where

h_p is the height of the propeller axis above the bed [m]

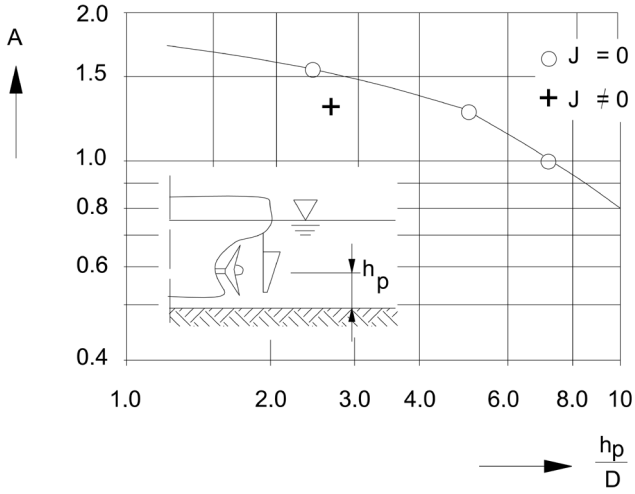

Figure 5.27 Coefficient A = function of (h_p/D) (standard situation 2)

(3) For twin-screw drives $A = 0.9$ = constant (approximation) (the interaction of the jets outweighing the influence of the water depth).

(4) Where the dispersion field is limited by a deflecting wall located in the direction of propagation of the jet (for the jets reflected from the bed and wall, $x \ge L+h_p$), (standard situation 4, see Figure 5.28):

$$A = \left(\frac{v_{x\max}\ (L)}{v_0}\right)\left(\frac{L+h_p}{D}\right)^{1.62} \qquad (5\text{-}73)$$

where

h_p is the height of the propeller axis above the bed (length of the jet deflected downwards at the wall, measured from wall to bed) [m]

L is the distance between the deflecting wall and the plane of the propeller [m]

D is the propeller diameter [m]

$v_{xmax}(L)$ is the main velocity at distance L behind the plane of the propeller [m/s]

The jet velocity relevant to scour at the toe of the quay wall is taken as the velocity occurring at the point where $x = L$ (see Figure 5.28).

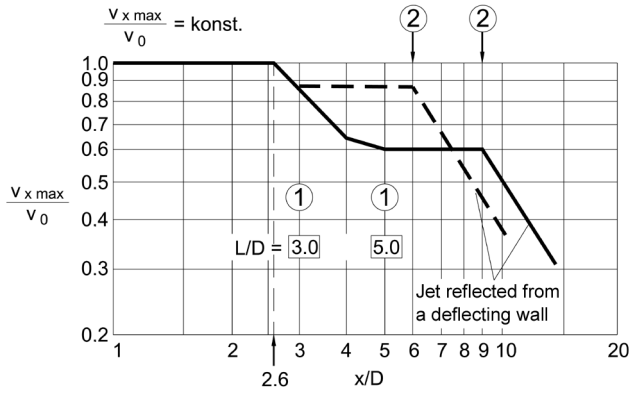

① Point of impact on the deflecting wall

② Point of impact on the bed

Figure 5.28 Jet dispersion characteristics for an ocean-going vessel with a twin-screw drive where the jet is reflected from a deflecting wall, for L / D = 3.0 and 5.0 (standard situation 4) /Römisch 1975/

5.6.3.3 Calculation of the distribution of the jet velocity orthogonal to the jet axis

The distribution of the jet velocity v_{xr} orthogonal to the jet axis in the area of jet impact is governed by

- the position of the jet axis above or at the bed at a distance x from the plane of the propeller (see 5.6.3.1) and
- the main velocity v_{xmax}

  N.B.: v_{xmax} is calculated in eqs. (5-67), (5-68), and (5-70) with

  $\rightarrow v_0$ where $v_S = 0$ bzw. $J = 0$

  $\rightarrow v_{0J}$ where $v_S \ne 0$ bzw. $J \ne 0$

taking into account the radial velocity distribution:

$$\frac{v_{xr}}{v_{x\max}} = e^{-22.2\ (r_x/x)^2} \qquad (5\text{-}74)$$

where

r_x is the radial distance of the considered point, e.g. the bed, from the jet axis at a distance x from the plane of the propeller [m]

v_{xr} is the jet velocity relative to the ship at a distance of radius r_x [m/s]

The jet velocity v_{xr1} at and relative to the bed, taking the ship speed into account, is calculated as follows:

$$v_{xr1} = v_{xr}\left(1-\frac{v_S}{n\,D}\right) \tag{5-75}$$

where

D is the diameter of the propeller [m]

n is the propeller rotation rate [1/s]

v_{xr} is the jet velocity relative to the ship at a distance of radius r_x [m/s]

v_S is the ship speed [m/s]
note: v_s is negative if the movement of the ship and the propeller jet point in the same direction, e.g. when the vessel is stopping.

The following correlation between r_x, x and h_p is obtained for loads on a plane river or canal bed (cf. Figure 5.29):

$$r_x = \left(h_p - x\,\sin\alpha_0\right)/\cos\alpha_0 \tag{5-76}$$

$$x_S = x\,\cos\alpha_0 - r_x\,\sin\alpha_0 \tag{5-77}$$

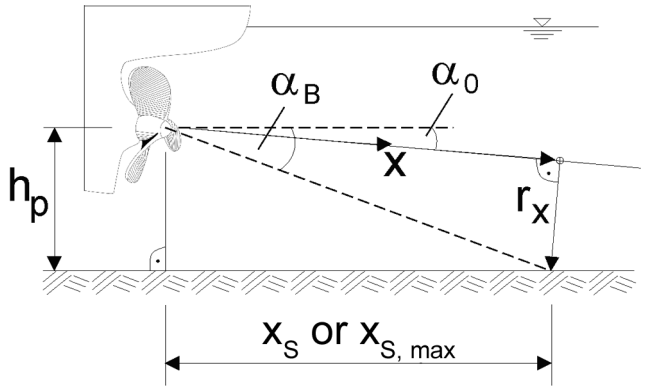

Figure 5.29 Geometrical definitions for the calculation of the distributions of near bed flow velocities orthogonal to the jet axis

The near bed flow velocity calculated using eqs. (5-74) to (5-77) initially increases in the x-direction, before diminishing again. The maximum near bed flow velocity v_{xr} is referred to as v_{Bmax} for the purpose of determining the size of the stones. The following equation can be used to calculate the position of the maximum near bed flow velocity for rough estimates:

$$x_{S,max} = \frac{h_p}{\tan\alpha_B} \tag{5-78}$$

where

h_p is the height of the propeller axis above the bed [m]

$x_{S,max}$ is the position of the maximum near bed flow velocity behind the rotation centre of the propeller plane [m]

α_B is the mean angle of diversion
α_B = 8.5° for standard situations 1 and 4 for $x_{S,max} < L$
α_B = 13° for standard situations 2 and 3 (see 5.6.3.1)

Allowance for the influence of the propeller advance ratio on v_0 and thus on v_{xmax} and v_{Bmax} has already been made in eqs. (5-61) to (5-65). However, the velocity of the impact on the bed of the waterway is also affected by the propeller advance ratio and is calculated approximately by eq. (5-80).

The standard situations describing the jet dispersion characteristics in 5.6.3.1 can be used to determine the loads on slopes rising in the same direction as the jet. The maximum flow velocity at the bed and slope must be determined by eq. (5-74), taking account of the geometrical boundary conditions shown in Figure 5.30 and Figure 6.4 and in accordance with eq. (6-8). A meaningful assumption of the largest angle between the ship's axis and the bank line must be made. Large angles occur when ships navigate bends, for example.

When a ship casts off, the jet strikes the bank after being deflected at the rudder. The smallest angle relevant to the design, β_{St}, between a perpendicular to the slope line and the axis of the deflected jet (see Figure 6.4) may be 15°. The deflection of the jet reduces the jet velocity to around 85 % of its initial value at the propeller.

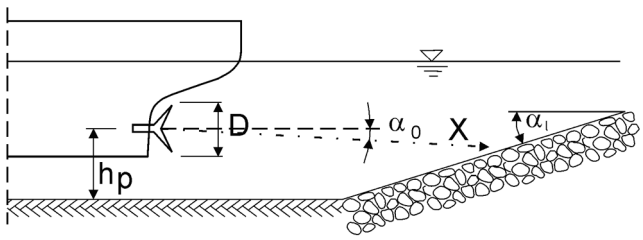

Figure 5.30 Diagram showing the impact of a jet on a sloping bank (longitudinal slope angle α_l see also 6.3.1)

5.6.3.4 Multi-screw drives

In the case of multi-screw drives, the jet dispersion for each propeller must first be considered separately by means of the algorithms given in 5.6.1 to 5.6.3.3 in accordance with /*Römisch 1994*/. The parameter *a* must be chosen as if there were two single-screw drives ($a \neq 0.25$). The values of v_{xr} can be added by way of approximation in order to determine how the drives act in combination. The geometrical boundary conditions shown in Figure 5.31 result for α_0 = 0° in standard situation 1.

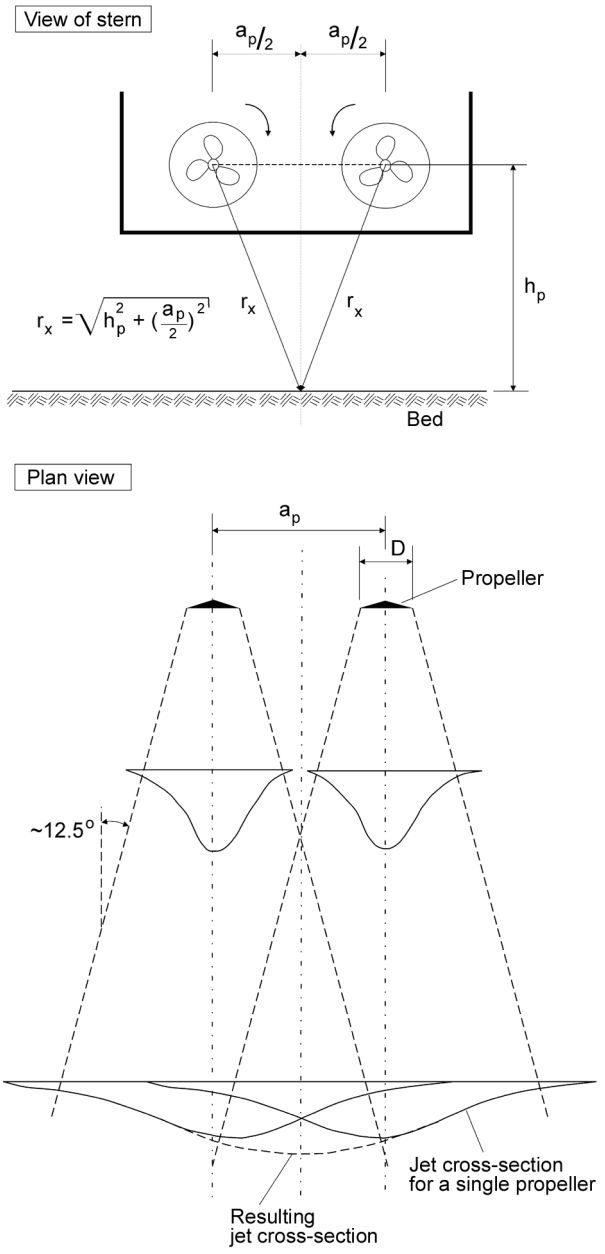

Figure 5.31 View of the stern of a twin-screw vessel with overlapping jets, standard situation 1, with α_0 = 0°

If $\alpha_0 \neq 0°$ or the jets are dispersed laterally or strike the bank at an angle, a sketch with all the relevant geometrical dimensions is recommended to obtain the overlap of the jets.

The values of the jet velocity at the bed obtained for twin-screw vessels when the propellers counter-rotate towards each other may be higher than those obtained by addition, as indicated in Figure 5.31.

5.6.4 Simplified calculation of the maximum near bed velocity

A simplified method of calculating the maximum near bed velocity for propeller advance ratios $J = 0$ and $J \neq 0$ follows for single- and multi-screw vessels; it is applicable to the cases referred to below. The method can only be used if the jets do not overlap.

- **Ship speed $v_S = 0$**

The maximum near bed velocity at the point of impact of the propeller jet v_{Bmax} can be estimated as follows for the standard jet dispersion situations 1, 2 and 3 (see 5.6.3.1) for $J = 0$.

Maximum near bed velocity at the point of impact v_{Bmax} für $J = 0$ (simplified calculation) [m/s]

$$v_{Bmax} = E \left(\frac{D}{h_p} \right) v_0 \qquad (5\text{-}79)$$

where

D is the propeller diameter [m]

h_p is the height of the propeller axis above the bed [m]

E is the coefficient for characterisation of stern shape and rudder configuration [-] (see Figure 5.32)

- E = 0.71 for slender sterns with a middle rudder
- E = 0.42 for slender sterns without a middle rudder
- E = 0.25 for modern inland navigation craft with a tunnel stern with twin rudders

v_0 is the induced initial velocity for $J = 0$ [m/s] see 5.6.1

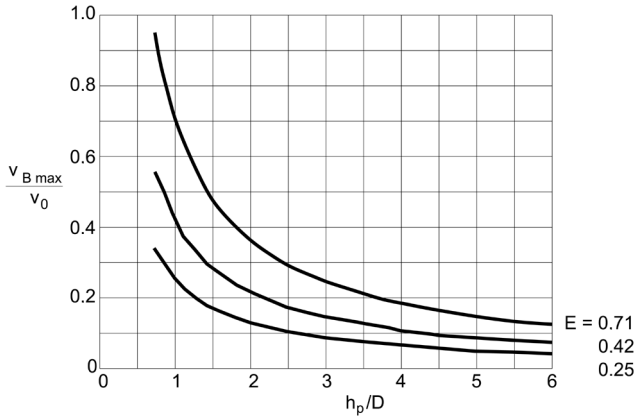

Figure 5.32 Relative maximum near bed velocity of the propeller jet v_{Bmax} / v_0 = as function of (h_p/D, E)

- **Ship speed $v_S \neq 0$**

When a ship casts off, i.e. when the propeller advance ratio is increasing, there is a decrease in the induced initial velocity and the associated velocity at which the propeller jet strikes the surfaces of the fairway.

The maximum near bed velocity v_{Bmax1} at a propeller advance ratio $J \neq 0$ can be calculated approximately in this case as follows:

Maximum near bed velocity at the point of impact v_{Bmax1} for $J \neq 0$ (simplified calculation) [m/s]

$$v_{Bmax1} = v_{Bmax} \left(1 - \frac{v_S}{n\,D}\right) \qquad (5\text{-}80)$$

where

D is the propeller diameter [m]

n is the propeller rotation rate [1/s]

v_{Bmax} is the maximum near bed velocity at the point of impact for $J = 0$ [m/s]

v_S is the ship speed [m/s]
signed, where appropriate: v_s is negative if the movement of the ship and the propeller jet point in the same direction, e.g. when the vessel is stopping

This approach also applies when the reduction in the near bed velocities has to be determined for the calculation of the total impact velocity field in accordance with 5.6.3.3.

For narrow fairway conditions (e.g. lock exits), the reductions in the near bed velocities referred to above are negligible due to the very low ship speeds that are possible owing to the limitation of the fairway. In this case, the loads assumed are the same as for $J = 0$.

5.6.5 Loads due to bow thrusters

According to /*Schokking 2002*/, revetments can be damaged by bow thrusters operated in the vicinity of mooring places and such damage needs to be taken into account in the design. The ship speed over ground is negligible in this case and v_s is therefore taken to be equal to zero below ($v_S = 0$). A distinction is made between temporary loads during mooring, long-term loads, loads on a sloping bank (slope inclination < 45°) and loads on the bed in front of a vertical bank (quay wall), see Figure 5.33. Such loads are not generally relevant to the design if the vessel is moving ($v_s \neq 0$) as the jet is deflected.

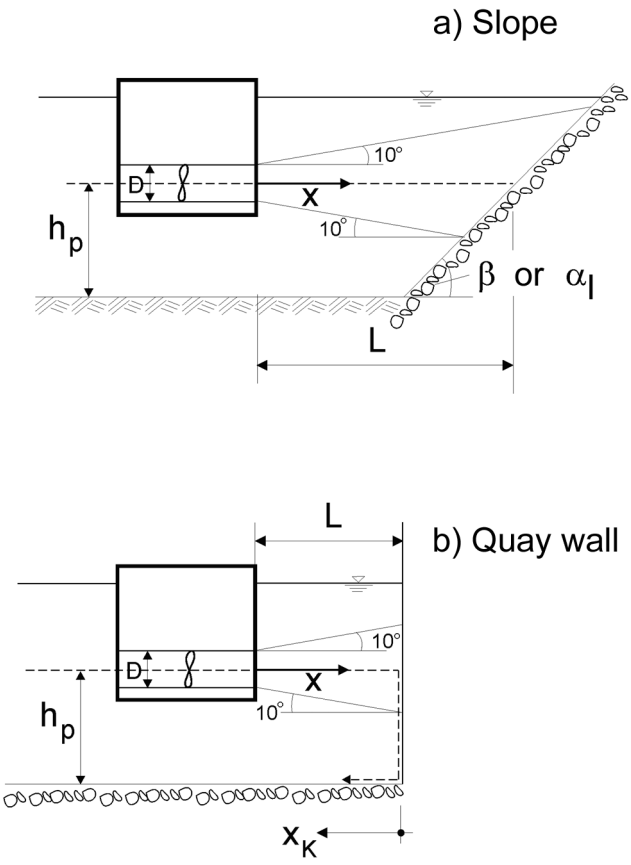

Figure 5.33 Jet dispersion for loads due to bow thrusters; (a): sloping bank, (b): quay wall where the jet is deflected towards the bed of the river or canal
β = slope angle
α_l = longitudinal slope angle, see Figure 6.4 and eq. (6-8)

The induced initial velocity v_0 corresponds approximately to that of a ducted propeller with an advance ratio J equal to 0. Depending on the power, the following equation applies in accordance with /*EAU 1996; Blaauw, Kaa 1978*/:

$$v_0 \approx 1.1 \left(\frac{P_{Bug}}{\rho_W \, D^2} \right)^{1/3} \tag{5-81}$$

where

P_{Bug} is the installed power of the bow thruster [W] see Table 5.1
N.B.: The value is stated in [kW] in Table 5.1

D is the duct diameter ≈ diameter of the propeller of the bow thruster [m]

ρ_W is the density of water [kg/m^3]

or eq. (5-58) applies where v_0 is a function of the thrust coefficient:

$$v_0 = 1.13 \; n \; D \sqrt{K_{T,DP}}$$

where

$K_{T,DP}$ is the thrust coefficient of a ducted propeller [-] for J = 0 as in eq. (5-58)

n is the propeller rotation rate of the bow thruster [1/min]

The reduction in the induced initial velocity is lower for bow thrusters than for free propellers. The following applies to the maximum axial flow velocity (main velocity) v_{xmax} at a sloping bank and has been derived from measurements by /*Schokking 2002*/:

Maximum axial flow velocity of a bow thruster at a sloping bank v_{xmax} [m/s]

$$\begin{cases} \boxed{v_{x\max} = v_0} & \text{for } \dfrac{x}{D} \le 1.0 \\ \boxed{v_{x\max} = v_0 \left(\dfrac{x}{D} \right)^{-1/3}} & \text{for } \dfrac{x}{D} > 1.0 \end{cases} \tag{5-82}$$

where

D is the duct diameter ≈ diameter of the propeller [m]

v_{xmax} is the maximum axial flow velocity, main velocity [m/s]

v_0 is the induced initial velocity [m/s]

x is the distance from the outlet side of the bow thruster [m]

The design value occurs at the slope where $x = L$.

The maximum jet velocity at the bed $v_{max,S,k}$ at the toe of a quay wall is as follows /*Blokland 1994*/:

$$\begin{cases} v_{max,S,K} = 1.0 \, \dfrac{v_0 \, D}{h_P} & \text{for } \dfrac{L}{h_P} < 1.8 \\ v_{max,S,K} = 2.8 \, \dfrac{v_0 \, D}{L + h_P} & \text{for } \dfrac{L}{h_P} \ge 1.8 \end{cases} \tag{5-83}$$

where

h_P is the hight of the propeller axis above the bed [m]

L is the distance between the plane of the bow thruster outlet and the quay wall [m]

$v_{max,S,K}$ is the maximum flow velocity at the bed at the toe of the quay wall [m/s]

The further reduction in the jet at the bed $v_{max,S,K}$ after deflection can be calculated as follows in the same way as for the propeller jet of the main drive as a function of the distance x_k from the quay wall:

$$v_{max,S,xK} = v_{max,S,K} \left(\frac{L + h_P}{x} \right)^{1.62} \tag{5-84}$$

where

x is the distance along the jet axis measured from the jet outlet to the quay wall and then to the bed of the river or canal [m]
$x = L + h_P + x_K$

x_K is the distance of the deflected jet from the quay wall measured along the bed of the river or canal [m]

$v_{max,S,xK}$ is the altered maximum flow velocity at the bed after deflection measured at a distance of x_k from the quay wall [m/s]

The size of stones required for unanchored revetments is determined in accordance with 6.3. Chapters 8 and 9 deal with how to take partial grouting into consideration.

5.7 Wind set-up and wind waves

5.7.1 General

Depending on its direction, velocity and duration the wind generates waves that must be considered in combination with other waves. This is important for waterways on large plains (Rhine Lowlands, North German Plain) and for long, wide reaches of waterways (impoundments). Wind waves can usually be

disregarded in the case of canals. However, wind set-up may be of relevance, especially in long impoundments.

5.7.2 Wind data

Data on wind directions, velocities and duration can be obtained from local meteorological offices or the statistical records kept by Germany's National Meteorological Service (DWD). Data on wind velocities for design purposes are also included in current German standards (DIN standards). In certain cases, it may be advisable to specify the wind data to be used in the calculations more precisely (e.g. by using statistics on extreme data classified according to direction for two-dimensional wind distribution). It will be necessary to consult experts on this matter. Local topographies may result in modification of the wind field.

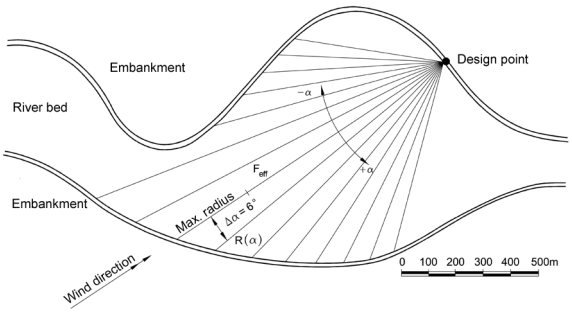

α [°]	cos α [-]	cos²α [-]	R(α) [m]	R(α) cos²α [m]
- 42	0.743	0.552	520	287
- 36	0.809	0.654	570	373
- 30	0.866	0.750	640	480
- 24	0.914	0.835	720	601
- 18	0.951	0.904	830	750
- 12	0.973	0.956	1340	1281
- 6	0.995	0.990	1240	1228
0	1.000	1.000	1140	1140
6	0.995	0.990	1050	1040
12	0.973	0.956	980	937
18	0.951	0.904	920	832
24	0.914	0.835	880	735
30	0.866	0.750	830	623
36	0.809	0.654	780	510
42	0.743	0.552	730	403
	∑13.512			∑11220

The effective fetch F_{eff} is:

$$F_{eff} = \frac{\sum R(\alpha) \cdot \cos^2\alpha}{\sum \cos\alpha}$$

$$F_{eff} = \frac{11220}{13.512}$$

F_{eff} = 830 m

Figure 5.34 Diagram and example illustrating how the effective fetch is calculated for a given wind direction in accordance with /CUR-TAW 1992/

5.7.3 Fetch and period of wind action

A fetch with a specific width-to-length ratio is needed for the prevailing wind to generate waves. The fetch length, or **effective fetch F_{eff}**, is used in the calculations. A method of calculating F_{eff} approximately using the sector method is described in /CUR-TAW 1992/; it takes into account the edges of the area of water in the vicinity of the revetment to be dimensioned. The calculation procedure is as follows (see Figure 5.34):

1. The prevailing wind is entered on a plan of the site, in relation to the design point.
2. The actual fetch lengths between the design point and the point on the opposite bank (or possibly a training wall, dry foreshore, etc.) are determined by drawing radial lines extending $\pm$ 45° to the left and right of the prevailing wind at selected intervals $\Delta\alpha$ (see table of examples in Figure 5.34: $\Delta\alpha$ = 6°).
3. The effective fetch is determined from the above input data by means of the following equation:

Effective fetch F_{eff} [m]

$$F_{eff} = \frac{\sum R(\alpha) \cos^2\alpha}{\sum \cos\alpha} \qquad (5\text{-}85)$$

where

F_{eff} is the effective fetch [m]

$R(\alpha)$ is the impact length to opposite bank at angle α [m]

α is the angle of influence direction [°]

The method described here can be used if the effective fetch obtained corresponds approximately to the straight-line fetch, which is the distance between the design point and the boundary of the body of water in the direction of the wind /*EAK 2002*/. The straight-line fetch can only be used for regular bank lines.

The prevailing wind velocity must continue for a certain minimum period of time in order for the maximum possible wave height to be generated in the fetch. The waves will be lower if the wind lasts for a shorter period of time.

The following applies to the required period of wind action. (N.B.: It is not dimensionally homogeneous ⇒ use the dimensions specified; see Figure 5.35) /*ACER 1992*/:

Minimum period of wind action t_{min} [h]

$$t_{min} = \frac{F_{eff}^{2/3}}{u^{0.41}} \qquad (5\text{-}86)$$

where

F_{eff} is the effective fetch [km]

t_{min} is the minimum period of wind action [h]

u is the wind velocity [m/s]
(representative mean value where appropriate)

A mean value of u can be obtained for highly variable wind velocities by determining the root mean square of the single values of a representative hydrograph for u for the period t_{min}. The period of time considered for the determination must be selected so as to obtain the highest possible value of u.

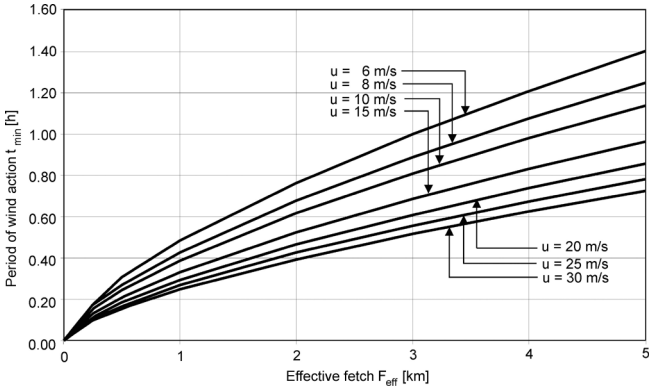

Figure 5.35 Period of wind action required for a given wave height to develop, as a function of the fetch and wind velocity, in accordance with /ACER 1992/

5.7.4 Wind set-up

If the wind blows from the same direction at a virtually constant velocity for a long period of time the critical shear stress between the air flow and the surface of the water causes a rise in the water level – known as wind set-up, Δh_w – at the lee of the fetch /*DVWK 246; Poweleit 1985*/. The "Zuider Zee equation" provides reference values. (N.B.: The equation is not dimensionally homogeneous ⇒ use the dimensions specified):

Height of wind set-up Δh_w at the end of the fetch [m]

$$\Delta h_w = \frac{u^2 \, S}{4861 \, h_m} \cos\alpha \qquad (5\text{-}87)$$

where

h_m is the mean depth of water [m]

S is the maximum fetch length [km]
(not the effective fetch)

u is the wind velocity [m/s]

α is the angle between the prevailing wind and the direction in which the slope falls [°]

Δh_w is the height of wind set-up at the lee of the fetch [m]

The most unfavourable value of Δh_w is obtained when $\cos\alpha$ = 1. The graph illustrating the equation (see Figure 5.36) indicates possible wind set-up values.

For the sake of simplification, a value of 0.05 m can be taken for the height of the wind set-up Δh_w if the mean fetch length S_m is less than 1500 m and the mean water depth h_m is greater than 6 m, cf. /*DVWK 246*/.

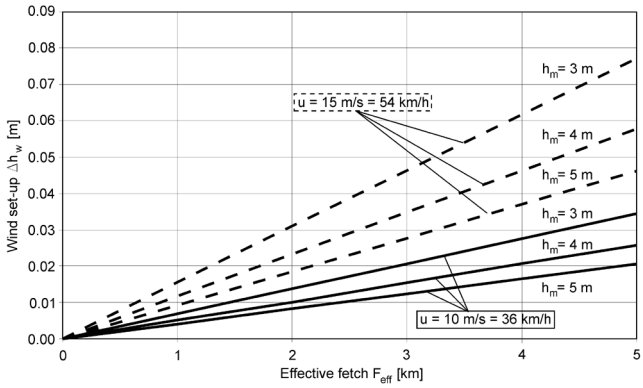

Figure 5.36 Height of wind set-up Δh_w as a function of the maximum fetch length S and the mean water depth h_m for two wind velocities u and $\cos\alpha$ = 1

5.7.5 Wind waves

There is very little data available on the possible height of wind-generated waves on inland waterways and estuaries. The significant, or design, wave height and associated wave period depend directly on the predetermined wind velocity, the mean water depth and the effective fetch.

One possibility of determining the wave height and period is to use Brettschneider's equations for deep water waves, for example. The equations also apply to inland waterways owing to the smaller waves that occur there, according to /*CUR-TAW 1992*/, and can be used for wind velocities u of up to 12 m/s (corresponding to wind force 5 on the Beaufort scale). This upper limit is sufficient as vessels on empty runs and with container cargoes only sail up to a maximum wind force of 8 m/s and the superimposition of ship-induced and wind waves is only relevant for such situations. Reference should be made to the literature, e.g. /*CEM 2002; Wagner 1996*/ if waves that act alone are to be taken into account in the design.

The conditional equation for the significant wave height H_s = Fkt. (h_m, u, F_{eff}) is as follows:

Conditional equation for the significant wave height H_s [m]

$$\frac{g\,H_s}{u^2} = 0.283 \tanh\left[0.530\left(\frac{g\,h_m}{u^2}\right)^{0.750}\right] \cdot \tanh\frac{0.0125\left(\frac{g\,F_{eff}}{u^2}\right)^{0.42}}{\tanh\left[0.530\left(\frac{g\,h_m}{u^2}\right)^{0.750}\right]} \qquad (5\text{-}88)$$

where

F_{eff} is the effective fetch [m]

g is the acceleration due to gravity [m/s^2]

h_m is the mean water depth [m]

H_s is the significant wave height [m]

u is the wind velocity [m/s]

The following applies to the associated characteristic wave period T = Fkt. (h_m, u, F_{eff}):

Conditional equation for the associated characteristic wave period T [s]

$$\frac{g\,T}{u} = 2\pi\ 1.2 \tanh\left[0.833\left(\frac{g\,h_m}{u^2}\right)^{0.375}\right] \cdot \tanh\frac{0.077\left(\frac{g\,F_{eff}}{u^2}\right)^{0.25}}{\tanh\left[0.833\left(\frac{g\,h_m}{u^2}\right)^{0.375}\right]} \qquad (5\text{-}89)$$

where

T is the wave periode [s]

Adapted to small effective fetch lengths, such as those on inland waterways, the above equations provide a means of determining design wave heights directly, without a great deal of computing. Water depths between 1 and 6 m, wind velocities between 8 and 14 m/s and fetch lengths up to 5 km have been incorporated into the graphs (see Figure 5.37). Water depths greater than a mean water depth h_m of 6 m result in only insignificantly greater wave heights. Wave heights can be determined by means of eq. (5-88) in special cases.

A mean value of the water depth must be used. Local shallows may be disregarded. Areas in the vicinity of side embankments must be considered separately owing to the influence of variable water depths on the wave height (see 5.8.2, 5.8.4).

Characteristic values of waves may be determined from measurements by using statistical methods as an alternative to obtaining the values by calculation only.

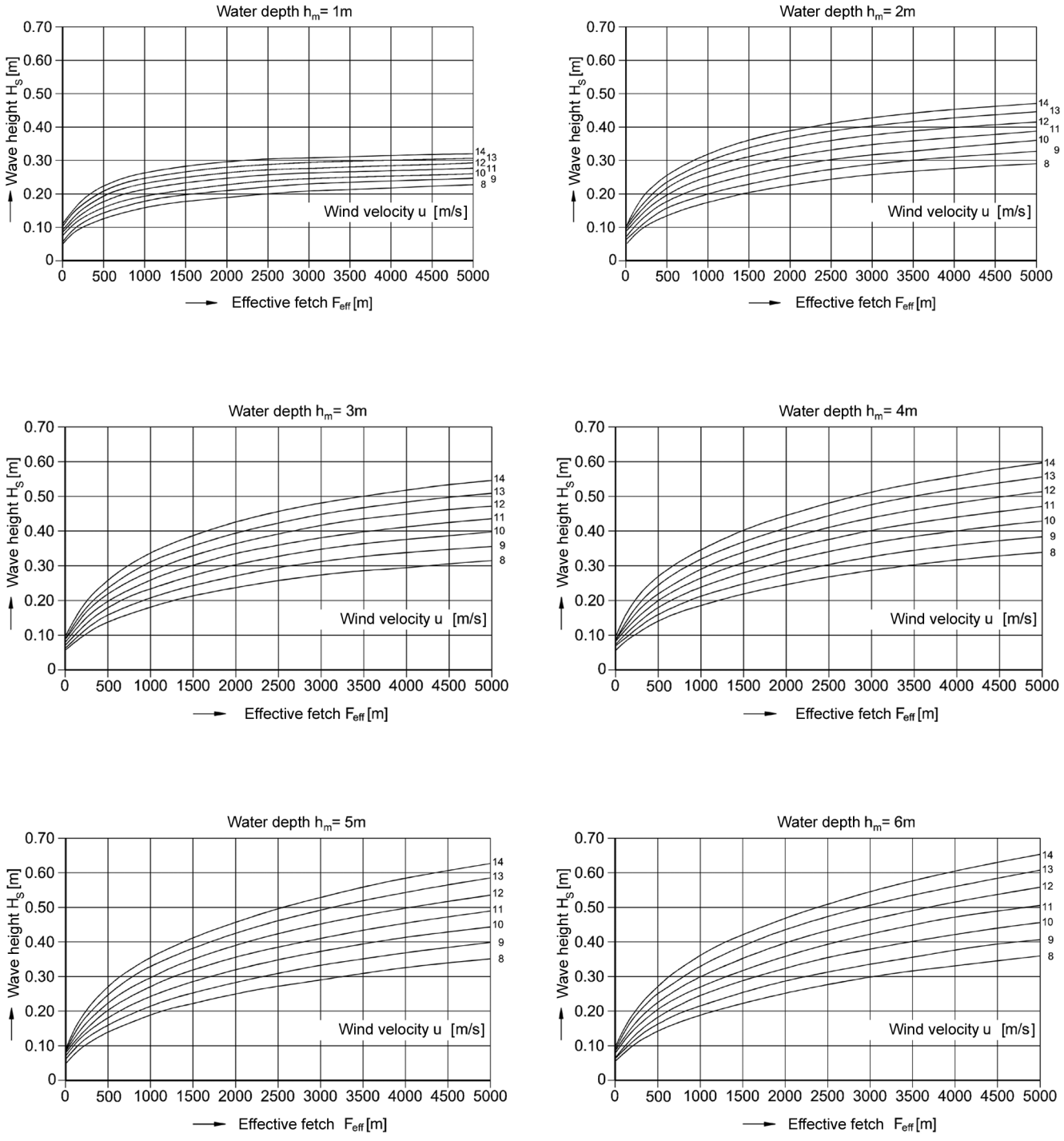

Figure 5.37 Significant wave height H_S as a function of the wind velocity u and the effective fetch F_{eff} for various water depths h_m, in accordance with /CUR-TAW 1992/

The associated wave length L can generally be determined implicitly by means of the following equation:

Wave length L, in general [m]

$$\frac{L}{T} = c = \sqrt{\frac{g\,L}{2\pi}\tanh\left(2\pi\,\frac{h_m}{L}\right)} \qquad (5\text{-}90)$$

where

c is the wave celerity [m/s]

L is the wave length [m]

The following applies to shallow water waves where $h_m/L << 1$ (i.e. $\tanh(2\pi h_m/L) \approx 2\pi h_m/L$):

Wave length L, in shallow water [m]

$$\frac{L}{T} = c = \sqrt{g\,h_m} \qquad (5\text{-}91)$$

The drawdown time of waves is of interest in geotechnical assessments and can be roughly estimated as follows:

Drawdown time $t_{a,W}$ [s]

$$t_{a,W} \approx \frac{1}{2}T \qquad (5\text{-}92)$$

where

$t_{a,W}$ is the drawdown time of a wave [s]

5.8 Wave deformation

5.8.1 General

The wave heights determined up to this point depend on waves being able to propagate unhindered. This applies in most design cases. However, in certain situations, the wave front is subject to numerous disturbances and influences (structures, variations in the depth of the water, approach angles) that change the height of the wave. The environment around the planned revetment must therefore be examined to determine how it is likely to affect the wave height at the design point. **Wave shoaling** and **breaking of waves** (see 5.8.2), **diffraction** (see 5.8.3), **refraction** (see 5.8.4) and/or **reflection** (see 5.8.5) may occur (see chapter 2 for terms and definitions).

5.8.2 Wave shoaling and breaking of waves

The shoaling of a wave (see chapter 2) in water of decreasing depth is described by the shoaling coefficient K_{sh}:

Wave height H_{sh} due to shoaling [m]

$$H_{sh} = K_{sh}\,H_{ein} \qquad (5\text{-}93)$$

$$K_{sh} = \frac{1}{\sqrt{\left(1+\frac{4\pi\,h_m/L_{ein}}{\sinh(4\pi\,h_m/L_{ein})}\right)\tanh(4\pi\,h_m/L_{ein})}} \qquad (5\text{-}94)$$

where

h_m is the mean depth of water [m]

H_{ein} is the height of the incoming waves [m]

H_{sh} is the wave height due to shoaling [m]

K_{sh} is the Shoaling-coefficient [-]

L_{ein} is the length of the incoming waves [m] ($L_{ein} = L$)

The graph of the shoaling coefficient (see Figure 5.38) indicates that wave shoaling in shallow water is preceded by a reduction in the wave height in the transitional zone.

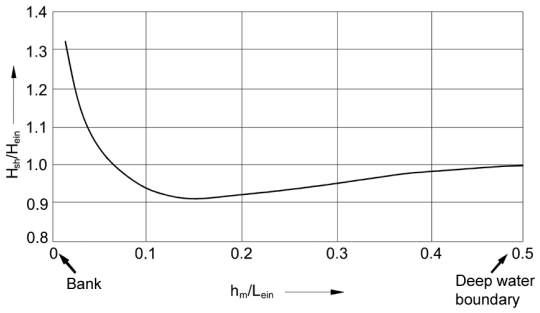

Figure 5.38 Graph showing shoaling coefficient K_{sh} for a decreasing mean water depth h_m

The following applies to the change in the wave length:

Wave length L_{sh} during shoaling [m]

$$\frac{L_{sh}}{L_{ein}} = \tanh\left(2\pi\ h_m / L_{sh}\right) \qquad (5\text{-}95)$$

where

L_{sh} is the wave length due to wave shoaling [m]

The fact that the height and length of the waves are continuously changing means that the steepness of the waves also changes. The latter is described by the following equation:

Wave steepness H_{sh}/L_{sh} [-]

$$\frac{H_{sh}}{L_{sh}} = \frac{H_{ein}}{L_{ein}} \cdot \sqrt{\frac{1+\cosh\left(4\pi h_m / L_{sh}\right)}{\left(4\pi h_m / L_{sh} + \sinh\left(4\pi h_m / L_{sh}\right)\right)\tanh^2\left(2\pi h_m / L_{sh}\right)}} \quad (5\text{-}96)$$

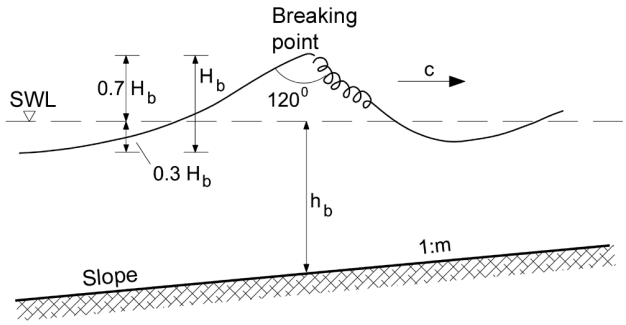

Figure 5.39 Diagram of a breaking wave
c – wave celerity
h_b – depth of water at the point of breaking
H_b – height of wave at the point of breaking
Maximum angle at wave crest: 120°

The upper limit of the wave steepness can be determined by means of the following equation:

Upper limit of wave steepness H_{sh}/L_{sh} [-]

$$\left[\frac{H_{sh}}{L_{sh}}\right]_{max} = 0.142 \tanh\frac{2\pi h_m}{L_{sh}} \quad (5\text{-}97)$$

The wave will break if this limit is exceeded. Depending on the inclination of the slope, various types of breaker, such as spilling breakers, plunging breakers or surging breakers, can occur (see chapter 2) /*Le Méhauté 1976; Press, Schröder 1966; SPM 1984*/.

The wave height at the point of breaking H_b is of relevance to the design as the maximum kinetic energy is available at the moment the wave breaks. H_b is obtained as follows for low initial steepnesses (H_{ein} / L_{ein} < 0.006):

Wave height H_b at the point of breaking [m]

$$\frac{H_b}{H_{ein}} = 0.303 \sqrt[3]{\frac{L_{ein}}{H_{ein}}} \quad (5\text{-}98)$$

where

H_b is the wave height at the point of breaking [m]

Reference may be made to Figure 5.40 for other initial steepnesses. The water depth h_b at the point of breaking can be estimated by means of Figure 5.41.

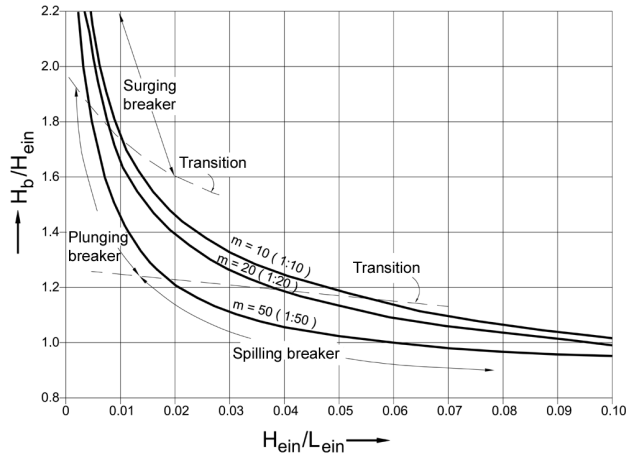

Figure 5.40 Wave height H_b at the point of breaking as a function of the initial steepness in accordance with /SPM 1977; EAK 2002/

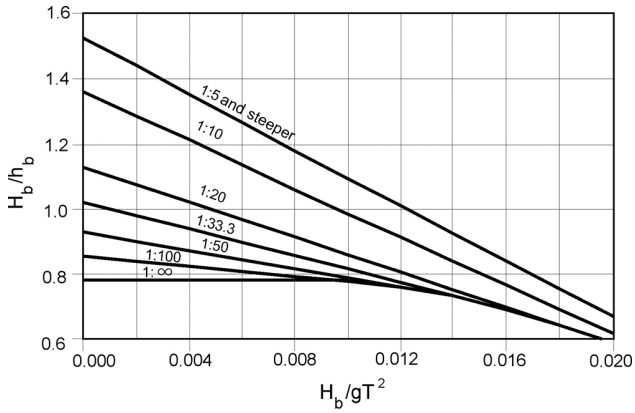

Figure 5.41 Water depth h_b at the point of breaking for $T = T_{ein}$ = constant, in accordance with /CEM 2002/

A surf similarity parameter can be obtained on the basis of the wave and slope geometry /*Pilarczyk 1990*/:

Surf similarity parameter ξ [-]

$$\xi = \frac{\tan\beta}{\sqrt{H_{ein} / L_{ein}}} \qquad (5\text{-}99)$$

where

H_{ein} is the height of the incoming wave [m]

L_{ein} is the length of the incoming wave [m]

β is the slope angle [°]

ξ is the surf similarity parameter [-]

The surf similarity parameter enables the type of breaker to be determined (see Figure 5.42). Either the breaker with the greatest wave height or the one with the greatest wave steepness is relevant to the design. The correlation between the slope inclination, the surf similarity parameter and the shape of the breaker can be seen in Table 5.2. The designations, which are not used consistently in the literature published in German, have been selected according to current recommendations /*EAK 1993; EAK 2002; EAU 1996*/.

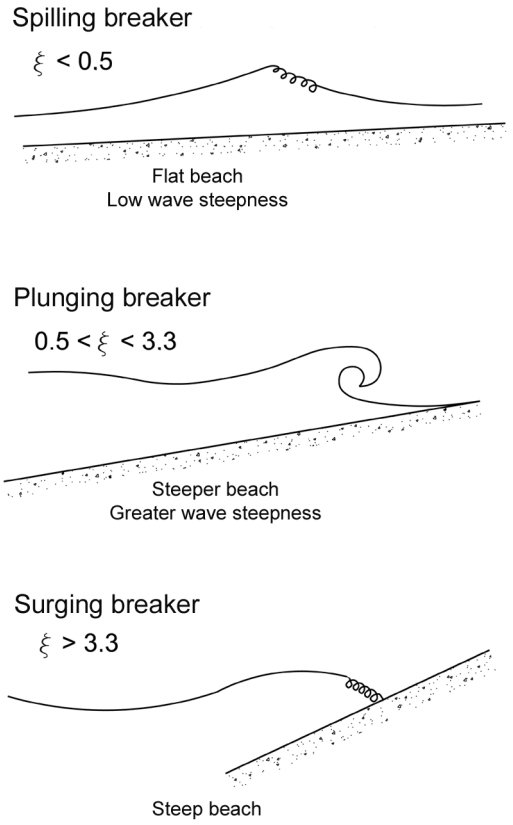

Figure 5.42 Types of breaker as a function of the surf similarity parameter for slope inclinations between 1:5 - 1:20, in accordance with /CEM 2002; EAK 2002/

Slope inclination	Surf similarity parameter	Type of breaker
1 : 5 to 1 : 20	$\xi < 0.5$	Spilling breaker
	$0.5 < \xi < 3.3$	Plunging breaker
	$\xi > 3.3$	Surging breaker
1 : 1.5 to 1: 4	$\xi < 2.5$	Spilling breaker
	$2.5 < \xi < 3.4$	Plunging breaker
	$\xi > 3.4$	Surging breaker

Table 5.2 Type of breaker as a function of the slope inclination and surf similarity parameter

5.8.3 Diffraction

Changes in the wave height due to diffraction (see chapter 2) at obstacles or structures (training walls, groynes etc., see Figure 5.43) are determined with the aid of a diffraction coefficient:

Wave height H_{diff} due to diffraction [m]

$$H_{diff} = K' H_{ein} \qquad (5\text{-}100)$$

where

H_{diff} is the wave height due to diffraction [m]

K' is the diffraction coefficient [-]

Diffraction charts showing lines representing the same values of K' are available for design purposes (see Figure 5.44 and Figure 5.45). They enable the wave height behind obstacles (e.g. groynes) to be estimated. It should be noted that local increases in the wave heights may also occur. The increase is around 10 % for common angles between a ship-induced wave and a groyne (see Figure 5.44). The height of waves that are parallel on reaching an opening in a training wall and are diffracted there may increase by around 20 % (see Figure 5.45). Further diagrams are available in the literature if the actual direction of the approaching wave does not correspond to that shown in the figures /*CEM 2002; Daemrich 1978a; Daemrich 1978b; SPM 1984*/.

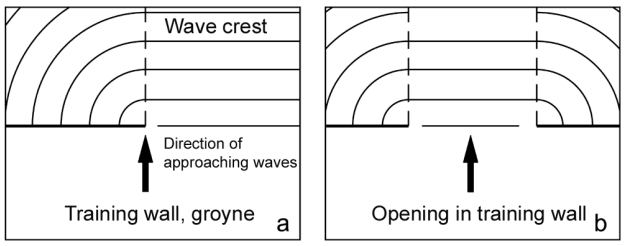

Figure 5.43 Configurations of (a) groynes and (b) openings in training walls causing diffraction

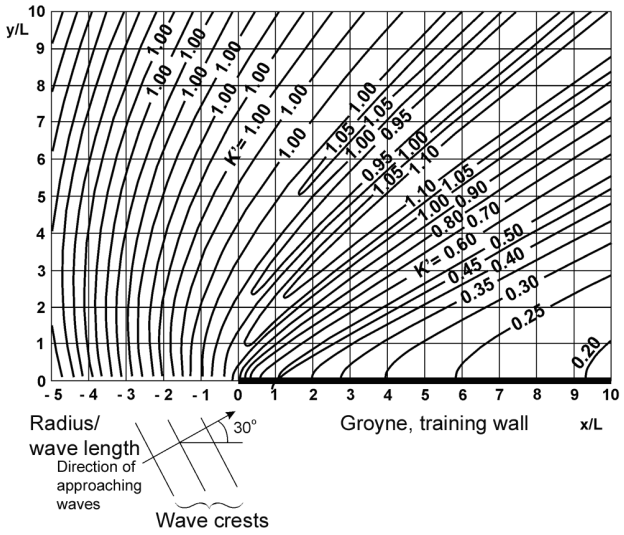

Figure 5.44 Diffraction chart showing wave propagation at a semi-infinite obstacle (groyne, training wall) at a constant mean water depth h_m and a wave attack angle of 30°, in accordance with /Daemrich 1978b/

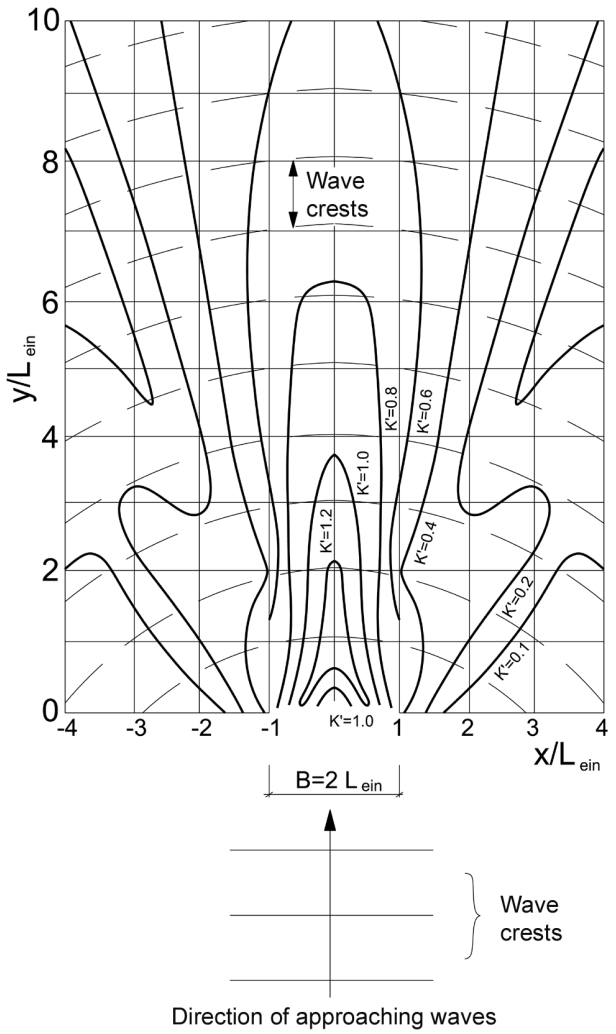

Figure 5.45 Diffraction chart showing wave propagation behind the opening in a training wall of width B at a constant mean water depth h_m for $B/L_{ein} = 2$ for attack by waves parallel to the opening, in accordance with /SPM 1984/

5.8.4 Refraction

Refraction occurs when the front of a ship-induced secondary wave strikes a bank line at an angle, for instance (see chapter 2). One side of the wave crest is in shallower water than the other. As the wave celerity of shallow water waves decreases with the water depth, the wave flank nearest the bank moves more slowly than the one furthest from the bank. The entire wave crest is bent towards the bank and refraction causes the height of the ship-induced waves in the canal to diminish (see Figure 5.46). However, it should be noted that wave shoaling may lead to an increase in the wave height (see 5.8.2). These effects must always be considered together.

It is very difficult to show the wave deformation due to refraction on a graph or to represent it numerically. A revetment design will be conservative if the wave deformation due to refraction is disregarded as refracted waves are always lower than incoming ones.

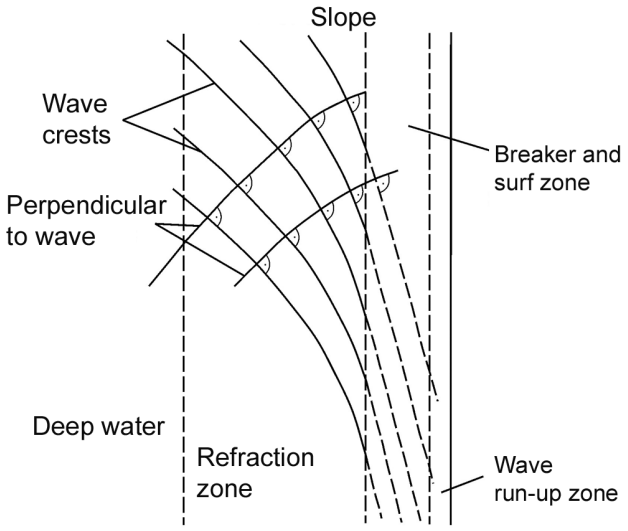

Figure 5.46 Diagram showing the refraction of ship-induced waves

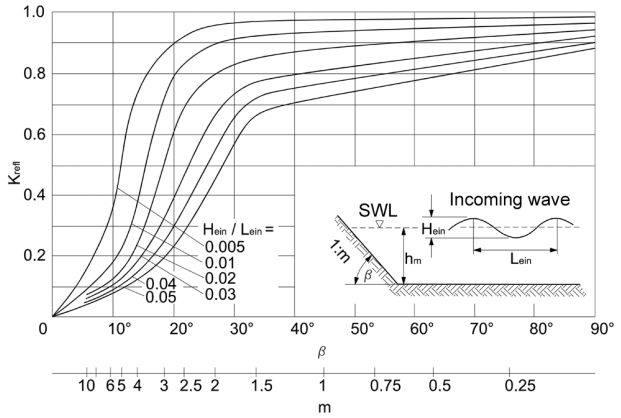

Figure 5.47 Reflection coefficient K_{refl} as a function of the mean water depth and of the height and length of the incoming wave for shallow water waves and sloping obstacles, in accordance with /Press, Schröder 1966/

5.8.5 Reflection

Waves are partially reflected when they strike a boundary surface (wall, groyne, training wall, steep bank, etc.). This is known as "reflection" (see chapter 2). The loss of wave energy causes the wave height to diminish ($H_{refl} < H_{ein}$), the process being described by the reflection coefficient as follows:

Wave height H_{refl} of the reflected wave [m]

$$H_{refl} = K_{refl}\, H_{ein} \quad 0 \le K_{refl} \le 1 \qquad (5\text{-}101)$$

where

H_{refl} is the height of the reflected wave [m]

K_{refl} is the reflection coefficient [-]

Reflected waves are superimposed on the incoming waves. Total reflection occurs in the limiting case where K_{refl} equals unity (vertical obstacle). By contrast, there is no reflection when K_{refl} is equal to zero (flat bank) (as the wave energy is dissipated fully when the wave breaks). Figure 5.47 can be used to estimate K_{refl} for shallow water waves striking a sloping obstacle.

5.8.6 Wave run-up

The wave run-up height z_{AL} of wind waves and secondary diverging waves is defined as the distance from the still-water level (SWL) to the highest run-up point on the slope when measured vertically.

The highest wave run-up heights occur when the waves propagate at right angles to the bank (wave crests parallel to the bank). The run-up height decreases as the angle β_W between the direction of propagation of waves and the fall of slope increases (see 5.8.6.1).

When wave propagation is parallel to the bank, as in the case of ship-induced transversal stern waves, it may be assumed that there will be no change in the wave height at the bank. The asymmetrical shape of secondary waves must be considered here. The greatest elevation of the water level above the still-water level exceeds half the height of the wave. It is also referred to below as the "run-up height" (see 5.8.6.2).

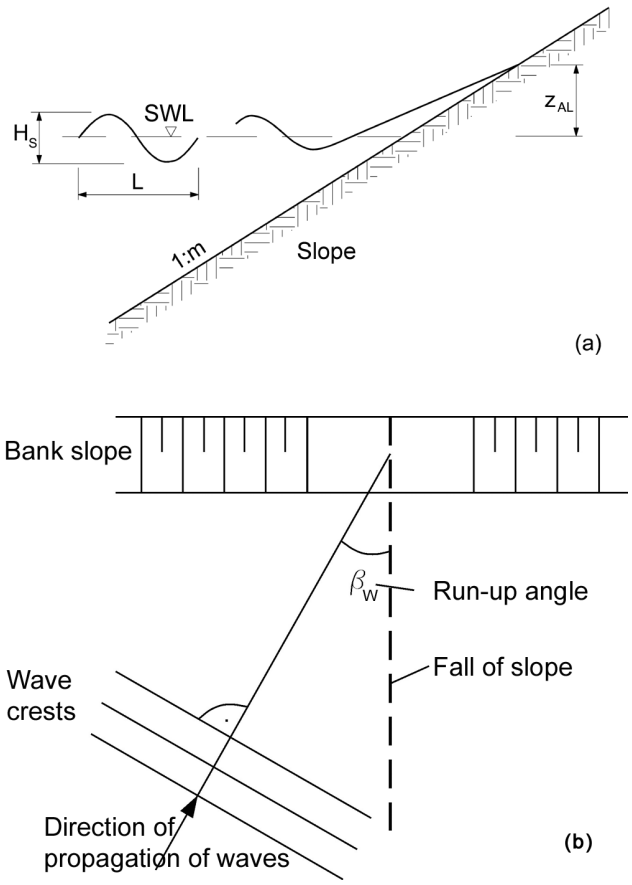

Figure 5.48 Definitions relating to the wave run-up height z_{AL}: (a) cross-section, (b) top view

There are numerous empirical equations available for the determination of the run-up height. The equations include wave height, length and period, slope inclination and profile (concave/convex) and the water depth, depending on how they were developed.

5.8.6.1 Incoming waves

Generally speaking, an increase in the percentage of voids in a slope and in the roughness of a slope surface will result in a lower run-up height while an increase in the steepness of the slope, wave height and wave period will result in a greater run-up height.

An equation for wave run-up that also takes into account the angle between the wave front and the slope as well as the roughness of the revetment surface is included in /CUR-TAW 1992/.

Wave run-up height z_{AL} [m] of diverging waves

$$z_{AL} = C_A \cos\beta_W \quad f_{red} \frac{1}{m} T \sqrt{g H_S} \geq \frac{H_S}{2} \qquad (5\text{-}102)$$

where

C_A is a constant for wave run-up [-]

$C_A = 0.4$ for regular waves and ship-induced waves /*EAK 1993*/

$C_A = 0.74$ for irregular wind waves /*CUR-TAW 1992*/

f_{red} is the reduction factor for energy losses during wave run-up [-] (see Table 5.3)

H_S is the design wave height [m]
Maximum secondary wave height in accordance with eq. (5-43) in 5.5.5.2 (diverging waves) and eq. (5-52) in 5.5.5.4 taking into account eq. (5-50) in 5.5.5.3 and the height of the wind waves in 5.7.5

m is the slope inclination [-]

T is the mean wave period [s]

β_W is the angle between a perpendicular to the wave crest and the fall of the slope [°] (see Figure 5.48)
N.B.: $\beta_W \approx 55°$ for diverging waves of the secondary wave system when a ship sails close to a bank and $Fr_h < 0.7$ (or up to 0.8 for rough approximations)

z_{AL} is the wave run-up height [m]

g is the acceleration due to gravity [m/s^2]

The equation applies to slope inclinations m of up to 1:3 (m = 3) and run-up angles of up to approx. 55°. A similar equation, which takes more input parameters into account, is included in /*EAK 2002*/. The result is also a reference value for the component of the freeboard (distance from the still-water level to the crown of the slope) that is dependent on the wave run-up. Adequate safety against wave overtopping is thus ensured. Statistically, only 2% of all waves exceed the calculated wave run-up.

If the slope features a berm, reference should be made to more specialised literature to enable the wave run-up to be calculated /*Przedwojski et al. 1995*/.

Increasing the surface roughness and voids content of a slope surface considerably reduces wave run-up. This is covered by a reduction factor f_{red} (see Table 5.3). For natural slopes, f_{red} must be estimated on the basis of the data in Table 5.3.

The wave run-up height of ship-induced waves on slope revetments comprising riprap and granular materials decreases as follows, depending on the voids content of the revetment, according to /*Abromeit 1997*/:

$$z_{AL,St} = \frac{H_S - d_D\, n}{H_S} z_{AL,0} \geq 0 \qquad (5\text{-}103)$$

where

d_D is the thickness of the cover layer [m]

H_S is the design wave height [m]

n is the voids content [-]

$z_{AL,St}$ is the wave run-up height on riprap [m]

$z_{AL,0}$ is the wave run-up height when f_{red} = 1 [m]

A filter layer comprising coarse gravel or an equivalent layer may be added to the cover layer.

Revetment	Reduction factor f_{red}
Smooth, layered	1
Precast concrete blocks	0.9
Slope protection, e.g. with basalt blocks, blocks of stone or a grass covering	0.85 - 0.9
A layer of riprap on an impermeable base	0.8
Placed stones	0.75 - 0.8
Loose round stones	0.6 - 0.65
Loose broken rock	0.5 - 0.6
Loose broken rock, partially grouted(*)	0.6 - 0.9

Table 5.3 Reduction factor f_{red} for wave run-up for different types of cover layer, in accordance with /CUR-TAW 1992/ including an amendment (*)

5.8.6.2 Parallel waves

There is an upper limit to the run-up height as calculated by eqs. (5-102) and (5-103) for high values of β_W. The following applies in the limiting case where $\beta_W = 90°$ (transversal waves generated by ships sailing parallel to a bank):

Wave run-up height z_{AL} [m] of parallel waves

$$z_{AL} \le \Delta H_{S,oWl} \approx \approx \frac{\pi}{8}\frac{{H_S}^2}{\lambda_q}\frac{\cosh\frac{2\pi h}{\lambda_q}}{\left(\sinh\frac{2\pi h}{\lambda_q}\right)^3}\left[2+\cosh\left(\frac{4\pi h}{\lambda_q}\right)\right]+\frac{H_S}{2} \quad (5\text{-}104)$$

where

h is the local water depth ≈ H_S at the point of the wave at breaking [m]

$\Delta H_{S,oWl}$ the component of the wave height above the still-water level [m]

H_S is the design wave height [m]
Maximum height of secondary waves in accordance with 5.5.5.2, eq. (5-43) (transversal bow and stern waves), eq. (5-47) (transversal stern waves) and 5.5.5.4, eq. (5-52) (diverging and stern waves generated by small fast boats) taking account of eq. (5-49) and (5-50) (from 5.5.5.3)

z_{AL} is the wave run-up height [m]

λ_q is the wave length of transversal waves [m] in accordance with 5.5.5.1, eq. (5-42)

5.8.7 Change in wave height at the transition from a vertical bank to a slope revetment

A particular type of reflection, known as the Mach reflection, must be taken into account at the transition from a vertical bank to a slope revetment. The Mach reflection results in an increase in the wave height when a wave front moves virtually at right angles to a vertical bank. In the most unfavourable cases, there may be an approximately two-fold increase in the height of the incident wave. The waves are still effective over a certain distance after striking the adjacent sloping bank. This situation must be taken into account in the design (see 6.13).

5.9 Other waves

5.9.1 General

Variations in the water level may also be caused by waves with long periods (positive surge/drawdown waves, tide waves, flood waves). Depending on the design situation and problem, these types of wave must be regarded as being superimposed on those originating in other ways (wind, ship) and therefore added to them.

The drawdown velocities for the types of wave dealt with below must be determined separately for geotechnical analyses.

5.9.2 Positive surge/drawdown waves

Positive surge/drawdown waves are caused by a variety of factors relating to the operation of industrial plant or works located on the waterway, such as:

- turbines starting up or being shut down suddenly (on rivers controlled by weirs or other works),
- lockage (on rivers controlled by weirs or other works, canals),
- the cooling plant of power stations being switched on or off (rivers),

- sudden influx of discharge (rivers),
- impoundment.

Information on the magnitude, duration and frequency of the probable variations in flow must be obtained from the originators (operators of hydroelectric power plants and locks, thermal power plants, sewage treatment plants; indirectly at tributaries) when determining the above types of positive surge/drawdown waves. The discharge from locks is usually restricted to 70 - 90 m^3/s to avoid extreme positive surge and drawdown /*EAU 1996*/.

The change in the water level due to a single positive surge/drawdown wave can be determined as stated in /*EAU 1996*/. For a given wave celerity

$$c = \sqrt{g\, h_m} \qquad (5\text{-}105)$$

where

c is the wave celerity,
is the wave celerity in shallow water [m/s]

g is the acceleration due to gravity [m/s^2]

h_m is the mean water depth [m]

the rise and fall in the water level Δh can be roughly estimated for low ratios ($\Delta h/h_m$) of the rise and fall in the water level Δh to the mean water depth h_m:

Rise and fall in the water level Δh due to positive surge and drawdown [m]

$$\Delta h = \pm \frac{\Delta Q}{c\, b_m} \qquad (5\text{-}106)$$

where

b_m is the mean width at water level [m] in the area of the positive surge/drawdown

$b_m = b_{WS} \pm m\, \Delta h$

b_{WS} is the width at water level [m]

m is the slope inclination [-]

ΔQ is the sudden change in discharge [m^3/s]

Δh is the increase and decrease in water level [m]

The above equations have been analysed, by way of an example, for a mean water depth of 3.0 m, which is a typical value for standard trapezoidal cross-sections (see Figure 5.49).

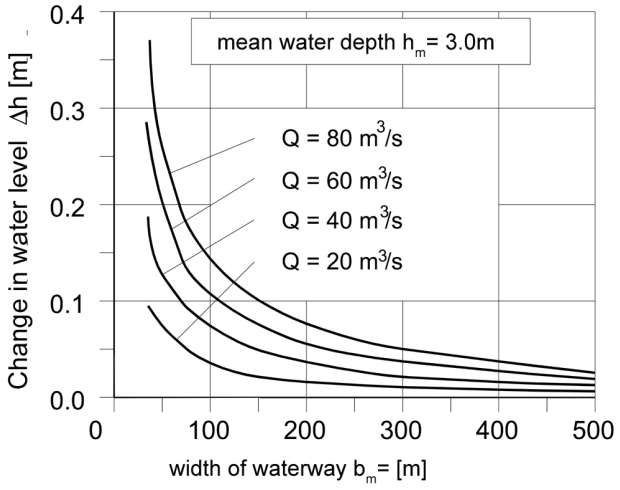

Figure 5.49 Changes in the water level due to positive surge and drawdown for a mean water depth of 3.0 m as a function of the width at water level for various discharge levels ΔQ

The wave height determined may increase or decrease due to reflection or superimposed subsequent positive surge and drawdown waves. Attenuation effects are marginal in uniform canal cross-sections, for straight channel orientations and smooth linings. Such waves may therefore travel backwards and forwards several times, particularly in short impoundments.

Changes in discharge over time must be estimated in accordance with the laws relating to lockage and the times at which turbines are started and shut down.

5.9.3 Flood waves

Flood waves occur during certain seasons and weather conditions and their height, duration and frequency can vary to a great extent. These parameters are affected by the origin and history of the wave as well as by the distance it travels so it is not possible to make any generalised statements. In exceptional cases, a rapid decrease in the level of the flood wave in impoundments may also be relevant to the design /*Köhler 1997*/.

Data (e.g. records of flood levels) must be obtained from the relevant authorities to enable the speed at which the water level drops, v_{za}, to be determined.

The pore water pressures in the soil may be considerably higher than the hydrostatic still-water level when a flood is receding, depending on the permeability of the soil in the vicinity of the bank (see Figure 5.50).

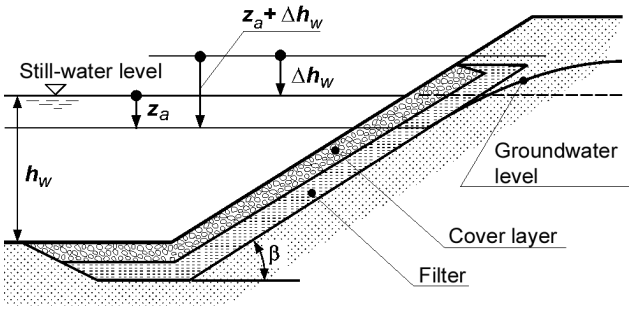

Figure 5.50 Determination of the relevant magnitude of drawdown after saturation of the soil or a rise in the groundwater level by Δh_w above the still-water level
*h_w water depth at still-water level (*SWL*)*
Δh_w temporary rise in water level
z_a maximum rapid drawdown below SWL

The difference Δh_w between the groundwater level and the still-water level must be taken into account in the geotechnical design.

Local experience and observations of the groundwater over many years must be referred to when ascertaining the relevant groundwater level. The exact value of Δh_w must be determined from the point at which the groundwater level intersects the failure surface being considered.

5.10 Excess pore water pressure as a function of rapid drawdown z_a

5.10.1 General

The following input parameters are required for the geotechnical design of permeable revetments as described in chapter 7:

- maximum rapid drawdown z_a and the associated drawdown velocity v_{za}
- maximum excess pore water pressure at the depth of the critical failure surface d_{krit} as a function of z_a and v_{za}.

5.10.2 Maximum drawdown z_a and drawdown velocity v_{za}

The rapid drawdown z_a can be determined for the following cases by means of the calculation methods and recommendations given in this publication:

- shipping (see 5.5.4)
- wind waves (see 5.7)
- positive surge and drawdown (see 5.9.2)
- flood waves (see 5.9.3)

The maximum drawdown z_a relevant to the design must be determined for the most unfavourable case in which several instances of drawdown are superimposed as described in 4.3.

Information on the drawdown velocity v_{za} is given in the following subsections:

- for shipping (primary waves (see 5.5.4.7))
- for wind waves and ship-induced secondary waves (see 5.5.4.7)
- for positive surge and drawdown (see 5.9.2)
- for flood waves (see 5.9.3)

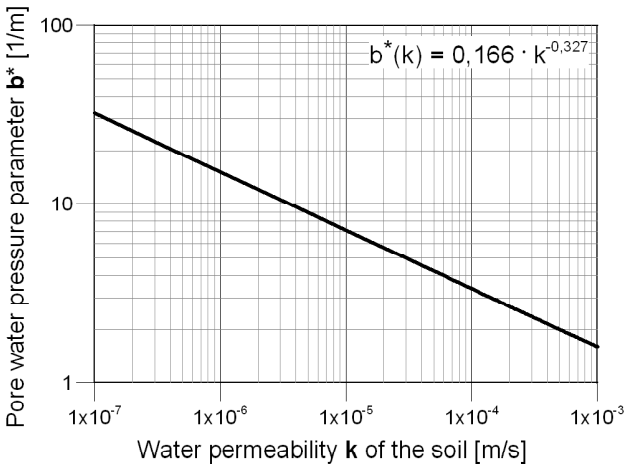

Figure 5.51 Pore water pressure parameter b as a function of the permeability k of the soil for a drawdown velocity v_{za} of 0.12 m/s /Köhler 1997/ or a drawdown time $t_a^* = 5s$*

5.10.3 Magnitude of excess pore water pressure Δu

The excess pore water pressure Δu resulting from rapid drawdown can be determined as a function of the depth z below the slope or bed of the river or canal by means of the following equation. It is an input parameter for the geotechnical design of permeable revetments /*Köhler 1989*/:

Excess pore water pressure Δu [kN/m^2]

$$\Delta u(z) = \gamma_W \, z_a (1 - a \, e^{-bz}) \qquad (5\text{-}107)$$

where

a is a pore water pressure parameter [-]
a = 1, unless other values are obtained from the mathematical description of the measurement results

b is a pore water pressure parameter [1/m] in accordance with eq. (5-109)
it depends on the drawdown time (see 5.5.4.7) and permeability (see also Figure 5.51)

e is Euler's constant [-]
$e \approx 2.718$

z is the depth below the surface of the slope [m] or the bed of the river or canal, normal to the bed

z_a is the maximum rapid drawdown [m]
- $z_a = z_{a,B}$ is the maximum rapid drawdown [m] for the relevant drawdown at the bow in accordance with eq. (7-0a)
- $z_a = z_{a,H}$ is the maximum rapid drawdown [m] for the relevant drawdown at the stern in accordance with eq. (7-0b)

γ_W is the weight density of water [kN/m^3]
$\gamma_W = \rho_W \, g$

ρ_W is the density of water [kg/m^3]

The pore water pressure parameter b is a measure of the decrease in the excess pore water pressure Δu with the depth. The reciprocal value of b corresponds approximately to the depth z_h at which Δu reaches half its maximum value (see Figure 3.4). An exact value is obtained by:

$$b = \frac{\ln 2}{z_h} \tag{5-108}$$

This means that b is inversely proportional to the depth z_h or proportional to the excess pore water pressure Δu at a given depth in the subsoil. The higher the value of b, the greater its destabilizing effect on the revetment will be.

The pore water pressure parameter b can be determined as a function of the water permeability k of the soil for a drawdown time $t_a = t_a^* = 5$s in accordance with Figure 5.51 or eq. (5-110). This parameter b ($k, t_a = 5\,\text{s}$) is referred to below as b^*. Allowance for other influence quantities such as the oedometer modulus of soil E_S and the degree of saturation S of the soil has been made in Figure 5.51 eq. (5-110) /*Köhler 1997*/. The pore water pressure parameter b^* can be converted into a parameter b for a different drawdown time where $t_a \neq 5$s by means of the factor $\sqrt{t_a^* / t_a}$:

$$b = b^* \sqrt{\frac{t_a^*}{t_a}} \tag{5-109}$$

where

b is a pore water pressure parameter [1/m]

b^* is a pore water pressure parameter [1/m] in accordance with Figure 5.51 or eq. (5-110) for

$t_a^* = 5\,\text{s}$

$$b^* = 0{,}166\, k^{-0{,}327} \tag{5-110}$$

t_a is the drawdown time [s] in accordance with 5.5.4.7
- $t_a = t_{a,B}$ in accordance with eq. (5-37) to (5-39) if the the drawdown at the bow is considered
- $t_a = t_{a,H}$ in accordance with eq. (5-40) if the drawdown at the stern is considered

k is the water permeability [m/s] of the soil

Lower values of b are obtained for longer drawdown times, i.e. where $t_a > 5$s, and conversely higher values of b are obtained for shorter drawdown times, i.e. where $t_a < 5$s, when using eq. (5-109).

In cases of doubt, the value of b must be determined from measurements of the excess pore water pressure.

6 Hydraulic design of unbound armourstone cover layers

6.1 General

The hydraulic design of unbound armourstone cover layers must be based on the actions of waves and/or currents described in chapter 5.

Experience and tests conducted with models have shown that the resistance of such cover layers to erosion due to the actions of waves or currents is affected by the following parameters:

- stone weight or size (grain size) and dry density
- thickness of the stone layer
- pore size and thickness of the substructure

Many methods of designing armourstone cover layers exposed to loads due to waves and currents are based on determining the required mean weight of the stones G_{50} (see Figure 6.1), which has been shown to be a relevant parameter for the erosion resistance of riprap armour /*Dietz 1973; Fuehrer, Römisch 1985; Hudson 1959*/.

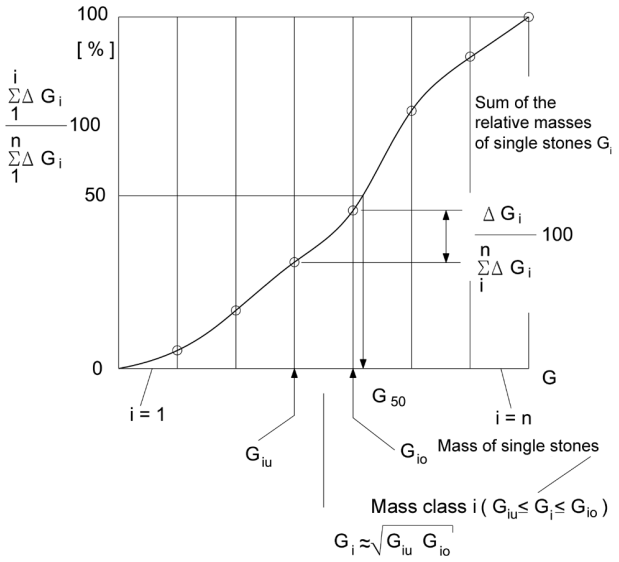

Figure 6.1 Definition of the mean stone mass G_{50}

The required stone size is calculated after initially determining the nominal stone size D_{n50} from G_{50} and the selected dry density. The nominal stone size corresponds to the length of the sides of a cube weighing G_{50}.

$$D_{n50} = \left(\frac{G_{50}}{\rho_S} \right)^{1/3} \qquad (6\text{-}1)$$

where

G_{50} is the mass [kg] at the 50 % value of the cumulative frequency line of the stone masses, see Figure 6.1

ρ_S is the density of the armourstones [kg/m^3]

Other design methods use sizes of screened stones such as D_{50} or D_{85}. The design sizes stated here apply to screening performed with a sieve with square perforations. The grain size D_x is defined in Figure 6.2.

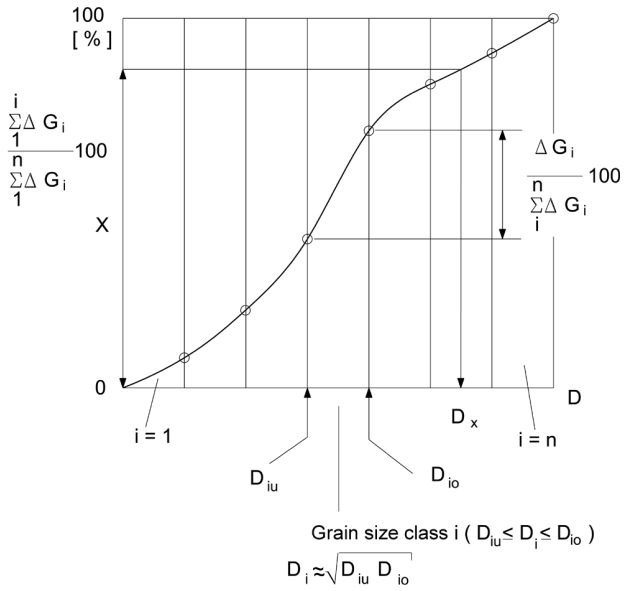

Figure 6.2 Definition of grain size D_x
Explanatory remark: ΔG_i corresponds to the percentage by weight of a screening sample that passes a sieve with opening size D_{io} but is retained on a sieve with opening size D_{iu}

The most frequently used parameters D_{n50} and D_{50} are linked approximately by the shape factor *SF*:

$$D_{n50} \approx SF^{1/3} \, D_{50} \qquad (6\text{-}2)$$

$$SF = \frac{c}{\sqrt{ba}}$$

where

a is the largest dimension of an armourstone [m] in accordance with Figure 6.3

b is the medium dimension of an armourstone [m] in accordance with Figure 6.3

c is the smallest dimension of an armourstone [m] in accordance with Figure 6.3

D_{50} is the grain size at 50 % of particles passing [m]

D_{n50} is the nominal stone size [m] (grain size)

SF is the shape factor [-]

$0.5 \le SF \le 0.8$ armourstones in accordance with /*TLW*/

$SF = 0.65$ typical mean value for armourstones

Reference should be made to 6.9 for the correlation between the nominal stone size D_{n50} and the stone length specified in /*TLW*/.

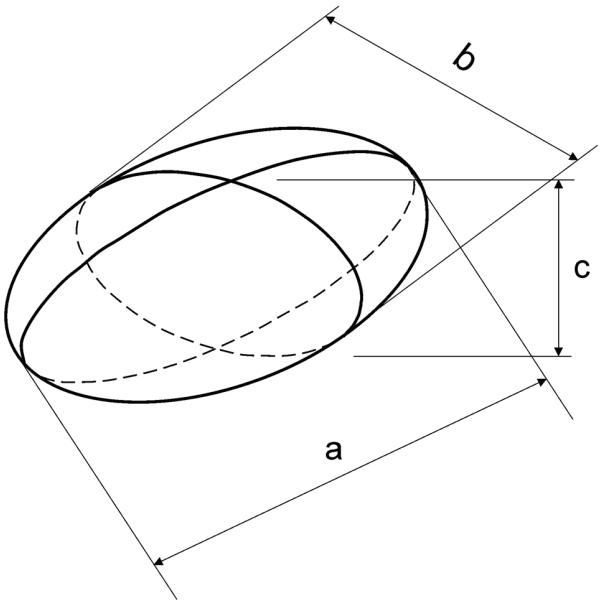

Figure 6.3 Definition of the dimensions a, b and c of an armourstone

6.2 Stone size required to resist loading due to transversal stern waves

The minimum mean stone size D_{50} of the cover layer material of bank revetments that is required to resist displacement under normal sailing conditions can be calculated for the maximum height of any transversal stern wave by means of the following equation:

Stone size D_{50} required to resist transversal stern waves [m]

$$D_{50} \ge \frac{H_{Bem}}{B'_B \left(\frac{\rho_S - \rho_W}{\rho_W} \right) m^{1/3}} \qquad (6\text{-}3)$$

where

B'_B is the stability coefficient [-], derived from field tests /BAW 2002/

B'_B= 1.5 (lower limit of measured values) to 2.3 (mean measured value)

The following is recommended for the design:

B'_B=1.5 if the design case occurs frequently and/or if damage to the revetment is intended to be avoided as far as possible

B'_B=2.3 if the design case occurs infrequently and/or if a certain amount of maintenance is allowed for

D_{50} is the required stone size (grain size) at 50 % of particles passing [m]

H_{Bem} is the design wave height [m]
Maximum value of $H_{u,Heck}$ bzw. $H_{Sek,q}$

$H_{u,Heck}$ height of stern waves of the primary wave system in accordance with 5.5.4.4, eq. (5-32) and Figure 5.13

$H_{Sek,q}$ height of pure transversal stern waves of the secondary wave system in accordance with 5.5.5.2, eq. (5-47), limited by eq. (5-50)

m is the slope inclination, $m = \cot \beta$ [-]
$2 \le m \le 5$
N.B.: Use the actual slope inclination m_{rts} or m_{lks} instead of $m_{K,äqui}$ in this case.

β is the slope angle [°]

ρ_W is the density of water [kg/m^3]

ρ_S is the density of the armourstones [kg/m^3]
N.B.: As specified in the current version of /*TLW*/

The design equation is based on Hudson's equation for determining the stone size required to withstand wave run-up. The slope inclination influences the type of breaker and the run-off velocity of the wave, which is what produces the greatest loads. For such waves, which are usually parallel to the bank, the influence $m^{-1/3}$ on D_{50} is overestimated, particularly for gentle slope inclinations. Eq. (6-3) should therefore only be used for engineered slopes with inclinations *m* of approx. 2 to 5.

The following can be assumed to allow for the influence of the effective angle of shearing resistance φ'_D and slope angle β in a first approximation in analogy to the design for slope supply flow:

$$D_{50} \geq \frac{H_{u,Heck}\, C_{Bö}}{B_B^* \dfrac{\rho_S - \rho_W}{\rho_W}} \qquad (6\text{-}4)$$

where

B^*_B is the coefficient for the frequency of recurrence [-]
- $B^*_B \approx 2.0$ if the design case occurs frequently and/or if damage to the revetment is intended to be avoided as far as possible
- $B^*_B \approx 3.0$ if the design case occurs infrequently and/or if a certain amount of maintenance is allowed for

$C_{Bö}$ is a factor for consideration of the influence of the slope [-]
Definition below eq. (6-12) in 6.7.1,

$H_{u,Heck}$ is the height of stern waves [m] in accordance with 5.5.4.4, eq. (5-32) and Figure 5.13 and the height of the secondary waves in accordance with 5.5.5.2, eq. (5-47), limited by eq. (5-50)

Observations have shown that steep waves are potentially more destructive than waves with a small degree of steepness, given the same wave height. The following applies, based on the design to resist wave run-up:

$$D_{50} \geq \frac{H_{u,Heck}^{3/4}\, L_H^{1/4}\, C_{Bö}}{\tilde{B}_B \dfrac{\rho_S - \rho_W}{\rho_W}} \qquad (6\text{-}5)$$

where

$\tilde{B}_B$ is the coefficient for the frequency of recurrence [-]
- $\tilde{B}_B \approx 6$ if the design case occurs frequently and/or if damage to the revetment is intended to be avoided as far as possible
- $\tilde{B}_B \approx 9$ if the design case occurs infrequently and/or if a certain amount of maintenance is allowed for

L_H is the wave length of the breaking transversal stern wave, determined in analogy to deep-water waves [m] see eq. (6-6)

The wave length L_H depends on the shape of the stern of the ship and on the bank distance in particular. The following approximation applies to large inland cargo vessels, tugs and push-tow units sailing close to a bank:

$$L_H \approx 2.5\, u_{eff} \qquad (6\text{-}6)$$

where

u_{eff} is the effective bank distance [m] in accordance with Figure 5.19 in 5.5.4.7

Small craft sailing extremely close to a bank can therefore be of significance to the design in spite of the fact that the wave heights are likely to be smaller.

6.3 Stone size required to resist flow due to propulsion

6.3.1 Stone size required to resist jet attack

For the load case covering manoeuvring or bollard pull propeller tests, the mean stone size D_{50} of the cover layer material of bed revetments that is required to ensure the stability of the bed without a significant degree of scouring must be determined for the maximum velocity v_{Bmax} (see 5.6.4) in accordance with the following relationship:

Stone size D_{50} required to resist propeller wash [m]

$$D_{50} \geq B_S \frac{v_{max,S}^2}{g} \frac{\rho_W}{\rho_S - \rho_W} \qquad (6\text{-}7)$$

where

B_S is the coefficient for jet attack on a plane bed [-]
- $B_S \approx 1.23$ for ships without a middle rudder and inland navigation vessels with a tunnel stern, standard situations 1 and 4 (see 5.6.3.1) and bow thrusters (see 5.6.5)
- $B_S \approx 0.64$ for ships with a middle rudder, standard situations 2 and 3 (see 5.6.3.1)

$v_{max,S}$ is the maximum flow velocity at the bed [m/s]

$v_{max,S} = v_{xr}$ or v_{xr1} for an exact calculation see 5.6.3.3

$v_{max,S} = v_{Bmax}$ or v_{Bmax1} for a simplified calculation see 5.6.4

N.B.: Part of the surrounding flow field must be taken into account (vectorial addition of the relevant flow velocities near the bed), see the following note.

Note: For moving ships, the relevant flow velocity near the bed comprises the return flow, the wake and the current in the canal or river. It must be noted that

- the flow velocity near the bed is lower,
- the return flow beneath the ship may be obstructed by the ship's hull,
- even the wake (water carried along by a ship in the direction of travel) may act against the flow due to propulsion.

A design method has not been specified here as the appropriate method will need to be selected on a case-to-case basis.

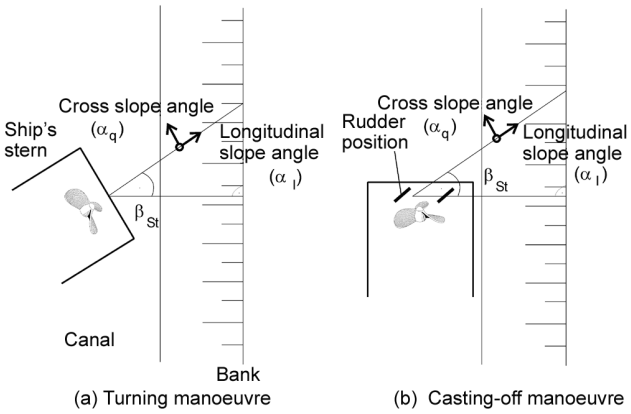

Figure 6.4 Diagram showing jet attack on a bank during (a) a turning manoeuvre or during (b) deflection of the jet during a casting-off manoeuvre

If the jet from the main drive or bow thrusters strikes a bank the value of B_S stated above will depend on the longitudinal slope angle and the cross slope angle in the direction of the jet (see Figure 6.4) and must be replaced with $B_{S,Bö}$:

$$\left\{ \begin{array}{l} B_{S,Bö} = B_S / K \\ \\ K = K_l \, K_q \\ \\ K_l = \dfrac{\sin(\alpha_l + \varphi'_D)}{\sin \varphi'_D} \\ \\ K_q = \cos \alpha_q \sqrt{1 - \dfrac{(\tan \alpha_q)^2}{(\tan \varphi'_D)^2}} \\ \\ \tan \alpha_l = \tan \beta \cos \beta_{St} \\ \\ \tan \alpha_q = \tan \beta \sin \beta_{St} \end{array} \right\} \qquad (6\text{-}8)$$

where

K is the inclination coefficient [-]

K_l is the longitudinal slope coefficient [-]

K_q is the cross slope coefficient [-]

α_l is the longitudinal slope angle [°]

α_q is the cross slope angle [°]

β is the slope angle [°]
β = arctan (1/m)

β_{St} is the angle between the jet axis and slope line normal (angle of impact) [°]

φ'_D is the angle of shearing resistance of the revetment [°] in accordance with 4.3

6.3.2 Stone size required to limit the depth of scour due to propeller wash

The equations stated by /*Römisch 1975*/ and /*Ducker, Miller 1996*/ can be used to estimate the depth of scour caused by propeller wash or the stone size required for a given tolerated scour depth:

$$\begin{cases} \dfrac{h_{Kolk}}{D_{85}} = C_m \; 0.1 \left(\dfrac{B^*}{B^*_{85}} \right)^{13} \text{ for } 1 \le \dfrac{B^*}{B^*_{85}} \le 1.4 \\ \dfrac{h_{Kolk}}{D_{85}} = C_m \; 4.6 \left(\dfrac{B^*}{B^*_{85}} \right)^{2.25} \text{ for } \dfrac{B^*}{B^*_{85}} > 1.4 \\ B^* = \dfrac{v_{max,S}}{\sqrt{g' \, D_{85}}} \\ B^*_{85} = B^*_{85,0} \sqrt{K} \end{cases} \quad (6\text{-}9)$$

where

B^* is the load coefficient [-]

B^*_{85} is the stability coefficient for slopes [-]

$B^*_{85,0}$ is the stability coefficient, in general [-]

$B^*_{85,0} = 1.25$ for standard situations 1 and 4 (see 5.6.3.1) and bow thrusters (see 5.6.5

$B^*_{85,0} = 1.73$ for standard situations 2 and 3 (see 5.6.3.1)

C_m is the coefficient for the duration of the load [-]

C_m = 1.0 for permanent loads

C_m = 0.3 for temporary loads for manoeuvres and for scouring in revetments comprising common types of armourstone (does not apply to sand or gravel)

g' is the relative density [m/s^2]
$g' = g((\rho_S - \rho_W)/\rho_W)$

h_{Kolk} is the depth of scour below the bed of the river or canal [m]

K is the inclination coefficient [-] (see eq. (6-8))

$v_{max,S}$ is the maximum flow velocity at the bed [m/s]
– for the main drive v_{Bmax} or v_{Bmax1} in accordance with 5.6.4
– for bow thrusters v_{xmax} or $v_{max,S,K}$ in accordance with 5.6.5

ρ_W is the density of water [kg/m^3]

ρ_S is the density of the riprap [kg/m^3]

The development of scour over time must be observed in the case of small grain sizes and large scour depths /*Gaudio et al. 2003*/.

6.4 Stone size required to resist loading due to secondary diverging waves

The wave crests of the diverging waves propagating from the bow and stern of a ship strike the bank at an angle β_W of approx. 55° when the ship is sailing parallel to the bank and when $v_S / \sqrt{g \, h_m} < 0.8$ (see Figure 5.20). The ship-induced secondary waves can be treated as incident waves according to /*Verhey, Bogaerts 1989*/ if the wave height is reduced as follows by the factor cos β_W:

Nominal stone size D_{n50} required to resist secondary diverging waves [m]

$$D_{n50} \ge \frac{H_{Sek} (\cos\beta_W)^{1/2} \, \xi^{1/2}}{\dfrac{\rho_S - \rho_W}{\rho_W} \, 2.25 \, (\cos\beta + \sin\beta)} \quad (6\text{-}10)$$

$$\xi = \tan\beta \left(\frac{\lambda_S}{H_{Sek}} \right)^{1/2}$$

where

H_{Sek} is the height of the secondary waves [m] in accordance with 5.5.5, possibly with superimposed wind waves as described in 5.7

λ_S is the wave length of the secondary diverging wave [m] in accordance with eq. (5-46)

β is the slope angle [°]

β_W is the angle between the wave crest of the secondary diverging wave and the bank line [°]; usually β_W = 55° (see Figure 5.20)

ξ is the surf similarity parameter [-]

Equations (6-3) and (6-4) may be used approximatively for transversal stern waves parallel to the bank. H_{Sek} in accordance with eq. (5-47) and limited by eq. (5-50) must then be substituted for $H_{u,Heck}$.

6.5 Stone size required to resist wind waves

The mean nominal stone size D_{n50} of a cover layer required to resist loading due solely to wind waves must be determined by the following equation /*PIANC 1987a*/:

Nominal stone size D_{n50} required to resist wind waves [m]

$$D_{n50} \ge \frac{H_s \sqrt{\xi}}{2.25} \frac{\rho_W}{\rho_S - \rho_W} \quad (6\text{-}11)$$

where

D_{n50} is the required mean nominal stone size [m]

H_s is the significant wave height (design wave height for wind waves) [m]

ρ_W is the density of water [kg/m^3]

ρ_S is the density of the armourstones [kg/m^3]

ξ is the surf similarity parameter [-] see 5.8.2

6.6 Stone size required to resist combined loads due to ship-induced waves and wind waves

Secondary diverging waves and wind waves may very occasionally be superimposed unfavourably, usually behind the ship. The wave heights are added together if the wave lengths are similar. If there are great differences in the wave lengths, the resulting wave height can be taken to be

$$½\, H_{Sek} + H_s \qquad (H_s > H_{Sek})$$

or

$$½\, H_s + H_{Sek} \qquad (H_{Sek} > H_s)$$

The equation in either 6.4 or 6.5 is used to determine the required stone size, depending on which component of the wave height forms the greater part of the resultant value.

6.7 Stone size required to resist attack by currents

In addition to loads due to ship-induced waves and wind waves, the planned cover layer must also withstand attack by currents flowing parallel to the bank and bottom of the river or canal. This type of attack results from natural currents, return flows and in some cases from the superimposition of these parameters or from the slope supply flow of the breaking stern wave.

6.7.1 Stone size required to resist attack by currents flowing largely parallel to the slope

The following equation may be used to obtain a rough estimate of the stone size /*PIANC 1987a*/:

Stone size D_{50} required to resist currents [m]

$$D_{50} \geq C_{lsb}\; C_{Bö}\; \frac{v_{max}^2}{g}\; \frac{1}{\frac{\rho_S - \rho_W}{\rho_W}} \qquad (6\text{-}12)$$

where

$C_{Bö}$ is a factor for considering the influence of the slope [-]
$C_{Bö}=1/k$
$k = \cos\beta\,[1 - (\tan^2\beta/\tan^2\varphi'_D)]^{0.5}$

C_{lsb} is a factor according to Isbash [-]
$C_{lsb} \approx 0.7$

D_{50} is the required stone size (grain size) at 50 % of particles passing [m]

g is the acceleration due to gravity [m/s^2]

v_{max} is the maximum flow velocity [m/s] composed of the return flow and flow velocity

Flow velocity in the direction of travel (downstream):
$v_{max} = \hat{v}_{rück} - v_{Str}$
Flow velocity opposite to the direction of travel (upstream):
$v_{max} = \hat{v}_{rück} + v_{Str}$

$\hat{v}_{rück}$ is the maximum return flow velocity [m/s]
$\hat{v}_{rück,u,Bug}$ for the bow section in accordance with 5.5.4.2
$\hat{v}_{rück,u,Heck}$ for the stern section in accordance with 5.5.4.3

v_{Str} is the flow velocity without shipping [m/s] near the slope

β is the slope angle [°]

φ'_D is the angle of shearing resistance [°]
approx. 55° for common cover layer materials

ρ_W is the density of water [kg/m^3]

ρ_S is the density of riprap [kg/m^3]

Eq. (6-12) is based on a limit definition by Isbash /*DVWK 118*/ that ensures stability against pure attack by currents for horizontal and gently sloping river and canal beds. It yields higher values than other methods /*DVWK 118; Söhngen, Koll 1997*/.

Extending the basic equation to include the factor $C_{Bö}$ describes the increase in the required nominal stone size D_{n50} due to the slope angle β and the angle of shearing resistance φ'_D of the riprap. The relationship $C_{Bö}$ = Fkt. (β, φ'_D) can be seen in Figure 6.5.

The point at which the natural bed material (adjacent to the toe of the revetment) begins to move can be estimated by means of the methods described by **Hjulström** (empirical method; correlation between the mean flow velocity and mean grain size), **Shields** (semi-empirical method; correlation between the velocity of the shear stress at the bed and the roughness of the bed; iterative solution) or **Bonnefille** (same as for Shields; direct solution), as

explained in detail in /*Dittrich 1998*/. All of these methods apply to uniform bed material ($U = D_{60}/D_{10} < 3$) with grain sizes D less than 100 mm.

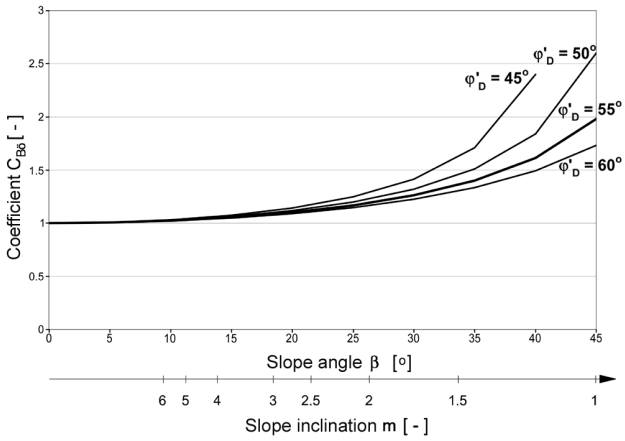

Figure 6.5 Dependence of factor $C_{Bö}$ on the slope angle β or the slope inclination m and the angle of shearing resistance φ'_D

6.7.2 Stone size required to resist loads on the slope due to slope supply flow

The coefficient C_{lsb} in eq. (6-12) must be reduced for loads due to the temporary, highly turbulent currents, partly mixed with air and flowing parallel to the slope, that occur when a transversal stern wave breaks (surf similarity parameter, see 5.5.4.5) and the resulting depression is filled from astern. The following grain size D_{50} is obtained using the maximum flow velocity u_{max}, allowing for the bed current:

Stone size D_{50} required to resist slope supply flow [m]

$$D_{50} \geq 0.5\, C_{Bö}\, \frac{u_{max,B}^2}{g}\, \frac{1}{\frac{\rho_S - \rho_W}{\rho_W}} \qquad (6\text{-}13)$$

where

$u_{max,B}$ is the design velocity of the slope supply flow [m/s]
maximum velocity of the slope supply flow u_{max} in accordance with eq. (5-33) in 5.5.4.5 plus a component of the bed current (mean flow velocity near the slope) v_{Str}

Flow velocity in direction v_s (vessel travelling downstream):
$u_{max,B} = u_{max} + v_{Str}$

Flow velocity opposite to direction v_s (vessel travelling upstream):
$u_{max,B} = u_{max} - v_{Str}$

Allowance must be made for boundary effects as the depth of water in the slope supply flow is small, corresponding more or less to the wave height. The loads acting on a slope are therefore greater for rough slopes than for slopes stabilised with small stone sizes. This effect can be taken into account approximately by introducing the height of the stern waves as follows in accordance with /BAW 2002/:

Stone size D_{50} [m] taking into account of the stern wave height

$$D_{50} \geq \left(\frac{u_{max,B}^2\, C_{Bö}}{\frac{\rho_S - \rho_W}{\rho_W}\, g\, 1.4\, H_{u,Heck}^{1/3}} \right)^{3/2} \qquad (6\text{-}14)$$

where

$H_{u,Heck}$ is the maximum height of the stern wave including the secondary wave component near the slope [m] in accordance with 5.5.4.4, eq. (5-32)

The above equations can only provide an initial estimate of the stone size required for a revetment owing to the uncertainties in the determination of $u_{max,B}$. However, they show that the ship speed and the height of the breaking stern wave, on which $u_{max,B}$ largely depends, are crucial to determining the stone size.

6.8 Stone size as specified in the Technical Supply Conditions for Armourstones (TLW)

The stone size D_{n50} is not the same as the mean size of armourstones if the stones are classified in accordance with the Technical Supply Conditions for Armourstones /*TLW*/. The classification of armourstones in /*TLW*/ (1997 edition) is based on the characteristic greatest stone length D_L (largest measured dimension of an armourstone, cf. length *a* in Figure 6.3), the class boundaries specified in that publication being D_{L0} and D_{L100}. Thus the stone sizes are not determined by screening. D_{L50} is not defined exactly in /*TLW*/. Permissible grading bands for the riprap classes 0 – V as specified in /*TLW*/ are shown in Figure 6.6. Generally speaking, D_{Lx} or D_{L50} for 50 % (see Figure 6.2) can be calculated as follows,

assuming a loglinear grain distribution that applies to the median line of the grading bands shown in Figure 6.6 (corresponding to the class boundaries in /*TLW*/):

$$\text{General :} \qquad D_{Lx} = D_{L0}\left(\frac{D_{L100}}{D_{L0}}\right)^{\frac{x}{100\%}}$$

$$\text{For } x = 50\ \%: \qquad D_{L50} = D_{L0}\left(\frac{D_{L100}}{D_{L0}}\right)^{0.50}$$

It must be checked whether the actual grading curve is reflected accurately enough by the median line of the grading bands shown in Figure 6.6. If not, the lower edge of the band applies.

According to /*Abromeit 1997; Kniess 1977*/ the relationship between the stone size of compact, i.e. neither flat or rod-shaped, stones as specified in /TLW/ and the nominal stone size D_n is as follows:

Stone size according to /*TLW*/ D_{TLW} [m]

$$D_{TLW} = D_L \approx 1.6\, D_n \qquad (6\text{-}15)$$

where

D_L is the characteristic greatest stone length [m]

D_n is the nominal stone size [m]

D_{TLW} is the stone size according to /*TLW*/ [m]

The relationship in eq. (6-15) is based on the shape of the armourstones, which is somewhere between a sphere and a cube /*Knieß 1977*/.

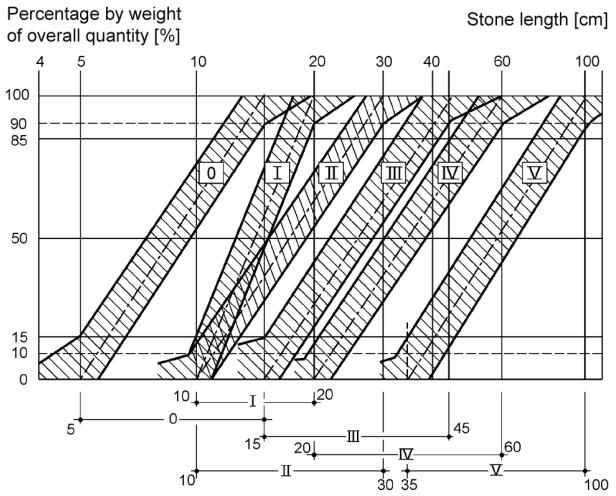

Figure 6.6 Permitted grading bands for riprap classes 0 – V as specified in /TLW/, taken from /MAK/ (1989 edition)

The factor of 1.6 stated in eq. (6-15) is an approximate value. It is often higher for armourstones of metamorphic sedimentary rock such as limestone, greywacke, gneiss, etc. and generally lower for plutonic rocks such as basalt. The ratio of the length of armourstones to their nominal size must be determined on a case-to-case basis by examining a sample of the stones intended for use.

Screening classes (criterion: grain size D_i) and weight classes (criterion: G_i) are specified in the 2003 edition of /*TLW*/ which was adopted in 2004. If D_{50} is determined, it can be used directly to establish the required screening class. If a nominal stone size D_{n50} is calculated, it can be converted into D_{50} as follows to enable a screening class to be selected, the calculation being based on eq. (6-2):

$D_{50} = 1.15\, D_{n50}$.

The nominal stone size D_{n50} can be converted as follows to enable a weight class G_{50} to be selected, the calculation being based on eq. (6-1):

$G_{50} = (D_{n50})^3\, \rho_S$ or

$G_{50} = 0.65\, (D_{50})^3\, \rho_S$

The 2003 edition of /*TLW*/ is based on /*DIN EN 13383*/. Further comments on this subject are included in /*Abromeit 2004*/.

6.9 Thickness of the cover layer

The uses of the design equations for the required stone size stated in 6.2 to 6.7 presuppose a minimum construction thickness d_D of the cover layer. This results from the boundary conditions of the various model tests on which the design methods are based /*Dietz 1973; Hudson 1959; Fuehrer, Römisch 1985*/:

Thickness of cover layer d_D [m]

$$d_D = (1.5 \div 2.0)\, D_{n50} \qquad (6\text{-}16)$$

where

d_D is the required construction thickness of a cover layer [m]

D_{n50} is the required mean nominal stone size [m]

Very permeable cover layer substructures (coarse gravel or coarse granular material) are also hydraulically effective in the case of actions due to waves and/or currents. The thickness of the substructure may therefore be taken into account fully in the hydraulic design of unbound riprap cover layers /*Abromeit 1997*/.

The following thickness is recommended as the smallest erosion-resistant construction thickness of riprap if the coefficient of uniformity U of the latter is taken into account /*Abromeit 1997*/:

Minimum required construction thickness
min d_D [m]

$$\min d_D = 1.5\, D_{n50}\, \sqrt{U} \qquad (6\text{-}17)$$

where

D_{n50} is the required mean nominal stone size [m]

min d_D is the minimum required construction thickness [m]

U is the coefficient of uniformity of the riprap [-]
$U = D_{60}/D_{10}$

6.10 Determination of hydraulically equivalent revetments

The design methods described above will only provide the mean stone size relevant to the minimum construction thickness. The stones may be smaller if the construction thickness is greater or the substructure of the cover layer is very permeable. The construction thickness of alternative hydraulically equivalent cover layers permitted for a particular design case can be determined approximately as follows for loads due to incident waves in accordance with /*Abromeit 1997*/:

Construction thickness of a hydraulically equivalent cover layer $d_{D\,(B)}$ [m]

$$d_{D\,(B)} = \frac{D_{nSt\,(A)}\; d_{D\,(A)}\; \rho'_A}{D_{nSt\,(B)}\; \rho'_B} \qquad (6\text{-}18)$$

where

$d_{D(A)}$ is the construction thickness of the initial cover layer (A) including a possibly very permeable granular substructure [m]

$d_{D(B)}$ is the construction thickness of the alternative hydraulically equivalent cover layer (B) including the thickness of a possibly very permeable granular substructure [m]

$D_{nSt(A)}$ is the nominal stone size of the initial cover layer for design case (A) [m]

$D_{nSt(B)}$ is the nominal stone size selected for the alternative hydraulically equivalent cover layer (B) [m]

ρ_W is the density of water [kg/m^3]
approx. 1000 kg/m^3

ρ_A is the dry density of a single stone in design case (A) [kg/m^3]

ρ'_A is the effective density of a single stone in design case (A) [kg/m^3]
$\rho'_A = \rho_A - \rho_W$

ρ_B is the dry density of a single stone in the alternative hydraulically equivalent cover layer (B) [kg/m^3]

ρ'_B is the effective density of a single stone in the alternative hydraulically equivalent cover layer (B) [kg/m^3]
$\rho'_B = \rho_B - \rho_W$

Conversion is recommended when the stone size of the initial cover layer determined for a particular design case does not correspond to the mean stone size of the size class specified in /*TLW*/ and a larger or smaller stone size must be selected, for example. The same applies when safety considerations require the use of a slightly greater cover layer thickness than that determined by the hydraulic design. In this case, the stone size may be slightly reduced. Using a lower stone size class may mean that it may be possible, for example, to extend the range of suitable filter grades or possibly even to omit a filter stage if granular filters are used /*MAK*/ or to dispense with a granular intermediate layer if a geotextile filter is used /*MAG*/.

The applicability of eq. (6-18) is restricted as regards the stone size $D_{nSt(B)}$ for reasons relating to the resistance of single grains to attack by waves and currents as there is a limit to the degree to which the hydraulic stability can be improved by increasing the thickness of the cover layer.

Conversely, there is a limit to the degree to which the thickness of the cover layer can be reduced in order to avoid endangering the bond of the stones. It is for this reason that stone sizes lower than those determined by means of eqs. (6-3) to (6-5), (6-10) and (6-12) to (6-14) must not used, irrespective of eq. (6-18).

Furthermore, the minimum thicknesses specified in 6.9 must be complied with.

6.11 Minimum thicknesses

The minimum thicknesses specified below must be complied with in addition to those determined under 6.9 to enable the revetment to withstand hydraulic actions /*Abromeit 1997*/.

The minimum thickness of a cover layer (on the **bed**) required to provide adequate safety against anchor cast is:

$$\left\{\begin{array}{ll} \min d_D \geq 0.5\ \text{m} + x & \text{(on granular filters)} \\ \min d_D \geq 0.6\ \text{m} + x & \text{(on geotextile filters)} \end{array}\right\} \qquad (6\text{-}19)$$

where

min d_D is the minimum thickness of the cover layer [m]

x is the additional thickness for the different kinds of stone [m]

x = 0 m when armourstones are used

x = 0.2 m for small-grained or ungraded materials

The minimum thickness (on the **slope**) required to provide adequate safety against impacts by ships is:

$$\left\{\begin{array}{ll}\min d_D \geq 0.3\ \text{m} + x & \text{(on granular filters)} \\ \min d_D \geq 0.5\ \text{m} + x & \text{(on geotextile filters)}\end{array}\right\} \quad (6\text{-}20)$$

Generally speaking, the following minimum thickness of the cover layer shall apply if a granular filter is used:

$$\min d_D \geq 1.5\, D_{50,TLW} + 0.10\ \text{m} \quad (6\text{-}21)$$

where

$D_{50,TLW}$ is the required mean size according to /*TLW*/ [m]

The following minimum thickness of the cover layer shall apply if a geotextile filter is used in order to ensure adequate protection against ultraviolet radiation:

$$\min d_D \geq \text{maximum of} \left\{\begin{array}{l}1.5\, D_{50,TLW} \\ 0.10\ \text{m}\end{array}\right\} \quad (6\text{-}22)$$

6.12 Length of revetments in the line of the slope required to resist wave loads

6.12.1 General

The slope revetment does not need to be continued down to the bed of a canal or river with same stone size and thickness in accordance with the design principles stated above if it is held in place on the slope by friction in accordance with 7.2.5.2 when exposed to wave action and the natural ground below the lower edge of the slope revetment is resistant to erosion as specified in /MAK/. There are no reliable data available for the design of revetments below the main stabilisation zone. It is recommended that the slope be stabilised in such a way that it is able to withstand the mean return flow velocity (eq. (5-23) in 5.5.3).

The length of a revetment in the direction of the slope line will depend on the still-water level SWL and on the types of wave.

6.12.2 Above the still-water level

The upper boundary of a revetment is determined by the wave run-up (see 5.8.6) and wind set-up (see 5.7.4), depending on the freeboard required.

6.12.3 Below the still-water level

The lower boundary of a revetment is determined by the required mean stone size D_{n50} /*PIANC 1987a*/.

For **primary waves**, the depth R'_d below the still-water level can be determined from Figure 6.7 using the maximum drawdown $\Delta\hat{h}_{u,Bug}$ (see 5.5.4.2) or $\Delta\hat{h}_{u,Heck}$ (see 5.5.4.3). Either the slope inclination or the slope angle must be taken into account when determining the length of the revetment below SWL.

For **secondary waves and wind waves**, the depth R'_d depends on the relevant wave height H and can be taken from Figure 6.8. The significant wave height H_s applies in the case of wind waves, for example (see 5.7.5).

The more unfavourable of the two values of R'_d shall be used in the design.

The revetment must extend at least below the bilge of a moving ship if the safety margin between ship and bank is small and there is a risk of ships colliding with the bank.

6.13 Design for the transition from a vertical bank to a slope revetment

The cover layer must be designed for twice the wave height over a length of 25 m in the transition zone from a vertical bank to a slope revetment to allow for the Mach reflection that may occur there (see 5.8.7).

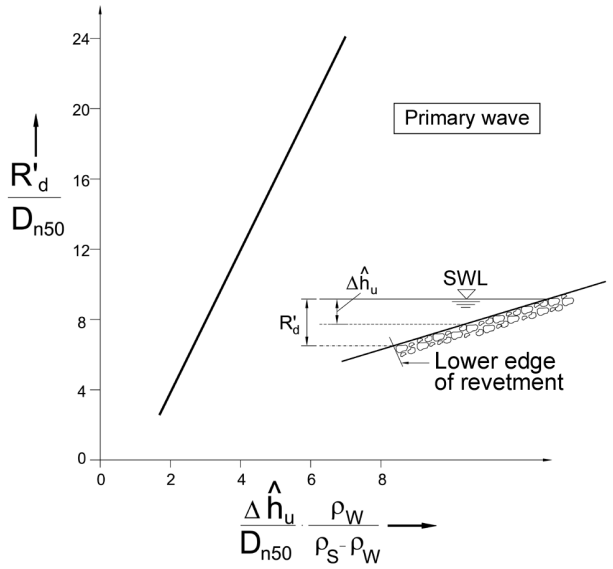

*Figure 6.7 Length of a revetment below SWL for **primary waves** in accordance with /PIANC 1987a/ ($\Delta h = z_A$ in chapter 5)*

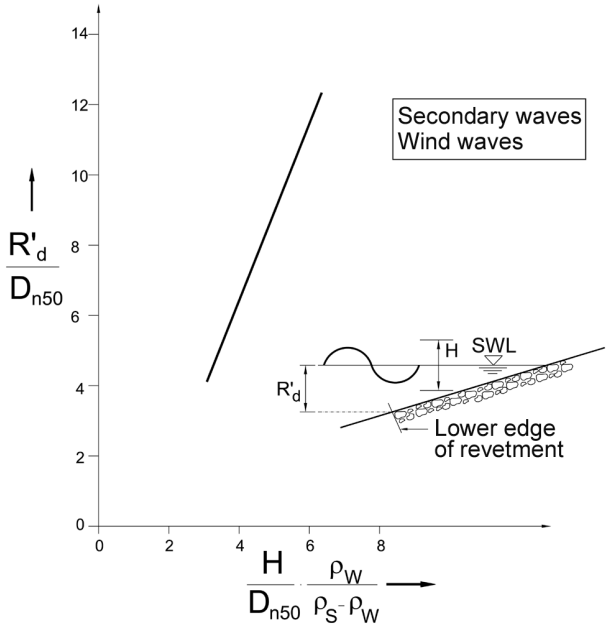

*Figure 6.8 Length of a revetment below SWL for **secondary waves and wind waves** in accordance with /PIANC 1987a/*

7 Geotechnical design of unbound cover layers

7.1 General

7.1.1 Guidance on design

A distinction between the local and global stability of permeable and impermeable revetments must be made in the geotechnical design of cover layers.

The design must ensure local stability for the load case in which excess pore water pressure occurs as a result of rapid drawdown of the water level and the required mass per unit area of the revetment must be determined. The global stability of the water-side slope must also be checked.

The weight of the granular filter may be added to the mass per unit area of the cover layer in each of the following analyses for the geotechnical design of cover layers.

The porosity n of granular filters with the weight densities γ_F and γ'_F can be taken as 0.45. Additional guidance on design is given in 4.3.

7.1.2 Input parameters

Hydraulic input parameters are required for the geotechnical design of unbound cover layers. They are derived from the hydraulic parameters determined in chapter 5.

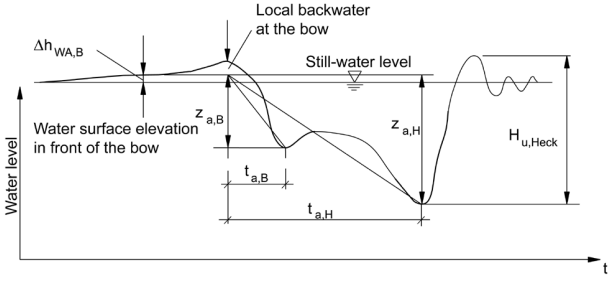

Figure 7.0-a Input parameters for geotechnical design (for a factor $f_{\Delta h_{WA,B}} = 1$)

In this case, it is above all the loads due to the maximum rapid water level drawdown that are of significance. Both the bow wave and the stern wave may be relevant to the design (see Figure 7.0-a). The drawdown time of the bow wave $t_{a,B}$ is shorter than that of the stern wave $t_{a,H}$, which means that, for a given soil, the pore water pressure parameter b (see 5.10.3) is greater for the bow wave than for the stern wave. However, the drawdown at the bow $z_{a,B}$ is generally less pronounced than that at the stern $z_{a,H}$. Both are included as non-linear parameters in the calculation of the excess pore water pressure Δu (see 5.10.3) and the critical depth (see 7.2.2) which subsequently affect the calculation of the required revetment thickness in opposite ways in the geotechnical design. As the non-linearity of the parameters means that their interplay cannot be predicted, both the fast, yet shallower, bow wave and the slower, yet larger, stern wave may be relevant to the design of a revetment. Accordingly, both cases need to be examined.

First, the drawdown times at the bow and stern are calculated (see 5.5.4.7). The pore water pressure parameter b (see 5.10.3) in each case can then be determined using the respective drawdown time and the water permeability k of the soil.

The geotechnically relevant drawdown comprises the water surface elevation in front of the ship's bow and the subsequent drawdown of the water level adjacent to the ship (see Figure 7.0-a). The water surface elevation in front of the bow occurs around not more than 120 s prior to drawdown. If the hydraulic permeability k of the ground is relatively low, the time is too short to cause a corresponding rise in the pore water pressure at the critical depth relevant to the subsequent drawdown. Accordingly, the water surface elevation in front of the bow $\Delta h_{WA,B}$ need not always be taken into account fully when determining the drawdown at the bow $z_{a,B}$ or the stern $z_{a,H}$ that is relevant to the geotechnical design. Depending on the permeability of the soil, it can be reduced using the factor $f_{\Delta h_{WA,B}}$ shown in Figure 7.0-b in accordance with eq. (7-0a) or eq. (7-0b).

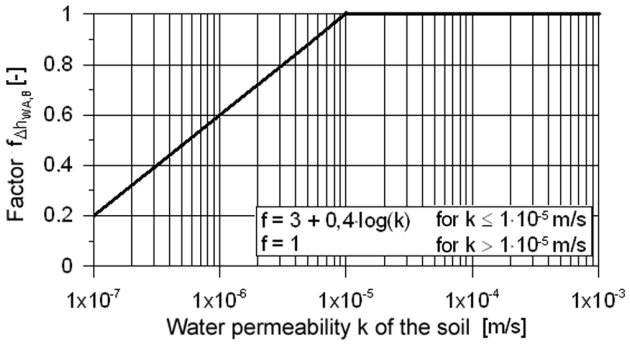

Figure 7.0-b Factor for reducing the effect of the water surface elevation in front of the bow on the maximum rapid water level drawdown z_a

Maximum rapid water level drawdown for the relevant drawdown at bow $z_{a,B}$ [m] or stern $z_{a,H}$ [m]

$$z_{a,B} = H_{u,Bug} \cdot (0{,}91 + 0{,}09 \cdot f_{\Delta h_{WA,B}}) \quad (7\text{-}0a)$$

$$z_{a,H} = 0{,}1 \cdot f_{\Delta h_{WA,B}} \cdot H_{u,Bug} + H_{u,Heck} - \frac{1}{2} H_{Sek,q} \quad (7\text{-}0b)$$

where

$H_{u,Bug}$ is the maximum height of the bow wave at the bank closest to the ship for eccentric sailing [m] in accordance with eq. (5-31)

$f_{\Delta h_{WA,B}}$ is the factor for reducing the effect of the water surface elevation in front of the bow as shown in Figure 7.0-b

$H_{u,Heck}$ is the maximum height of the stern wave at the bank closest to the ship for eccentric sailing [m] in accordance with eq. (5-32)

$H_{Sek,q}$ is the height of pure secondary transversal stern waves [m] in accordance with eq. (5-47).

7.2 Local stability of permeable revetments

7.2.1 General

The rapid drawdown of the water level of a river or canal is always accompanied by excess pore water pressures in the soil close to the surface of the bed and banks of the canal or river (see 3.4.3).

In the case of permeable revetments

- sliding may occur along a failure surface in the ground parallel to the slope at the critical depth d_{krit} below the revetment or
- hydrodynamic soil displacement may occur directly below the revetment

if the revetment has an insufficient weight per unit area, depending on the degree and velocity of drawdown.

Geotechnical analyses for both types of failure must always be carried out in order to determine the required weight per unit area of permeable revetments on banks, i.e. for the assessment of local stability. Such analyses can also be used to check the local stability of natural banks.

7.2.2 Depth of the critical failure surface d_{krit}

The shear resistance of the soil is lowest at the critical depth d_{krit} owing to the excess pore water pressure so that, on slopes, the soil layer above the critical depth may slide. The depth of the critical failure surface is required to enable the required weight per unit area of the cover layer to be calculated and is determined as follows:

Depth of the critical failure surface d_{krit} [m]

$$d_{krit} = \frac{1}{b} \ln \frac{\tan \varphi' \, \gamma_W \, z_a \, b}{\cos \beta \, \gamma' (\tan \varphi' - \tan \beta)} \geq 0 \quad (7\text{-}1)$$

The equation applies when $\varphi' > \beta$.

In the equation

b is a pore water pressure parameter [1/m] in accordance with Figure 5.51

z_a is the maximum rapid drawdown [m]

$z_a = H_{u,Bug}$ relevant drawdown at the bow (including water surface elevation in front of the bow and possibly long-wave components of the backwater at the bow) in accordance with eq. (5-31) (see also Figure 5.18)

$z_a = H^*_{u,H}$ relevant drawdown at the stern in accordance with eq. (5-41) (see also Figure 5.18)

β is the slope angle [°]

γ' is the effective weight density of the soil [kN/m^3]

γ_W is the weight density of water [kN/m^3]

φ' is the effective angle of shearing resistance of the soil [°]

If $d_{krit} \leq 0$, local stability is ensured, even without the weight of the revetment.

Eq. (7-1) is only defined for $\varphi' > \beta$. This calculation method cannot be used for the assessment if $\beta \geq \varphi'$. In that case, the cover layer must be designed in the same way as a retaining wall without bending stiffness.

7.2.3 Weight per unit area of cover layers required to protect slope revetments against sliding failure

7.2.3.1 General

The following method of calculating the required weight per unit area of a permeable cover layer on a bank is based on the failure mechanisms specified for the equilibrium of forces in the plastic limit state in accordance with Rankine's special case.

Initially, an infinitely long slope is considered, after which the additional influences resulting from a toe support or revetment suspension are included.

The shear stresses in the sliding surface are determined. Any other relevant forces (e.g. toe support) are converted into equivalent shear stresses.

The weight per unit area of the cover layer and the associated thickness of a permeable slope revetment are calculated for a failure surface close to the surface and parallel to the slope at the critical depth d_{krit}, determined as described in 7.2.2.

7.2.3.2 Method of calculation

The weight of the cover layer required to prevent sliding failure of a slope is calculated in accordance with the following equation /*Köhler 1989*/:

Weight per unit area g' of cover layer of a permeable slope revetment required to prevent sliding failure [kN/m^2]

$$g' = \gamma'_D \, d_D = \frac{\Delta u \tan\varphi' - c' - \tau_F - \tau_A}{\cos\beta \tan\varphi' - \sin\beta} - (\gamma'_F \, d_F + \gamma' d_{krit}) \quad (7\text{-}2)$$

The equation applies when $\varphi' > \beta$.

In the equation

c' is the effective cohesion of the soil [kN/m^2]

d_D is the thickness of the cover layer [m]

d_F is the thickness of the filter [m]

d_{krit} is the critical depth of the failure surface [m] in accordance with eq. (7-1)

g' is the weight per unit area of the cover layer [kN/m^2]

Δu is the excess pore water pressure [kN/m^2] in accordance with eq. (5-107) for $z = d_{krit}$ in accordance with eq. (7-1)

β is the slope angle [°]

γ' is the effective weight density of the soil [kN/m^3]

γ'_D is the effective weight density of the cover layer [kN/m^3]

γ'_F is the effective weight density of the filter at buoyancy [kN/m^3]
$\gamma'_F = 0$ for geotextile filters

φ' is the effective angle of shearing resistance of the soil [°]

τ_A is the additional stress [kN/m^2] from a revetment suspension (see 7.2.6)

τ_F is the additional stress [kN/m^2] from a toe support (see 7.2.5).

Eq. (7-2) is only defined for soils with an angle of shearing resistance φ' greater than β.

The effective weight density of the cover layer at buoyancy is calculated as follows:

Effective weight density of a permeable cover layer γ'_D [kN/m^3]

$$\gamma'_D = (1-n)(\gamma_S - \gamma_W) \quad (7\text{-}3)$$

where

n is the porosity of the revetment [-]

γ'_D is the effective weight density of the cover layer [kN/m^3]

γ_S is the weight density of the armourstone [kN/m^3]

γ_W is the weight density of water [kN/m^3]

The following values apply to n:

approx. 0.50 – 0.55 for dumping under water

approx. 0.45 for placing in a dry condition

approx. 0.30 – 0.40 for subsequent manual finishing work

If the effective cohesion of the soil c' is

$$c' \geq \Delta u \tan\beta$$

and is permanent, a revetment on such soil (i.e. cohesive soil) will have an adequate degree of safety against sliding failure. Permeable cover layers on a clay lining will also have an adequate level of safety against sliding failure as the clay lining is considered as being similar to a natural cohesive soil for the purpose of the analysis.

If a toe support or anchoring forces are considered, allowance is made for the resulting equivalent additional stresses τ_F (see 7.2.5) and τ_A (see 7.2.6) in eq. (7-2). In this case, attention is drawn to the fact that different types of deformation are required to mobilise such stresses and that only the degree to which they are mobilised must be taken into account.

The required equivalent shear stress erfτ for a selected cover layer thickness is obtained by means of eq. (7-2) as follows:

Required equivalent shear stress erf τ [kN/m^2]

$$\text{erf}\,\tau = (d_D \, \gamma'_D + d_F \, \gamma'_F + d_{krit} \, \gamma')(\sin\beta - \cos\beta \tan\varphi') + \Delta u \tan\varphi' - c' \quad (7\text{-}4)$$

where

c' is the effective cohesion of the soil [kN/m^2]

d_D is the thickness of the cover layer [m]

d_F is the thickness of the filter [m]

d_{krit} is the critical depth of the failure surface [m] in accordance with eq. (7-1)

erf τ is the required shear stress [kN/m^2]

τ_F additional shear stress from a toe support

τ_A additional shear stress from a revetment suspension

Δu is the excess pore water pressure [kN/m^2] in accordance with eq. (5-107) for $z = d_{krit}$ in accordance with eq. (7-1)

β is the slope angle [°]

γ' is the effective weight density of the soil [kN/m^3]

γ'_D is the effective weight density of the cover layer [kN/m^3]

γ'_F is the effective weight density of the filter [kN/m^3], $\gamma'_F = 0$ for geotextile filters

φ' is the effective angle of shearing resistance of the soil [°]

7.2.3.3 Procedure for stratified ground

If a revetment is placed on stratified ground, the stratum requiring the highest weight per unit area will determine the weight per unit area of the revetment as a whole.

7.2.4 Weight per unit area of cover layers to inhibit hydrodynamic soil displacement

7.2.4.1 General

In the presence of high toe support forces, revetment suspensions or very gentle slope inclinations the necessary weight per unit area of a revetment required to prevent sliding failure may theoretically be reduced to the point at which the excess pore water pressure may cause the surface of the soil to move upwards, resulting in loosening of the ground.

This may result in hydrodynamic soil displacement in **non-cohesive soils** (c' = 0) /*Köhler, Koenders 2003*/. In such cases, the weight per unit area selected for the design must be high enough to suppress the excess pore water pressure at the critical depth by applying a sufficiently high surcharge. As a rule, $b \leq 8$ applies to non-cohesive soils. Soils are usually cohesive at values of $b > 8$.

The above check is not required for **cohesive soils** (c' > 0) as hydrodynamic soil displacement does not occur in them.

7.2.4.2 Method of calculation

The weight per unit area at buoyancy g' of the cover layer that is required to inhibit hydrodynamic soil displacement is calculated as follows by analogy to hydraulic heave:

Weight per unit area g' of a permeable cover layer at buoyancy required to inhibit hydrodynamic soil displacement [kN/m^2]

$$g' = \gamma'_D \; d_D \geq \frac{\Delta u}{\cos \beta} - (\gamma'_F \; d_F + \gamma' \; d_{krithB}) \qquad (7\text{-}5)$$

where

b is the pore water pressure parameter [1/m] in accordance with Figure 5.51, as a function of the drawdown velocity

d_D is the thickness of the cover layer [m] (measured normally to the surface)

d_F is the thickness of the filter [m] (measured normally to the surface)

d_{krithB} is the critical depth of the failure surface [m] relevant to the hydrodynamic displacement of soil

$$d_{krithB} = \frac{1}{b} \ln\left(\frac{\gamma_w \; z_a \; b}{\gamma' \cos \beta}\right) \geq 0 \qquad (7\text{-}6)$$

g' weight per unit area of the cover layer [kN/m^2]

z_a is the maximum rapid drawdown [m] see below eq. (7-1)

β is the slope angle [°]

γ'_D is the effective weight density of the cover layer [kN/m^3]

γ' the effective weight density of the soil [kN/m^3]

γ'_F is the effective weight density of the filter [kN/m^3], $\gamma'_F = 0$ for geotextile filters

γ_W is the weight density of water [kN/m^3]

Δu is the excess pore water pressure [kN/m^2] according to eq. (5-107) for $z = d_{krithB}$ in accordance with eq. (7-6)

7.2.5 Weight per unit area of cover layers taking a toe support into account

7.2.5.1 General

If the revetment at the toe of the slope is designed as specified in /*MAR*/ (e.g. with a toe blanket, embedded toe or sheet pile wall at the toe) a toe support force can be taken into consideration when

determining the weight per unit area of the cover layer. The magnitude of the toe support force results from the shear strength of the revetment (failure mechanism 1) or from the stability of the toe of the revetment (failure mechanism 2).

The method of calculating the mobilisable toe support force is based on conservative simplifications of the failure geometry and the shear resistances. The toe support force is considered as an equivalent shear stress in the sliding surface.

Two failure mechanisms are possible for supported slope revetments:

- **Failure mechanism 1:** The revetment shears off in a horizontal joint passing through the upper edge of the toe of the revetment (see Figure 7.1)
- **Failure mechanism 2:** Failure of the toe of the revetment (see Figure 7.2, Figure 7.3 and Figure 7.4)

The failure mechanism relevant to the design is the one for which the higher cover layer weight is obtained and depends on the design of the toe of the slope.

7.2.5.2 Failure mechanism 1 at the toe of a slope

In the case of failure mechanism 1, the sliding surface is located at the upper edge of the toe of the revetment and passes horizontally through the revetment (Figure 7.1). This failure mechanism does not depend on the design of the toe.

In the case of stratified ground, the failure surface may also be located at the interface between two strata.

In the case of cover layers placed on a granular filter, the weighted mean of the individual weight densities of the cover layer and filter may be taken as the weight density of the overall system by way of simplification.

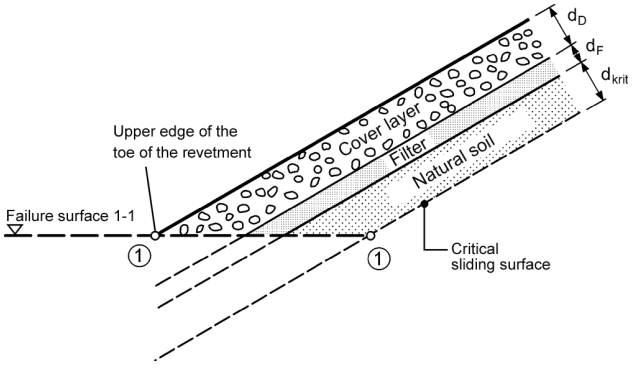

Figure 7.1 Failure mechanism 1 of a toe support

The equivalent shear stress resulting from the toe support force max τ_{F1} below the slope revetment cannot exceed the value required for equilibrium in the direction in which the slope falls.

The required weight per unit area g' of the cover layer or the associated cover layer thickness is obtained as follows for failure mechanism 1:

Required thickness of a permeable cover layer d_D for failure mechanism 1 [m]

$$d_D = \sqrt{A^2 + \frac{B}{0.5\, C\, \gamma'_D}} - A \qquad (7\text{-}7)$$

with the auxiliary functions

A = $(C\, \gamma'_D\, d_F - DE\, \gamma'_D) / C\, \gamma'_D$

B = $DE\, (d_F\, \gamma'_F + d_{krit}\, \gamma') + DF - G$

C = $\tan\varphi'_D \cos\beta$

D = $(\cos\beta - \sin\beta \tan\varphi'_D)\, (h_W - z_a)$

E = $\sin\beta - \cos\beta \tan\varphi'$

F = $\Delta u \tan\varphi' - c'$

G = $0.5\, d_F^2\, \gamma'_F$

and with the symbols

c' is the effective cohesion of the soil [kN/m^2]

d_F is the thickness of the filter [m]

d_{krit} is the critical depth of the failure surface [m] in accordance with eq. (7-1)

h_W is the water depth at still-water level [m]

z_a is the maximum rapid drawdown [m] see below eq. (7-1)

β is the slope angle [°]

γ'_D is the effective weight density of the cover layer [kN/m^3]

γ'_F is the effective weight density of the filter [kN/m^3], γ'_F = 0 for geotextile filters

γ' the effective weight density of the soil [kN/m^3]

φ' is the effective angle of shearing resistance of the soil [°]

φ'_D is the angle of shearing resistance of the cover layer material [°]
φ'_D = 55° for ungrouted cover layers

Δu is the excess pore water pressure [kN/m^2] according to eq. (5-107) for $z = d_{krit}$ in accordance with eq. (7-1)

The maximum equivalent shear stress max τ_{F1} due to shearing in the revetment in the direction in which the slope falls is obtained as follows:

Maximum equivalent shear stress max τ_{F1} for failure mechanism 1 [kN/m²]

$$\max \tau_{F1} = \frac{\left(\frac{1}{2} d_F^2 \gamma'_F + \left(d_D d_F + \frac{1}{2} d_D^2\right)\gamma'_D\right)\tan\varphi'_D \cos\beta}{(\cos\beta - \sin\beta \tan\varphi'_D)(h_w - z_a)} \quad (7\text{-}8)$$

where

d_D is the thickness of the cover layer [m]

d_F is the thickness of the filter layer [m]

γ'_F is the effective weight density of the filter [kN/m³]

max τ_{F1} is the maximum equivalent shear stress [kN/m²] below the slope revetment for failure mechanism 1

h_W is the water depth at still-water level [m]

z_a is the maximum rapid drawdown [m] see below eq. (7-1)

β is the slope angle [°]

γ'_D is the effective weight density of the cover layer [kN/m³]

φ'_D is the angle of shearing resistance of the cover layer material [°]
φ'_D = 55° for ungrouted cover layers

7.2.5.3 Failure mechanism 2 for toe blankets

If a toe blanket is used, the critical sliding surface in failure mechanism 2 will occur directly beneath the filter layer along the boundary between the subsoil and the toe blanket, petering out below the passive earth pressure wedge in front of the toe blanket at the same level as the bed of the river or canal (see Figure 7.2).

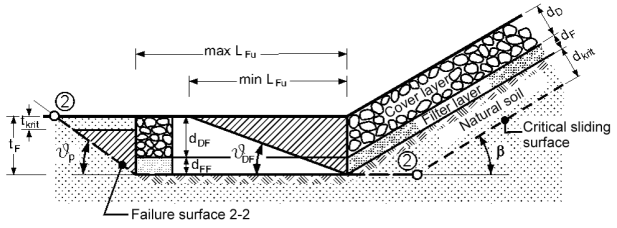

Figure 7.2 Failure mechanism 2 for a slope revetment with a toe blanket

The excess pore water pressure caused in the bed of the river or canal by drawdown z_a (see 5.10) generates an unsteady upward flow of pore water that can temporarily destabilise the soil at the bed. The flow results in the loss of the effective stress of the soil at the bed above the critical depth t_{krit} immediately after the maximum drawdown z_a has been reached. Consequently, there is a reduction in the supporting effect of the mobilisable passive earth pressure in front of the toe blanket /*Köhler, Koenders 2003*/. The difference between the vertical stress from the buoyant soil block *G'* and the excess pore water pressure at the bed, which varies with time, $\Delta u(z)$, results in a minimum in the critical depth t_{krit}. The surplus energy from the unsteady pore water flow is dissipated by the incipient vertical soil movement.

This critical depth t_{krit} at the bed of the river or canal (obtained by eq. (7-1) for a slope angle $\beta = 0$) is calculated as follows:

$$t_{krit} = \frac{1}{b} \ln\left(\frac{b\,\gamma_W\,z_a}{\gamma'}\right) \geq 0 \quad (7\text{-}9)$$

The maximum equivalent shear stress max τ_{F2} that can be assumed for the toe blanket is calculated from the required equilibrium conditions (see Annex A) of all forces acting within and outside the slope toe retaining structure (cf. Figure 7.2), where the following applies:

Maximum equivalent shear stress max τ_{F2} for failure mechanism 2 for a toe blanket [kN/m²]

(inside)

$$\max \tau_{F2,i} = \frac{\left(d_{DF}^2\,\gamma'_{DF} + d_{FF}^2\,\gamma'_{FF} + 2\,d_{DF}\,d_{FF}\,\gamma'_{DF}\right)\sin\beta}{\left[\cos\beta\,\cot\left(\varphi'_{DF} + \vartheta_{DF}\right) - \sin\beta\right] 2\tan\vartheta_{DF}\,(h_w - z_a)} \quad (7\text{-}10)$$

or

(outside)

$$\max \tau_{F2,a} = \frac{\left[\left(\sigma_v'\tan\varphi' + c'\right)L_{Fu} + E'_{ph}\right]\sin\beta}{\left(\cos\beta - \sin\beta\tan\varphi'\right)\left(h_w - z_a\right)} \quad (7\text{-}11)$$

with the equation

$$\sigma'_v = \gamma'_{DF}\,d_{DF} + \gamma'_{FF}\,d_{FF}$$

and with the symbols

b is the pore water pressure parameter [1/m] in accordance with Figure 5.51, depending on the drawdown speed

c' is the effective cohesion of the soil [kN/m^2]

d_{DF} is the thickness of the stone layer in the toe blanket [m]

d_{FF} is the thickness of the filter in the toe blanket [m]

E'_{ph} is the horizontal component of the passive earth pressure in front of the toe blanket [kN/m]

h_W is the water depth at still-water level [m]

L_{Fu} is the length of the toe blanket [m]

$\max \tau_{F2}$ is the maximum equivalent shear stress [kN/m^2] below the slope revetment due to the toe blanket

t_{krit} is the critical depth at the river or canal bed [m]

t_F is the thickness of the toe blanket as a whole [m]

z_a is the maximum rapid drawdown [m] see below eq. (7-1)

β is the slope angle [°]

γ' is the effective weight density of the soil [kN/m^3]

γ'_{DF} is the effective weight density of the cover layer in the toe blanket [kN/m^3]

γ'_{FF} is the effective weight density of the granular filter in the toe blanket [kN/m^3]
$\gamma'_{FF} = 0$ for geotextile filters

γ_W is the weight density of water [kN/m^3]

ϑ_{DF} is the angle of the sliding surface of the passive earth pressure wedge within the toe blanket [°]

ϑ_p is the angle of the sliding surface of the passive earth pressure wedge in the soil directly in front of the toe blanket [°]

σ'_V is the effective vertical stress [kN/m^2]

φ' is the effective angle of shearing resistance of the soil [°]

φ'_{DF} is the effective angle of shearing resistance of the riprap in the toe blanket [°]

The passive earth pressure may only be taken into account in the toe support force if scouring in front of the toe blanket can be ruled out. Otherwise, the passive earth pressure E'_{ph} must not be included in the numerator in eq. (7-11).

For assessments of the internal, maximum shear stress max $\tau_{F2,i}$ that can be mobilized if a toe support is used, the angle of shearing resistance φ'_{DF} must be limited to 35° as larger angles of shearing resistance will result in incorrect results being obtained when using the algorithms for rigid failure mechanisms to calculate the internal shear stress.

The thickness $t_F = d_{DF} + d_{FF}$ and length L_{Fu} of the toe blanket must first be specified. The dimensions finally selected for the toe blanket must satisfy the following three conditions:

(1) The safety against liquefaction of the soil for the selected thickness t_F must be verified in order to ensure a sufficient minimum thickness of the toe blanket. The following inequality must be satisfied, considering the critical depth t_{krit} below the river or canal bed ($\beta = 0$):

$$d_{DF} \geq \frac{\gamma_W \, z_a \left(1 - e^{-b \, t_{krit}}\right) - \gamma'_{FF} \, d_{FF} - \gamma' \, t_{krit}}{\gamma'_{DF}} \qquad (7\text{-}12)$$

The required minimum thickness of the cover layer d_{DF} must satisfy the above inequality for the selected thickness t_F of the toe blanket.

(2) The length L_{Fu} of the toe blanket to be specified must be determined in such a way that it does not exceed the maximum permissible length (max L_{Fu}) and the minimum length (min L_{Fu}) required for inner stability is ensured.

The following applies to the final specification of the length L_{Fu} of the toe blanket

$$\left\{ \begin{array}{l} \min L_{Fu} \leq L_{Fu} \leq \max L_{Fu} \\ \max L_{Fu} = 4 \, t_F \\ \min L_{Fu} = \dfrac{t_F}{\tan \vartheta_{DF}} \end{array} \right\} \qquad (7\text{-}13)$$

The equation includes the following simplifying and conservative assumption for the passive angle of the sliding surface ϑ_{DF} of the passive earth pressure wedge within the toe blanket (verification of internal shear stress):

$$\vartheta_{DF} = 35^\circ \qquad (7\text{-}14)$$

(3) The relevant angle of shearing resistance φ' of the soil at a bed of the river or canal is used to calculate the passive earth pressure in front of the toe blanket E'_{ph} as follows:

$$E'_{ph} = \left(G' - U_v + C \sin \vartheta_p\right) \tan\left(\varphi' + \vartheta_p\right) + C \cos \vartheta_p \qquad (7\text{-}15)$$

with the auxiliary functions

$$G' = \frac{(t_F - t_{krit})^2\ \gamma'}{2 \tan \vartheta_p} \quad \text{and} \quad \vartheta_p = 45° - \frac{\varphi'}{2}$$

$$C = \frac{c' (t_F - t_{krit})}{\sin \vartheta_p}$$

$$U_v = \frac{\gamma_w\ z_a}{\tan \vartheta_p} \left[\frac{e^{-b\,t_F} - e^{-b\,t_{krit}}}{b} + e^{-b\,t_{krit}} (t_F - t_{krit}) \right]$$

N.B.: Only applies when $U_v \geq 0$;
use $U_v < 0$ if $U_v = 0$

and with the symbols

b is the pore water pressure parameter [1/m] in accordance with Figure 5.51, depending on the drawdown speed

c' is the effective cohesion of the soil [kN/m^2]

E'_{ph} is the horizontal component of the passive earth pressure in front of the toe blanket [kN/m]

t_{krit} is the critical depth at the river or canal bed [m]

t_F is the thickness of the overall toe blanket [m]

z_a is the maximum rapid drawdown [m] see below eq. (7-1)

γ_W is the weight density of water [kN/m^3]

γ' is the effective weight density of the soil [kN/m^3]

φ' is the effective angle of shearing resistance of the soil [°]

ϑ_p is the angle of the sliding surface of the passive earth pressure wedge within the toe blanket [°]

The equivalent shear stress max τ_{F2} that can be exerted by the toe blanket is obtained by comparing the results for the external and internal shear stresses obtained in accordance with eqs. (7-10) und (7-11). The lower of the two calculated shear stress values shall be the one used in the following calculation of the required weight per unit area g' of the cover layer:

Required weight per unit area of a permeable cover layer g' for designs including a toe blanket [kN/m^2]

$$g' = \gamma'_D\ d_D = \frac{\max \tau_{F2} - \Delta u \tan \varphi' + c'}{\sin \beta - \cos \beta \tan \varphi' - (\gamma'_F\ d_F + d_{krit}\ \gamma')} \qquad (7\text{-}16)$$

where

c' is the effective cohesion of the soil [kN/m^2]

d_D is the thickness of the cover layer [m]

d_F is the thickness of the filter [m]

d_{krit} is the critical depth of the failure surface [m] in accordance with eq. (7-1)

g' is the required weight per unit area of the cover layer [kN/m^2] for failure mechanism 2

$\max \tau_{F2}$ is the maximum equivalent shear stress [kN/m^2] due to the toe blanket for failure mechanism 2

Δu is the excess pore water pressure [kN/m^2] in accordance with eq. (5-107) for $z = d_{krit}$ in accordance with eq. (7-1)

z_a is the maximum rapid drawdown [m] see below eq. (7-1)

β is the slope angle [°]

γ' is the effective weight density of the soil [kN/m^3]

γ'_D is the effective weight density of the cover layer [kN/m^3]

γ'_F is the effective weight density of the filter [kN/m^3], $\gamma'_F = 0$ for geotextile filters

φ' is the effective angle of shearing resistance of the soil [°]

7.2.5.4 Failure mechanism 2 for embedded toes

In failure mechanism 2 for an embedded toe, the failure surface considered occurs in the soil below the filter or at the interface between the filter and the soil and is located beneath the passive soil wedge (see Figure 7.3). The excess pore water pressure is also relevant to the revetment at the embedded toe below the bed of the river or canal as the pores in this area may be clogged with backfill. The permeability of the latter will then be relevant to the revetment too.

Rapid drawdown generates excess pore water pressure in the soil at the horizontal bed (see 5.10) and consequently a pore water flow. The pore water flow leads to a loss in the effective stresses (soil liquefaction) near the surface, the loss extending down to the critical depth t_{krit}. At this depth, the buoyant force resulting from the difference between the excess pore water pressure and the vertical stress due to the dead weight of the soil reaches its maximum value. The energy arising from the pore water flow is dissipated by the movement of the soil. The critical depth t_{krit} at the river or canal bed (slope angle $\beta = 0$) is calculated on the basis of eq. (7-9) as follows:

$$t_{krit} = \frac{1}{b} \ln \left(\frac{b\,\gamma_W\,z_a}{\gamma'} \right) \geq 0 \qquad (7\text{-}17)$$

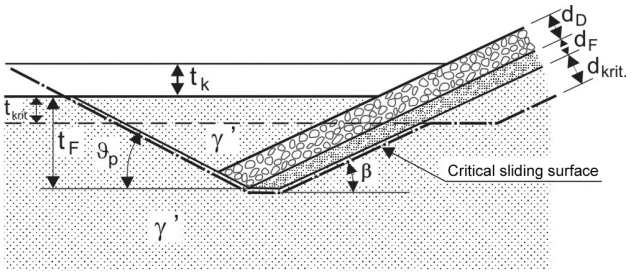

Figure 7.3 Failure mechanism 2 for a bank revetment with an embedded toe

The maximum equivalent shear stress max τ_{F2} is calculated from the equilibrium conditions for the sliding wedge shown in Figure 7.3.

Maximum equivalent shear stress max τ_{F2} for failure mechanism 2 for an embedded toe [kN/m^2]

$$\max \tau_{F2} = \frac{F_{F2}}{L_u} \geq 0$$

$$L_u = \frac{h_W - z_a + t_k + t_{krit}}{\sin\beta} \qquad (7\text{-}18)$$

$$F_{F2} = \frac{U_{v1} - G_1' - C_1' A}{B} + \frac{U_{v2} - G_2'}{D} + C_2'$$

with the auxiliary functions

$$A = \sin\vartheta_p + \cos\vartheta_p \cot(\varphi' + \vartheta_p)$$

$$B = \sin\beta - \cos\beta \cot(\varphi' + \vartheta_p)$$

$$D = \sin\beta - \cos\beta \cot(\varphi' - \beta)$$

$$U_{v1} = \frac{\gamma_W z_a}{\tan\vartheta_p}\left[\frac{e^{-b t_F} - e^{-b t_{krit}}}{b} + e^{-b t_{krit}}(t_F - t_{krit})\right]$$

$$U_{v2} = \frac{\gamma_W z_a}{\tan\beta}\left[\frac{e^{-b t_F} - e^{-b t_{krit}}}{b} + e^{-b t_{krit}}(t_F - t_{krit})\right]$$

$$G_1' = \frac{\gamma'(t_F - t_{krit})^2}{2\tan\vartheta_p}; \quad G_2' = \frac{\gamma'(t_F - t_{krit})^2}{2\tan\beta}$$

$$C_1' = \frac{c'(t_F - t_{krit})}{\sin\vartheta_p}; \quad C_2' = \frac{c'(t_F - t_{krit})}{\sin\beta}$$

$$\vartheta_p = \arctan\left(\sqrt{\frac{(1+\tan^2\varphi')\tan\varphi'}{\tan\varphi' + \tan\beta}} - \tan\varphi'\right)$$

and with the symbols

see below eq. (7-19)

The weight per unit area required in this case is then obtained as follows, taking into account the maximum attainable equivalent shear stress:

Weight per unit area required for a permeable cover layer g' for designs including an embedded toe [kN/m^2]

$$g' = \gamma_D' d_D = \frac{\Delta u \tan\varphi' - c' - \max\tau_{F2}}{\cos\beta\tan\varphi' - \sin\beta} - (\gamma_F' d_F + \gamma' d_{krit}) \qquad (7\text{-}19)$$

where

b is the pore water pressure parameter [1/m] in accordance with Figure 5.51, depending on the drawdown speed

c′ is the effective cohesion of the soil [kN/m^2]

d_D is the thickness of the cover layer [m]

d_F is the thickness of the filter [m]

d_{krit} is the critical depth within the slope [m]

h_W is the water depth at still-water level [m]

t_F is the thickness of the toe blanket [m]

t_k is the depth of scour at the bed in front of the toe of the revetment [m]

t_{krit} is the critical depth at the river or canal bed [m]

Δu is the excess pore water pressure [kN/m^2] in accordance with eq. (5-107) for $z = d_{krit}$ in accordance with eq. (7-1)

z_a is the maximum rapid drawdown [m] see below eq. (7-1)

β is the slope angle [°]

γ' is the effective weight density of the soil [kN/m^3]

γ'_D is the effective weight density of the cover layer [kN/m^3]

γ'_F is the effective weight density of the filter [kN/m^3]

γ_W is the weight density of water [kN/m^3]

φ' is the effective angle of shearing resistance of the soil [°]

ϑ_p is the angle of the sliding surface [°]

max τ_{F2} is the maximum equivalent shear stress due to the embedded toe [kN/m^2] in accordance with eq. (7-18)

Depending on local experience, scouring to a depth of t_k may need to be taken into account as shown in Figure 7.3 when specifying the embedment depth t_F.

Negative values may be obtained when determining the required thickness of the cover layer d_D. In such cases, a revetment is not required for the assessment of the embedded toe. The thickness of the revetment is then obtained by means of failure mechanism 1.

7.2.5.5 Failure mechanism 2 for a sheet pile wall at the toe

Failure mechanism 2 comprises failure of a fixed sheet pile wall installed at the lower edge of a slope revetment. The following influences must be taken into consideration when designing sheet pile walls (see Figure 7.4):

(a) The toe support force F acting on the head of the sheet-pile wall in the direction in which the cover layer falls; F is obtained from the additional shear stress erf τ_F in accordance with eq. (7-4) for the selected thickness d_D of the cover layer in conjunction with the following equation

$$F = \text{erf}\,\tau_F \; L_u \qquad (7\text{-}20)$$

where

h_W is the water depth at still-water level [m]

L_u is the length of the slope revetment below the water level [m]

$$L_u = \frac{h_W - z_a}{\sin \beta}$$

z_a is the maximum rapid drawdown [m] see below eq. (7-1)

β is the slope angle [°]

erf τ_F is the required shear stress [kN/m^2] for the sheet pile wall at the toe in accordance with eq. (7-4)

(b) the active earth pressure E'_a in the soil below the slope revetment

(c) a scour depth t_k, to be specified in accordance with /*MAR*/ or local experience

(d) the critical depth t_{krit} at which the buoyancy force due to the difference between the excess pore water pressure and the self-weight of the soil reaches its maximum

(e) the resulting excess water pressure $u_b = \Delta u(\Delta t_k)$ where $\Delta t_k > 0$ in accordance with Figure 7.4

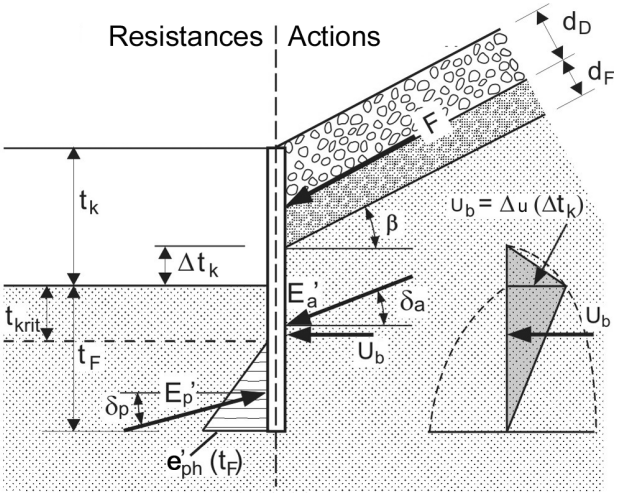

Figure 7.4 Toe support in the form of a sheet pile wall for a slope revetment (failure mechanism 2). Symbols: E'_a - active earth pressure, E'_p - passive earth pressure, F – force due to the revetment, t_k – depth of scour, U_b – resultant force of excess pore water pressure

Unanchored sheet pile walls are designed for full restraint in accordance with /*EAU 2004*/. If a scour depth t_k is assumed, the stresses shall be assessed for load case 2 /*EAU 2004*/ if the scour is only temporary.

The excess pore water pressure at the bed in accordance with eq. (5-107) must be taken into account when determining the earth resistance E'_p in front of the sheet pile wall. E'_p is the resultant of the earth resistance inclined at a wall friction angle $\delta_p = 2/3\ \varphi'$ in accordance with /*DIN 4085*/.

Conservative values of the horizontal earth pressure force E'_{ph} can be obtained in a simplified manner by using the earth pressure ordinates e'_{ph} in accordance with the following equation which includes the effect of the excess pore water pressure due to rapid drawdown. The passive earth pressure can be taken as increasing linearly with the depth (see Figure 7.4).

Earth pressure ordinate $e'_{ph}(t_F)$ [kN/m^2]

$$e'_{ph}(t_F) = \frac{2E'_{ph}\cos\delta_p}{(t_F - t_{krit})^2} \qquad (7\text{-}21)$$

with the auxiliary functions

$$E'_{ph} = \frac{U_v - G' - C'\left(\cos\vartheta_p \cot\left(\vartheta_p + \varphi'\right) - \sin\vartheta_p\right)}{\sin\delta_p - \cos\delta_p \cot\left(\vartheta_p + \varphi'\right)}$$

$$C' = \frac{c'\left(t_F - t_{krit}\right)}{\sin\vartheta_p}$$

$$G' = \frac{\gamma'\left(t_F - t_{krit}\right)^2}{2\tan\vartheta_p}$$

$$U_v = \frac{\gamma_w z_a}{\tan\vartheta_p}\left[\frac{e^{-bt_F} - e^{-bt_{krit}}}{b} + e^{-bt_{krit}}\left(t_F - t_{krit}\right)\right]$$

$$\vartheta_p = \arctan\left(\sqrt{\frac{(1+\tan^2\varphi')\tan\varphi'}{\tan\varphi' + \tan\delta_p}} - \tan\varphi'\right)$$

$$t_{krit} = \frac{1}{b}\ln\left(\frac{\gamma_w z_a b}{\gamma'}\right)$$

and with the symbols

b is the pore water pressure parameter [1/m] for the maximum drawdown time in accordance with Figure 5.51

c' is the effective cohesion of the soil [kN/m^2]

E'_{ph} is the horizontal component of the passive earth pressure [kN/m^2]

t is the depth below the river or canal bed [m]

t_{krit} is the critical depth at the river or canal bed (β = 0°)

t_F is the depth of the sheet pile wall [m] (the selected value of t_F must be greater than t_{krit})

z_a is the maximum rapid drawdown [m] see below eq. (7-1)

γ' is the effective weight density of the soil [kN/m^3]

δ_p is the wall friction angle [°], as a rule δ_p = 2/3 φ' for sheet pile walls

γ_W is the weight density of water [kN/m^3]

φ' is the effective angle of shearing resistance of the soil [°]

ϑ_p is the angle of the sliding surface [°]

The excess pore water pressure Δu in the area of the earth resistance has already been included in eq. (7-21)

The active earth pressure E'_a may be determined using the effective weight density of the soil in accordance with /*DIN 4085*/.

The resulting water pressure on the active side may be simplified by means of a triangle as shown in Figure 7.4, the ordinate of the triangle at the lower edge of the scour being obtained using eq. (5-107) for the depth z = Δt_k = t_k - (d_F+d_D)/cosβ and for the drawdown time t = t_a.

The cover layer will be stable if it is possible to design the sheet pile wall at the toe for the influences referred to in (a) to (c). The weight of the cover layer or the embedment depth and the moment of resistance of the sheet piles, if relevant, must otherwise be increased.

7.2.6 Weight per unit area of cover layers taking a suspension of the revetment into account

7.2.6.1 General

The stability of the revetment can be increased by anchoring the cover layer at the top ("suspended revetment") (see Figure 7.5). The means of suspension can either comprise individual anchors (steel cables, high-tensile fabric strips) or high-tensile sheets.

The tensile force Z that must be resisted is obtained by multiplying the required shear stress erf τ in accordance with eq. (7-4), which depends on the selected thickness of the cover layer d_D, by the length L_u of the cover layer below the lowered water level.

The simultaneous use of a toe support and an anchor at the top of the slope revetment is not recommended.

The following verifications must be performed if resistance to the tensile stress Z is to be provided by the weight of the cover layer above the lowered water level:

- Verification of the external load-bearing capacity (see 7.2.6.2)
- Verification of the internal load-bearing capacity (see 7.2.6.3)

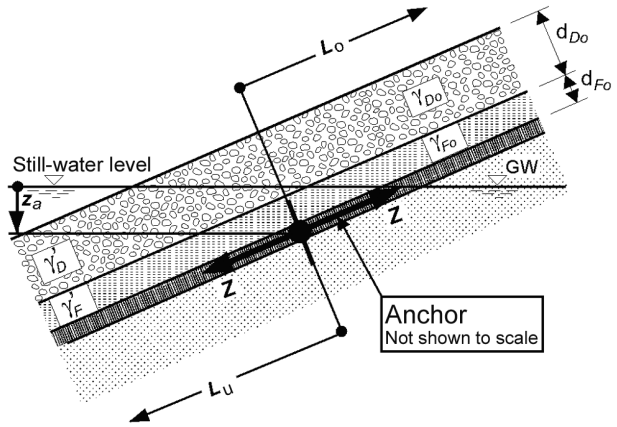

Figure 7.5 Diagram showing a method of suspending a slope revetment

7.2.6.2 Verification of the external load-bearing capacity

The external load-bearing capacity shall be verified as described below if the anchoring forces above the lowered water level are transferred into the ground by friction below the cover layer. The required weight per unit area g' of the cover layer is obtained as follows:

Required weight per unit area g' of a permeable cover layer, taking the suspension of the revetment into account [kN/m^2]

$$g' = \gamma_{Do}\, d_{Do} = \\ = \frac{Z \cos\varphi'_{AB} - c'_{AB}\, L_o \cos\varphi'_{AB}}{L_o \sin(\varphi'_{AB} - \beta)} - \gamma_{Fo}\, d_{Fo} \quad (7\text{-}22)$$

with the quantities

$$Z = \text{erf}\,\tau_A\, L_u$$

$$L_u = \frac{h_W + t_k - z_a}{\sin\beta}$$

and with the symbols

c'_{AB} is the cohesion/adhesion between the tension element and the soil above the lowered water level [kN/m^2]

d_{Do} is the thickness of the cover layer above the lowered water level [m]

d_{Fo} is the thickness of a mineral filter above the lowered water level [m]

erf τ_A is the required additional supporting shear stress [kN/m^2]
erf τ_A = erf τ in accordance with eq. (7-4)

L_u is the length of the slope revetment below the lowered water level [m]

L_o is the length of the slope revetment above the lowered water level [m]

h_W is the water depth at still-water level [m]

t_k is the depth of scour at the bed in front of the toe of the revetment [m], to be specified in accordance with local experience

z_a is the maximum rapid drawdown [m]
see below eq. (7-1)

Z is the tensile force in a revetment suspension [kN/m]

β is the slope angle [°]

γ_{Do} is the weight density of the cover layer above the lowered water level [kN/m^3]

γ_{Fo} is the weight density of a mineral filter above the lowered water level [kN/m^3]

φ'_{AB} is the effective angle of shearing resistance [°] between the tension element and the soil or tension element and the cover layer above the lowered water level, whichever is lower

Forms of load transfer other than by friction in the revetment (e.g. anchor trenches) must be assessed separately in respect of the tensile force Z.

7.2.6.3 Verification of the internal load-bearing capacity

The internal load-bearing capacity of the anchorage shall be verified in accordance with the methods of designing reinforcement elements, e.g. stress analysis or limit state GZ 1B in accordance with the safety concept involving partial safety factors as described in subclause 4.3.2 of /*DIN 1054*/. The strain under service load of geosynthetics must not exceed 2 % of the strain at failure as specified in /*DIN EN ISO 10319*/.

If the resulting thickness d_{Do} of the cover layer above the lowered water level is too high, the weight per unit area of the cover layer d_D below the lowered water level can be increased to reduce the tensile force that needs to be resisted. If permitted by the verification of the internal load-bearing capacity, the tension elements can be anchored in a trench at the shoulder of the embankment in accordance with the recommendation for geosynthetic reinforcements /*EBGEO*/.

7.2.7 Slope revetment above the lowered water level

The stability of a slope above the lowered water level is ensured if the revetment required to protect the slope against erosion extends up to the highest wave run-up point in accordance with 5.8.6.

If groundwater seeps from a slope in a steady-state above the slope revetment, the local stability of that part of the slope is ensured if the slope comprising non-cohesive soil satisfies the following condition (see 3.5):

$$\beta < \frac{\varphi'}{2}$$

where

β is the slope angle above the lowered water level [°]

φ' is the effective angle of shearing resistance of the soil [°]

If this condition is not satisfied other suitable measures will be required to prevent damage if it is not intended to extend the slope revetment over the area in which groundwater seepage occurs.

In this respect, cohesive soils are always stable.

7.3 Local stability of impermeable revetments

7.3.1 General

Impermeable revetments must be designed to withstand the maximum excess water pressure if the ground water level may be higher than the lowered water level in the canal.

The weight per unit area of impermeable revetments must be great enough to prevent the excess pressure below the lining resulting in local sliding on the slope or uplift at the bed.

If the slope lining is capable of resisting longitudinal forces and transferring them to the bed of the river or canal, the weight of the revetment must also be great enough to prevent uplift.

7.3.2 Weight per unit area of impermeable cover layers required to resist sliding

The weight per unit area of the cover layer of an impermeable slope revetment required to resist sliding without any additional support is calculated as follows:

Weight per unit area of an impermeable cover layer g' required to resist sliding [kN/m^2]

$$g' = \gamma'_D d_D + \gamma'_F d_F + \gamma'_{Di} d_{Di} = \frac{\Delta u \tan\varphi' - c'}{\cos\beta \tan\varphi' - \sin\beta} \qquad (7\text{-}23)$$

with the equation

$$\Delta u = (\Delta h_W + z_a)\, \gamma_W \qquad (7\text{-}24)$$

and with the symbols

c' is the effective cohesion of the soil [kN/m^2]

d_D is the thickness of the cover layer [m]

d_{Di} is the thickness of the impervious lining [m]

d_F is the thickness of the filter [m]

g' is the weight per unit area of the cover layer [kN/m^2]

Δu is the excess pore water pressure beneath the lining [kN/m^2]

z_a is the maximum rapid drawdown [m] see below eq. (7-1)

β is the slope angle [°]

Δh_W is the difference in height [m] between the groundwater level and the still-water level of the waterway. It is positive when the groundwater level is above the still-water level.

γ'_D is the effective weight density the cover layer [kN/m^3]

γ'_{Di} is the effective weight density of the lining material [kN/m^3]

γ'_F is the effective weight density of the filter [kN/m^3]

γ_W is the weight density of water [kN/m^3]

φ' is the effective angle of shearing resistance of the soil [°]

It must be examined whether a failure surface in the soil or in the lining will be relevant to the design. The strength of the lining must be introduced as the undrained shear strength.

7.3.3 Weight per unit area of impermeable cover layers required to resist uplift

It must be verified that the weight per unit area of impermeable revetments on the bed or of impermeable revetments on a slope with adequate toe support is sufficient to resist uplift.

The weight per unit area g' of the cover layer of an impermeable revetment required to resist uplift is obtained as follows:

Weight per unit area g' of an impermeable cover layer required to resist uplift [kN/m^2]

$$g' = \gamma'_D\, d_D + \gamma'_F\, d_F + \gamma'_{Di}\, d_{Di} \geq \frac{\Delta u\, \gamma_A}{\cos\beta} \qquad (7\text{-}25)$$

where

d_D the thickness of the cover layer [m]

d_{Di} is the thickness of the impervious lining [m]

d_F is the thickness of the filter [m]

g' is the weight per unit area of the cover layer [kN/m^2]

Δu is the excess pore water pressure below the lining [kN/m^2] in accordance with eq. (7-24)

z_a is the maximum rapid drawdown [m] see below eq. (7-1)

β is the slope angle [°]

Δh_W is the difference in height [m] between the groundwater level and the still-water level on the waterway. It is positive when the groundwater level is above the still-water level.

γ_A is the safety against uplift [-]
γ_A = 1.20

γ'_D is the effective weight density of the cover layer [kN/m^3]

γ'_{Di} the effective weight density of the lining material [kN/m^3]

γ'_F is the effective weight density of the filter [kN/m^3].

7.4 Verification of the global safety of the water-side slope

The global safety of the water-side slope including the revetment or any other surcharges must be verified using the safety margins specified in /*DIN 1054*/ and the methods described in /*DIN 4084*/ (slope failure). Failure mechanisms other than the failure of the revetment as described in 7.2 und 7.3 (sliding or uplift of a sliding wedge parallel to the slope at depth d_{krit} in accordance with 7.2.2 or beneath a lining) must be investigated. Generally speaking, these will be sliding wedges with failure surfaces usually penetrating into the slope over a considerable length (several decimetres or more) below the critical depth d_{krit}.

An analysis for the limit state GZ 1C as described in subclause 4.3.3 of /*DIN 1054*/ must be performed for the following cases:

(a) Operating water level BW or mean water level MW without drawdown with the partial safety factors for load case LC 1 in accordance with /*DIN 1054*/.

(b) Rapid drawdown of the water level (generally caused by a passing ship, but in some cases also after a rapidly receding flood wave), assuming pore water pressure on the failure surface but without allowing for any excess pore water pressure as described in 5.10, to be considered for load case LC 3 in accordance with /*DIN 1054*/.

(c) It is assumed that the excess pore water pressure as described in 5.10 acts on the sliding wedge in (b) with verification that the limit state is satisfied when the partial safety factors γ_φ and γ_c for the shear parameters are both equal to 1.0 ($\gamma_\varphi = \gamma_c = 1.0$).

8 Hydraulic design of partially grouted armourstone cover layers

Field tests and experience have shown that partially grouted cover layers comprising armourstones of size classes I - III and the quantities of grout as specified in /*MAV*/ and constructed in accordance with the specifications in /*MAV*/ have adequate resistance to all known hydraulic actions occurring on waterways when the distribution of the grout over and below the surface is as specified in /*MAV*/. Hydraulic design is not required in this case provided that the maximum flow velocity does not exceed 7.7 m/s /*LWI 1998*/, which is generally the case.

Experience has shown that adequate safety against damage caused by anchors (e.g. due to anchor cast) on navigable waterways is ensured if the cover layer is at least 40 cm deep and the quantity of grout is selected as specified in /*MAV*/.

9 Geotechnical design of partially grouted armourstone cover layers

9.1 General

For the sake of simplification, the design may be performed with an angle of shearing resistance φ'_D of 70° for the overall shear strength for grouting carried out in accordance with /*MAR*/ and /*MAV*/. The quantity of grout can be included in the calculation of the weight density of the revetment as follows:

Mass per unit area of a partially grouted revetment at buoyancy *g*' [kN/m^2]

$$g' = (1-n)(\gamma_D - \gamma_W)\, d_D + \frac{m_V}{1000}(\gamma_V - \gamma_W) \qquad (9\text{-}1)$$

where

d_D is the thickness of the cover layer [m]

g' is the mass per unit area of a partially grouted revetment at buoyancy [kN/m^2]

m_V is the quantity of grouting used [l/m^2] (Denominator of 1000 due to conversion of litres to cubic metres)

n is the voids ratio of the ungrouted revetment [-] in accordance with 7.2.3.2

γ_D is the weight density of the cover layer [kN/m^3]

γ_V is the weight density of the grouting material [kN/m^3]
generally γ_V = 22 kN/m^3

γ_W is the weight density of water [kN/m^3]

9.2 Local stability of permeable revetments with partially grouted cover layers

For the geotechnical design of partially grouted cover layers it must be verified that

- adequate safety against hydrodynamic soil displacement beneath the revetment is ensured as specified in 7.2.4 and
- adequate safety of the slope above the revetment is ensured as specified in 7.2.7.

Note: The extent of dynamic hydraulic actions on cover layers due to passing ships is limited. The internal bond of partially grouted cover layers is sufficient to transfer forces to lateral, unloaded areas. Consequently, verification that the cover layer provides safety against sliding and shearing is not required.

An embedded toe (toe extension as described in /*MAR*/) is required to provide protection against scour.

9.3 Local stability of impermeable revetments with partially grouted cover layers

For the geotechnical design of partially grouted cover layers placed on an impervious lining it must be verified that

- adequate safety against the revetment sliding on the slope is ensured as specified in 7.2.3 and
- adequate safety of the revetment against uplift is ensured as specified in 7.3.3.

9.4 Verification of the global stability of the water-side slope

The global stability of the slope must be verified as specified in 7.4.

10 Literature

/*Abromeit 1997*/ Abromeit, H.-U.

Ermittlung technisch gleichwertiger Deckwerke an Wasserstraßen und im Küstenbereich in Abhängigkeit von der Trockenrohdichte der verwendeten Wasserbausteine

Mitteilungsblatt der Bundesanstalt für Wasserbau Nr. 75,
Eigenverlag, Karlsruhe 1997

/*Abromeit 2004*/ Abromeit, H.-U.

Anpassung der Technischen Lieferbedingungen für Wasserbausteine (TLW) an die neue DIN EN 13383 - Wasserbausteine

BAW-Brief Nr. 1 – März 2004
Eigenverlag, Karlsruhe

/*ACER 1992*/ US Department of the Interior, Bureau of Reclamation

Freeboard criteria and guidelines for computing freeboard allowances for storage dams

Eigenverlag, Denver 1992

/*BAW 2002*/ Bundesanstalt für Wasserbau

Fahrversuche am Wesel-Datteln-Kanal zur Frage der Sohlen- und Deckwerks-stabilität bei Schifffahrt

Karlsruhe, unveröffentlicht

/*Binek, Müller 1991*/ Binek, H.; Müller, E.

Bestimmung der Wassertiefenabhängigkeit des Formfaktors eines Ein-Schrauben-Binnenschiffes

Versuchsanstalt für Binnenschiffbau e.V.
Eigenverlag, Duisburg 1991

/*Blaauw* Blaauw, H. G.; van der Knaap, F. C. M.; de Groot, M. T.; Pilarczyk, K. W.

et al. 1984/ **Design of bank protection of inland navigation fairways**

International conference on flexible armoured revetments incorporating geotextiles
Publ. No. 320
London 1984

/*Blaauw, Kaa 1978*/ Blaauw, H. G.; van de Kaa, E. J.

Erosion of bottom and sloping banks caused by the screw race of manoeuvering ships

WL publication 202; 1978

/*Blokland 1994*/ Blokland, T.

In-situ tests of current velocities and stone movements caused by a propeller jet against a vertical quay wall

Rotterdam public works 1994

/*BMV 1994*/ Bundesministerium für Verkehr

Richtlinien für Regelquerschnitte von Schifffahrtskanälen

Eigenverlag, Bonn 1994

/*BMV 1996*/ Bundesministerium für Verkehr

Bundeswasserstraßenkarte

Drucksachenstelle der WSV
Hannover 1996

/*Bouwmeester 1977*/ Bouwmeester, J.

Recent studies on push-towing as a base for dimensioning waterways

Publication No. 194, 39 p.
Delft Hydraulic Laboratory
Eigenverlag, Delft 1977

/*CEM 2002*/ US Army Corps of Engineers

Coastal engineering manual

USACE Internet Publishing Group
April 2002

/*CUR-TAW 1992*/ Centre for civil engineering research and codes (CUR),
Technical advisory committee on water defences (TAW)

Guide for design of river dikes
Volume 1 - upper river area

Report 142
Eigenverlag, Gouda/NL 1992

/*Daemrich 1978 a*/ Daemrich, K. F.

Diffraktion gebeugter Wellen
- Ein Beitrag zur Berechnung der Wellenunruhe in Häfen

Mitteilungen des Franzius-Instituts für Wasserbau und Küsteningenieurwesen
Technische Universität Hannover

Heft 47, S. 1-157
Eigenverlag, Hannover 1978

/*Daemrich 1978 b*/ Daemrich, K. F.

Diffraktion an halbunendlichen Wellenbrechern - Diagramme der Wellenhöhenverteilung hinter totalreflektierenden linienförmigen Bauwerken

Mitteilungen des Franzius-Instituts für Wasserbau und Küsteningenieurwesen Technische Universität Hannover

Heft 47, S. 196-213
Eigenverlag, Hannover 1978

/*Dand, White 1978*/ Dand, J. W.; White, W. R.

Design of navigation canals

Symposium on aspects of navigability of constraint waterways including harbour entrances
Delft 1978

/*Davidenkoff 1964*/ Davidenkoff, R.

Deiche und Erddämme, Sickerströmung-Standsicherheit

Werner Verlag, Düsseldorf 1964

/*Dettmann 1998*/ Dettmann, T.

Ein Beitrag zur Berechnung von Fahrrinnenverbreiterungen in Kanal- und Flusskrümmungen bei niedrigen Fließgeschwindigkeiten

Binnenschifffahrt Nr. 23, S. 38-40
Dezember 1998

/*Dettmann, Jurisch 2001*/ Dettmann, T.; Jurisch, R.

Beitrag zur Bemessung von Fahrrinnenbreiten in Kanälen und Flüssen

Binnenschifffahrt Nr. 6, S. 72-75
Juni 2001

/*Dietz 1973*/ Dietz, J. W.

Sicherung der Flusssohle unterhalb von Wehren und Sperrwerken

Wasserwirtschaft 63 (1973) 3, S. 76-83

/*DIN 1054*/ Deutsches Institut für Normung (Hrsg.)

Zulässige Belastung des Baugrunds

Beuth-Verlag, Berlin

/*DIN 4020*/ Deutsches Institut für Normung (Hrsg.)

Geotechnische Untersuchungen für bautechnische Zwecke

Beuth-Verlag, Berlin

/*DIN 4084*/ Deutsches Institut für Normung (Hrsg.)
Gelände- und Böschungsbruchberechnungen
Beuth-Verlag, Berlin

/*DIN 4085*/ Deutsches Institut für Normung (Hrsg.)
Berechnung des Erddrucks
Beuth-Verlag, Berlin

/*DIN 18196*/ Deutsches Institut für Normung (Hrsg.)
Erd- und Grundbau; Bodenklassifikation für bautechnische Zwecke
Beuth-Verlag, Berlin

/*DIN EN 13383*/ Deutsches Institut für Normung (Hrsg.)
Wasserbausteine
Teil 1 und Teil 2
Beuth-Verlag, Berlin

/*DIN EN ISO 10319*/ Deutsches Institut für Normung (Hrsg.)
Geotextilien- Zugversuch am breiten Streifen
ISO 10319:1993; Deutsche Fassung EN ISO 10319:1996
Beuth-Verlag, Berlin

/*Dittrich 1998*/ Dittrich, A.
Wechselwirkungen Morphologie/Strömung naturnaher Fließgewässer
Mitteilungen aus dem Institut für Wasserbau und Kulturtechnik,
Universität Karlsruhe, Heft 198
Eigenverlag, Karlsruhe 1998

/*Ducker, Miller 1996*/ Ducker, H. P.; Miller, C.
Harbour bottom erosion at berths due to propeller jets
Proceedings of the 11th International Harbour Congress
Antwerpen, 1996

/*DVPFIX 2002*/ **Programmdokumentation DVPFIX**
Institut für Energie- und Umwelttechnik, Universität Rostock 2002

/*DVWK 118*/ Deutscher Verband für Wasserwirtschaft und Kulturbau e. V., DVWK (Hrsg.)
Maßnahmen zur naturnahen Gewässerstabilisierung
DVWK Schriften, Heft 118
Wirtschafts- und Verlagsgesellschaft mbH, Bonn 1997

/*DVWK 246*/ Deutscher Verband für Wasserwirtschaft und Kulturbau e. V., DVWK (Hrsg.)

Freibordbemessung an Stauanlagen

DVWK Schriften, Heft 246
Wirtschafts- und Verlagsgesellschaft Gas und Wasser mbH, Bonn 1997

/*EAK 1993*/ Deutsche Gesellschaft für Erd- und Grundbau (DGEG), Hafenbautechnische Gesellschaft (HTG)

Empfehlungen für die Ausführung von Küstenschutzbauwerken

Die Küste
Westholsteinische Verlagsanstalt Boyens & Co., Heide in Holstein 1993

/*EAK 2002*/ Deutsche Gesellschaft für Geotechnik e. V. (DGGT), Hafenbautechnische Gesellschaft e.V. (HTG)

Empfehlungen für die Ausführung von Küstenschutzwerken

Die Küste, Heft 65, 2002

/*EBGEO*/ Deutsche Gesellschaft für Geotechnik e. V. (DGGT)

Empfehlungen für Bewehrungen aus Geokunststoffen

Verlag Wilhelm Ernst & Sohn, Berlin 1997

/*EAU 1996*/ Hafenbautechnische Gesellschaft e. V. (HTG), Deutsche Gesellschaft für Geotechnik e. V. (DGGT)

Empfehlungen des Arbeitsausschusses "Ufereinfassungen"

Verlag Wilhelm Ernst & Sohn, Berlin 1997

/*Fuehrer, Römisch 1985*/ Fuehrer, M.; Römisch, K.

Dimensionierung von Sohlen- und Böschungsbefestigungen an Schiffahrtskanälen

Mitteilungen der Forschungsanstalt für Schiffahrt, Wasser- und Grundbau
Schriftenreihe Wasser- und Grundbau, Nr. 47, Berlin 1985

/*Führböter 1974*/ Führböter, A.

Einige Ergebnisse aus Naturuntersuchungen in Brandungszonen

Mitteilungen aus dem Leichweiß-Institut für Wasserbau, Universität Braunschweig, Heft 40/74
Eigenverlag, Braunschweig 1974

/*Führböter et al. 1983*/ Führböter, A.; Dette, H. H.; Jensen, J.

Ergebnisse von Wind- und Schiffswellenmessungen an der Unterelbe in den Jahren 1980/1981

Bericht Nr. 546 (unveröffentlicht)
Leichtweiß-Institut, Universität Braunschweig
Eigenverlag 1983

/*Gates, Herbich 1977*/ Gates, E. T.; Herbich, J. B.

Mathematical model to predict the behavior of deep-draft vessels in restricted waterways

Texas A and M University, Sea Grant College
Report TAMU-SG-77-206, 1977

/*Gaudio, Marion 2003*/ Gaudio, R.; Marion, A.

Time evolution of scouring downstream of bed sills

Journal of Hydraulic Research
Vol. 41, No. 3 (2003), pp. 271 -284

/*Henschke 1952*/ Henschke, W.

Schiffbautechnisches Handbuch

Verlag Technik, Berlin 1952

/*Horn 1928*/ Horn, F.

Theorie des Schiffes

in: „Mechanik der Flüssigkeiten nebst technischen Anwendungsgebieten“
von Auerbach, F.; Hort, W.
S. 552-718
Verlag von Johann Ambrosius Barth, Leipzig 1928

/*Hudson 1959*/ Hudson, R. Y.

Laboratory investigations of rubble mound breakwaters

Journal of Waterways and Harbours
ASCE, New York 1959

/*Jansen, Schijf 1953*/ Jansen, P. Ph.; Schijf, J. B.

ohne Titel

PIANC's 18th International Navigation Congress
Section I - Communication I, pp. 175 - 197
Eigenverlag, Rom 1953

/*Knieß 1977*/ Knieß, H.-G.

Bemessung von Schüttsteindeckwerken im Verkehrswasserbau
Teil 1: Lose Steinschüttungen

Mitteilungsblatt der Bundesanstalt für Wasserbau Nr. 42
Eigenverlag, Karlsruhe 1977

/*Kuhn 1985*/ Kuhn, R.

Binnenverkehrswasserbau

Verlag Wilhelm Ernst & Sohn, Berlin 1985

/*Köhler 1989*/ Köhler, H.-J.

Messung von Porenwasserüberdrücken im Untergrund

Mitteilungsblatt der Bundesanstalt für Wasserbau Nr. 66, S. 155 - 174
Eigenverlag, Karlsruhe 1989

/*Köhler 1993*/ Köhler, H.-J.

The influence of hydraulic head and hydraulic gradient on the filtration process

in: "Filters in Geotechnical and Hydraulic Engineering"
Proceedings of the 1st International Conference 'Geofilters'
Karlsruhe 1992, pp. 225 - 240
A. A. Balkema Verlag, Rotterdam 1993

/*Köhler 1997*/ Köhler, H.-J.

Boden und Wasser - Druck und Strömung

Mitteilungsblatt der Bundesanstalt für Wasserbau, Nr. 76, S. 15 - 33
Eigenverlag, Karlsruhe 1997

/*Köhler, Koenders 2003*/ Köhler, H.-J.; Koenders, M. A.

Direct visualization of underwater phenomena in soil-fluid interaction and analysis of the effects of an ambient pressure drop on unsaturated media

Journal of Hydraulic Research, Vol. 41, Issue 1 (2003), pp. 69 – 78

/*Kohlhase 1983*/ Kohlhase, S.

Ozeanographisch-seebauliche Grundlagen der Hafenplanung

Mitteilungen des Franzius-Instituts für Wasserbau und Küsteningenieurwesen der Universität Hannover
Eigenverlag, Hannover 1983

/*Kriebel 2003*/ Kriebel, D.

Development of unified description of ship generated waves

U. S. Section PIANC Annual Meeting
27. – 30. Oktober 2003, Portland, Oregon/USA
Passing Vessel Issues Workshop

/*Le Méhauté 1976*/ Le Méhauté, B.

An introduction to hydrodynamics and water waves

Springer-Verlag, Berlin 1976

/*LWI 1998*/ N.N.

Stabilität von verklammerten Deckwerken

Bericht Nr. 833
Leichtweiß-Institut für Wasserbau / TU Braunschweig, August 1998

/*MAG*/ Bundesanstalt für Wasserbau

Merkblatt Anwendungen von geotextilen Filtern an Wasserstraßen

Eigenverlag, Karlsruhe 1993

/*MAK*/ Bundesanstalt für Wasserbau

Merkblatt Anwendung von Kornfiltern an Wasserstraßen

Eigenverlag, Karlsruhe 1989

/*MAR*/ Bundesanstalt für Wasserbau

Merkblatt Anwendung von Regelbauweisen für Böschungs- und Sohlensicherungen an Wasserstraßen

Eigenverlag, Karlsruhe 1993

/*MAV*/ Bundesanstalt für Wasserbau

Merkblatt Anwendung von hydraulisch- und bitumengebundenen Stoffen zum Verguß von Wasserbausteinen

Eigenverlag, Karlsruhe 1990

/*Oosterveld, Oossanen 1975*/ Oosterveld, M. W. C.; van Oossanen, P.

Further computer-analysed data of the Wageningen B-Screw Series

International shipbuilding progress, Vol 22, No. 251. July 1975, pp. 251-262

/*Peters 2002*/ Peters, H.-E.

Stellungnahme und Vorschläge zur Abschätzung der Strahlgeschwindigkeit von Propellern und Düsenpropellern

Ausarbeitung im Auftrag der BAW (unveröffentlicht)
Rostock 2002

/*PIANC 1987a*/ Permanent International Association of Navigation Congresses - PIANC (Hrsg.)

Guidelines for the design and construction of flexible revetments incorporating geotextiles for inland waterways

Report of the Working Group 4 of the Permanent Technical Committee I
Supplement to Bulletin No. 57
Eigenverlag, Brüssel 1987

/*PIANC 1987b*/ Permanent International Association of Navigation Congresses - PIANC (Hrsg.)

Risk consideration when determining bank protection requirements

Supplement to Bulletin No. 87, 1987, pp. 202 ff.
Eigenverlag, Brüssel 1987

/*PIANC 1992*/ Permanent International Association of Navigation Congresses - PIANC (Hrsg.)

Guidelines for the design and construction of flexible revetments incorporating geotextiles in marine environment

Report of Working Group 21 of the Permanent Technical Committee II
Supplement to Bulletins Nos. 78/79, 1992

/*Pilarczyk 1990*/ Pilarczyk, K.W.

Design of seawalls and dikes including overview of revetments

Proceedings of the short course on coastal protection
Balkema, Rotterdam 1990

/*Poweleit 1985*/ Poweleit, A.

Bemessung des Freibords im Erddammbau

Wasserwirtschaft 75 (1985) 10, S. 434-439

/*Press, Schröder 1966*/ Press, H.; Schröder, R.

Hydromechanik im Wasserbau

Verlag Wilhelm Ernst & Sohn, Berlin 1966

/*PROFIX 2002*/ **Programmdokumentation PROFIX**

Institut für Energie- und Umwelttechnik, Universität Rostock 2002

/*Przedwojski et al. 1995*/ Przedwojski, B.; Blazejewski, R.; Pilarczyk, K. W.

River training techniques - fundamentals, design and application

Balkema, Rotterdam 1995

/*Römisch 1975*/ Römisch, K.

Der Propellerstrahl als erodierendes Element bei An- und Ablegemanövern in Hafenbecken

Seewirtschaft Heft 7 (1975)
Berlin

/*Römisch 1989*/ Römisch, K.

Empfehlungen zur Bemessung von Hafeneinfahrten

Technische Universität Dresden, Sektion Wasserwesen
Wasserbauliche Mitteilungen, Heft 1, S. 2-84
Eigenverlag, Dresden 1989

/*Römisch 1994*/ Römisch, K.

Propellerstrahlinduzierte Erosionserscheinungen

HANSA – Schiffahrt – Schiffbau – Hafen
Nr. 9 / 1994 (131. Jg.), S. 231-234

/*RPG*/ Bundesanstalt für Wasserbau

Richtlinien für die Prüfung von Geotextilien im Verkehrswasserbau

Eigenverlag, Karlsruhe 1994

/*Schäle*, *Mollus 1971*/ Schäle, E.; Mollus, G.

Bildbericht über die Versuche auf Rhein und Main sowie in den Haltungen Hausen und Kriegenbrunn

Kanal- und Schiffahrtsversuche, 3. Folge
Versuchsanstalt für Binnenschiffbau, Duisburg 1971

/*Schokking 2002*/ Schokking, L. A.

Bowthruster-induced damage

Master of Science Thesis
TU Delft 2002

/*Schuster 1952*/ Schuster, S.

Untersuchungen über die Strömungs- und Widerstandsverhältnisse bei der Fahrt von Schiffen in beschränktem Wasser

Jahrbuch der Schiffbautechnischen Gesellschaft 1952

/*Söhngen 1992*/ Söhngen, B.

Dimensionierung von Fahrrinnenquerschnitten im Rahmen der Planung von Staustufen

13. Duisburger Kolloquium für Schiffs- und Meerestechnik, Mai 1992

/*Söhngen, Koll 1997*/ Söhngen, B.; Koll, K.

Bemessung von Sohlendeckwerken unter starkem Strömungsangriff

in DVWK-Schrift 118, 1997

/*SPM 1977*/ Department of the Army, Waterways Experiment Station (WES)
Corps of Engineers, Coastal Engineering Research Center

Shore Protection Manual, Vol. 1, 2

Eigenverlag, Vicksburg 1977

/*SPM 1984*/ Department of the Army, Waterways Experiment Station (WES)
Corps of Engineers, Coastal Engineering Research Center

Shore Protection Manual, Vol. 1, 2

Eigenverlag, Vicksburg 1984

/*TLW*/ Bundesministerium für Verkehr

Technische Lieferbedingungen für Wasserbausteine

Eigenverlag, Bonn 1997 bzw. 2003

/Verhey, *Bogaerts 1989*/ Verhey, H. J.; Bogaerts, M. P.

Ship waves and the stability of armour layers protecting slopes

9th International Harbour Congress
Antwerpen, Belgien, Juni 1989
Delft Hydraulics Publication No. 428 (von 1989)

/Wagner 1996/ Wagner, H.

Konzeption zur Prognose von durch Wind erzeugten Wellen für kleinere Seegebiete

Institut für Wasserbau und Technische Hydromechanik, TU Dresden
Dresdner Wasserbauliche Mitteilungen, Heft 9, S. 91 ff.
Dresden 1996

/*Yosifov et al. 1986*/ Yosifov, K.; Zlatev, Z.; Staneva, A.

Optimum characteristics equations for K-J ducted propeller design charts

Bulgarian Ship Hydrodynamics Centre, Selected Papers Volume 1, Book 1, Varna 1986, pp. 73-84

/*ZfB 1993*/ N.N.

Antriebstechnik für Binnenschiffe

Binnenschiffahrt - ZfB
Heft 8/1993, S. 14-19

/*ZTV-W 210*/ Wasser- und Schifffahrtsverwaltung (Hrsg.)

Zusätzliche Technische Vertragsbedingungen - Wasserbau für Böschungs- und Sohlensicherung (Leistungsbereich 210)

Drucksachenstelle bei der Wasser- und Schiffahrtsdirektion Mitte,
Eigenverlag, Hannover 1991

11 Nomenclature

11.1 Abbreviations

BF	toe of slope
BinSchStrO	Code for Inland Waterways
BW	operating water level
BWStr	inland waterway(s)
DEK	Dortmund-Ems Canal
DWD	German National Meteorological Service
ES	inland waterway vessel of “Europe“ type
Fkt.	function of (...)
Gl(n).	equation(s)
GMS	large inland cargo vessel, large self-propelled barge
GW	ground water level
KA	centre line of canal / canal axis
MW	mean water level
MS	motor ship
RHK	Rhine-Herne Canal
R-Profil	standard rectangular profile
RWS	still-water level (SWL) (German abbreviation)
SV	push tow unit
SWL	still-water level
T-Profil	standard trapezoidal profile
WDK	Wesel-Datteln Canal
Wsp.	water level
1D	one-dimensional
2SV/4SV	push tow unit with 2 or 4 lighters

11.2 Symbols

a	[m]	largest dimension of an armourstone
a	[-]	exponent for describing the situation of jet dispersion
a	[-]	pore water pressure parameter
a_p	[m]	distance of propeller axes of a twin-screw drive
A	[-]	coefficient for describing the jet dispersion
A	[m^2]	flow cross-section, river cross-section, canal cross-section
A'	[m^2]	cross-sectional area between ship’s axis and bank
A_0	[m^2]	cross-sectional area at the narrowest jet contraction behind propeller

A_A	[m²]	area of approach flow in front of the propeller
A_E	[m²]	area of inlet into the plane of the propeller
A_K	[m²]	unmodified cross-sectional area of the canal
$A_{K,äqui}$	[m²]	equivalent canal cross-section
A_M	[m²]	plunged midship section
$A_{S,äqui}$	[m²]	equivalent cross-sectional area of ship
$A_{S,B}$	[m²]	cross-sectional area of ship at bow
$A_{S,eff}$	[m²]	effective plunged midship section
$A_{S,eff,B}$	[m²]	effective plunged midship section at bow
$A_{S,eff,D}$	[m²]	virtually increased effective plunged midship section of a ship sailing with drift
$A_{S,eff,H}$	[m²]	effective plunged midship section at stern
$A_{S,H}$	[m²]	cross-sectional area of ship at stern
A_W	[-]	wave height coefficient depending on the shape of the ship, dimensions of the ship, draught and water depth
b	[1/m]	pore water pressure parameter
b	[m]	medium dimension of an armourstone
b'	[m]	fairway width
b^*	[1/m]	pore water pressure parameter for $t_a = t_a^* = 5$s
b_E	[m]	influence width of return flow field, equivalent canal width for a ship sailing in shallow water conditions
b_F	[m]	fairway width
b_m	[m]	mean width at water level in the area of water level increase/drawdown
b_r	[m]	equivalent canal width, equivalent waterway width
$b_{r,äqui}$	[m]	width of equivalent canal profile [m]
b_S	[m]	width of the canal bed, bed width
b_{WS}	[m]	width at water level
$b_{WS,äqui}$	[m]	equivalent width at water level
B	[m]	width of inlet of longitudinal groyne
B	[m]	beam width
B^*	[-]	load coefficient
B_1	[m]	width of single lane
B_{85}^*	[-]	stability coefficient for slopes
$B_{85,0}^*$	[-]	stability coefficient (general)
B_B	[m]	beam width at bow
B'_B	[-]	stability coefficient
B_B^*	[-]	coefficient for frequency of recurrence
$\tilde{B}_B$	[-]	coefficient for recurrence frequency
B_H	[m]	beam width at stern
B_m	[m]	mean beam width between bow and stern

B_S	[-]	coefficient at jet attack on plane bed
$B_{S,Bö}$	[-]	coefficient at jet attack on bank
BW_o	[m+NN]	upper operating water level
BW_u	[m+NN]	lower operating water level
c	[-]	calibration parameter
c	[m]	smallest dimension of an armourstone
c	[m/s]	wave celerity
c'	[kN/m^2]	effective cohesion of soil, effective cohesion
c_0	[m/s]	wave celerity in shallow water
c'_{AB}	[kN/m^2]	cohesion, adhesion between tension element and soil above the lowered water level
c'_D	[kN/m^2]	cohesion of cover layer
c_F	[-]	constant of pivot point
C	[-]	constant for the approximation of the drawdown time
C	[-]	coefficient (for induced initial velocity based on the engine power)
C_A	[-]	constant for wave run-up
$C_{Bö}$	[-]	factor for considering the influence of the slope
C_H	[-]	factor for considering the influence of the type of the ship, draught and trim
C_{Isb}	[-]	factor according to Isbash
C_m	[-]	coefficient for load duration
d_0	[m]	jet diameter at point of maximum contraction
d_A	[m]	jet diameter in region of approach flow
d_D	[m]	thickness of cover layer (measured normally to the surface)
$d_{D(A)}$	[m]	construction thickness of the initial cover layer (A)
$d_{D(B)}$	[m]	construction thickness of the hydraulically equivalent cover layer (B)
d_{DF}	[m]	thickness of stone layer in toe blanket
d_{Di}	[m]	thickness of impervious lining
d_{Do}	[m]	thickness of cover layer above the lowered water level
d_F	[m]	thickness of filter
d_{FF}	[m]	thickness of filter in toe blanket
d_{Fkrit}	[m]	critical depth in toe blanket
d_{Fo}	[m]	thickness of mineral filter above the lowered water level
d_{krit}	[m]	critical depth of failure surface, depth of critical failure surface
d_{krithB}	[m]	critical depth of failure surface to prevent hydrodynamic soil displacement
d_x	[m]	diameter of cone of propeller jet
D	[m]	grain size
D	[m]	propeller diameter
D_{10}	[m]	grain size at 10 % of particles passing
D_{15}	[m]	grain size at 15 % of particles passing
D_{50}	[m]	grain size at 50 % of particles passing

$D_{50,TLW}$	[m]	required mean grain size corresponding to /*TLW*/
D_{60}	[m]	grain size at 60 % of particles passing
D_{85}	[m]	grain size at 85 % of particles passing
D_{90}	[m]	grain size at 90 % of particles passing
D_i	[m]	representative grain size of class i, corresponding to the geometric mean of D_{io} and D_{iu}
D_{io}	[m]	upper limit of grain size class i (square sieve opening size)
D_{iu}	[m]	lower limit of grain size class i (square sieve opening size)
D_L	[m]	characteristic largest stone size (largest measured length of an armourstone)
D_n	[m]	nominal stone size
D_{n50}	[m]	necessary mean nominal stone size, nominal stone size
$D_{nSt(A)}$	[m]	nominal stone size of initial cover layer for design case (A)
$D_{nSt(B)}$	[m]	selected nominal stone size of alternative hydraulically effective cover layer (B)
D_{TLW}	[m]	stone size according to TLW
D_x	[m]	grain size at x % of particles passing
e	[-]	Euler‘s constant e ≈ 2,718
e'_{ph}	[kN/m^2]	horizontal component of the passive earth pressure
erf τ	[kN/m^2]	required shear stress
erf τ_A	[kN/m^2]	required additional supporting shear stress
erf τ_F	[kN/m^2]	required shear stress at a toe sheet pile wall
E	[-]	coefficient for characterisation of stern shape and rudder configuration
E'_a	[kN/m]	active earth pressure in the soil below the slope revetment
E'_p	[kN/m]	passive earth pressure, earth resistance
E'_{ph}	[kN/m]	horizontal component of the passive earth pressure in the toe blanket
E_S	[MN/m^2]	Oedometer modulus of soil
$\tilde{f}$	[-]	form parameter
f_B	[-]	factor of influence width dependent on type of ship
f_{cr}	[-]	coefficient of velocity
f_N	[-]	factor for selected propeller rotation rate
f_P	[-]	factor for applicable engine power
f_{red}	[-]	reduction factor for energy loss at wave run-up
f_λ	[-]	wave length coefficient
F	[kN/m]	toe support force, force from revetment
F_{eff}	[m]	effective fetch
Fr	[-]	Froude number at stern
$\tilde{F}r$	[-]	Froude number at point of maximum height of stern waves
Fr_h	[-]	Froude number based on depth
g	[m/s^2]	acceleration due to gravity

g'	[kN/m^2]	mass per unit area of the cover layer
G	[kg]	mass of stone
G'	[kN]	effective weight of soil block
G_i	[kg]	representative mass of stone of class i, corresponding to the geometric mean of G_{io} and G_{iu}
G_{io}	[kg]	upper limit of mass of stone of class i
G_{iu}	[kg]	lower limit of mass of stone of class i
G_{50}	[kg]	required mean mass of stone
h	[m]	water depth, canal water depth
h'	[m]	fairway depth
h_b	[m]	water depth at point of breaking
h_{Kolk}	[m]	scour depth below bed of river or canal
h_m	[m]	mean water depth
h_p	[m]	level of the propeller axis above bed
h_W	[m]	water depth at still-water level
h_x	[m]	water depth at narrowest flow cross-section
H	[m]	wave height, height of ship-induced waves, design wave height
H_b	[m]	wave height at point of breaking
H_{Bem}	[m]	design wave height
H_{diff}	[m]	wave height due to diffraction
H_{ein}	[m]	height of incident wave
H_{refl}	[m]	wave height due to reflection
H_s	[m]	significant wave height, design wave height of wind waves
H_{Sek}	[m]	height of secondary waves, height of additional secondary waves
$H_{Sek,gl}$	[m]	height of secondary waves for ships sailing at sliding speed
$H_{Sek,q}$	[m]	height of pure secondary transversal stern waves
H_{sh}	[m]	wave height due to wave shoaling
H_{tol}	[m]	tolerated wave height
$H_{u,Bug}$	[m]	maximum height of bow wave at the bank for eccentric sailing
$H^*_{u,H}$	[m]	relevant weight height near the bank at stern for calculating the drawdown time
$H_{u,Heck}$	[m]	maximum height of stern waves at the bank for eccentric sailing
i_p	[kN/m^3]	seepage pressure
J	[-]	propeller advance ratio
k	[-]	blockage coefficient
k	[m/s]	permeability of soil, water permeability of soil
K	[-]	inclination coefficient
K'	[-]	diffraction coefficient

K_l	[-]	longitudinal slope coefficient
K_q	[-]	cross slope coefficient
K_{refl}	[-]	reflection coefficient
K_{sh}	[-]	shoaling coefficient
K_{SS}	[m]	equivalent sand roughness of ship's hull
K_T	[-]	thrust coefficient of propeller for $J = 0$
$K_{T,DP}$	[-]	thrust coefficient of ducted propeller for $J = 0$
$K_{T,DPJ}$	[m]	thrust coefficient of ducted propeller for $J \neq 0$
K_{TJ}	[-]	thrust coefficient of unducted propeller for $J \neq 0$
l_u	[m]	wetted perimeter
L	[m]	ship's length, length of recreational craft
L	[m]	distance between the propeller plane and quay wall
L	[m]	wave length
L_{eff}	[m]	effective ship's length
L_{ein}	[m]	length of incoming wave
L_{Fu}	[m]	length of toe blanket
L_H	[m]	length of breaking transversal stern wave
L_o	[m]	length of slope revetment above the lowered water level
L_{pris}	[m]	length of the prismatic part of hull
L_{Sek}	[m]	length of secondary waves
L_{sh}	[m]	wave length due to shoaling
L_u	[m]	length of slope revetment below the lowered water level length of slope revetment below water level
L_W	[m]	wave-generating length of ship
m	[-]	slope inclination (attention: definition differs from that of the slope of a straight line)
$m_{K,äqui}$	[-]	equivalent slope inclination
m_{lks}	[-]	slope inclination at left bank
m_{rts}	[-]	slope inclination at right bank
m_v	[l/m^2]	quantity of grouting material
max L_{Fu}	[m]	maximum permitted length of the toe blanket
max v_{za}	[m/s]	maximum rate of drawdown
max τ_{F1}	[kN/m^2]	maximum equivalent shear stress for failure mechanism 1
max τ_{F2}	[kN/m^2]	maximum equivalent shear stress at a toe blanket
min d_D	[m]	minimum thickness of the cover layer
min L_{Fu}	[m]	minimum length of the toe blanket
n	[-]	voids ratio of the mineral granular filter or the revetment
n	[1/min]	propeller rotation rate, propeller rotation rate of the bow thruster
n	[-]	blockage ratio

$n_{äqui}$	[-]	equivalent blockage ratio
n_{Nenn}	[1/min]	design propeller rotation rate
p	[bar; Pa]	pressure
P	[m]	design pitch
P_{Bug}	[kW]	power of the bow thruster
$P_{d,Nenn}$	[kW]	nominal power
r_x	[m]	radial distance of impact point below jet axis at distance x behind propeller plane
R	[m]	inner, smaller radius of a curved fairway
R'_d	[m]	vertical depth of the revetment below still-water level (SWL)
$R(\alpha)$	[m]	impact length to opposite bank at angle α
S	[-]	degree of saturation of the soil
S	[km]	maximum fetch length
S_m	[km]	medium fetch length
SF	[-]	shape factor of armourstones
t	[s]	time
t	[m]	depth below the bed of the river or canal
t_a	[s]	drawdown time (in general)
t_a^*	[s]	drawdown time $t_a = t_a^* = 5$ s
$t_{a,B}$	[s]	drawdown time at bow
$t_{a,B,Sek}$	[s]	drawdown time of secondary bow wave
$t_{a,H}$	[s]	drawdown time at stern
$t_{a,W}$	[s]	drawdown time of a wave
t_f	[m]	underkeel clearance
t_F	[m]	depth of the embedded toe / depth of the toe sheet pile wall / depth of the total toe blanket
t_{fl}	[m]	dynamic underkeel clearance
$t_{fl,min}$	[m]	minimum dynamic underkeel clearance
t_k	[m]	scour depth in front of the toe of the revetment, scour depth
t_{krit}	[m]	critical depth below the bed of the river or canal
t_{min}	[h]	minimum period of wind action
t_v	[m]	draught while sailing
T	[s]	mean wave period, wave period, characteristic wave period
T	[m]	draught, midship draught while sailing
T_a	[s]	drawdown period
T_B	[m]	draught at bow section
T_{ein}	[s]	period of incoming wave
T_H	[m]	draught at stern section

T_m	[m]	mean draught between bow and stern
u	[m]	bank distance (middle of ship to bank line at SWL)
u	[m/s]	wind velocity
u'	[m]	distance ship's side to bank line
u^*	[m]	bank distance at the moment of impact of the first interference wave group on the bank
u_b	[kN/m^2]	resulting excess pore water pressure
U_b	[kN/m]	resultant force of the excess pore water pressure
u_{eff}	[m]	effective bank distance
u_{max}	[m/s]	maximum velocity of slope supply flow on revetment
$u_{max,B}$	[m/s]	design speed of slope supply flow
u_r	[m]	equivalent bank distance, distance to equivalent bank
$u_{r,lks}$	[m]	distance to the left bank in the equivalent canal cross-section
$u_{r,max}$	[m]	maximum bank distance in equivalent cross-section
$u_{r,min}$	[m]	minimum bank distance in equivalent cross-section
$u_{r,rts}$	[m]	distance to the right bank in the equivalent canal cross-section
U	[-]	coefficient of uniformity of the riprap
v	[m/s]	velocity
v_0	[m/s]	induced initial velocity at $J = 0$
v_{0J}	[m/s]	induced initial velocity at $J > 0$
v_A	[m/s]	velocity of approach flow towards the propeller
v_{Bmax}	[m/s]	maximum near bed flow velocity at the impact point of the propeller jet for $J = 0$
v_{Bmax1}	[m/s]	maximum near bed flow velocity at the impact point of the propeller jet for $J \neq 0$
v_{krit}	[m/s]	critical ship speed
v_{max}	[m/s]	maximum flow velocity composed of return flow velocity and flow velocity
$v_{max,S}$	[m/s]	maximum flow velocity at the bed of the river or canal
$v_{max,S,K}$	[m/s]	maximum flow velocity at the bed of the river or canal at the toe of the quay wall
$v_{max,S,xK}$	[m/s]	modified maximum flow velocity at the the bed of the river or canal after deflection at the toe of the quay wall at distance x_K
v_P	[m/s]	velocity in the propeller plane
$\overline{v}_{rück}$	[m/s]	mean return flow velocity, return flow velocity averaged in the longitudinal and transverse directions
$\overline{v}_{rück,u}$	[m/s]	mean return flow velocity near the bank, return flow velocity averaged in the longitudinal direction at bank
$\overline{v}_{rück,u,lks}$	[m/s]	return flow velocity averaged in the longitudinal direction at the left bank
$\overline{v}_{rück,u,rts}$	[m/s]	return flow velocity averaged in the longitudinal direction at the right bank
$\hat{v}_{rück}$	[m/s]	maximum return flow velocity
$\hat{v}_{rück,u,Bug}$	[m/s]	maximum return flow velocity at bow near the bank
$\hat{v}_{rück,u,Heck}$	[m/s]	maximum return flow velocity at stern near the bank

v_S	[m/s]	ship speed, ship speed through water
$v_{S,gl}$	[m/s]	sliding speed
$v_{S,zul}$	[m/s]	permitted ship speed through water
v_{Str}	[m/s]	flow velocity
$v_{SüG}$	[m/s]	ship speed over ground
v_{xmax}	[m/s]	main velocity
v_{xr}	[m/s]	jet velocity relative to ship at a distance of radius r_x from the jet axis (impact point) for $J = 0$
v_{xr1}	[m/s]	jet velocity relative to ship at a distance of radius r_x from the jet axis (impact point) for $J \neq 0$
v_{za}	[m/s]	drawdown rate of water level
$\overline{v}_{za}$	[m/s]	mean drawdown rate
$\overline{v}_{za,B}$	[m/s]	mean drawdown rate at the bow (average gained by field measurements)
$\overline{v}_{za,Bug}$	[m/s]	mean drawdown rate at the bow
$\overline{v}_{za,Heck}$	[m/s]	mean drawdown rate at the stern
v_{zul}	[m/s]	permitted speed according to the Code for Inland Waterways (BinSchStrO)
w	[-]	wake factor
x	[m]	coordinate
x	[m]	distance from the propeller plane within the jet axis
x	[m]	additional thickness to allow for the different kinds of stone material
x_{gr}	[m]	distance beyond which jet dispersion is obstructed
x_K	[m]	distance of the deflected jet on the bed of the river or canal, measured from the quay wall
x_S	[m]	distance from the rotation centre of the propeller plane, measured on the bed of the river or canal
$x_{S,max}$	[m]	position of the maximum near bed flow velocity behind the rotation centre of the propeller plane
y	[m]	coordinate
y	[m]	distance of sailing line from canal axis, distance between the axis of the sailing line and the canal axis
$y_{äqui}$	[m]	eccentricity of the sailing line in the equivalent canal cross-section
z	[-]	number of blades on a propeller
z	[m]	depth
z	[m]	depth below the slope surface or below the bed of the river or canal, normal to the bed of the river or canal
z_a	[m]	maximum rapid drawdown, drawdown
$z_{a,B}$	[m]	is the maximum rapid drawdown for the relevant drawdown at the bow
$z_{a,H}$	[m]	is the maximum rapid drawdown for the relevant drawdown at the stern
z_{AL}	[m]	wave run-up height
$z_{AL,0}$	[m]	wave run-up height for $f_{red} = 1$

$z_{AL,St}$	[m]	wave run-up height on riprap
z_h	[m]	depth at which the excess pore water pressure increases to half of its maximum value
Z	[kN/m]	tensile force in a revetment suspension
α	[°]	angle of outer jet boundary
α	[°]	angle of influence direction
α	[°]	angle between wind direction and a perpendicular to the slope line
α_1	[-]	correction coefficient describing nearness to critical ship speed
α_0	[°]	angle between propeller axis and jet axis
α_B	[°]	mean angle of diversion
α_K	[°]	Kelvin angle ($\alpha_K \approx 19°$)
α_l	[°]	trim angle; longitudinal slope angle
α_q	[°]	cross slope angle
α_z	[°]	angle of outer jet boundary, measured vertically
β	[°]	slope angle, slope angle above the lowered water level
β_D	[°]	drift angle
β_K	[°]	angle between wave crest of secondary diverging wave and bank line (mostly: β_K = 54,74°)
β_{St}	[°]	angle between jet axis and a perpendicular to the slope line (angle of impact)
β_W	[°]	angle between a perpendicular to the wave crest and fall of slope line, angle between wave crest of secondary diverging wave and bank line
β_λ	[-]	coefficient considering wave-generating length of ship
γ	[kN/m^3]	weight density of soil
γ'	[kN/m^3]	effective weight density of soil at buoyancy
γ_A	[-]	safety against uplift
γ_B	[-]	block coefficient of ship cross-section at bow section
γ_c	[-]	partial factor of safety for cohesion
γ'_D	[kN/m^3]	effective weight density of the cover layer at buoyancy
γ'_{DF}	[kN/m^3]	effective weight density of the cover layer in the toe blanket at buoyancy
γ'_{Di}	[kN/m^3]	effective weight density of the sealing material at buoyancy
γ_{Do}	[kN/m^3]	effective weight density of the cover layer above the lowered water level
γ_F	[kN/m^3]	effective weight density of the filter
γ'_F	[kN/m^3]	effective weight density of the (grain) filter at buoyancy
γ'_{FF}	[kN/m^3]	effective weight of the filter in the toe blanket at buoyancy
γ_{Fo}	[kN/m^3]	weight density of a mineral filter above the lowered water level
γ_H	[-]	block coefficient of ship cross-section at stern section
γ_S	[kN/m^3]	weight density of the riprap
γ_V	[kN/m^3]	weight density of the grouting material
γ_W	[kN/m^3]	weight density of water

γ_φ	[-]	partial factor of the safety for angle of shearing resistance
δ	[°]	trim angle
δ_a	[°]	wall friction angle (active side)
δ_p	[°]	wall friction angle (passive side)
δ_{1H}	[m]	thickness of boundary layer at bow section
ΔA	[m^2]	reduction of cross-section in the canal due to ship cross-section and drawdown
ΔG_i	[kg]	mass of all single stones of a grading i
Δh	[m]	rise/fall of the water level (depending on index)
$\Delta\overline{h}$	[m]	maximum drawdown averaged for canal width at narrowest flow cross-section, mean drawdown according to 1D canal theory, drawdown averaged in the longitudinal and transverse directions
$\Delta\hat{h}$	[m]	maximum drawdown near the bank
Δh_B	[m]	water level increase in front of bow
$\Delta\hat{h}_{Heck}$	[m]	drawdown at stern
$\Delta\overline{h}_{krit}$	[m]	mean drawdown at critical ship speed
$\Delta H_{s,oWl}$	[m]	ratio of wave height above still-water level
Δh_{Sek}	[m]	maximum water level increase of secondary wave system
$\Delta\overline{h}_u$	[m]	drawdown averaged in longitudinal direction at bank
$\Delta\overline{h}_{u,Bug}$	[m]	drawdown averaged at bank in the bow section for ships sailing in the centre of a river or canal
$\Delta\hat{h}_{u,Bug}$	[m]	maximum drawdown at bow near the bank without the influence of eccentricity
$\Delta\overline{h}_{u,Heck}$	[m]	drawdown averaged at the stern section at bank for ships sailing in the centre of a river or canal
$\Delta\hat{h}_{u,Heck}$	[m]	maximum drawdown at stern near the bank without the influence of eccentricity
$\Delta\overline{h}_{u,lks}$	[m]	drawdown averaged in longitudinal direction at left bank
$\Delta\overline{h}_{u,rts}$	[m]	drawdown averaged in longitudinal direction at right bank
Δh_W	[m]	height difference between groundwater level and still-water level, temporary rise in water level
Δh_W	[m]	height of wind set-up at lee of fetch
$\Delta h_{WA,B}$	[m]	rise in water level in front of bow
Δp	[bar; Pa]	pressure difference
ΔQ	[m^3/s]	sudden change in discharge
Δt	[m]	dynamic squat
Δt_k	[m]	scour depth below bottom of the filter
Δu	[kN/m^2]	excess pore water pressure
$\Delta\alpha$	[°]	increment of the sector method for the determination of the fetch

ϑ_p	[°]	angle of sliding surface
ϑ_{DF}	[°]	angle of sliding surface of the passive earth pressure wedge within the toe blanket
λ_q	[m]	length of transversal wave
λ_S	[m]	length of diverging wave
ξ	[-]	surf similarity parameter
ρ	[kg/m^3]	density of soil
ρ'	[m/s^2]	relative gravity acceleration
ρ_A	[kg/m^3]	dry density of a single stone for design case A
ρ'_A	[kg/m^3]	effective density of the single stone at buoyancy for design case A
ρ_B	[kg/m^3]	dry density of a single stone of the hydraulically equivalent cover layer B
ρ'_B	[kg/m^3]	effective density of a single stone at buoyancy of the hydraulically equivalent cover layer B
ρ_S	[kg/m^3]	density of riprap, density of armourstones
ρ_W	[kg/m^3]	density of water
σ'_V	[kN/m^2]	effective vertical stress
τ_A	[kN/m^2]	additional stress from a revetment suspension
τ_F	[kN/m^2]	additional stress from a toe support
φ'	[°]	effective angle of shearing resistance of the soil
φ'_{AB}	[°]	effective angle of shearing resistance between tension element and soil or between tension element and cover layer above the lowered water level, whichever is smaller
φ'_D	[°]	effective angle of shearing resistance of the riprap or the cover layer material
φ'_{DF}	[°]	effective angle of shearing resistance of the riprap at the toe blanket
φ'_F	[°]	effective angle of shearing resistance of the granular filter

Annex A:

Derivation of the formulae for geotechnical analyses of revetments with a toe support

For 7.2.5.3 Failure mechanism 2 with a toe blanket

Diagram showing the determination of max F_{F2} (internal analysis)

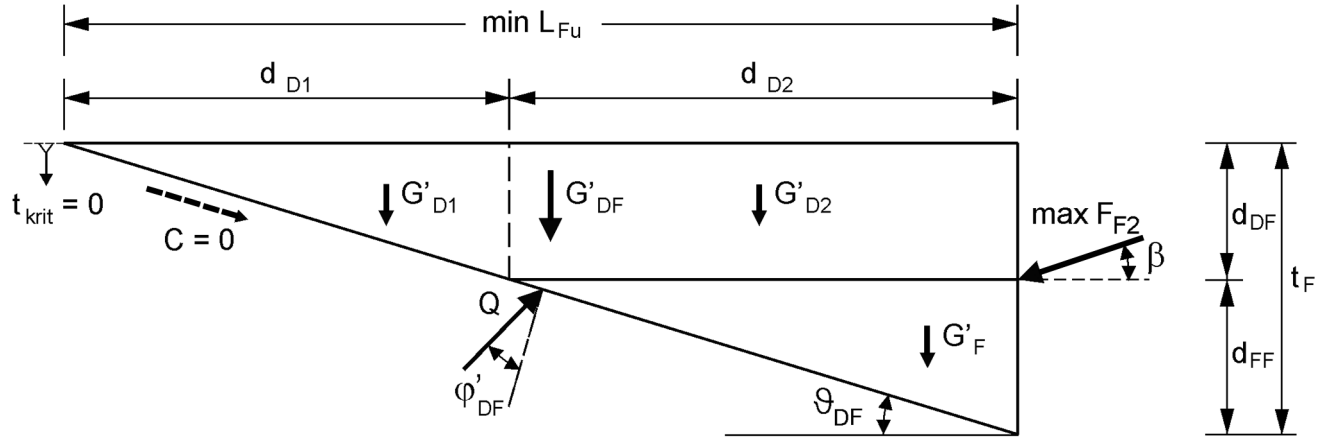

max F_{F2} = toe support force

(1) ΣV = 0: $Q\cos\left(\varphi'_{DF}+\vartheta_{DF}\right)-G'_{DF}-\max F_{F2}\sin\beta=0$

(2) ΣH = 0: $-Q\sin\left(\varphi'_{DF}+\vartheta_{DF}\right)+\max F_{F2}\cos\beta=0$

from (2) $\Rightarrow$ $$Q=\frac{\max F_{F2}\cos\beta}{\sin\left(\varphi'_{DF}+\vartheta_{DF}\right)}$$

inserted in (1) where

(3) $$\vartheta_{DF}=45^\circ-\frac{\varphi'_{DF}}{2}$$

it follows that

(4) $$\max F_{F2}=\frac{G'}{\cos\beta\,\cot\left(\varphi'_{DF}+\vartheta_{DF}\right)-\sin\beta}$$

where

(5) $$G'=\frac{{d_{DF}}^2\,\gamma'_{DF}}{2\tan\vartheta_{DF}}+\frac{{d_{FF}}^2\,\gamma'_{FF}}{2\tan\vartheta_{DF}}+\frac{d_{DF}\,d_{FF}\,\gamma'_{DF}}{\tan\vartheta_{DF}}$$

From (4) is derived the maximum equivalent shear stress that can be calculated as given in equation (7-10) (internal analysis)

(6) $$\max\tau_{F2,i}=\frac{\max F_{F2}}{L_u}$$

(where L_u is the length of the slope under water)

for the internal earth pressure wedge of the toe blanket.

The passive earth pressure E'_{ph} acting in front of the toe blanket may also be taken into account in the determination of the maximum equivalent shear stress $\tau_{F2,a}$ in accordance with equation (7-11) (external analysis).

Diagram showing the determination of the passive earth pressure in front of the toe blanket:

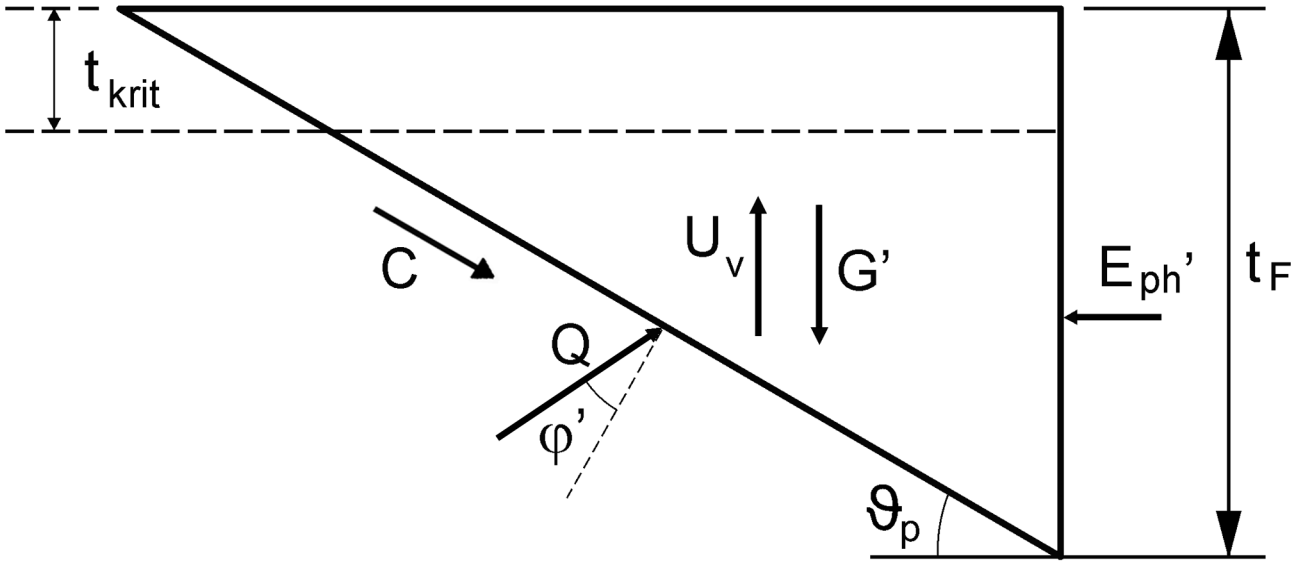

(7) ΣV = 0: $$-C\sin\vartheta_p + Q\cos(\varphi'+\vartheta_p) + U_v - G' = 0$$

(8) ΣH = 0: $$-C\cos\vartheta_p - Q'\sin(\varphi'+\vartheta_p) + E'_{ph} = 0$$

from (7) $\Rightarrow$ $$Q' = \frac{G' - U_v + C\sin\vartheta_p}{\cos(\varphi'+\vartheta_p)}$$ inserted in (8)

the passive earth pressure E'_{ph} in front of the toe blanket is calculated as follows:

$$E'_{ph} = (G' - U_v + C\sin\vartheta_p)\tan(\varphi'+\vartheta_p) + C\cos\vartheta_p \qquad (7\text{-}15)$$

with the auxiliary functions

$$\vartheta_p = 45^\circ - \frac{\varphi'}{2}$$

and

$$G' = \frac{(t_F - t_{krit})^2\,\gamma'}{2\tan\vartheta_p}$$

and

$$C = \frac{c'(t_F - t_{krit})}{\sin\vartheta_p}$$

and

$$U_v = \frac{\gamma_W z_a}{\tan\vartheta_p}\left[\frac{e^{-b t_F} - e^{-b t_{krit}}}{b} + e^{-b t_{krit}}(t_F - t_{krit})\right]$$

For 7.2.5.4 Failure mechanism 2 with an embedded toe

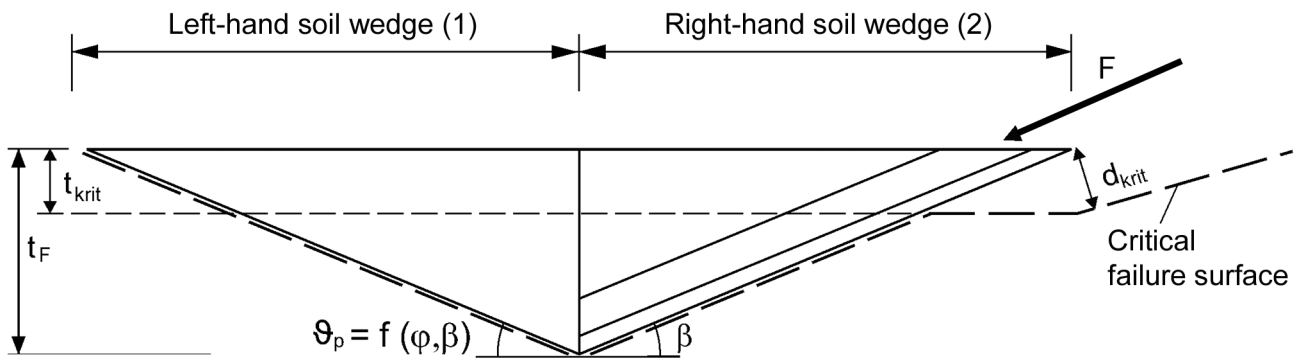

$$L_u = \frac{h_W - z_a + t_k + t_{krit}}{\sin\beta}$$

$$\vartheta_p = \arctan\left[\sqrt{\frac{\left(1+\tan^2\varphi'\right)\tan\varphi'}{\tan\varphi'+\tan\beta}} - \tan\varphi'\right]$$

The critical depth is the fluidisation depth: $t_{krit} = \frac{1}{b}\ln\left(\frac{b\,\gamma_W z_a}{\gamma'}\right)$ (7-17)

Left-hand soil wedge

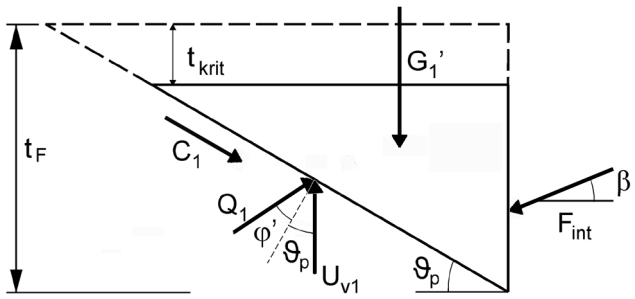

F_{int} = internal force

Vertical excess pore water pressure U_{v1}

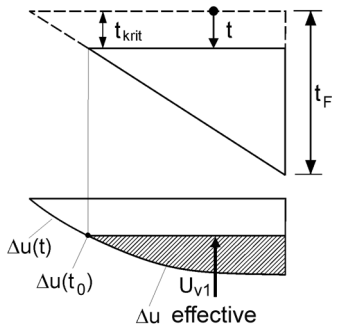

$$U_{v1} = \int \Delta u(x)\,\mathrm{d}x - \Delta u(t_{krit})\frac{t_F - t_{krit}}{\tan\vartheta_P}$$

$$\text{with } \mathrm{d}x = \frac{\mathrm{d}t}{\tan\vartheta_p} \quad \text{and} \quad \Delta u(t) = \gamma_W z_a\left(1-e^{-bt}\right)$$

$$U_{v1} = \frac{\gamma_W z_a}{\tan\vartheta_P}\cdot\int_{t_{krit}}^{t_F}\left(1-e^{-bt}\right)\mathrm{d}t - \frac{\gamma_W z_a}{\tan\vartheta_p}\left(1-e^{-bt_{krit}}\right)\left(t_F - t_{krit}\right)$$

$$= \frac{\gamma_W z_a}{\tan\vartheta_p}\left[t_F + \frac{1}{b}e^{-bt_F} - t_0 - \frac{1}{b}e^{-bt_{krit}} - t_F + t_F e^{-bt_{krit}} + t_0 - t_0\,e^{-bt_{krit}}\right]$$

$$U_{v1} = \frac{\gamma_W z_a}{\tan\vartheta_p}\left[\frac{e^{-bt_F} - e^{-bt_{krit}}}{b} + e^{-bt_{krit}}\left(t_F - t_{krit}\right)\right] \qquad \text{(s.7–18)}$$

(1) $\sum V = 0:$ $\quad -C_1' \sin\vartheta_p + Q_1 \cos(\varphi' + \vartheta_p) + U_{v1} - G_1' - F_{int} \sin\beta = 0$

(2) $\sum H = 0:$ $\quad -C_1' \cos\vartheta_p - Q_1 \sin(\varphi' + \vartheta_p) + F_{int} \cos\beta = 0$

from (2) $\Rightarrow$ (2′) $\quad Q_1 = \dfrac{F_{int}\cos\beta - C_1 \cos\vartheta_p}{\tan(\varphi' + \vartheta_p)}$

(2') in (1): $\quad -C_1' \sin\vartheta_p + \dfrac{F_{int}\cos\beta - C_1\cos\vartheta_p}{\tan(\varphi' + \vartheta_p)} + U_{v1} - G_1' - F_{int}\sin\beta = 0$

$$F_{int}\left(\frac{\cos\beta}{\tan(\varphi' + \vartheta_p)} - \sin\beta\right) = C_1 \sin\vartheta_p + G_1' - U_{v1} + C_1' \frac{\cos\vartheta_p}{\tan(\varphi' + \vartheta_p)}$$

(3) $$F_{int} = \frac{-U_{v1} + G_1' + C_1'\left(\sin\vartheta_p + \dfrac{\cos\vartheta_p}{\tan(\varphi' + \vartheta_p)}\right)}{-\sin\beta + \dfrac{\cos\beta}{\tan(\varphi' + \vartheta_p)}}$$

with: $\quad G_1' = \dfrac{\frac{1}{2}(t_F - t_{krit})^2 \gamma'}{\tan\vartheta_p}$ $\quad$ and $\quad C_1' = \dfrac{c'(t_F - t_{krit})}{\sin\vartheta_p}$

Right-hand soil wedge

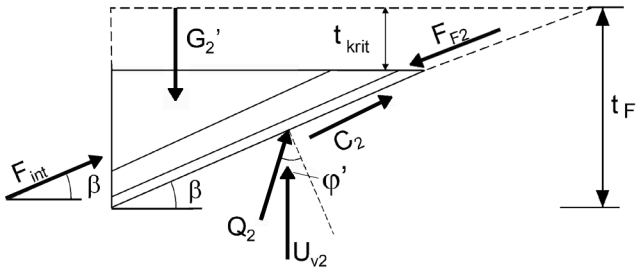

Vertical excess pore water pressure U_{v2}

$$U_{v2} = \frac{\gamma_W z_a}{\tan\beta}\left[\frac{e^{-bt_F} - e^{-bt_{krit}}}{b} + e^{-bt_{krit}}(t_F - t_{krit})\right]$$

(4) $\sum V = 0:$ $\quad G_2' - U_{v2} - Q_2\cos(\varphi' - \beta) - C_2\sin\beta - F_{int}\sin\beta + F_{F2}\sin\beta = 0$

(5) $\sum H = 0:$ $\quad F_{int}\cos\beta + Q_2\sin(\varphi' - \beta) + C_2\cos\beta - F_{F2}\cos\beta = 0$

$\Rightarrow$ (5b) $\quad Q_2 = \dfrac{(F_{F2} - F_{int} - C_2')\cos\beta}{\sin(\rho' - \beta)}$

(5b) in (4): $G_2' - U_{v\,2} - (F_{F\,2} - F_{int} - C_2')\cos\beta\cot(\varphi' - \beta) - C_2'\sin\beta - F_{int}\sin\beta + F_{F\,2}\sin\beta = 0$

$$F_{F\,2}(-\cos\beta\cot(\varphi' - \beta) + \sin\beta) = U_{v\,2} + C_2'\sin\beta + F_{int}(\sin\beta - \cos\beta\cot(\varphi' - \beta)) - G_2' + \\ - C_2'\cos\beta\cos(\varphi' - \beta) \\ = U_{v2} - G_2' + (C_2' + F_{int})(\sin\beta - \cos\beta\cot(\varphi' - \beta))$$

$$F_{F\,2} = \frac{U_{v\,2} + G_2'}{\sin\beta - \cos\beta\cot(\varphi' - \beta)} + C_2' + F_{int}$$

with $G_2' = \dfrac{\frac{1}{2}(t_F - t_{krit})^2\gamma'}{\tan\beta}$ and $C_2' = \dfrac{c'(t_F - t_{krit})}{\sin\beta}$

with (3): $$F_{F\,2} = \frac{U_{v1} - G_1' - C_1'(\sin\vartheta_p + \cos\vartheta_p\cot(\varphi' + \vartheta_p))}{\sin\beta - \cos\beta\cot(\varphi' + \vartheta_p)} + \frac{U_{v2} - G_2'}{\sin\beta - \cos\beta\cot(\varphi' - \beta)} + C_2'$$

$$= \frac{U_{v1} - G_1' - C_1'\,A}{B} + \frac{U_{v2} - G_2'}{D} + C_2'$$

with $A = \sin\vartheta_p + \cos\vartheta_p\cot(\varphi' + \vartheta_p)$

$B = \sin\beta - \cos\beta\cot(\varphi' + \vartheta_p)$

$D = \sin\beta - \cos\beta\cot(\varphi' - \beta)$

For 7.2.5.5 Sheet pile wall at toe

Determination of e_{ph} for a sheet pile wall at the toe:

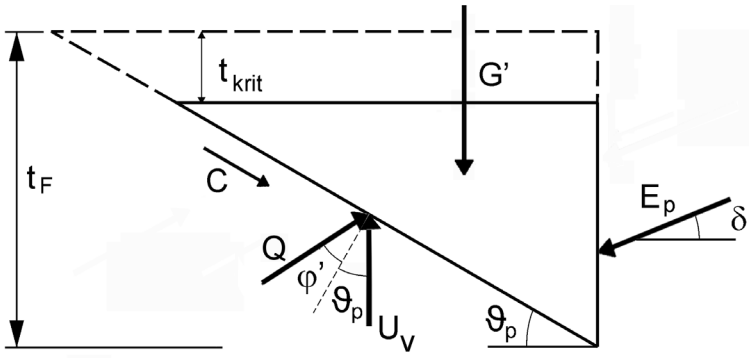

$$\vartheta_p = \arctan\left[\sqrt{\frac{(1 + \tan^2\varphi'\tan\varphi')}{\tan\varphi' + \tan\delta}} - \tan\varphi'\right]$$

The critical depth is the fluidisation depth: $t_{krit} = \dfrac{1}{b}\ln\left(\dfrac{\gamma_W z_a b}{\gamma'}\right)$

$$U_v = \frac{\gamma_W z_a}{\tan\vartheta_P}\left[\frac{e^{-bt_F} - e^{-bt_{krit}}}{b} + e^{-bt_{krit}}(t_F - t_{krit})\right]$$

(1) $\sum V = 0:\quad G' - U_v - Q\cos(\vartheta_p + \varphi') + C\sin\vartheta_p + E_p\sin\delta = 0$

(2) $\sum H = 0:\quad C\cos\vartheta_p + Q\sin(\vartheta_p + \varphi') - E_p\cos\delta = 0$

$$\Rightarrow (2'):\qquad Q = \frac{E_p\cos\delta - C\cos\vartheta_p}{\sin(\vartheta_p + \varphi')}$$

in (1):
$$G' - U_v - (E_p\cos\delta - C\cos\vartheta_p)\cot(\vartheta_p + \varphi') + C\sin\vartheta_p + E_p\sin\delta = 0$$

$$\Rightarrow\qquad E_p(-\cos\delta\cot(\vartheta_p + \varphi') + \sin\vartheta_p) = U_v - G' - C\sin\vartheta_p - C\cos\vartheta_p\cot(\vartheta_p + \varphi')$$

$$\Rightarrow\qquad E_p = \frac{U_v - G' - C(\cos\vartheta_p\cot(\vartheta_p + \varphi') - \sin\vartheta)}{-\cos\delta\cot(\vartheta_p + \varphi') + \sin\delta}$$

with $C = \dfrac{c'(t_F - t_{krit})}{\sin\vartheta_p}$ and $G' = \dfrac{(t_F - t_{krit})^2\gamma'}{2\tan\vartheta_p}$

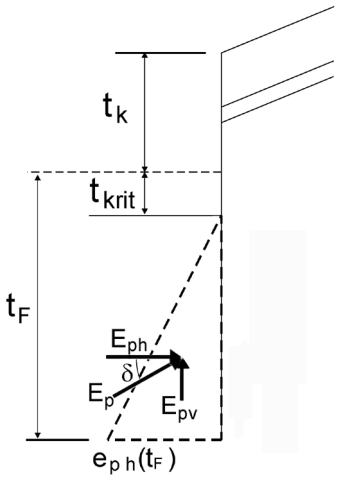

Horizontal component of the passive earth resistance (see figure)

$$E_{ph} = E_p\cos\delta = \frac{1}{2}(t_F - t_{krit})^2 e_{ph}(t_F)$$

$$\Rightarrow\qquad e_{ph}(t_F) = \frac{2E_p\cos\delta}{(t_F - t_{krit})^2}$$

Gesamtinhaltsverzeichnis aller bisher erschienenen Mitteilungsblätter

Hinweis: Die erste Zahl steht für die fortlaufende Nummerierung, die zweite Zahl für das Erscheinungsjahr, danach werden Autor und Titel des Beitrages aufgeführt.

1/53 Jambor: Erhöhung der festen Wehrschwelle bei gleicher hydraulischer Leistung
Burghart: Die Verteilung der Abflußmenge über den Querschnitt
Türk: Untersuchung über die Geschiebebewegung in Flüssen und Stauanlagen. Das elektro-akustische Geschiebe-Abhörverfahren
Zweck: Flach- und Pfahlgründungen in weichem tonigem Schluff
Canisius: Aus der Arbeit der Bundesanstalt
Liebs: Ausbau der Unteren Hunte
Schleiermacher: Sicherung der Schiffahrtsrinne in der Donau im Bereich der Innmündung bei Passau
Boos: Vom wasserbaulichen Versuchswesen in England

2/53 Canisius: Technische Entwicklung im Wasserbau
Pichl: Der Ortungstachygraph und seine Anwendung
Burghart/Gehrig: Beitrag zur Frage der Geschwindigkeitsverteilung in offenen Gerinnen
Davidenkoff: Grundwasserzufluß zu Brunnen und Gräben
Sagawe: Der Dehnungsmeßstreifen als Meßelement bei erd- und wasserbaulichen Modellversuchen
Zweck: Zur Ermittlung der Tragfähigkeit von Pfählen (I)

3/54 Canisius: Die Bodenmechanik im Dienste des Wasserbaues
Wehrkamp: Ein neues Flußprofilmeßgerät
Liebs: Abzweigung einer verhältnisgleichen Teilwassermenge an einem Meßwehr
Schleiermacher: Gestaltung schräg angeströmter Brückenpfeiler
Zweck: Zur Ermittlung der Tragfähigkeit von Pfählen (II)
Meenen: Reiseeindrücke von einem Einsatz der Bundesanstalt in Venezuela

4/54 Jambor: Die Gestaltung von Kanalabzweigungen unter besonderer Berücksichtigung von Schwingungen im Kanal
Herr: Spülvermögen bei Verschlammung und Geschiebeablagerung in einem Wehrfeld mit höckerartig erhöhter Wehrschwelle
Wehrkamp: Das Flußprofilzeichengerät von Dr. Fahrentholz
Davidenkoff: Gefährdung der Stauwerke bei Unterströmung
Zweck: Zur Ermittlung der Tragfähigkeit von Pfählen (III)

5/55 Canisius: Die Bundesanstalt für Wasserbau. Ein Rückblick auf ihre Entwicklung 1948 -1955
Niebuhr: Kritische Betrachtungen zur Frage der Modellrauhigkeit (I)
Schleiermacher: Wasserspiegelaufnahmen in Flußkrümmungen und Wasserspiegelquergefälle
Gehrig: Überprüfung hydrographischer Angaben durch den Modellversuch
Poggensee: Die Grundformel zur Bestimmung der Schleusenleistung
Zweck/Davidenkoff: Die versuchstechnischen Verfahren zur Berechnung des Netzes einer Grundwasserströmung

6/56 Schleiermacher: Geschwindigkeits-Verlagerung in Querschnitten mittels Buhnen oder Leitwerken
Gehrig: Messung und Berechnung von Kräften an Schiffen im Modell
Wigand: Verhinderung von Geschiebeablagerungen vor den unteren Schleusenvorhäfen und Staustufen
Zweck/Davidenkoff: Über die Zusammensetzung von Filtern
Poggensee: Anwendung und Kritik von Rammformeln

7/56 Gehrig: Strömungsmessung mit einem Kreiszylinder
Zweck/Davidenkoff: Untersuchung von Sicherungsmaßnahmen an Flußdeichen durch Modellversuche
Schleiermacher: Einfache Darstellung des zeitlichen Ablaufes von Anschwellungen in Wasserläufen
Niebuhr: Beitrag zur Erfassung der Räumkraft einer ungleichförmigen Strömung unter besonderer Berücksichtigung der Verhältnisse im Tidegebiet
Davidenkoff: Angenäherte Ermittlung des Grundwasserzuflusses zu einer in einem durchlässigen Boden ausgehobenen Grube

7/56 Liebs: Abflußbeiwerte für grasbewachsene Deiche
Jambor: Formgebung des Trennpfeilers in Flußkraftwerken

8/57 Yalin: Die theoretische Analyse der Mechanik der Geschiebebewegung
Davidenkoff: Durchsickerung durch Deiche und Erddämme (I)

9/57 Zweck/Davidenkoff: Auftrieb unter Wehren auf durchlässigem Grund
Davidenkoff: Wirkung der Sickerströmung auf die Standsicherheit eines Erddammes (II)
Schleiermacher: Versuch einer morphologischen Begründung von Rauhigkeits-Beiwerten für die Berechnung des Wasserspiegel-Gefälles
Yalin: Ermittlung des Querschnittes mit maximalem Geschiebetransportvermögen

10/58 Magens: Untersuchung der Ursachen und des Vorganges der Verschlickung der Schleusenvorhäfen zu Brunsbüttelkoog

11/58 Rubbert: Die Vertiefung der Tideflüsse und ihre Problematik
Gruhle: Verformungsmessungen an den Spundwänden der Schleuse Friedrichsfeld
Gehrig: Der Verbau von Übertiefen und die Erhaltung des Fahrwassers
Davidenkoff: Durchsickerung durch Deiche und Erddämme (Schluß aus 8 und 9)

12/59 Zweck/Dietrich: Zur Ermittlung der Verteilung des Coulomb'schen Erddruckes
Zweck: Versuchsergebnisse über die Zusammensetzung von Filtern
Rubbert: Die Tiderechnung als Problem der Numerischen Analysis

13/59 Zweck/Dietrich: Die Berechnung verankerter Spundwände in nicht bindigen Böden nach ROWE
Felkel: Der Schwellbetrieb der Flußkraftwerke
Steinfeld: Über den Erddruck an Schacht- und Brunnenwandungen

14/60 Felkel: Walzenbucht und Ringgraben als Mittel zur Verminderung der Schwebstoffablagerungen in Flußhäfen
Davidenkoff: Neue Forschungsarbeiten über die Konsolidierung wassergesättigter bindiger Böden
Gehrig/Herr: Beitrag zur Ermittlung des Wasserdruckes auf gekrümmte Flächen

15/60 Jambor: Lage und Gestaltung der Schleusen und ihrer Zufahrten
Felkel: Wasserspiegelmessungen an einer festen Wehrschwelle
Felkel: Gemessene Abflüsse in Gerinnen mit Weidenbewuchs

16/61 Felkel: Die Modelluntersuchungen für zehn Moselstaustufen
Davidenkoff: Sickerverluste bei Durch- und Unterströmung von Deichen
Dietrich: Schnittgrößen und Randspannungen in der Sohlfuge einer Kaimauer oder Stützmauer von rechteckigem Querschnitt

17/62 Kleinschmidt/Schröder: Sonderheft Korrosionsversuche

18/62 Felkel: Der Einsatz frei fahrender Modellschiffe beim flußbaulichen Versuch
Vollmer: Erfahrungen an einem Tidemodell mit beweglicher Sohle und Vergleich zwischen Modell- und Naturmessungen
Felkel: Ein einfaches Rundbecken zum Mischen von Wasser und Koagulieren von Schmutzstoffen
Davidenkoff: Über die Berechnung der Sickerverluste aus Kanälen

19/63 Zweck/Dietrich: Modellversuche mit steifen Dalben in bindigen Böden bei plötzlicher Belastung
Jansen: Die Neukonstruktion von Fahrstühlen für Kraftmessungen an Modellschiffen
Felkel: Die Neckartalplanung im Raume Heilbronn
Jänke: Überprüfung der Brauchbarkeit von Pfahlformeln anhand von Probebelastungen und Messungen an Stahlpfählen

20/64 Franke: Die Strömungsvorgänge bei unvollkommenen Brunnen

21/64 Naujoks: Untersuchungen zum Nachweis eines spezifischen Sättigungsgrades
Dietrich: Zur Berechnung der Tragfähigkeit starrer Dalben in homogenen Böden
Liebs: Die Abschirmung von Seehäfen gegen Seegang
Franke: Der Einfluß des Neigungswinkels der wasserführenden Schicht und einer partiellen Auskleidung des durchlässigen Brunnenschachtes auf die Zuflußmenge zu einem artesischen Brunnen

22/65 Rubbert: Tidewellenberechnungen nach dem Universalprogramm der BAW „Anwendung zur Berechnung der Tidebewegung der Oberelbe"
Jambor: Schutz der Sohle in Flüssen

22/65 Davidenkoff/Franke: Untersuchung der räumlichen Sickerströmung in eine umspundete Baugrube in offenen Gewässern

23/66 Dietrich: Modellversuche mit biegsamen langen Dalben unter wiederholten Belastungen im Sand
Ruck: Untersuchungen der Sandwandungsverhältnisse im Küstenbereich zwischen Stohl und Brauner Berg
Dietz: Einfluß der Saugschlauchbeaufschlagung bei Kaplanturbinen auf die Schiffahrtsverhältnisse im Unterwasser von Staustufen
Felkel/Canisius: Elektronische Berechnung von Wasserspiegellagen

24/66 Völpel/Samu: Reliefänderungen in der Tidestromrinne des Wangerooger Fahrwassers im Verlaufe einer Sturmperiode und in der darauf folgenden Periode mit ruhigeren Wetterlagen
Schnoor: Über neue Verfahren zur Berechnung des Reflexionsdruckes von Wasserwellen auf senkrechte Wände
Zweck: Baugrunduntersuchungen mit Sonden gem. DIN 4094 mit Auswertungsmöglichkeiten
Davidenkoff/Franke: Räumliche Sickerströmung in eine umspundete Baugrube im Grundwasser

25/67 Schnoor: Über verschiedene Verfahren zur Berechnung der Wellenangriffskräfte nicht brechender Wellen auf senkrechte Pfähle und Wände
Davidenkoff: Dimensionierung von Brunnenfiltern
Franke: Die Wirkungen des Wassers auf die Standsicherheit von Böschungen
Schulz/Ruck: Die Sandwanderungsverhältnisse an der Nordküste der Insel Fehmarn zwischen Westermarkelsdorf und Puttgarden
Lambert: Die Erscheinung der Gezeiten und ihre Erklärung

26/68 Schnoor: Über verschiedene Verfahren zur Berechnung der Wellenangriffskräfte auf senkrechte Pfähle und Wände
Samu: Ergebnisse der Sandwanderungsuntersuchungen in der südlichen Nordsee
Ruck: Auswirkung der geologischen Verhältnisse im Küstengebiet auf Baumaßnahmen im Wasserbau

27/68 Schäle/Kuhn/Schröder/Hofmann: Kanal- und Schiffahrtsversuche Bamberg 1967

28/69 Jänke: Untersuchungen der Zusammendrückbarkeit und Scherfestigkeit von Sanden und Kiesen sowie der sie bestimmenden Einflüsse
Felkel: Der Weg zum vollständigen mathematischen Flußmodell

29/69 Dietz: Kolksickerung durch Befestigungsstrecken für das Eidersiel
Dietz: Kolksicherung am Elbewehr Geesthacht

30/70 Franke/Manzke: Zwei interessante Beispiele von den Erdbauaufgaben am Elbe-Seitenkanal
Franke: Einige Beispiele zur Strömungsdruckwirkung des Grundwassers
Felkel: Ideestudie über die Möglichkeiten der Verhütung von Sohlenerosionen durch Geschiebezufuhr aus der Talaue ins Flußbett, dargestellt am Beispiel des Oberrheins
Jurisch: Beitrag zur Verwendung von Durchflußgleichung bei Dreieck-Überfällen
Sindern/Rohde: Zur Vorgeschichte der Abdämmung der Eider in der Linie Hundeknöll-Vollerwiek
Harten: Abdämmung der Eider; Modellversuche im Tidemodell
Dietz: Abdämmung der Eider; Modellversuche für das Sielbauwerk

31/72 Giese/Teichert/Vollmers: Das Tideregime der Elbe - Hydraulisches Modell mit beweglicher Sohle
Dorer: Berechnung der nichtstationären Abflüsse in nicht-prismatischen offenen Gerinnen
Dietz: Ausbildung von langen Pfeilern bei Schräganströmung am Beispiel der BAB-Mainbrücke Eddersheim
Dietz: Systematische Modellversuche über die Pfeilerkolkbildung

32/72 Niebuhr: Einfluß der Seitenwände bei hydraulischen Versuchen in einer rechteckigen Glasrinne
Ache: Ergebnisse von Sondierungen neben einem eingespülten Gründungskörper einer Leuchtbake
Franke/Ache: Ein Verfahren zur Berechnung eingespannter gedrungener Gründungskörper
Franke/Garbrecht/Kiekbusch: Meßfehler infolge unvollkommener Volumenkonstanz von Porenwasserdruckgebern beim Scherversuch
Franke/Bernhard: Erddruckansatz bei trogförmigen Bauwerken und Wechselwirkung zwischen Erd- und Sohldruck am Beispiel des Schiffshebewerkes Lüneburg
Felkel: Das Sohlenkorn des Rheins zwischen Straßburg und Bingen
Giese: Fahrwasserumbildungen in der Unter- und Außenelbe

33/72 Rohde/Meyn: Untersuchungen über das hydrodynamische Verhalten oberflächenmarkierten Sandes und über die Einbringmethode bei Leitstoffuntersuchungen
Ruck: Erfahrungen beim Präparieren von Sand für Leitstoffuntersuchungen
Dietz: Kolksicherung am Störsperrwerk
Hein: Verhalten von Rost unter nicht absolut dichten Beschichtungen bei Anlegen von kathodischem Schutz im Stahlwasserbau

34/73 Hovers: Der Einfluß von Strombauwerken auf die morphologische Entwicklung der Stromrinnen im Mündungsgebiet eines Tideflusses, untersucht am Beispiel der Außenweser

35/73 Davidenkoff: Anwendung von Bodenfiltern im Wasserbau
Tödten: Beitrag zur Energiedissipation von Tosbecken im Modellversuch
Hein: Sulfatangriff des Meerwassers auf Beton? Ein Beitrag zur Klärung der Frage, warum Meerwasser trotz hohen Sulfatgehaltes Beton nicht angreift
Jurisch: Messung der Momentangeschwindigkeiten mit Hilfe der Laser-Doppler-Anemometrie
Pulina: Geschwindigkeitsmessungen an einer Bootsgasse
Dietz: Modelluntersuchung der Schleusenvorhäfen an der Rheinstaustufe Iffezheim
List: Untersuchungen von instationär belasteten Kunststoff-Filtern für den Wasserbau

36/74 Dietz: Hydraulische Probleme bei der Planung von Staustufen
Felkel: Modellversuche mit Grundschwellen und Schiffahrt
Dietz/Pulina: Wahl der Wehrverschlüsse beim Ausbau der Saar zur Schiffahrtsstraße

37/75 Tödten: Untersuchung der Strömungsvorgänge an Buhnen
Schuppener: Erddruckmessungen am Schiffshebewerk Lüneburg
Harten/Knieß: Eiderdamm - Natur- und Modellmessungen
Dietz: Wellenmessungen im Hafen Travemünde - Vergleich zwischen Natur und Modell

38/75 Schuppener: Der Erddruck einer rolligen Hinterfüllung auf eine unverschiebliche Stützwand infolge der Verdichtung
Felkel: Untersuchungen der Veränderungen der Höhenlage der Sohle des Oberrheins
Samu: Beitrag zur morphologischen Entwicklung der Außenjade

39/76 Dietz/Pulina: Modelluntersuchungen zur Gestaltung der Hauptbauwerke an der Rheinstaustufe Iffezheim

40/76 Dietz/Pulina: Zur Wahl des Zugsegmentes als Wehrverschluß bei Ausbau der Saar
Knieß: Eiderdamm - Wiederauffüllung von Baggerlöchern im Watt
Annuß/Dehm/Hein/Schröder: Korrosion an Spundwänden - Wand-Dickenmessungen mit Ultraschall
Dietz/Pulina: Zur Problematik der Querströmungen in Vorhafenzufahrten und ihre Untersuchung im Modell
Dietz: Zur Frage der Nachbildung von Kolkvorgängen im Modell

41/77 Armbruster: Vergleich berechneter und gemessener Grundwasserstände am Beispiel Kehl
Döscher: Die Suspensionswand
Feddersen: Querbelastete Verankerungen
Franke/Garbrecht: Drei Serien von Probebelastungen an Großbohrpfählen in Sand-Ziel-Methode - Ergebnisse
Franke/Schuppener: Besonderheiten beim Gründungsgutachten für ein flachgegründetes off-shore-Bauwerk
Hauß: Beispiele für die Anwendung statistischer Methoden in der Bodenmechanik
Kiekbusch: Elektrisches Messen von Volumenänderungen beim Triaxialversuch
Ruck: Sondierungen zur Erkundung unterhalb der Gewässersohle von schwimmender Arbeitsplattform
Sagawe: Kraft- und Spannungsmessungen an der Containerkaje in Bremerhaven
Schulz: Überlegungen zur Führung des Nachweises der Standsicherheit in der tiefen Gleitfuge

42/77 Hein: Untersuchung über den Korrosionsablauf an wetterfesten Stählen in Abhängigkeit von der Entfernung zum Meer
Knieß: Bemessung von Schüttstein-Deckwerken im Verkehrswasserbau; Teil I: Lose Steinschüttungen
Hein: Zum Korrosionsverhalten von Zink in salzhaltigen Wässern

43/78 Dietz: Strömungsabweiser und/oder durchbrochene Trennmole als Mittel zur Verminderung der Querströmung in oberen Vorhafenzufahrten am Beispiel der neuen Mainstaustufe Krotzenburg
Knieß: Belastungen der Böschung des NOK durch Schiffsverkehr - Ergebnisse von Naturmessungen

44/79 Pulina: Modelluntersuchungen für die Saarstaustufe Rehlingen
Jurisch: Untersuchungen über die Abflußverhältnisse im Bereich einer Grundschwelle

45/79 Dietz/Pulina: Zur Frage des Wehrschwellenprofils beim Zugsegment
Dorer/Siem Hou Lie: Schwall- und Sunkberechnungen mit impliziten Differenzenverfahren

46/80 Garbrecht: Auswertung von Setzungsmessungen - zwei Beispiele -
Liebig: Stabilitätsuntersuchungen von Mehrfachregelkreisen an hydraulischen Modellen im wasserbaulichen Versuchswesen
Franke: Studie zur Frage des Einflusses von Meereswellen auf die Größe des Sohlwasserdruckes unter Offshore-Flachgründungen
Armbruster: Die Sickerwasserströmung im Bereich der Stauanlage Kulturwehr Kehl -
Teil I: Unterströmung und Standsicherheit im Endzustand

47/80 Felkel: Die Geschiebezugabe als flußbauliche Lösung des Erosionsproblems des Oberrheins

48/80 Giese: Das Tideregime der Elbe - Hydraulisches-Modell mit beweglicher Sohle
Schulz/Feddersen/Weichert: Zwängungskräfte infolge Sohlreibung

49/81 Pulina/Voigt: Hydrodynamische Belastung der Wehrverschlüsse an den Saarstufen Rehlingen, Mettlach und Schoden sowie Abflußleistungen bei spezifischen Betriebsfällen – Modelluntersuchungen

50/81 Schulz: Zur Festigkeit überverdichteter Tone
Gehrig: Die Berechnung des Geschiebetriebanfanges
Knieß: Schütten von Steinen unter Wasser
Wulzinger: Sedimenttransport und Sohlausbildung im Tidemodell der Elbe mit beweglicher Sohle

51/82 Pulina/Voigt: Einfluß der Randbedingungen auf die Abflußleistung unterströmter Wehrverschlüsse
Kemnitz: Beitrag zur Verringerung der Quergeschwindigkeiten im unteren Schleusenvorhafen einer Staustufe
Hein/Klein: Untersuchung über den Temperatureinfluß auf das Korrosionsverhalten von ungeschütztem Stahl im Emder Hafenwasser

52/83 Pulina/Voigt: Neubau eines Wehres im Zitadellengraben Berlin-Spandau
Knieß: Untersuchung zum Nachweis der Wirtschaftlichkeit von Uferdeckwerken an Wasserstraßen

53/83 Knieß: Kriterien und Ansätze für die technische und wirtschaftliche Bemessung von Auskleidungen in Binnenschiffahrtskanälen

54/84 Dorer: Ähnlichkeit bei flußbaulichen Modellen

55/84 Knieß: Untersuchung und Begutachtung alter Massivbauwerke an Wasserstraßen
Wagner: Die Untersuchung von Stahlwasserbauten
Hein: Korrosion über und unter dem Wasserspiegel
Hallauer: Grundsätzliche Betrachtungen über den Schutz und die Instandsetzung von Betonbauwerken
Abromeit: Anwendung von geotextilen Filtern bei Uferdeckwerken von Wasserstraßen in der BRD
Knieß/Köhler: Untersuchung gebundener Steinschüttungen auf Flexibilität, Verbundfestgkeit und Wasserdurchlässigkeit
Kellner/Annuß/Kretschmer: Kurzberichte über Arbeiten des Referats „Meßtechnik“

56/85 Schulz: Die Ermittlung des Seitendrucks in überkonsolidierten Tonen mit Hilfe von Laborversuchen
Schuppener: Verformungsmessungen im Erd- und Grundbau
Köhler: Modellversuche für die Dimensionierung von Deckwerken an Wasserstraßen - Stabilität loser Steinschüttungen

57/85 Armbruster: Messungen, Inspektion und Kontrolle an Dämmen
Pulina/Voigt: Lastbeanspruchungen langgestreckter Bauwerke in der Wasserstraße

58/86 Dorer: Stabilitätsformeln für lose Deckschichten von Böschungs- und Sohlenbefestigungen
Schulz: Kompressibilität und Porenwasserüberdruck - Bedeutung für Gewässersohlen
Hallauer: Vergußstoffe für Uferdeckwerke
Eißfeldt: Standsicherheitsbeurteilung alter Hafenanlagen am Beispiel der Woltmann Kaje Cuxhaven
Reiner/Schuppener: Gründungsbeurteilung und Sicherung des Weserwehres in Bremen
Knieß: Verfahren zur Untersuchung von Spanngliedern

59/86 Samu: Ein Beitrag zu den Sedimentationsverhältnissen im Emder Fahrwasser und Emder Hafen
Armbruster/Venetis: Der Einfluß von zeitweilig überstauten Polderflächen auf das Grundwasser
Müller/Renz: Erfahrungen bei der Untersuchung von Dükern und Durchlässen
Hein: Über das Korrosionsverhalten von Stahlspundwänden im Mittellandkanal

60/87 Rohde: 25 Jahre Außenstelle Küste
Dietz: Untersuchungen in den Tidemodellen der Außenstelle Küste
Kiekbusch: Entwicklung des Hamburger Bodenmechanischen Labors der BAW
Schuppener: Erfahrungen mit Bodenmechanischen Laborversuchen an Klei
Manzke: Erd- und grundbauliche Beratung beim Bau des Elbeseitenkanals
Schuppener/Eißfeldt: Standsicherheitsbeurteilung der Gründungen alter Wasserbauwerke
Alberts: Wanddickenmessungen an Stahlspundwänden
Harten: Das Staustufenmodell Weserwehr bei Bremen
Giese: Aufbau eines hydraulischen Tidemodells für das Lagunengebiet von Abu Dhabi
Fahse: Traceruntersuchungen in der Natur
Samu: Geomorphologische Untersuchungen im Bereich der Brammerbank und des Krautsander Watts in der Unterelbe
Jensen: Überlegung zur künftigen Entwicklung der Sturmflutwasserstände an der Nordseeküste

61/87 Teil I: Beiträge zum Ehrenkolloquium für Herrn Prof. Gehrig am 27. März 1987
Lohrberg: Prof. W. Gehrig und seine Bedeutung für die Entwicklung des Modellversuchswesens in der WSV
Garbrecht: Erosion, Transport, Sedimentations-Probleme und Überlegungen im Altertum
Mosonyi: Geschiebeprobleme bei Hochdruckwasserkraftwerken
Vollmers: Probleme bei der praktischen Berechnung des Geschiebebetriebs
Nestmann/Bachmeier: Anwendung von Luftmodellen im strömungsmechanischen Versuchswesen des Flußbaus

Teil II:
Haferburg/Müller: Instandsetzung der Mittellandkanalbrücke 144 b über die Weser in Minden

62/88 Weichert: Kenngrößen von Bentonit-Zement-Suspensionen und ihre Bedeutung für die Eigenschaften von Dichtungswandmaterialien

63/88 40-Jahre Bundesanstalt für Wasserbau

64/88 Rohde-Kolloquium am 9. Mai 1988:
Keil: Zur Untersuchung von Naturvorgängen als Grundlage für Ausbau und Unterhaltung der Bundeswasserstraßen im Küstenbereich
Holz: Moderne Konzepte für Tidemodelle
Vollmers: Reflexionen über Modelle mit beweglicher Sohle

Festakt „40 Jahre Bundesanstalt für Wasserbau“ am 8. November 1988:
Knieß: Einführungsansprache beim Festakt zur 40 Jahr-Feier der BAW am 08.11.88
Knittel: Ansprache anläßlich des 40jährigen Jubiläums der BAW in Karlsruhe am 08.11.88
Lenk: Verantwortungsprobleme im Wasserbau

Vortragsveranstaltung „Umwelt und Wasserstraßen“ am 8. November 1988:
Zimmermann/Nestmann: Ströme und Kanäle als Ingenieurbauwerke oder gestaltete Natur
Schulz: Standsicherheiten, Bemessungskriterien und Normen - Kontraindikationen eines naturnahen Flußbaus?
Lankenau: Technische Zwänge, Entwicklungen und Notwendigkeiten bei modernen Wasserstraßen
Reinhardt: Rechtliche Zwänge, Entwicklungen und Notwendigkeiten bei modernen Wasserstraßen
Kolb: Grundsätze der Landschaftsplanung bei der Gestaltung von Wasserstraßen
Larsen: Notwendiges Umdenken beim Ingenieur in Ausbildung und Praxis
Kennedy: Sediment, flood-control and navigation aspects of the Three Gorges Project, Yangtse river, China

65/89 Schröder: Auswirkung der Harmonisierung des EG-Binnenmarktes auf das Bauwesen
Flach: Normung für das Bauwesen im Rahmen eines europäischen Binnenmarktes
Litzner: Welche Auswirkungen haben die vorgesehenen europäischen Regelungen auf die deutschen Stahlbeton-Bestimmungen
Hallauer: Die Entwicklung der Zusammensetzung von Beton für Wasserbauten

65/89 Bayer: Einsatz der Betonbauweise bei Offshore-Bauwerken
Lamprecht: Verwendung von Beton bei Wasserbauten in der Antike
Rassmus: Entwicklung des Stahlbrückenbaus am Nord-Ostsee-Kanal (NOK)
Roehle: Der technische Fortschritt bei der Konstruktion und betrieblichen Ausbildung von Stahlwasserbauverschlüssen
Wagner: Untersuchung von Stahlwasserbauverschlüssen, vergleichende Auswertung und Folgerungen

66/89 Vorträge des gemeinsamen Symposiums „Deckwerke“ des Franzius-Instituts für Küsteningenieurwesen, Hannover, und der Bundesanstalt für Wasserbau am 8./9. Juni 1988:
Mühring: Entwicklung und Stand der Deckwerksbauweisen im Bereich der Wasser- und Schiffahrtsdirektion Mitte
Bartnik: Entwicklung und Stand der Deckwerksbauweisen im Bereich der Wasser- und Schiffahrtsdirektion West
Paul, W.: Deckwerksbauweisen an Rhein, Neckar, Saar
Paul, H. J.: Deckwerke unter ausführungstechnischen Gesichtspunkten
Möbius: Abrollen von Geotextilien unter Wasser
Saggau: Deichschlußmaßnahme Nordstrander Bucht
Laustrup: Dünensicherungsmaßnahmen an der dänischen Nordseeküste
de Groot: Allgemeine Grundlagen zur Standsicherheit des Untergrundes unter Deckwerken
Oumeraci: Zur äußeren Beanspruchung von Deckschichten
Richwien: Seegang und Bodenmechanik - Geotechnische Versagensmechanismen von Seedeichen
Köhler: Messungen von Porenwasserüberdrücken im Untergrund
Bezuijen: Wasserüberdruck bei Betonsteindeckwerken
Sparboom: Naturmaßstäbliche Untersuchungen an einem Deckwerk im Großen Wellenkanal
Heerten: Analogiebetrachtungen von Filtern
Hallauer: Baustoffe für Deckwerke
Saathoff: Prüfung an Geotextilien
Schulz: Überblick über neue nationale und internationale Empfehlungen

67/90 Hein: Zur Korrosion von Stahlspundwänden in Wasser
Kunz: Risikoorientierte Lastkonzeption für Schiffsstoß auf Bauwerke
Pulina/Voigt: Untersuchungen beim Umbau und Neubau von Wehranlagen an Bundeswasserstraßen
Zimmermann: Zur Frage zulässiger Querströmungen an Bundeswasserstraßen
Tsakiris: Kombinierte Anwendung der Dezimalklassifikation und von Titelstichwörtern zur Inhaltserschließung von Dokumenten

68/91 Knieß: Erweiterte Bundesanstalt für Wasserbau
Alf/Theurer: Prognose zur Entwicklung des Ladungspotentials für die Binnenschiffahrt in den neuen Bundesländern
Schulz: Zur Mobilisierung von Bewehrungskräften in nichtbindigen Böden
Ehmann: Bauwerksmessungen am Beispiel des Weserwehres
Hamfler: Temperatur- und Dehnungsmessungen während der Erhärtungsphase des Betons
Hauß: Verwendbarkeit von Waschbergen im Verkehrswasserbau
Köhler/Feddersen: Porenwasserdruckmessungen in Böden, Mauerwerk und Beton

69/92 Ohde: Nachdruck seiner Veröffentlichungen zu „Bodenmechanischen Problemen“
Themenkreise: Bodenmechanische Kennwerte, Erddruck, Standsicherheit, Sonstige Probleme und Gesamtdarstellungen

70/93 Knieß: 90 Jahre Versuchsanstalt für Wasserbau
Pulina: Bestimmung der zulässigen Strömungsgröße für seitliche Einleitungsbauwerke an Bundeswasserstraßen
Köhler u. a. m.: Wellenamplitudenmessungen mittels videometrischer Bildverarbeitung
Kuhl: Die Geschiebezugabe unterhalb der Staustufe Iffezheim von 1978 - 1992
Siebert: Simulation von Erosion und Deposition mit grobem Geschiebe unterhalb Iffezheim
Nestmann: Oberrheinausbau, Unterwasser Iffezheim

71/94 Nestmann/Theobald: Numerisches Modell zur Steuerung und Regelung einer Staustufenkette am Beispiel von Rhein und Neckar
Dietz/Nestmann: Strömungsuntersuchungen für das Eider-Sperrwerk

72/95 Vorträge zum OHDE-Kolloquium „Praktische Probleme der Baugrunddynamik“ am 14. September 1995
Fritsche: Modellversuche zur Bestimmung des dynamischen Verhaltens von Fundamenten
Huth: Modellierung des zyklischen Materialverhaltens von Lockergestein
Holzlöhner: Einfluß des Bodens beim Schiffsstoß auf Bauwerke
Schuppener: Eine Proberammung vor einer Stützwand mit unzureichender Standsicherheit
Palloks/Zierach: Zum Problem der Prognose von Schwingungen und Setzungen durch Pfahlrammungen mit Vibrationsrammbären
Haupt: Sackungen im Boden durch Erschütterungseinwirkungen
Zerrenthin/Palloks: Beiträge zur Prognose von Rammerschütterungen mit Hilfe von Fallversuchen
Palloks/Dietrich: Erfahrungen mit Lockerungssprengungen für das Einbringen von Spundbohlen im Mergelgestein
Huber: Ein Beitrag zur Erschütterungsausbreitung bei Zügen
Achilles/Hebener: Untersuchungen der Erschütterungsemission für den Ausbau von Straßenbahnstrecken mit angrenzender historischer Bebauung

73/95 Westendarp: Untersuchungen und Instandsetzungsmaßnahmen an den Massivbauteilen des Eidersperrwerkes
Dietz: Strömungsverhältnisse, Kolkbildung und Sohlensicherung am Eider-Sperrwerk
Heibaum: Sanierung der Kolke am Eidersperrwerk - Geotechnische Stabilität von Deckwerk und Untergrund

74/96 Vorträge zum BAW-Kolloquium „Flußbauliche Untersuchungen zur Stabilisierung der Erosionsstrecke der Elbe“ am 9. März 1995
Faist: Langfristige Wasserspiegelsenkungen und Grundsätze der Strombaumaßnahmen in der Erosionsstrecke der Elbe
Glazik: Flußmorphologische Bewertung der Erosionsstrecke der Elbe unterhalb von Mühlberg
Faulhaber: Flußbauliche Analyse und Bewertung der Erosionsstrecke der Elbe
Schmidt: Ergebnisse neuerer Untersuchungen zu Gewässersohle und Feststofftransport in der Erosionsstrecke
Alexy: Hydronumerische Untersuchungen zur Felsabgrabung und zum Einbau von Grundschwellen in der Elbe bei Torgau
Fuehrer: Untersuchungen der Einsinktiefe von Bergfahrern im Stromabschnitt Torgau
Schoßig: Sohlenstabilisierung der Elbe km 154,62 - 155,70 im Bereich der Torgauer Brücken - praktische Durchführung -
Kühne: Sohleninstandsetzung im Stromabschnitt Klöden (El-km 188,8 - km 192,2)

75/97 Abromeit: Ermittlung technisch gleichwertiger Deckwerke an Wasserstraßen und im Küstenbereich in Abhängigkeit von der Trockenrohdichte der verwendeten Wasserbausteine
Alberts/Heeling: Wanddickenmessungen an korrodierten Stahlspundwänden - Statistische Datenauswertung zur Abschätzung der maximalen Abrostung -
Köhler: Porenwasserdruckausbreitung im Boden, Messverfahren und Berechnungsansätze

76/97 Vorträge zum BAW-Kolloquium zur Verabschiedung von LBDir a. D. Prof. Dr.-Ing. H. Schulz und zur Amtseinführung von LBDir Dr.-Ing. B. Schuppener am 18. Oktober 1996
Krause: Ansprache anläßlich der Verabschiedung von Prof. Dr.-Ing. Schulz
Schwieger: Monitoringsystem zur Überwachung der Fugendichtigkeit an der Schleuse Uelzen
Köhler: Boden und Wasser - Druck und Strömung
Armbruster-Veneti: Leckageortung an Bauwerken der WSV mittels thermischer Messungen
Schulz: Rückblick auf 23 Jahre Geotechnik in der BAW
Schuppener: Gedanken zu den zukünftigen Aufgaben der Geotechnik in der BAW

77/98 Armbruster-Veneti et al.: Das Schawan-Wehr in Karelien - Zustand und Lebensdauer
Fuehrer: Untersuchungen zur hydraulischen Beanspruchung der Wasserstraßen durch die Schiffahrt
Jurisch: Untersuchung der Genauigkeiten von Tachymeter- und DGPS-Ortungen zur Ermittlung hydraulischer und hydrologischer Daten in Flüssen
Lasar/Voigt: Gestaltung des Allerentlastungsbauwerkes I am MLK

78/98 50 Jahre Bundesanstalt für Wasserbau

79/98 Vorträge zum Gemeinsamen Kolloquium von BAW und BfG „Eisbildung und Eisaufbruch auf Binnenwasserstraßen“ am 26. Mai 1998
Heinz: Konzeptionelle Überlegungen zur Nutzung der Wasserstraßen bei Eis
Barjenbruch: Wärmehaushalt von Kanälen
Klüssendorf-Mediger: Prognose von Eiserscheinungen auf ostdeutschen Wasserstraßen
Brydda: Chancen eines garantierten Ganzjahresverkehrs auf mitteleuropäischen Kanälen
Busch: Eissituation an den Wasserstraßen der WSD Süd
Voß: Eisbildung und Eisaufbruch auf den Binnenwasserstraßen der WSD Ost
Rupp: Eisbrechende Fahrzeuge und deren Einsatzmöglichkeiten bei Eisbedeckung
Kaschubowski: Eisfreihaltung mit Luftsprudelanlagen
Sachs: Tauchmotorpropellerpumpen zur Eisfreihaltung von Stemmtoren
Alexy: Eisdruck auf Kanalbrücken
Alexy: Optimierung der Eisabführung an Brücken

80/99 Vorträge zum BAW-Kolloquium „Donauausbau Straubing-Vilshofen / vertiefte Untersuchungen“ am 14. Oktober 1999
Kirchdörfer: Donauausbau Straubing - Vilshofen - vertiefte Untersuchungen - Ziele, Varianten, Organisationsstruktur
Hochschopf: Donauausbau Straubing - Vilshofen - vertiefte Untersuchungen - Baumaßnahmen Naturversuch Sohlendeckwerk
Jurisch/Orlovius: Durchführung und Rohdatenauswertung
Strobl: Steinschlaguntersuchungen zur Ermittlung vertikaler Sicherheitsabstände in der Schifffahrt
Zöllner: Fahrdynamische Untersuchungen der Versuchsanstalt für Binnenschiffbau e. V., Duisburg, zum Donauausbau Straubing - Vilshofen
Neuner: Untersuchungen zu den horizontalen Sicherheitsabständen in einem mit Buhnen geregelten Flussabschnitt
Nestmann: Luftmodelluntersuchungen zu Kolkverbaumaßnahmen
Kellermann: Donauausbau Straubing - Vilshofen - vertiefte Untersuchungen - 1D-Modellverfahren - Modelltechnik, 3D-Untersuchungen, Buhnen, flussmorphologische Änderungen
Söhngen: Fahrdynamische Modelluntersuchungen
Roßbach/Kauppert: Physikalischer Modellversuch Isarmündung

81/00 Dienststelle Ilmenau
Beuke: Festvortrag - Bauinformatik als Verbundstelle zwischen Bauingenieurwesen und Informatik
Siebels: Wie kam es zum Standort Ilmenau
KSP Engel und Zimmermann Architekten: Neubau der Dienststelle der Bundesanstalt für Wasserbau in Ilmenau
Siebels: Kunstwettbewerb für den Neubau der Dienststelle der Bundesanstalt für Wasserbau in Ilmenau
Paul: Erwartungen der WSV an die BAW-Dienststelle in Ilmenau
Bruns: Informations- und Kommunikationstechnik - Perspektiven und Visionen -
Bruns: Zur Geschichte der Datenverarbeitung in der BAW
Fleischer: Zur Begutachtung der Standsicherheit alter, massiver Verkehrswasserbauten
Palloks: Die Entwicklung der Aufgaben des Referats Baugrunddynamik (BD)
Palloks: Bericht über das BAW - Kolloquium „Setzungen durch Bodenschwingungen“ in der Außenstelle Berlin am 29.09.1999

82/00 Oebius: Charakterisierung der Einflussgrößen Schiffsumströmung und Propellerstrahl auf die Wasserstraßen
Zöllner: Schiffbauliche Maßnahmen zur Reduzierung der Sohlbeanspruchung
Rieck/Abdel-Maksoud/Hellwig: Numerische Berechnung der induzierten Geschwindigkeiten eines Binnenschiffes im Flussbett bei Bergfahrt
Fuehrer/Pagel: Formparameter- und Tiefgangseinflüsse auf die erreichbare Schiffsgeschwindigkeit und schiffsinduzierte Sohlströmung im allseitig begrenzten Fahrwasser – Ergebnisse der 3D-Modellierung der Schiffsumströmung nach FANKAN
Willamowski: Anwendung hydraulischer und fahrdynamischer Bewertungskriterien zur Beurteilung der Befahrbarkeit von Flüssen am Beispiel der Unteren Saale
Söhngen/Heer: Einfluss des mittleren Rückströmungsfeldes auf den Geschiebetransport am Beispiel des Rheins bei Westhoven
Abromeit: Deckwerksschäden durch Verockerung des geotextilen Filters und Sanierungsmethode

82/00 Alexy: Ermittlung der Kolktiefen und der erforderlichen Sohlenbefestigung im Bereich einer Brückenbaustelle in der Elbe
Faulhaber: Veränderung von hydraulischen Parametern der Elbe in den letzten 100 Jahren
Hentschel/Kauther: Hochgeschwindigkeitsvideokamera im wasserbaulichen und geotechnischen Versuchswesen
Gladkow/Söhngen: Modellierung des Geschiebetransports mit unterschiedlicher Korngröße in Flüssen
Glazik: Historische Entwicklung des wasserbaulichen Modellversuchswesens in den Versuchsanstalten Berlin-Karlshorst und Potsdam

83/01 Vorträge zum BAW-Kolloquium „Instandhaltung der Wasserbauwerke - eine Kernaufgabe der WSV", Abschiedskolloquium für Herrn LBDir R. Wagner am 22. März 2001
Aster: Bauwerksinstandsetzung und Kernaufgaben - Ein Widerspruch?
Hermening: Anforderungen der WSV an die BAW bezüglich der Beratung bei der Instandhaltung der Anlagen
Kunz/Bödefeld: Von der Bauwerksinspektion zum Bauwerksmanagement
Westendarp: Betoninstandsetzung - Neue Anforderungen und Entwicklungen
Strobl/Wildner: Injektion mit hydraulischem Bindemittel im porösen Massenbeton
Meinhold: Instandsetzungsmöglichkeiten und -grenzen für Stahlwasserbauten
Binder: Arbeits- und Umweltschutz bei Korrosionsschutzarbeiten
Beuke: Gestalterische Aspekte bei der Modernisierung der Schleuse Woltersdorf

84/02 10 Jahre deutsch-russische Kooperation im Bereich der Binnenwasserstraßen 1991-2001, Vorträge aus Symposien 9. September 2001 in Sankt Petersburg und 11. Dezember 2001 in Karlsruhe (in deutscher und russischer Sprache)
Butow: Zusammenarbeit der Sankt-Petersburger Staatlichen Universität für Wasserkommunikationen mit der Bundesanstalt für Wasserbau
Armbruster: Ausgewählte Aspekte der Zusammenarbeit auf dem Gebiet der Geotechnik
Kljujew: Deformationen der Schleusenkammerwände an der Wolga-Ostsee-Wasserstraße
Ogarjow/Koblew: Zustand und Entwicklungsperspektiven der Kaspi-Schwarzmeer-Wasserstraße
Radionow: Rekonstruktion des Moskau-Kanals
Bödefeld: Auswertung der Bauwerksinspektion
Dettmann/Zentgraf: Pegelabhängige Fahrspurberechnung in fließenden Gewässern
Kemnitz: Modellierung des Geschiebetransports in Flüssen
Kemnitz: Untersuchung von Schleusenfüllsystemen am Beispiel der neuen Hafenschleuse Magdeburg
Lausen: Numerische 3D-Simulation der Moselstaustufe Lehmen
Odenwald: Prüfung und Beurteilung der Baugrubenabdichtung für den Schleusenneubau Uelzen II im Elbe-Seitenkanal
Paul: Donauausbau Straubing - Vilshofen
Stenglein: Unterhaltungskonzept für den freifließenden Rhein

85/02 Oberflächendichtungen an Sohle und Böschung von Wasserstraßen:
Empfehlungen zur Anwendung von Oberflächendichtungen an Sohle und Böschung von Wasserstraßen

Kolke an Gründungen / Scour of Foundations - Workshop 5 der XV. Internationalen Tagung über Bodenmechanik und Geotechnik in Istanbul im August 2001 (in deutscher und englischer Sprache):
Annandale et al.: Fallstudien zur Kolkbildung / Scour Case Studies
Heibaum: Geotechnische Aspekte von Kolkentwicklung und Kolkschutz / Geotechnical Parameters of Scouring and Scour Countermeasures
Richardson et al.: Praktische Berechnungen zu Kolken an Brücken in den USA / United States Practice for Bridge Scour Analysis

Schiffbautechnisches Kolloquium der Bundesanstalt für Wasserbau am 24./25. April 2002:
Bielke: Funktionale Leistungsbeschreibung bei der Ausschreibung von Wasserfahrzeugen
Dobinsky/Sosna: Einsatz dieselelektrischer Schiffsantriebe
Lenkeit/Stryi: Modernisierung der Fähren entlang des NOK
Stumpe: Verlängerung MzS MELLUM
Garber: Entwicklung eines Sandhobels
Claußen: Entwickung und Einsatz von flachgehenden Aufsichts- und Arbeitsschiffen (Typ Spatz)
Kühnlein: Modellversuchswesen im Schiffbau
Germer: Antifouling (TBT-Alternativen)
Christiansen: Umweltverträgliche Schmierstoffe und Hydrauliköle

85/02 Hoffmann: Fächerlot- und Sonarsysteme
Preuß: Einsatz von AIS/VDR an Bord

86/03 Themenschwerpunkt: Wasserbau im Küstenbereich
Beschreibung und Analyse der Ästuardynamik in den Seeschifffahrtsstraßen:
Jürges/Winkel: Ein Beitrag zur Tidedynamik der Unterems
Lang: Ein Beitrag zur Tidedynamik der Innenjade und des Jadebusens
Schüttrumpf/Kahlfeld: Hydraulische Wirkungsweise des JadeWeserPorts
Schubert/Rahlf: Hydrodynamik des Weserästuars
Boehlich: Tidedynamik der Elbe
Seiß/Plüß: Tideverhältnisse in der Deutschen Bucht
Winkel: Das morphologische System des Warnow-Ästuars
Rudolph: Sturmfluten in den deutschen Ästuaren

Grundlagen für die Sicherheit und Leichtigkeit des Schiffsverkehrs:
Liebetruth/Eißfeldt: Untersuchungen zur Nautischen Sohle
Uliczka/Kondziella: Dynamisches Fahrverhalten extrem großer Containerschiffe unter Flachwasserbedingungen
Bielke/Siebeneicher: Entwicklung, Planung und Neubau von Wasserfahrzeugen

Die mathematische Modellierung als unverzichtbare Beratungsgrundlage:
Heyer: Zur Bedeutung mathematischer Modelle im Küstenwasserbau
Lang: Analyse von HN-Modell-Ergebnissen im Tidegebiet
Weilbeer: Zur dreidimensionalen Simulation von Strömungs- und Transportprozessen in Ästuaren
Malcherek: Vom Sohlevolutions- zum vollständigen Morphologiemodell: Eine Road Map zur SediMorph-Entwicklung
Vierfuss: Seegangsmodellierung in der BAW

87/04 Grundlagen zur Bemessung von Böschungs- und Sohlensicherungen an Binnenwasserstraßen

88/05 Principles for the Design of Bank and Bottom Protection for Inland Waterways
(Englische Fassung des Mitteilungsblatts Nr. 87/2004)